PhD-FSTM-2021-025
The Faculty of Science, Technology and Medicine

DISSERTATION

Presented on 29/04/2021 in Luxembourg

to obtain the degree of

DOCTEUR DE L'UNIVERSITÉ DU LUXEMBOURG

EN BIOLOGIE

by

Andrés, CANO GALIANO
Born on 23 January 1992 in Santander (Spain)

IDENTIFYING AND TARGETING METABOLIC VULNERABILITIES IN IDH MUTANT GLIOMAS

Dissertation defense committee

Dr. Simone Niclou, dissertation supervisor
Head of the Department of Oncology, Luxembourg Institute of Health
Adjunct Professor, University of Bergen, Norway

Dr. Saverio Tardito
Junior Group Leader, Cancer Research UK Beatson Institute, Glasgow, United Kingdom

Dr. Carole Linster, Chairman
Head of Enzymology and Metabolism Group, Luxembourg Centre for Systems Biomedicine
Assistant Professor, Université du Luxembourg

Dr. Almut Schulze
Professor, Julius-Maximilians Universität
Head of Tumor Metabolism and Microenvironment Group, German Cancer Research Center, Heidelberg, Germany

Dr. Dirk Brenner, Vice Chairman
Professor, Université du Luxembourg
Head of Experimental and Molecular Immonology, Luxembourg Institute of Health

The Faculty of Sciences, Technology and Communications

DISSERTATION

Defense held on 29.04.2021
to obtain the degree of

DOCTEUR DE L'UNIVERSITÉ DU LUXEMBOURG
EN BIOLOGIE

by

Andrés Cano Galiano
Born on 23rd of January 1992 in Santander (Spain)

IDENTIFYING AND TARGETING METABOLIC VULNERABILITIES IN IDH MUTANT GLIOMAS

Dissertation defense committee

Prof. Dr. Simone Niclou, dissertation supervisor
Luxembourg Institute of Health, Luxembourg

Dr. Carole Linster, chairman
University of Luxembourg, Luxembourg

Prof. Dr. Dirk Brenner, vice-chairman
University of Luxembourg, Luxembourg

Dr. Saverio Tardito, external jury member
Cancer Research UK Beatson Institute, Glasgow, United Kingdom

Prof. Dr. Almut Schulze, external jury member
German Cancer Research Center, Heidelberg, Germany

Dissertation Supervisor

Prof. Dr. Simone Niclou

Norlux Neuro-Oncology Laboratory, Department of Oncology, Luxembourg Institute of Health, Luxembourg

Dissertation Supervision Committee

Dr. Carole Linster

Department of Enzymology and Metabolism, University of Luxembourg, Luxembourg

Dr. Saverio Tardito

Oncometabolism Research Group, Cancer Research UK Beatson Institute, Glasgow, United Kingdom

Prof. Dr. Simone Niclou

Norlux Neuro-Oncology Laboratory, Department of Oncology, Luxembourg Institute of Health, Luxembourg

The work presented in this thesis was conducted at the:

Norlux Neuro-Oncology Laboratory

Luxembourg Institute of Health

The work presented in this thesis was sponsored by:

CANBIO Doctoral Training in Cancer Biology

Luxembourg National Research Fund

Doctoral Program in Systems and Molecular Biomedicine

Doctoral School in Science and Engineering

University of Luxembourg

Fondation du Pélican de Mie et Pierre Hippert-Faber

Under the aegis of the Fondation de Luxembourg

Affidavit

I hereby confirm that the PhD thesis entitled “IDENTIFYING AND TARGETING METABOLIC VULNERABILITIES IN IDH MUTANT GLIOMAS” has been written independently and without any other sources than cited. All necessary ethical approvals have been obtained in accordance with the law (on the use of clinical samples and on the Care and Use of laboratory animals, where applicable).

Luxembourg, February 15, 2021 Andrés Cano Galiano

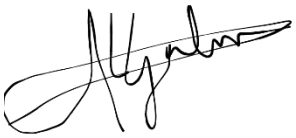

To my parents, Román and Elena

Acknowledgments

First of all, I have to mention all those who have accompanied me on this journey. Simply and bluntly, thank you very much. Getting here would have been impossible without the help of so many people who lent themselves to collaborate, to advise, or just to be close in this process. I hope I do not miss too many.

I start with Simone. You were the one who allowed this to begin in the first place. And for that I will be eternally grateful. You brought me to life in this project, trusting me and giving me the opportunity to enter the scientific world. It has not been easy, but where would the fun be then? Together we have been shaping ideas, sharing and disagreeing opinions, step by step making this story fructify. Not everything has gone as planned, and although expectations were high and reality turned out to be different, what comforts me the most is having your approval and appreciation for the effort made. Despite your busy agenda, I never felt like I lacked time to talk to you when I needed it. You always gave me a solid perspective on my ideas and from you I feel I have learned a lot about how to pose and approach my scientific challenges. It has been a complete honor to have been your pupil. I will always be available and I hope to keep in touch once I continue on my way. If one day you want to visit the mountains in northern Spain, don't hesitate to let me know.

Of course, now it's Fred's turn. My inseparable companion in fatigue, side by side (literally) for four years. I feel incredibly lucky to have had your support from the first day I arrived. You made my adaptation to a new job, a new country, a new life, as comfortable and pleasant as possible. You were always there, helping, listening, solving my mistakes, being patient with me and helping without blinking any time I needed it, inside but also outside the lab. You have always given me a sense of calm and peace that has helped me countless times when facing difficult stages of the PhD. I still hope to enjoy some more time with you on a kayak, or to share that beer which we have been planning for too long. Whatever happens in the time ahead, you know Fred here you have a friend. Thanks for everything.

Many thanks to all the people at NORLUX, this great team with great scientists. I have always felt a good vibe floating over us, and I have never felt self-conscious when I have needed you. Without the

magical hands of Anaïs and Virginie with the *in vivo* work, a large part of this project would not have worked, thank you. Also to Anna, who from the beginning was attentive and advised me during the adventures and misadventures with my dammed cells. Thanks to Sabrina and Monika, who put up with me for almost a year, at the beginning of this project, trying to complete the most difficult task ever attempted, correcting the IDH1 mutation. Thanks to you I learnt a lot about CRISPR/Cas9, and at least we got our IDH1m knock-in. Ann-Christin and Alfonso, thank you for helping me quickly and efficiently with the patient samples at a critical time. Thanks also to Rolf, for lending the patient samples, and Christel Herold-Mende, for the cell lines. Thanks to Siu-Thinh, for so much patience and poise in solving my paperwork. Amandine, Vanessa and all of you who were going to the cantine together when I arrived, you welcomed me very sweetly from the first moment, thank you from the heart.

What about the other big part of NORLUX and LIH in general, the PhD community? Thank you all for having shared this burden at some point. We are the ones who understand each other best. When I arrived there were not so many of us. Thanks to Mathieu, Carole, Anne Dirkse, Hélène, the old guard who introduced me to what was coming to me. The old ones left, and I was one of the first in this new herd that is now growing so much. But there we were for a while at the beginning, alone, Moha, Yolanda, Miriam and me. Months and months when we only had each other. How many Tuesdays and Thursdays at Liquid saved us? Without all those moments of de-stress and disconnection, everything would have been much more uphill. Thanks guys. Now the family has increased, Lia, Carina, Yahaya, Hugo, Rédouane... and all those who continue to arrive. There are many of us now, and although the annoying COVID situation and the hustle of our PhD life have distanced us, I hope that we can all celebrate together properly when all this calms down.

Not only do the people at NORLUX deserve thanks, great people at LIH have helped me take my PhD with a special attitude and motivation. Giuliuca, *trimona*, you're amaaazing. Soon we will finally walk around the contour of the bull. Iria, you will always have me here waiting for you to stop looking at the ceiling. Ilaria, Andrea, thank you for those Spritz and Bora Bora moments.

And here we are, at LIH still. I thank this center for providing the means that allowed me to do my PhD, giving me the opportunity to participate in such a rich and multicultural research environment.

Obviously I do not forget who feeds me, and I am very grateful that FNR and CANBIO have supported my progress and have allowed me to evolve from start to finish. In addition to the University of Luxembourg, which offers so many opportunities and commodities that make me feel tremendously lucky to have landed to this country to do my PhD.

The beauty of science and biomedicine in particular is that it is not possible to carry out a project all by yourself. You will always need people to help you, collaborations. How to summarize the work of Johannes and all that he has helped me at the time I needed it most? In the middle of my PhD, when motivation waned, you came in and pulled me out of the hole. You redirected my path and thanks to that the project went ahead. Once I was doing better, you continued to be there, to give advice and discuss ideas. I could not be more grateful to you. I am very happy to see how your team of Cancer Metabolism Group (CMG) is growing and progressing. Many thanks also to all of you there at CMG for your aid in this beautiful field that unites us. Also through Johannes, I was able to collaborate with the people from the Metabolomics platform of the Luxembourg Center for Systems and Biomedicine (LCSB), Carole, Nicole, Xiangyi, Christian, thank you for your help.

Much of what achieved in this project is also owed to the LIH Quantitative Biology Unit, and in particular to Elena. How much you have helped me... With the proteomics experiments but also as a therapist with whom I can have long conversations over our coffees, thinking about Costa Ricas and calimotxos. *Mil gracias Elena, eres una grande.*

When I started my PhD, it was impossible to foresee how many experiences I would have. Indeed, thanks to the Fondation du Pélican and the members of the jury who granted me their scholarship, I have been able to expand academically beyond Luxembourg. I could attend to internationally renowned conferences in Glasgow, Paris or Bilbao, where for instance, I had the opportunity to speak with someone who would end up winning the Nobel Prize in Medicine later on, William G. Kaelin. Thanks to the Pelican grant I was also able to attend, for three weeks, one of the most important courses in metabolomics in the world, at Cold Spring Harbor Laboratory (CSHL), New York. A temple of science and molecular biology where the greatest have been. In all these experiences I have been able to meet

some of the most renowned scientists in my field, but most importantly incredible and nice people, opening new doors and opportunities for my future paths.

However, one of my internships abroad that has enriched me the most has undoubtedly been during my two-week stay at the Cancer Research UK Beatson Institute, in Glasgow. There I have been able to collaborate and learn from Saverio. I thank you very much for how well you welcomed me there, I have a great memory of those days in Glasgow, of our conversations in the car and in the lab. Thank you very much for all your support with this project and your always accurate criticism. You have given me a great insight into the functioning of cellular metabolism, and it has been a pleasure and an honor to be able to learn and live the experience in your laboratory. Thanks also to Saverio's team at Beatson, especially to Francesca. You are the best, you treated me great when I was there, you took me to see Scotland and you took care of always including me in cool plans with you and your friends. I am looking forward to seeing each other again, but maybe next time further south, where the sun shines a little more. Many thanks also to David and his mastery of the Beatson metabolomics platform. You were also the coolest teacher at CSHL, a billiards star and a professional beer taster.

I want also to give a special mention to the members of my CET. Carole, Saverio and Simone. I have always felt very comfortable with our annual meetings, you transmitted calm to me while helping a lot with the project. You have been able to see how it all started and where it ended. Thanks for the support. I also want to thank the other members of my defense jury, Dirk Brenner and Almut Schulze. Thank you for having accepted to evaluate my thesis, and dedicate some of your time to read what with effort and dedication I have compiled during these four years.

I would now like to thank all those people who have been present in my adventure outside the scientific world. Obviously, my parents, who from the first day of my life supported me and made me believe that I could achieve anything I set my mind to. I dedicate my thesis to you, as it is an extension of your work and effort. Thanks to my brother, an example that is worth fighting for your dreams in life. Thanks also to my whole family, to all the Galianos, for always remembering me even if I could not be with you all I wanted. To my grandmother for her inspiring strength and love. To my aunt Sofía, that if it had been necessary she would have crossed Europe in the midst of a pandemic to see me defending my thesis.

Of course, I have to thank my other family, the one I chose, my childhood friends, those who have seen me grow and evolve and with whom I have always counted on any of my adventures. Romans, Pau, Tinuca, Wey, Divi, and the whole family of *bezanosos* and *tierruqueros*, who put up with my stories every time we see each other, as if we had never parted. I feel a millionaire in friends. Thank you. And of course, I am not forgetting you Rut. You have been a crucial support for much of this journey, and you are a very important chapter in my PhD. Thanks for sharing it with me.

I also want to thank my friends from Luxembourg for being there, making my stay so cool. Thanks to Kobi, Acerina and Alvar, our regular dinners and trips fill my life here. Always faithful, since we met a lifetime ago at Unival II. Also thanks to those friends who have been taking me out of the routine and showing me new life perspectives, to María, Luca, Rubén, Natasa, Shameek, to the entire Shamrock team... you are great. Paradoxically, the pandemic brought us closer together, and I feel lucky for that.

I feel tremendously grateful to have had the opportunity to do this PhD. It has been a slow process, intense, exhausting, with ups and downs, but it has been insurmountable. I would not change a thing about how this path has played out (well… maybe some smaller error bars here and there). The difficulty of the journey makes the taste of the end especially pleasant, and once everything is coming to an end it is easier to appreciate that it has been worth it. A very important stage of my life ends here, and I still don't know where or how the next one will be. I only wish I will continue being as well surrounded as I have been here. Thank you so much to everyone. *Merci beaucoup. Villmols merci. Vielen Dank. Grazie mille. Muchas gracias.*

List of abbreviations

α-KG	- α-ketoglutarate
ANLS	- Astrocyte-neuron lactate shuttle
AS	- Astrocytoma
ATP	- Adenosine triphosphate
BBB	- Blood brain barrier
Cas9	- CRISPR associated protein 9
CBS	- Cystathionine β-synthase
CBTRUS	- Central Brain Tumor Registry of the United States
CNS	- Central nervous system
CRISPR	- Clustered regularly interspaced short palindromic repeats)
CSE	- Cystathionine γ-lyase
CSF	- Cerebrospinal fluid
D2HG	- D-2-hydroxyglutarate
DCFDA	- 2',7'-dichlorodihydrofluorescein diacetate
ECAR	- Extracellular acidification rate
ETC	- Electron transport chain
GBM	- Glioblastoma
GCLC	- Glutamate—cysteine ligase catalytic subunit
GOBP	- Gene ontology biological process
GSC	- Glioma stem-like cell
GSH	- Glutathione
GSSG	- Glutathione disulfide
HIF1-α	- Hypoxia-inducible factor 1-alpha
HMDB	- Human metabolome database
IDH1m	- Isocitrate dehydrogenase 1 mutant
IDHwt	- Isocytrate dehydrogenase wild type
ICGC	- International Cancer Genome Consortium
KEGG	- Kyoto Encyclopedia of Genes and Genomes
LCMS	- Liquid chromatography - mass spectrometry
NADH	- Nicotinamide adenine dinucleotide
NADPH	- Nicotinamide adenine dinucleotide phosphate

NCT	- National Center for Tumor diseases
OCR	- Oxygen consumption rate
OD	- Oligodendroglioma
PAG	- Propargylglycine
PDC	- Patient-derived cell line
PDX	- Patient-derived xenograft
PPP	- Pentose phosphate pathway
Redox	- Reduction-oxidation
ROS	- Reactive oxygen species
SAM	- S-adenosymethionine
SAH	- S-aednosylhomocysteine
shRNA	- Short hairpin ribonucleic acid
sgRNA	- Single guide ribonucleic acid
TCGA	- The Cancer Genome Atlas
TP	- Transsulfuration pathway
XCT	- Cysteine/glutamate transporter

Summary

Diffuse gliomas are a group of central nervous system (CNS) tumors with a poor patient prognosis. Within these diffuse gliomas, isocitrate dehydrogenase (IDH) mutation defines the different tumor subtypes and is considered to be an initiating event in gliomagenesis. IDH is a metabolic enzyme that in normal conditions mediates the conversion of isocitrate into α-ketoglutarate (α-KG), producing the reducing equivalent NADPH. IDH mutation (IDHm) leads to a neomorphic reaction where α-KG is consumed to generate the oncometabolite D-2-hydroxyglutarate (D-2HG), using NADPH as reducing agent. It has been reported that IDHm-dependent D-2HG synthesis has a direct impact on DNA and histone methylation, however the metabolic repercussions are not yet well defined. Due to the consumption of NADPH by IDHm reaction, some groups including us have hypothesized that IDHm cells may bear an imbalance of reducing equivalents, that may trigger a defective antioxidant defense. In the present study we made use of patient-derived cell lines and xenografts thereof as well as clinical samples in order to study the metabolic vulnerabilities of IDHm gliomas.

In the first part of the thesis experimental data, we generated an integrative liquid chromatography-mass spectrometry (LCMS)-based proteomic-metabolomic characterization of IDHm metabolism. We made use of patients, cell lines and xenografts to address the direct effect of the mutation. We observed that IDHm gliomas have altered regulation of key processes in central carbon metabolism through glucose and glutamate processing as well as glutathione (GSH) metabolism and fatty acid production.

In the second part of experimental data, we investigated the redox vulnerabilities of IDHm gliomas. Here we discovered that IDHm astrocytomas specifically upregulate cystathionine-γ-lyase (CSE) enabling them to synthesize GSH independently of NADPH. CSE is the only known enzyme capable of synthesizing cysteine. We found that genetic and chemical inhibition of CSE led to a decrease in cell viability upon cysteine restriction. Finally inhibition of CSE *in vivo* led to a delay in tumor growth rate.

In conclusion, in the present PhD dissertation we expose a comprehensive study of the metabolic behavior of IDHm human gliomas, and we propose a novel therapeutic strategy that might improve patient prognosis, by inflicting oxidative damage to the tumor.

Contents

CHAPTER I. THEORETICAL FRAMEWORK

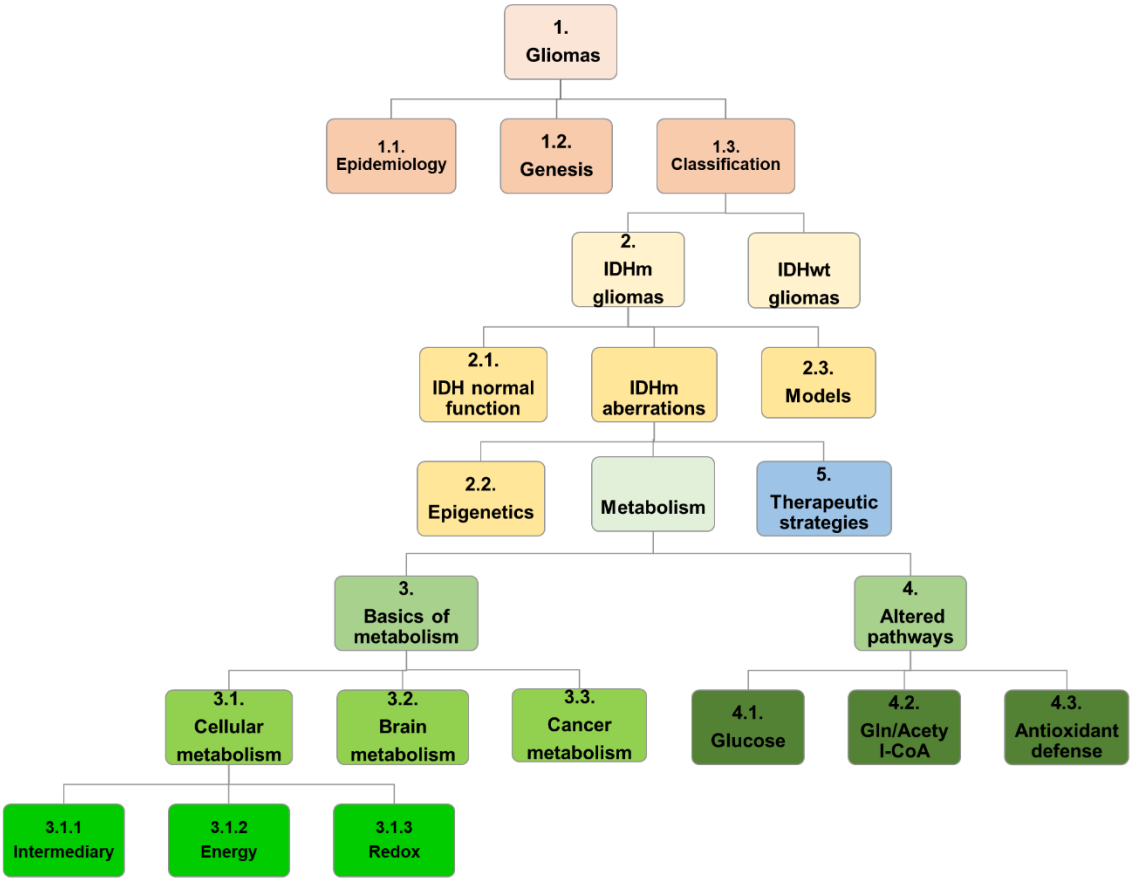

Organigram of theoretical framework. Schematic representation of the rationale behind the structure.

1. Gliomas

1.1. Epidemiology

Gliomas are commonly defined as malignant primary tumors of the glial tissue of the nervous system. Gliomas together with all the tumors of the central nervous system (CNS) correspond to a highly heterogeneous type of cancer. The Central Brain Tumor Registry of the United States (CBTRUS) is the largest population-based registry of tumors of the brain and CNS worldwide, and recently published a report containing age-adjusted data from 2012-2016 and presented per 100.000 population (Ostrom et al., 2019). According to CBTRUS, brain and other CNS tumors (both malignant and non-malignant) are the cancer type with highest incidence rate in 0-14 year old children population, being leukemia in second place. The incidence of CNS tumors decreases at older ages, been the third most common cancer type after breast and thyroid in 15-39 years old population. Finally in older adults, at age >40 years, these tumors are the eighth cancer type in incidence, being prostate and breast the two most common (**Figure 1**). It is important to clarify that overall cancer occurrence increases with age. Therefore, although the incidence of CNS tumors over total cancer is higher in younger patients, the absolute incidence of this cancer type is yet higher in eldest patients. With regard to mortality rate, CNS tumors contribute as the top reason for cancer mortality in children of age 0-14 years at death. Among persons age 15-39 years CNS tumors were the second most common cause of cancer death and for older population of age >40 years this cancer type rises up to thirteenth in death rate position. Similarly as before, although CNS tumors are the top cancer-relative mortality for youngest patients, the absolute mortality is still higher for eldest patients.

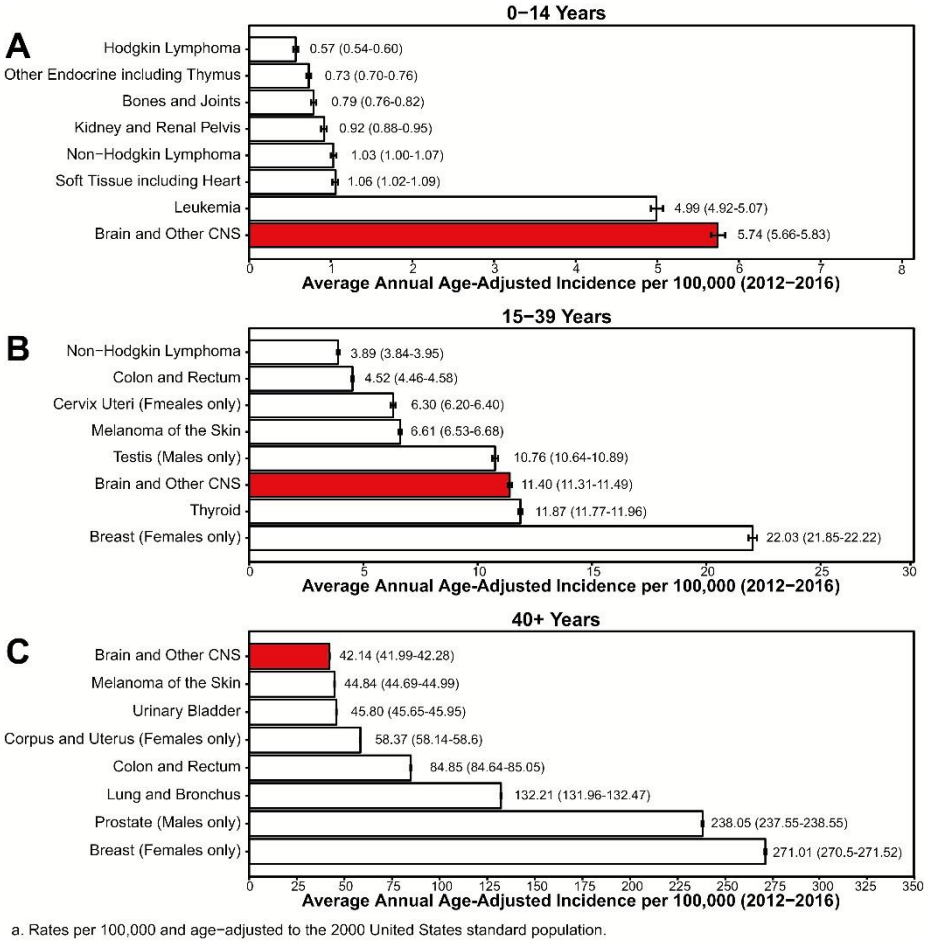

a. Rates per 100,000 and age–adjusted to the 2000 United States standard population.

Figure 1. Annual average age-adjusted incidence rates of all CNS tumors in comparison to other common cancers in the US.
A. Children at age 0-14 years. B. Adolescents and young adults at age 15-39 years, and C. older adults at age 40+ years, CBTRUS statistical report: US Cancer Statistics - NPCR and SEER 2012–2016 (Ostrom et al., 2019).

When considering all the CNS tumors, CBTRUS accounts malignant ones to 30.2% of the cases, however gliomas correspond to the majority of all these cases, been only 1.1% of the total CNS tumors non-malignant gliomas (**Figure 2**). The most common tumor type of all the ones of the CNS is the non-malignant meningioma (37.2%) and the most common of the malignant cases is glioblastoma (14.6%), the most aggressive subtype of all gliomas and CNS tumors (**Figure 2**).

Indeed, glioblastomas together with astrocytomas (5.1%) and oligodendrogliomas (1.3%) correspond to the so-called diffuse glioma group, the deadliest group of gliomas and CNS tumors (Ostrom et al., 2019). The detailed histological and molecular classification of diffuse

gliomas according to the up-to-date regulation of the World Health Organization (WHO) (Louis et al., 2016b) is forthcoming discussed in section 1.3. Other important malignant non-glioma CNS tumors, which account to 5.4% over the total (**Figure 2**), include choroid plexus tumors, neuronal and mixed neuronal-glial tumors, tumors of the pineal region, embryonal tumors, tumors of the pituitary, craniopharyngiomas or nerve sheath tumors, among others.

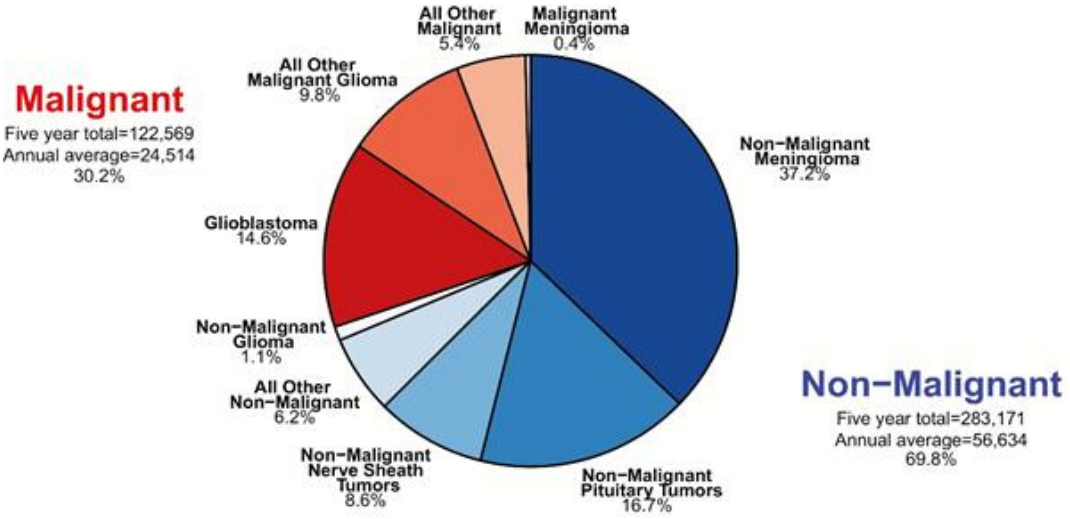

Figure 2. Distribution of CNS tumors by behavior and histology.
Rates for selected sub-types (where there is a sufficient number of cases to calculate rates). CBTRUS statistical report: US Cancer Statistics - NPCR and SEER 2012–2016 (Ostrom et al., 2019).

Time trends are important to understand the progression of cancer impact in the society, however it is worth considering that many factors can fluctuate time trend rates and not be related with real changes in incidence of these tumors e.g. demographic changes, changes in classification or changes in registration procedures. In cancer overall incidence rates have decreased over time (McCarthy et al., 2013). Regarding to malignant brain and other CNS tumors, between 2000 and 2016, CBTRUS has registered a small but statistically significant decrease of incidence. However, there has been an increase in incidence of these tumors in children at age 0-14 years. Moreover, the annual incidence rate of malignant tumors has always been higher that of non-malignant ones in children at 0-14 years (since the beginning of non-malignant registration procedures started, in 2004), whereas all the older ages experience the opposite trend (**Figure 3**).

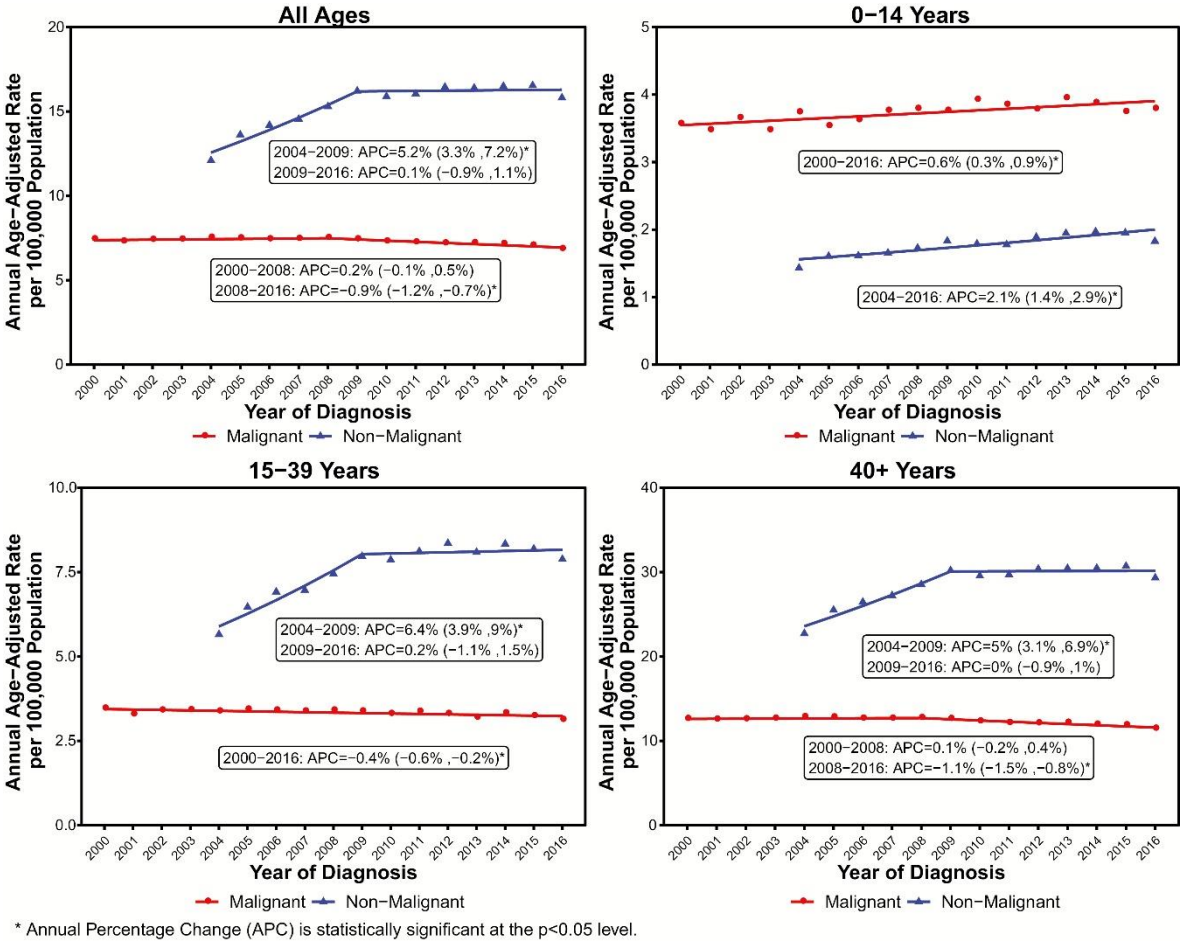

Figure 3. Annual age-adjusted incidence rates of CNS tumors and incidence trends between 2000 and 2016, ordered by behavior and age group.
CBTRUS statistical report: US Cancer Statistics - NPCR and SEER 2000–2016 (Ostrom et al., 2019).

In synthesis, this study reflects that although cancer overall is a disease far more prevalent in eldest population, the high incidence and mortality of CNS tumors in children and young adults when relative to other cancer types highlights its relevance in youngest patient sector. Thus, the study and understanding of glioma carcinogenesis is a crucial milestone to overcome for the future of our society. Before analyzing the detailed classification of CNS tumors, we will first address the definition of glial cells and its link with the genesis of gliomas.

1.2. Gliomagenesis

The origin of gliomas represents nowadays a controversial research area. It is not clear whether these tumors arise from differentiated glial cells or neural precursor cells since there is experimental evidence supporting both. Yet, gliomagenesis is likely linked to intrinsic plasticity rather than cancer stem cell (CSC) multipotency (Laug et al., 2018, Dirkse et al., 2019, Neftel et al., 2019).

Neuroglia. Glial cells, also known as neuroglia, are non-synaptic nervous cells with different functions of support of neural tissue. There exist different types of glia in both central nervous system (CNS) and peripheral nervous system (PNS), with astrocytes and oligodendrocytes being the two most prevalent in the CNS (**Figure 4**).

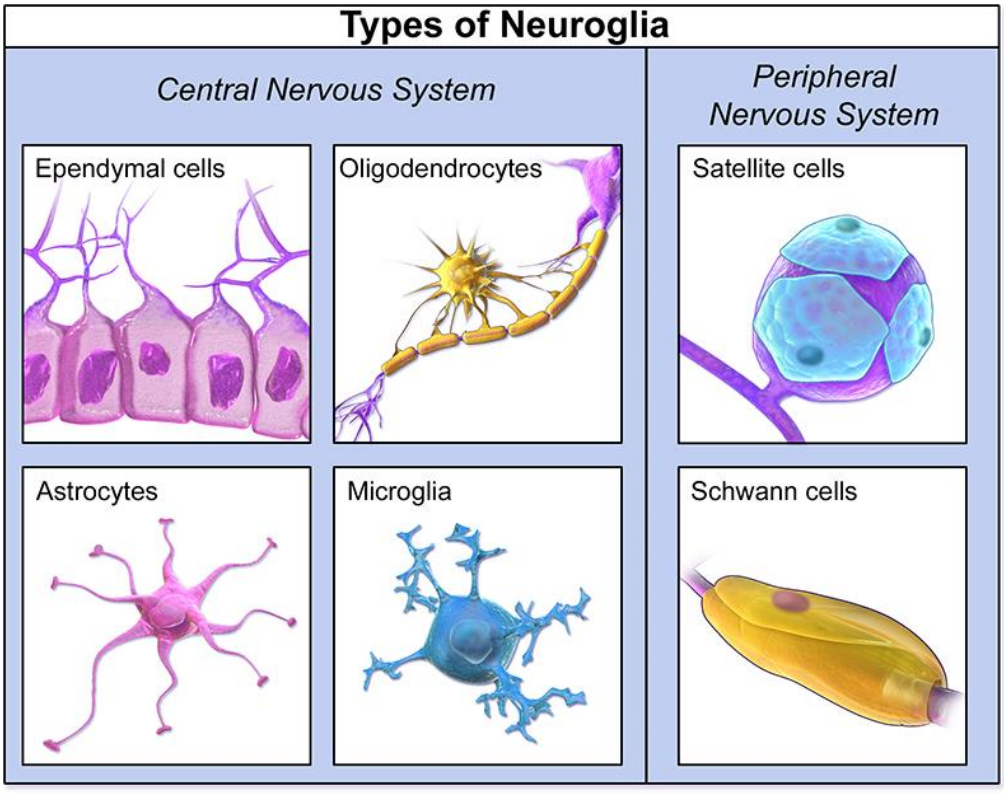

Figure 4. Different types of neuroglia.
Used from https://qbi.uq.edu.au/brain-basics/brain/brain-physiology/types-glia

Astrocytes are star-shaped cells which represent the most abundant glial cell type in the CNS. Astrocytes have different functions such as provision of nutrients to neurons, formation of the blood-brain barrier (BBB), buffering neurotransmitter levels or formation of synapses (Molofsky and Deneen, 2015). A detailed explanation on the metabolic interactions of astrocytes within the CNS will be forthcoming discussed in section 3.2. Oligodendrocytes are cells in charge of the myelination of neuronal axons in the CNS. The myelin sheath formed by these cells provides insulation across the axon and is essential for saltatory nerve conduction (Baumann and Pham-Dinh, 2001) (**Figure 5**).

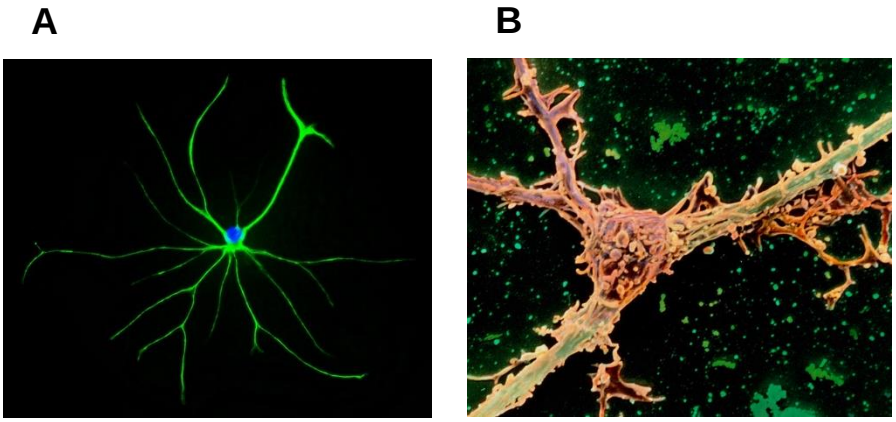

Figure 5. Glial cells.
A. Immunopanning imaging of an astrocyte from a rat pup. Used from (Landhuis, 2018). **B**. Scanning electron microscope (SEM) imaging of an oligodendrocyte ensheathing an axon. Used from Dr John Zajicek/science Photo Library, fineartamerica.com

Origin of gliomas. Diffuse gliomas are amongst the most common glioma subtype and bear the worst patient prognosis. The three main categories of diffuse gliomas are oligodendrogliomas, astrocytomas and glioblastomas (Louis et al., 2016b). As suggested by their names, oligodendrogliomas and astrocytomas share histological features with their natural counterpart cell types. In addition, astrocytomas can as well give rise to secondary glioblastoma (Laug et al., 2018). As noted previously, the exact mechanism behind gliomagenesis is yet unknown. Different perspectives have been considered in an attempt to understand how gliomas are originated. Some studies are currently investigating the link between neural stem and cancer stem cells and gliomagenesis. According to these, certain

molecular factors which are essential in glial differentiation (e.g. NFIA, Sox9), have also been found to play important roles in tumorigenesis (Glasgow et al., 2013, Glasgow et al., 2017).

On the other hand, other groups argue that differentiated glial cells may bear an advanced grade of plasticity that in some cases enable them to undergo malignancy and initiate tumorigenesis. In fact, the hypothesis of cancer stem cell (CSC) as driver of tumor initiation is contradicted by the observation that glioma cells expressing CSC associated cell membrane markers do not represent a clonal entity with distinct functional properties, but rather a plastic state that can be adopted by any cancer cell (Dirkse et al., 2019, Neftel et al., 2019).

An important breakthrough with regard to gliomagenic aberrations, was the discovery of a point mutation in the enzyme isocitrate dehydrogenase (IDH) during early stages of tumorigenesis (Parsons et al., 2008). In fact, recent large-scale sequencing studies demonstrated that IDH mutation may be linked to the acquisition of a variety of tertiary alterations related with tumor progression including PI3k/Akt, K-ras, PDGFRA, Met and n-Myc pathways (Bai et al., 2016, Brat et al., 2015). The direct implications of IDH mutation in tumorigenesis and epigenetic reprogramming will be discussed in section 2.2. Before that, we will first review the specific classification of the different glioma subtypes, in which IDH plays a central role.

1.3. Glioma classification

As we have already introduced there is not just a unique type of glioma. In fact, during the past decades there has been a constant refinement and evolution of glioma classification. At the onset of glioma research, the first grouping variables were based on histological features observed through different microscopic techniques, such as hematoxylin-eosin staining, immunohistochemistry or ultrastructural characterization (**Figure 6**). With the beginning of the present millennium, the exponential development of molecular based studies has revealed a new step on the classification of the tumors of the central nervous system. Although within the previous World Health Organization (WHO) Classification of Tumors of the Central Nervous

System (2007 CNS WHO) some of these molecular findings were already mentioned (Louis et al., 2007), it was not until the most recent report (2016 CNS WHO) that these parameters have been fully integrated (Louis et al., 2016a).

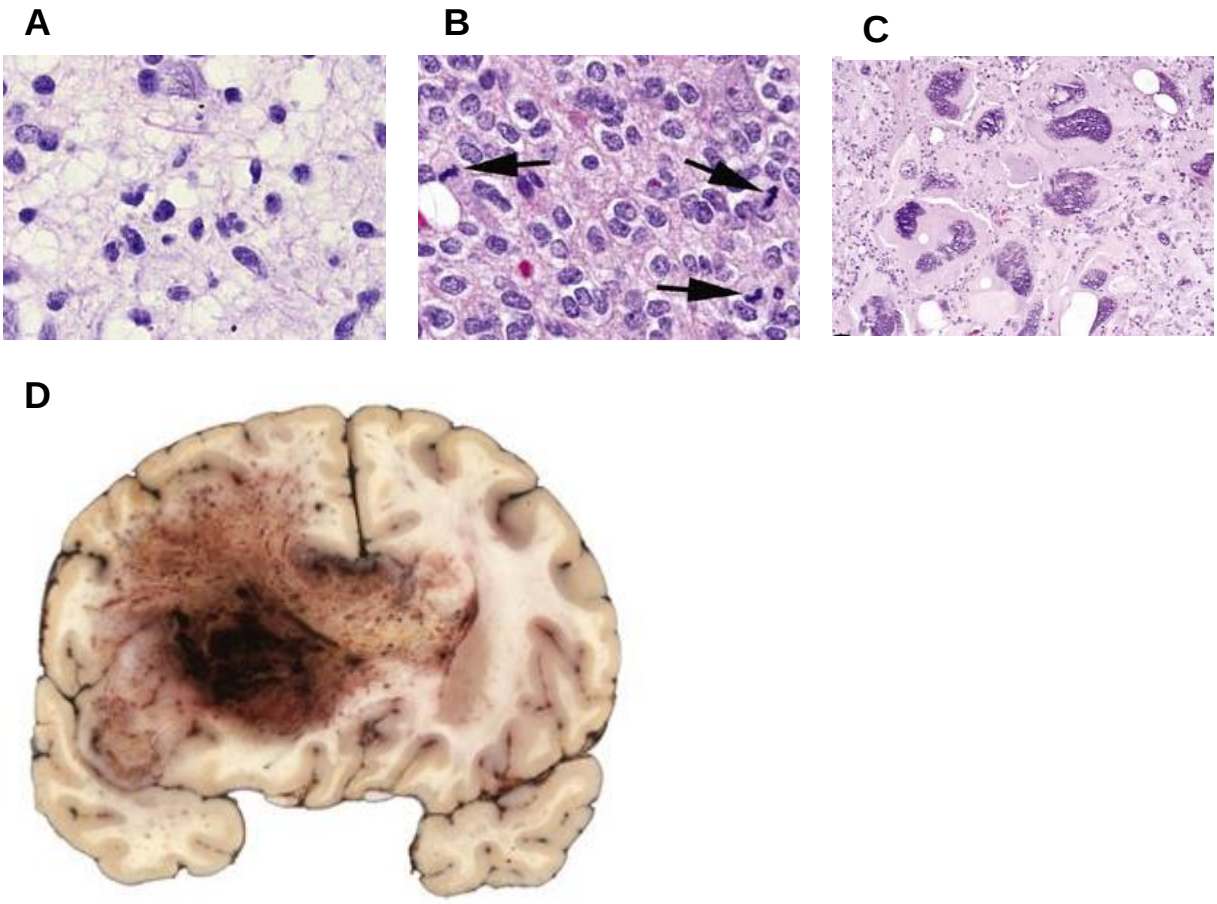

Figure 6. Histological classification of gliomas.
Microscopic hematoxylin and eosin (H&E) staining of **A.** Astrocytoma. Cells with hyperchromasia (intensely stained nuclei) and irregular contours. **B.** Oligodendroglioma. Cells typically show increased mitotic activity (arrows). **C.** Glioblastoma. Large, highly pleomorphic and multinucleated cells. Adapted from (Perry and Wesseling, 2016). **D.** Coronal brain section of glioblastoma tumor showing necrotic core with hemorrhages (PubCan, 2014).

To update the new CNS WHO report an international collaboration of 35 neuropathologists, neuro-oncological clinical advisors and scientists from 10 countries during a three-day conference held in 2014 in Haarlem, the Netherlands, established the guidelines for how to incorporate molecular findings into brain tumor diagnoses. Therefore, the new standards stipulate that each glioma subtype may be classified taking into account both the original

histological phenotype and the specific genotypic signature altogether. In case of discordant results, the genotype trumps the histological phenotype.

The classical WHO grading system of CNS tumors (Burger, 1995) is also included in the 2016 CNS WHO. With this regard, grade I corresponds to slow-growing tumors, non-malignant and associated with long-term survival; grade II are relatively slow-growing tumors that can recur as higher grade tumors and can be malignant or non-malignant; grade III are always malignant tumors that often recur as higher grade; grade IV tumors reproduce rapidly and are very aggressive malignant tumors.

Diffuse glioma, the most frequent and aggressive type of CNS tumors, include astrocytomas, oligodendrogliomas and glioblastoma. Commonly, astrocytomas and oligodendrogliomas represent grade II or III tumors, therefore are also known as low grade gliomas (LGG). On the other hand, glioblastomas are commonly grade IV, and known as high grade gliomas (HGG). The most relevant update on gliomas in the new 2016 CNS WHO is indeed within these diffuse gliomas. Currently, all diffusely infiltrating gliomas are classified based on point mutations in the isocitrate dehydrogenase 1 (IDH1) or isocitrate dehydrogenase 2 (IDH2) genes. Thus, in this new classification IDH mutation define astrocytomas, oligodendrogliomas, whereas IDHwt genotype define primary glioblastoma (**Figure 7**). Furthermore, in order to differentiate IDH mutant oligodendroglioma from IDH mutant astrocytoma there are other established molecular markers. The most consensual one is the presence of a 1p/19q chromosomal co-deletion in the oligodendroglial tumors. As a complementary testing, although not required for diagnosis, the ATRX loss and TP53 mutation are specific markers in astrocytoma (**Figure 7**). With regard to glioblastomas, around 90% of the tumors are IDH wild type which corresponds most frequently with the clinically defined primary glioblastoma and predominates in patients over 55 years of age. The rest of glioblastomas correspond to so-called secondary glioblastoma which bear the IDH mutation since it arises from prior lower grade astrocytoma, frequently observed in younger patients (Ohgaki and Kleihues, 2013).

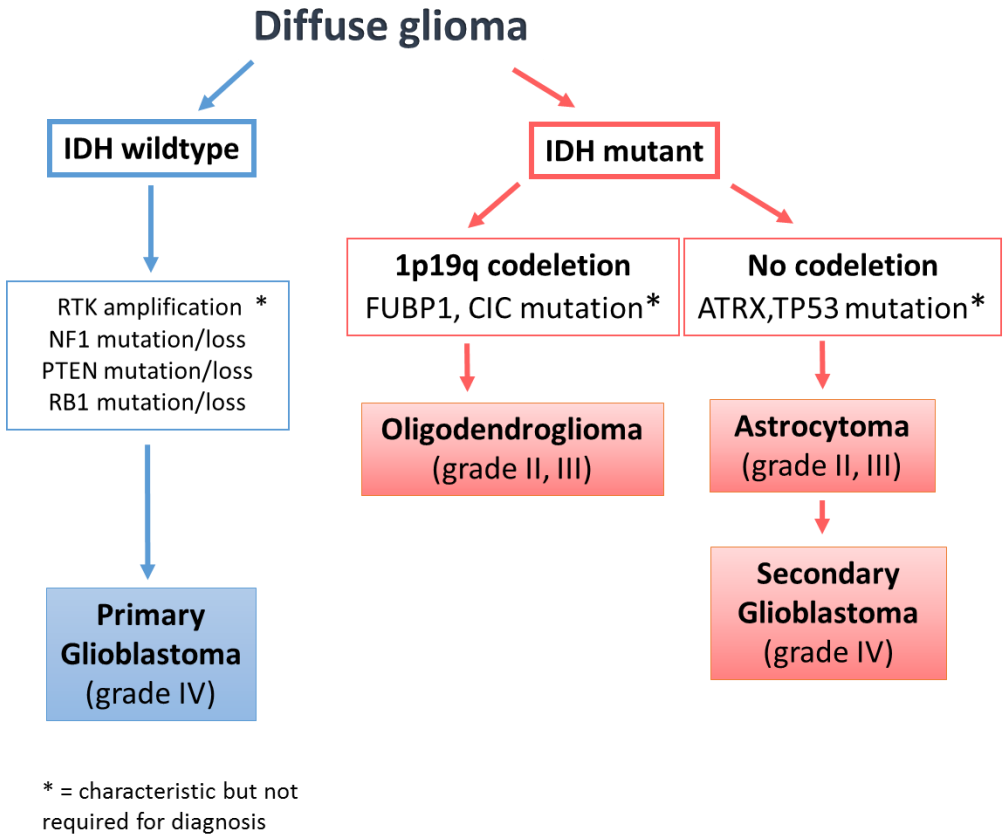

Figure 7. **Molecular classification of diffuse gliomas.**
Schematic algorithm for classification of diffuse gliomas combining both histological and genetic characteristics.

Each specific molecular subtype of diffuse glioma bear different clinical outcomes (**Figure 8**). IDHwt glioblastoma (GBM) is the most aggressive glioma type with an average survival time of 12-18 months. Only 25% of patients survive more than one year and 5% more than five years. IDHm gliomas are associated with a better patient prognosis when compared to GBM, although yet averaging a poor survival time of 7 years (Claus et al., 2015). Within IDHm gliomas the different life expectancy is as well disparate. Whereas IDHm 1p/19q codeleted gliomas (i.e. oligodendrogliomas) show a 80% of 5-year survival rate, this number decays down to 50% in the case of IDHm non-codeleted gliomas (i.e. astrocytomas) (Ostrom et al., 2019).

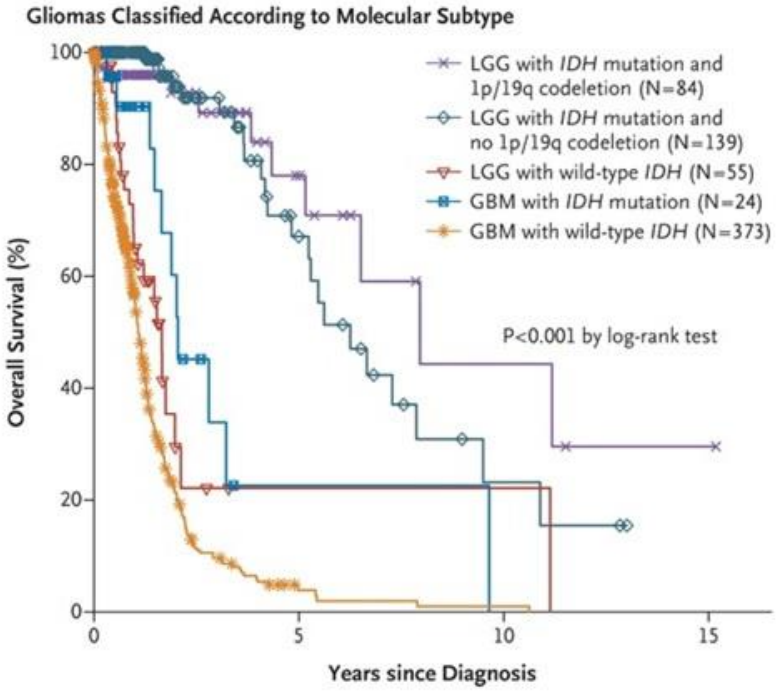

Figure 8. Overall survival time of glioma patients.
Kaplan-Meier estimates of overall survival among patients with different gliomas classified according to molecular subtype. Used from (Brat et al., 2015). LGG: Low grade glioma; GBM: glioblastoma.

Table 1 summarizes the main classification and epidemiologic features of the three most relevant types of gliomas (glioblastoma, astrocytoma and oligodendroglioma).

Table 1. Summary of genetic characteristics of diffuse gliomas.
All data is based on (Ostrom et al., 2019), except IDHm % (Yan et al., 2009). GBM: glioblastoma, AS: astrocytoma, OD: oligodendroglioma, HGG: high grade glioma, LGG: low grade glioma. * considering both primary and secondary glioblastomas.

Glioma subtype	Grade	IDHm (% over total cases)	1p/19q codeletion	Median age	Incidence over all malignant CNS tumors (%)	5-year survival rate (%)
GBM	HGG	13*	No	65	48.3	6.8
AS	LGG	90	No	47	5.9	51.6
OD	LGG	85	Yes	43	2.9	82.7

Improving classification based on molecular profiling. In order to develop a more accurate pathological diagnosis and improve clinical outcome of glioma patients some recent studies have shown notable advances in the molecular profiling of gliomas. In a study of 1,122 diffuse grade II-III-IV gliomas it was integrated new parameters of classification such as DNA methylation patterns or telomere length correlating with the official CNS WHO groups (Ceccarelli et al., 2016). In this study they analyzed six different cytosine-phosphate-guanine (CpG) island methylation clusters (LGm1-6) and compared its presence in both IDHm and IDHwt glioma sub-groups. They observed that the methylation clusters associated with genome-wide hypermethylation (LGm1/LGm2/LGm3) were enriched in IDH mutant tumors, documenting the association between IDH mutation and increased DNA methylation (Noushmehr et al., 2010, Turcan et al., 2012). In fact, profound analysis of different CpG status in tumors lead to the observation that IDH1m 1p/19q intact gliomas (i.e. astrocytomas), can be subsequently divided in Glioma-CpG island methylator phenotype (G-CIMP) high and G-CIMP low tumors, further refining glioma classification (Ceccarelli et al., 2016). Moreover, a recent study on the approximately 100 different CNS tumor entities shows a comprehensive approach for DNA methylation-based classification and demonstrates its application in a routine diagnostic setting (Capper et al., 2018). These studies lay the groundwork of DNA-methylation as a blueprint for the future of CNS tumors classification, where IDH mutation play a pivotal

role. In section 2 we will describe its DNA and histone methylation and other epigenetic repercussions associated with IDH mutation.

Besides the methylation factors, different important signaling pathways have been shown to be altered in glioma tumors, promoting tumor malignancy and aggressiveness. Whether these pathways occur in parallel or in later steps of tumorigenesis has not yet been clarified (Laug et al., 2018). As aforementioned, besides IDH mutation, loss or mutation of *ATRX* and *TP53* are among the most common molecular aberrations in astrocytomas (Ceccarelli et al., 2016). *TP53* signaling, plays a key role in several cellular processes including cell cycle, cell differentiation, and neovascularization. In fact, this pathway is found to be mutated not only in astrocytomas but also in secondary GBM (Bögler et al., 1995). Oligodendrogliomas, known for their 1p/19q chromosomal co-deletion as well as IDH mutation, bear commonly wild type expression of *ATRX* and *TP53*. However, these tumors usually present *TERT* mutation, an alteration also observed in the majority IDHwt GBM (Ceccarelli et al., 2016). Indeed, within GBM group, the diverse signaling pathways involved in malignancy have been more extensively studied. Among these pathways EGFR signaling plays a key role in primary GBM development (**Figure 9**). The overexpression of EGFR through amplification of the *EGFR* gene initiates a molecular cascade that involves PI3K and PIP3 and activates Akt and mTOR pathways, resulting in cell proliferation and increased cell survival by stimulating energetic and biosynthetic metabolism and blocking apoptosis. PTEN, which normally stops this cascade by inhibiting PIP3 signal, is mutated in most of these primary GBM (Mellinghoff et al., 2005) (**Figure 9**). Interestingly, PI3K/Akt cascade seems to be inhibited by IDH1 mutation (Birner et al., 2014). Moreover, $P16^{INK4a}$/RB1 pathway is important in both primary and secondary GBM. These tumors commonly bear $P16^{INK4a}$ deletion or promoter methylation, what impedes to enter in cell cycle arrest due to the over activation of cyclin D family and RB1 protein phosphorylation (Ohgaki and Kleihues, 2007) (**Figure 9**).

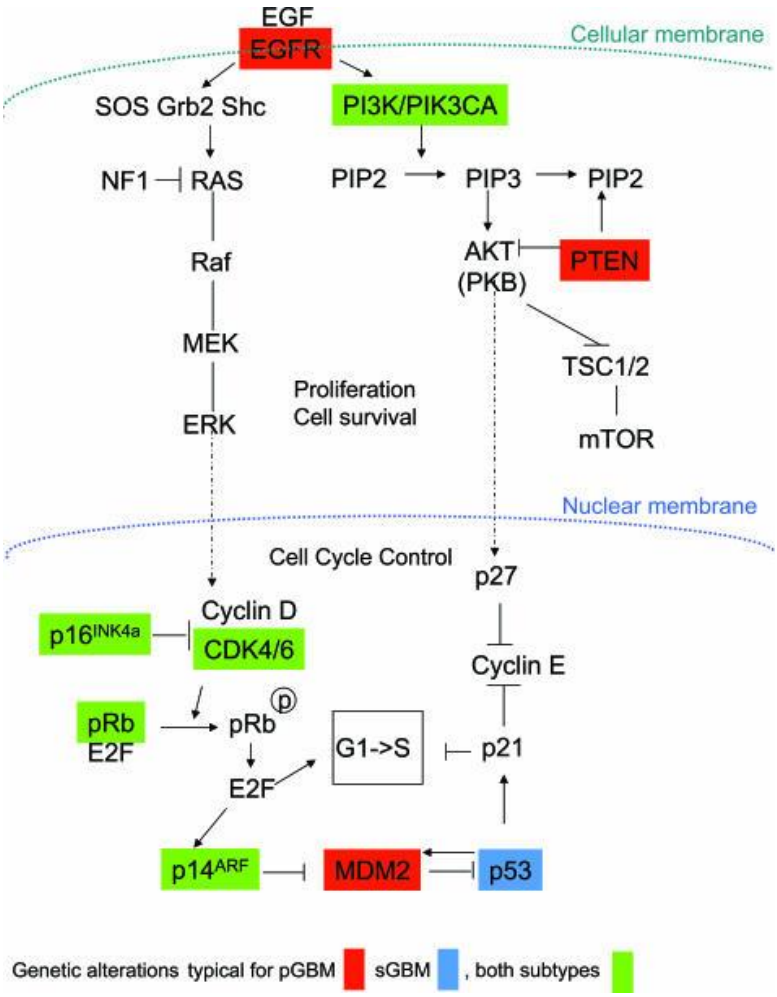

Figure 9. Major signaling pathways involved in glioblastoma malignancy.
Pathways highlighted in red are common for pGBM (primary glioblastoma), in blue for sGBM (secondary glioblastoma, and astrocytomas) and in green for both subtypes. Used from (Ohgaki and Kleihues, 2007)

2. Isocitrate dehydrogenase

Isocitrate dehydrogenase (IDH) enzymes are essential in several major metabolic processes, such as tricarboxylic acid (TCA) cycle, lipogenesis, glutamine metabolism or reduction-oxidation (redox) regulation (Lee et al., 2002, Badur et al., 2018). There exist three different isoforms of IDH. While mutations in IDH1 and IDH2 lead to a carcinogenic gain-of-function (i.e. neomorphic allele), IDH3 mutations have not been reported in cancer. Besides gliomas, IDH mutations are also found in acute myeloid leukemia (AML; 16% of all clinical cases), intrahepatic cholangiocarcinoma (23%) and central/periostal chondrosarcoma (56%) (Han et al., 2020). Thus, the study and comprehension of the role in tumor malignancy of this frequent mutation is nowadays one of the main goals in the field of cancer, and especially of glioma research, aiming to improve the clinical outcome of patients. In order to understand the molecular mechanisms derived from the mutation in IDH we will first analyze the physiological roles of these enzymes.

2.1. IDH structure and function

IDH1 is located in the cytoplasm and cell peroxisomes while IDH2 and IDH3 are present in the mitochondria (Leighton et al., 1969). Yet, *IDH1* and *IDH2*, presenting 70% of gene sequence similarity in humans (Waitkus et al., 2016), bear a more comparable structure and function. *IDH1* gene is present on 2q33.3 chromosomal region and *IDH2* gene on 15q26.1. Both enzymes are homodimers that catalyze the reversible oxidative decarboxylation of isocitrate to α-ketoglutarate (α-KG). They have one active site per monomer with affinity to a divalent metal cation (e.g. calcium or magnesium) and to nicotinamide adenine dinucleotide phosphate ($NADP^+$). The reaction leads to reduction of $NADP^+$ to NADPH liberating CO_2 (Stoddard et al., 1993) (**Figure 10A**). Individual IDH subunits contain a large domain, a small domain and a clasp domain (**Figure 10B**), and IDH2 has an additional mitochondrial targeting sequence. The catalytic activity involves the binding of $NADP^+$ cofactor in an inactive open conformation

characterized by a regulatory loop segment involving the residue Ser^{94} of the large domain. Isocitrate binding displaces the regulatory loop by its interaction with residues of both dimer subunits, including Ser^{94} and multiple conserved arginines in the active site (**Figure 10C**). Isocitrate interaction induces a conformational change to a closed catalytically active state that promotes decarboxylation of isocitrate into α-KG (Xu et al., 2004).

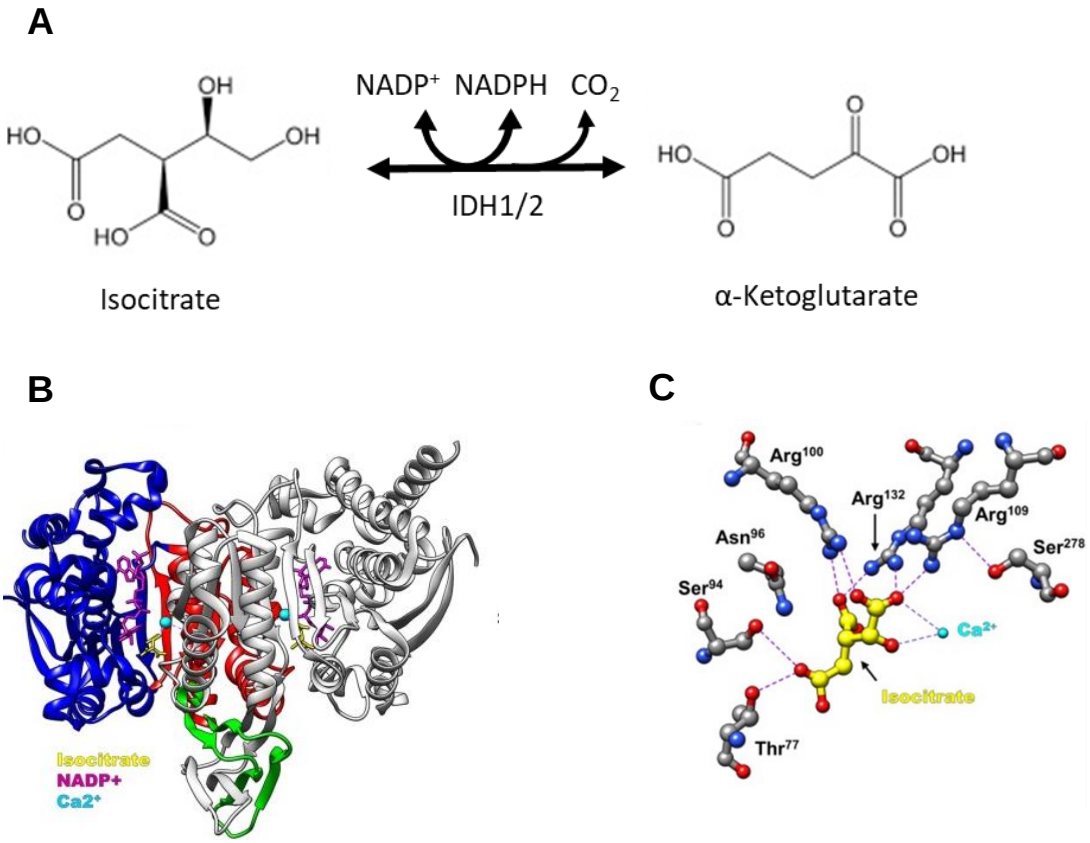

Figure 10. IDH1/2 reaction and structure.
A. Reversible oxidative decarboxylation of isocitrate to generate α-ketoglutarate (α-KG) using $NADP^+$ and producing NADPH and CO_2. **B.** Crystal structure of IDH1 homodimer. Each monomer is composed by a large domain (blue), small domain (red) and clasp domain (green). Only one monomer is colored for clarity. The substrate binding pocket contains isocitrate (yellow), calcium (blue) and $NADP^+$ (purple). Used from (Waitkus et al., 2016). **C**. Residue interaction in IDH1 active site. Hydrophilic interactions between active site residues, cofactor (Ca^{2+}) and substrate (isocitrate) are depicted as dashed lines. Used from (Waitkus et al., 2016).

On the other hand, IDH3 is an evolutionary distinct multisubunit complex composed of 3 proteins encoded by different genes. It is conformed as a heterotetramer with two α-subunits

encoded by IDH3A gene on 15q25.1-q25.2, one β-subunit encoded by IDH3B on 20p13, and one γ-subunit encoded by IDH3G on Xq28. The α-subunits are catalytic and β, γ-subunits are regulatory (Ramachandran and Colman, 1980). Unlike its homologous counterparts, IDH3 is nicotinamide adenine dinucleotide (NAD)-dependent and is in charge of the conversion of isocitrate to α-KG while generating NADH, a central reaction in the tricarboxylic acid (TCA) cycle. The high negative free energy change during mitochondrial isocitrate to α-KG conversion and the increased number of regulatory domains make IDH3 reaction virtually irreversible (Ramachandran and Colman, 1980). The α-KG generated by IDH3 continues being metabolized within the TCA cycle and the NADH is used as electron donor in the electron transport chain (ETC) to generate ATP in the process of oxidative phosphorylation. This IDH isoform is regulated by substrate availability and cell requirements: whereas calcium, ADP and citrate activates it, ATP and NADH inhibit its activity (Gabriel et al., 1986). Therefore, when there is high NADH/NAD ratio due to high energy levels or there is increased α-KG due to high production from secondary sources (e.g. glutamate and glutamine), mitochondrial isocitrate will increase due to IDH3 inhibition (Al-Khallaf, 2017). Some isocitrate molecules will be then consumed by IDH2 within the mitochondria in order to generate NADPH, which is used as reducing power for antioxidant synthesis such as glutathione (GSH) (Dickinson and Forman, 2002). Other isocitrate molecules may be converted back to citrate by mitochondrial aconitase (ACO) and subsequently transported to the cytosol where can be used to produce acetyl-CoA by ATP-citrate lyase (ACL) or to generate cytoplasmic NADPH by IDH1 (Srere, 1959) (**Figure 11**). Both cytosolic acetyl-CoA and NADPH are required in lipogenesis. The α-KG that is not processed in the TCA cycle or biosynthetic pathways, will act as cofactor for dioxygenases. There are more than 60 different α-KG-dependent dioxigenases in humans and they are associated with DNA and histone demethylation, HIF-1α degradation and collagen folding and maturation (Ohba and Hirose, 2016).

The reverse reaction carried out by IDH1 and 2 of reductive carboxylation of α-KG to isocitrate, may be as important as the forward one. Reductive carboxylation, which leads to NADPH and

CO_2 consumption, largely depends on the relative K_m values of forward/reverse reactions as well as the relative levels of isocitrate, α-KG or NADPH within the cell (Lemons et al., 2010).

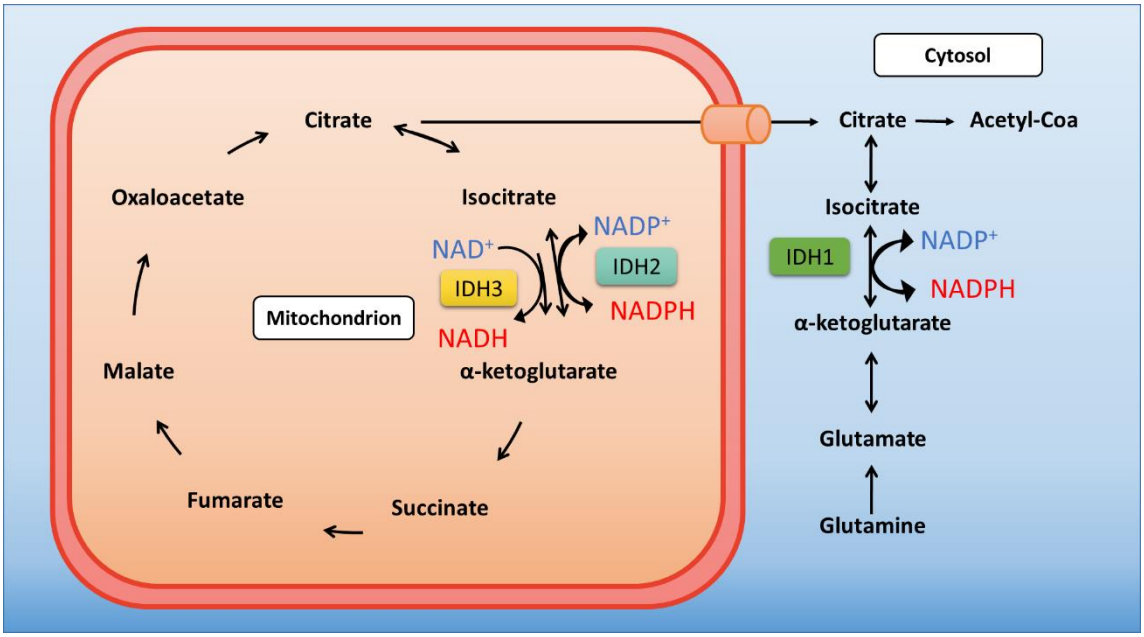

Figure 11. IDH isoforms and their role and localization. IDH3 is in charge of α-KG and NADH production in the mitochondrial TCA cycle. IDH2 (mitochondrial) and IDH1 (cytosolic) are both NADP-dependent enzymes with roles in different biosynthesis pathways.

In summary, IDH1 and IDH2 are in charge of regulation of synthetic pathways when energy levels are high enough to keep IDH3 inhibited, enabling to redirect isocitrate or α-KG out of the TCA cycle (Al-Khallaf, 2017). From a physiological perspective, the roles of IDH1/2 enzymes are thought to have a crucial impact in human metabolic regulation. Indeed, IDH represents the major NADPH source in various tissues, together with the pentose phosphate pathway (PPP). Depending on the tissue, the importance of IDH over PPP for NADPH synthesis will vary, e.g. IDH is the main producer of this reducing agent within the human brain (Atai et al., 2011). Diverse studies point to a key impact of IDH1/2 in oxidative stress defense. It has been shown that NADPH production via IDH1/2 has a direct effect in the protection against replicative senescence by reducing oxidative DNA damage and lipid peroxidation in cell culture (Lee et al., 2002, Kil et al., 2006). Consistent with an antioxidant function of IDH, other studies

show how its NADPH-producing activity protects against UVB-induced phototoxicity (Jo et al., 2002), reduces reactive oxygen species (Kim and Park, 2003) and limits ischemia-reperfusion injury in the kidney (Kim et al., 2009, Kim et al., 2011). IDH1 has been also probed to display an important lipogenic role. During hypoxia, IDH1 reverse reaction of α-KG to isocitrate reductive carboxylation is stimulated in order to increase the cytosolic acetyl-CoA pool for lipid synthesis (Metallo et al., 2011). Overexpression of liver and adipose IDH1 leads to diverse metabolic diseases such as obesity, hyperlipidemia and fatty liver in transgenic mice (Koh et al., 2004). Within the CNS, IDH1 has shown to regulate phospholipid metabolism in astrocytes of developing mice (Bogdanovic et al., 2014). Regarding IDH2, the reductive carboxylation of α-KG has also been shown to promote synthesis of lipids by reductive glutamine metabolism (Ward et al., 2010). In addition, it has been shown how mitochondrial IDH2/3 regulate glucose-stimulated insulin secretion in pancreatic cells (MacDonald et al., 2013).

2.2. IDH mutation and epigenetic reprogramming

The contribution of IDH in multiple biochemical pathways makes the study of IDH mutation in cancer highly relevant for the understanding of the disease. Nevertheless, before discussing in section 4 all the diverse effects in glioma metabolism that IDH mutation may inflict, we will first address the different repercussions of this mutation in epigenetic reprogramming, an extensively studied mechanism in the field of IDH mutant tumors.

IDH mutation. IDH mutations are universally missense substitutions and tend to occur in the arginine residue on the active site. Missense mutations in *IDH1/2* genes result in the replacement of a strong positively charged residue such as arginine (R) with a lower-polarity amino acid such as histidine (H), lysine (K) or cysteine (C). In IDH1, the most common missense is from the arginine in position 132 (Arg^{132}) for a histidine (R132H). IDH2 mutations occur at Arg^{172}, the analogous residue to IDH1 Arg^{132}, and are most commonly substituted by a lysine (K) (R172K) (**Table 2**) (Ward et al., 2012). IDH1 Arg^{132} and IDH2 Arg^{172} are

evolutionary conserved residues that participate in isocitrate binding in the catalytic pocket (**Figure 10C**).

Table 2. Frequency of each specific IDH mutation in glioma patients according to (Yan et al., 2009, Hartmann et al., 2009). In the mutation nomenclature c refers to change of a DNA base, the number of the base that is changed, the original base and the new substituted base.

Gene	Mutation	Amino Acid Change	Frequency (%)
IDH1	c.395G.A	R132H	83.5–88.9
	c.394C.T	R132C	3.9–4.1
	c.394C.A	R132S	1.5–2.4
	c.394C.G	R132G	0.6–1.3
	c.395G.T	R132L	0.3–4.1
IDH2	c.515G.A	R172K	2.4–2.7
	c.515G.T	R172M	0.8–1.8
	c.514A.T	R172W	0.0–0.7
	c.514A.G	R172G	0.0–1.2

The substitution from a high positively-charged amino acid to a low polar one impedes the formation of hydrogen bonds with the α-carboxyl and β-carboxyl groups of isocitrate, which translates in a loss of affinity for isocitrate and an elevated preference for α-KG. This substrate affinity switch triggers a gain-of-function activity which leads to the reduction of α-KG to produce the metabolite D-2-hydroxyglutarate (D-2HG). Due to the reductive nature of this neomorphic activity, mutant IDH will consume NADPH (**Figure 12A**), unlike for the oxidative wildtype reaction where $NADP^+$ is required (Dang et al., 2009b).

Nevertheless, this being a heterozygous mutation, only one copy of *IDH* gene is mutated in these tumors, resulting in the protein translation of a heterodimer that contains an IDH wildtype (IDHwt) and an IDH mutant (IDHm) subunit. As a result, the IDHwt monomer produces α-KG from isocitrate generating NADPH whereas the IDHm monomer consumes both the α-KG and NADPH to generate D-2HG. Biochemical studies indicate that a homodimer formed by two IDHm subunits is catalytically inactive (Han et al., 2020) (**Figure 12B**). This mutation can occur

in either IDH1 or IDH2 and only very rare cases showed both mutations at the same time (Hartmann et al., 2009).

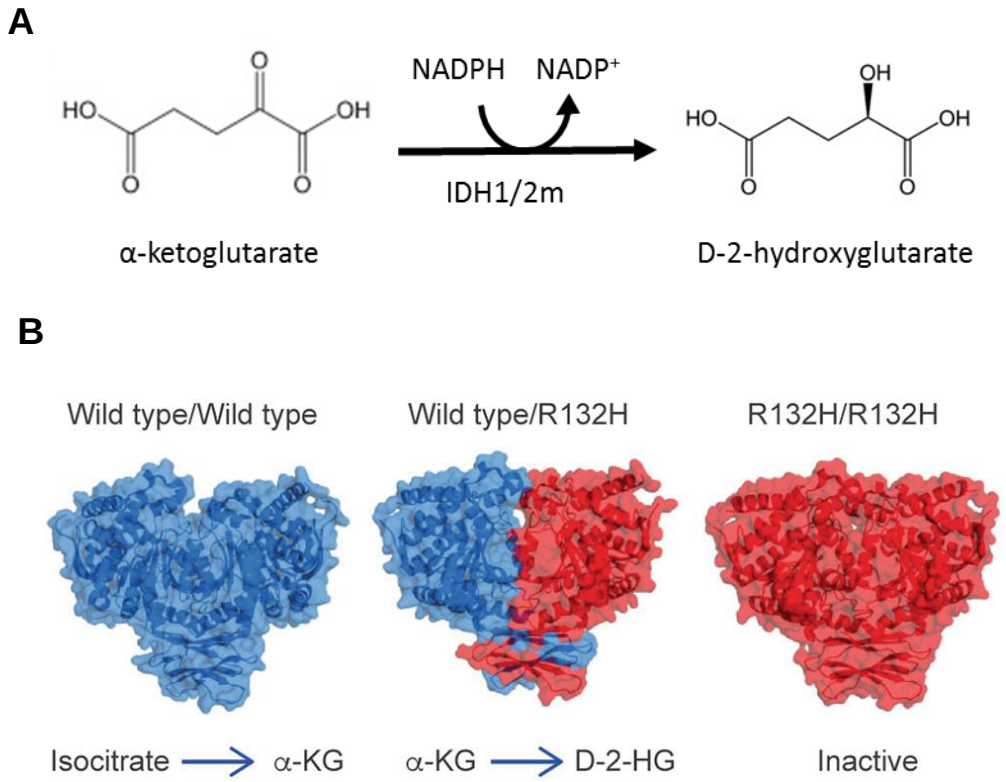

Figure 12. IDH1/2 mutant reaction and dimerization. A. IDH gain-of-function mutation leads to the neomorphic reduction of α-KG into D-2HG consuming NADPH. **B.** Wildtype IDH1 enzyme is composed of two wildtype monomers which transform isocitrate into α-KG. In IDH1 mutant cells, a heterodimer is formed with one wildtype monomer and one R132H mutant. This enzyme is able to generate D-2HG. The rare case of homodimer formed by two IDH1m subunits it has been shown to be catalytically inactive. Used from (Han et al., 2020).

IDHm epigenetic reprogramming. Due to its tumorigenic potential, D-2HG is commonly categorized as an oncometabolite. 2HG molecule is a five-carbon dicarboxylic acid and its second carbon is chiral, meaning that it has two enantiomers: D-2HG and L-2HG. The D enantiomer is the one exclusively produced by the neomorphic reaction of IDHm cells (Dang et al., 2009b). In healthy tissue both enantiomers can also be found although they are thought to be metabolic "waste" originated in the mitochondria in a small amount, and that can be converted into α-KG by D-2HG and L-2HG dehydrogenases (D2HGD, L2HGD) (Steenweg et al., 2010). Yet, the D-2HG levels of IDH1m gliomas are found to be >100-fold higher than in

normal tissue (Dang et al., 2009b). D-2HG and α-KG are two structurally similar metabolites which only differ in the presence of a C2 hydroxyl group in D-2HG instead of the C2 carbonyl group of α-KG (**Figure 12A**). This similarity is what confers to D-2HG the capacity of competitively inhibit α-KG-dependent dioxygenases, enzymes in charge of hydroxylating target proteins by using α-KG as substrate and incorporating both atoms of molecular oxygen (O_2).

One of the most important dioxygenases in which D-2HG has a direct inhibitory effect are histone demethylases, and some of the most frequently inhibited are JHMD1A, JMJD2A, JMJD2C and FBXL11, members of Jumonji-C (JmjC) domain-containing family. These histone demethylases commonly act by removing methyl groups from lysine residues of different histones, and for these reason they are also known as histone lysine demethylases (KDM) (Waitkus et al., 2016) (**Figure 13**). It has been reported that administration of D-2HG is sufficient to increase methylation of H3K9 and H3K79 histones in U87 GBM cells (Xu et al., 2011a). Moreover, it has been observed how $IDH1^{R132H}$ and $IDH2^{R172K}$ overexpression lead to trimethylation of histone H3 at Lys^{9} and Lys^{27} in immortalized human astrocytes (Lu et al., 2012).

As mentioned in section 1.3 IDH mutation is closely associated with CpG island hypermethylation (G-CIMP). Indeed, several studies showed that neomorphic IDHm activity triggers as well a direct DNA methylation mechanism. Similar as with the competitive inhibition of histone demethylases, D-2HG is also able to block the activity of TET 5-methylcytosine hydroxylases (Xu et al., 2011a). TET family are α-KG-dependent enzymes that catalyze the first step of the DNA demethylation process. This first step consists of the hydroxylation of 5-methylcytosines to convert them into 5-hydroxymethylcytosines (5-hmC), which are intermediates that will be eventually turned into cytosines (Han et al., 2020) (**Figure 13**). The observations in clinical glioma tissues that 5-hmC levels are lower in IDHm tumors relative to IDHwt are consistent with *in vitro* and *in vivo* mechanistic studies in which the overexpression of $IDH1^{R132H}$ and $IDH2^{R172K}$ lead to a decrease in 5-hmC abundance by direct D-2HG-mediated inhibition of TET1 and TET2 (Sasaki et al., 2012, Xu et al., 2011a).

Epigenetic aberrations generated after histone and DNA hypermethylation in IDHm gliomas is reported to inhibit cell differentiation (Lu et al., 2012). In fact, IDHm activity increases histone methylation at promoters of astrocytic lineage markers. This mechanism has shown to confer a block in differentiation in patient-derived glioma xenografts (PDX). Furthermore, it has been demonstrated how IDH1m inhibition leads to differentiation of neural stem cells as well as tumor growth delay of an IDHm subcutaneous xenograft model (Rohle et al., 2013). A similar differentiation mechanism has been observed after IDH1m inhibition of glioma stem like cells (GSCs) *in vitro* (Rohle et al., 2013). Surprisingly, this differentiation effect did not lead to a change in DNA hypermethylation. Moreover, a study in which IDH1m GSCs were treated with the hypomethylating agent decitabine observed a similar differentiating effect without observed change in D-2HG levels (Turcan et al., 2013). It is possible that IDH mutation occurring in progenitor glial cells may lead to a specific stop in differentiation that promotes malignant transformation and gliomagenesis. Yet, further work is required to definitively identify IDHm-dependent epigenetic reprogramming mechanism in glioma.

The association of IDHm with hypoxia-inducible factor 1-α (HIF1-α) regulation has also raised controversial hypotheses. HIF1-α is considered as the master transcriptional regulator of cellular and developmental response to hypoxia (Ivan et al., 2001). Accumulation of D-2HG was also shown to inhibit α-KG-dependent prolyl-hydroxylases (PHDs). Under normoxia, these enzymes hydroxylate specific proline residues of HIF1- α creating a binding site for the von Hippel-Lindau (VHL) ubiquitin-ligase protein complex and therefore leading to HIF1-α proteasomal degradation. On the other hand, under hypoxic conditions, oxygen-dependent hydroxylation of PHD dioxygenases does not occur, which results in HIF1- α accumulation. This leads to the translocation of HIF1-α into the nucleus and activation of its downstream target genes such as *VEGF, GLUT1* or *PGK1* (Ivan et al., 2001). Competitive inhibition of D-2HG block similarly the degradation of HIF1- α leading to the overexpression of its target genes which might promote tumor proliferation, invasion, angiogenesis and metastasis (Xu et al., 2011a, Semenza, 2003) (**Figure 13**). Moreover, α-KG has been shown to revert this

mechanism and promote a decrease in HIF1-α levels (Zhao et al., 2009). However, the controversy was propelled by a study which showed that D-2HG indeed enhanced PHD2 activity leading to a decreased expression of HIF1-α, an effect that led to cellular transformation (Koivunen et al., 2012). Although further work will be required to fully elucidate the link between HIF1-α and IDHm in gliomas, it is possible that environmental factors play a key role in determining whether D-2HG inhibits or stimulates HIF hydroxylases.

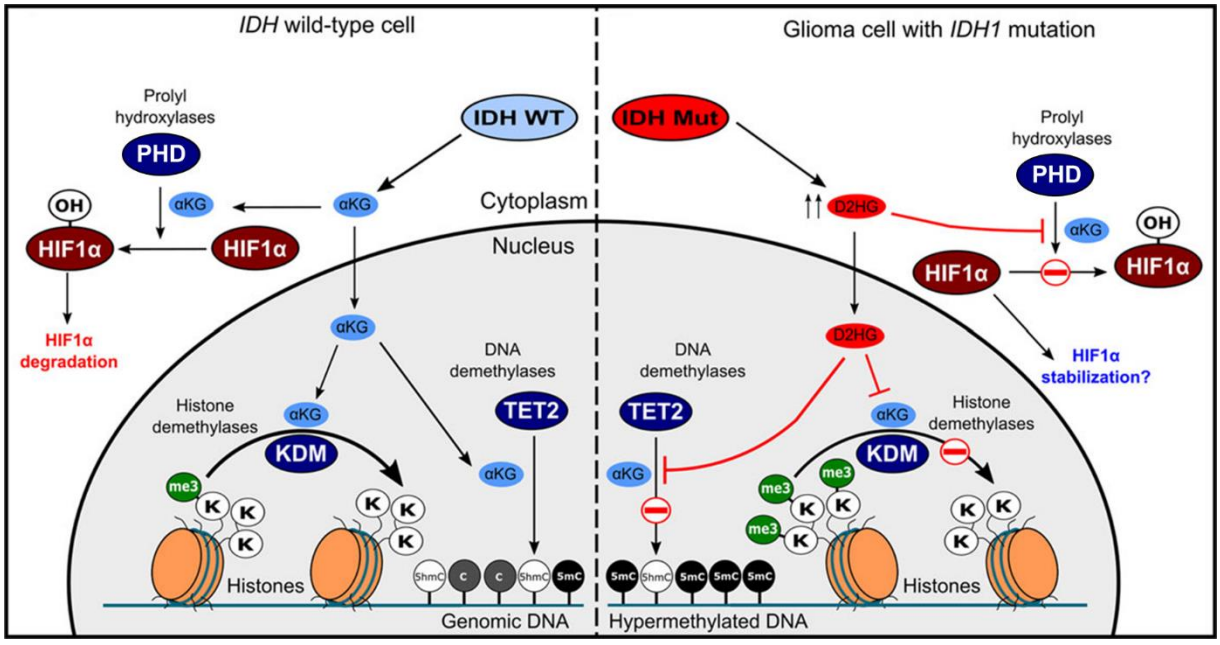

Figure 13. Epigenetic reprogramming in IDHm glioma cells.
The mutation of IDH in glioma cells lead to the accumulation of D-2HG which competitively inhibits several α-KG-dependent dioxygenases. The inhibition of KDMs leads to a block in the histone demethylation process. TETs inhibition promotes an accumulation of methylated citosines within the genome leading to hypermethylation of DNA. Both DNA and histone methylation may promote a dedifferentiated status in glioma cells. On the other hand PHD enzymes inhibition prevents HIF1-a degradation which may lead to different carcinogenic effects such as tumor cells invasion or angiogenesis. Used from (Waitkus et al., 2016).

It has been extensively investigated how IDH gain-of-function mutation and subsequent D-2HG generation lead to numerous epigenetic mechanisms that alter and reprogram the cellular and developmental fate of glioma cells. However, these are not the only repercussions derived from this frequent mutation. Being such an important metabolic enzyme, IDH plays a central role in several biosynthetic, energetic and antioxidant pathways that may be equally or even

more crucial for the understanding of glioma malignancy, and uncovering potential vulnerabilities. In section 4 we will dissect the IDHm-related metabolic alterations so far discovered, in the special context of brain tumors.

2.3. Experimental models for IDH mutant gliomas

Cancer models should ideally present biological features similar to those encountered on human cancers. Experimental models for the study of cancer include human cell lines and organisms such as mice or rats to investigate cancer biochemical mechanisms and pathology. Cell lines are commonly known as *in vitro* models, which are obtained from normal human tissue and are kept in long term culture under special sterile conditions. The use of cell lines allows the study and manipulation of cancer under ideal growth and analytical conditions. Commonly, these cells are genetically immortalized to improve their growing capacities and to grow adhered to the culture surface in serum-containing medium, and that are commonly kept and commercialized in different laboratories internationally. On the other hand, patient-derived cancer cell lines are directly resected from patient tumors and kept in culture preserving the original genetic background. Such cells have long been grown as adherent cell lines and have spread over many years and different laboratories, which led to the accumulation of additional genetic aberrations not found in the parental tumors (e.g. U87, U251). More recently, researchers have switched to glioma patient-derived cell lines grown as 3D spheres in serum-free medium, thought to better recapitulate the tumor of origin (e.g. NCH551b). With regard to animal experimental systems, these are commonly known as *in vivo* models. When generated from implantation of human tumor cells, these are referred to as xenograft models, meaning a tissue or cellular transplant that belongs to a donor from a different species than the host. Mice are commonly used as animal model, which in most cases are genetically modified to attenuate the immunological response to the transplant (e.g. immunodeficient mice). Mouse models can be generated from immortalized cell lines, or from patient derived cells, also known as patient-

derived xenografts (PDXs). Indeed, certain human cancer cells are not capable of growing *in vitro*, but they are stable once implanted into a mouse host. Finally, human samples can also be analyzed in order to collect genomics or proteomics blueprints of the cancer entity. However, these samples are not amenable to manipulation, thus they are not considered experimental models *per se*.

In the study of IDHm gliomas there are a number of different experimental models that have been used. Whereas GBM cell lines are normally easy-to-handle models, the presence of IDH mutation is generally associated with increased vulnerability and slower growth. Diverse stable cell lines genetically engineered to present IDH mutation, have facilitated the analysis of this cancer type (Dang et al., 2009b). On the other hand, patient-derived cells are usually more difficult to manipulate displaying slow growth capacity or frequent loss of IDHm heterozygosity (Luchman et al., 2013). Within the last decade there has been promising improvements in the design and maintenance of appropriate models for this elusive cancer type, ranging from the direct use of human samples, to the basic principles of *in vitro* cell lines and the *in vivo* implantation of tumors in mice.

Human samples. The first report of the existence of the IDH mutation within gliomas was observed in a set of 22 human samples where a complete genomics analysis was applied (Parsons et al., 2008). In fact, in order to preserve the material, 15 of these samples were implanted in mice to be analyzed later, unlike the other 7 samples which were directly used for sequencing. Since then, different groups made key findings in the research of IDHm glioma by using human samples, not only analyzing their genetic features but also protein or metabolite profiles. The clear advantage of using clinical material is the direct analysis of the patient reality. Yet, clinical samples represent a snapshot in time and most studies using clinical samples are restricted to the classification and molecular characterization of tumors. For this reason, several studies use clinical samples as complementary material to validate more detailed mechanistic observations made on *in vitro* or *in vivo* models (Dang et al., 2009b, Zhao et al., 2009, Turcan et al., 2012). Interestingly, some groups have made use of innovative

strategies to analyze *in situ* the features of IDHm gliomas in patients, such as the use of metabolic mapping (Bleeker et al., 2010). Nonetheless, this approach is far less versatile than the direct manipulation of cell lines and animal models. When the purpose is to present a complete characterization of IDHm gliomas, large scale patient cohorts have been used, which led to the establishment of genomic databases with a thorough molecular profiling of the disease (i.e. TCGA, ICGC, NCT) (Hartmann et al., 2009, Ceccarelli et al., 2016, Bowman et al., 2017, Capper et al., 2018).

In vitro models. The most commonly used *in vitro* model consists of the transfection of the *IDH1m* gene into a stable fast growing cell line. Diverse groups have opted for this easy-to-handle cellular set-up in order to understand the cellular impact of the IDH mutation. In some cases the IDHm is directly introduced into a fast growing GBM cell line which also expresses the IDHwt enzyme. Some of the most common GBM cell lines used for this purpose are U87, U373, LN229 or LN18 (Dang et al., 2009b, Zhao et al., 2009, Li et al., 2013, Pusch et al., 2017). However, sometimes researchers use cell lines that are not even derived from gliomas, but are routinely used for transgenic manipulation, such as HEK293T derived from human embryonic kidney cells, A549 from epithelial cancer or NCIH82 from lung cancer (Dang et al., 2009b, Zhao et al., 2009, Turcan et al., 2012, Pusch et al., 2017, McBrayer et al., 2018). These IDHm transfected cell lines are normally generated by using IDHm overexpression plasmids, which carries the disadvantage of increasing vastly the expression of this enzyme which recedes from the patient reality. In order to circumvent this, recently some groups have made use of clustered regularly interspaced short palindromic repeats (CRISPR)-cas9 technology to introduce the IDH mutation (Brabetz et al., 2017). The main advantages of using this IDH1m transfection set-up is that it generates isogenic models of IDHm with a heterozygous expression of IDHm. The transfected and the parental wild type cell line have the same genetic background (isogenic) with the exception of the transgenic *IDHm* insert, which is only expressed from one allele, thus reproducing IDHm heterozygosity of patient tumors. This allows to understand the acute impact of this mutation, which is not possible when comparing

patient-derived tumor cells with or without the mutation, since they represent different tumor entities which bear various other mutations and chromosomal alterations. However, patient-derived tumor models with endogenous IDH mutation better reflect IDHm glioma biology, since they carry the genetic background of the original tumor. In any case, the drawback of slow growing capacity and vulnerability of these cell lines, often determines the decision of which model to use. So far only few groups have used these patient-derived IDHm cell lines such as NCH551b, TS603, MGG152 or BT142 (Rohle et al., 2013, Chesnelong et al., 2014, Pusch et al., 2017, McBrayer et al., 2018). Moreover, in some cases non-glioma IDHm patient-derived cell lines have also been used as complementary model to brain tumors, such as the fibrosarcoma cell line HT1080 (Rohle et al., 2013, Pusch et al., 2017).

In vivo models. In order to mimic the physiological environment of the tumor, *in vivo* approaches are essential. This is particularly important for investigation of tumor metabolism which is highly dependent on the surrounding microenvironment and nutrient supply. Commonly used *in vivo* models are immunodeficient mouse xenografts. Once more, the slow growing nature of IDHm cells limits the development of these tumors after implantation. Some groups perform these tumor cell implantation in the flanks of the mice, subcutaneously (Rohle et al., 2013, Schumacher et al., 2014, McBrayer et al., 2018), an easier procedure than orthotopic implantation, i.e. transplantation into the original organ of the tumor. However, orthotopic xenografts are crucial to understand the behavior of the tumor in the particular context of the brain (e.g. BBB, microenvironment, myelin sheaths). In our group we have showed the efficacy of establishing IDH1m patient-derived orthotopic xenografts (PDOXs) (**Figure 14**) (Golebiewska et al., 2020). Our PDOX models are generated from primary tumors directly resected from patients, without intermediate *in vitro* amplification, and have proven to be suitable models for metabolomics and drug efficacy studies (Fack et al., 2017, Golebiewska et al., 2020). Interestingly, many IDH mutant tumors, do not grow *in vitro* but do grow *in vivo* as PDOX. In addition to *in vivo* models, in the recent years different groups including us, have shown the potential of patient-derived tumor organoids as optimal experimental models, which

preserve intra-tumor heterogeneity and to some extent can be adapted to recapitulate the immune compartment (**Figure 14**) (Klein et al., 2020, Golebiewska et al., 2020). These models can be manipulated in culture therefore representing an intermediate level between an *in vitro* and *in vivo* set up, commonly known as *ex vivo*. Nonetheless, while GBM organoids have been established by several groups, as of today, no one has been able to generate IDHm organoids.

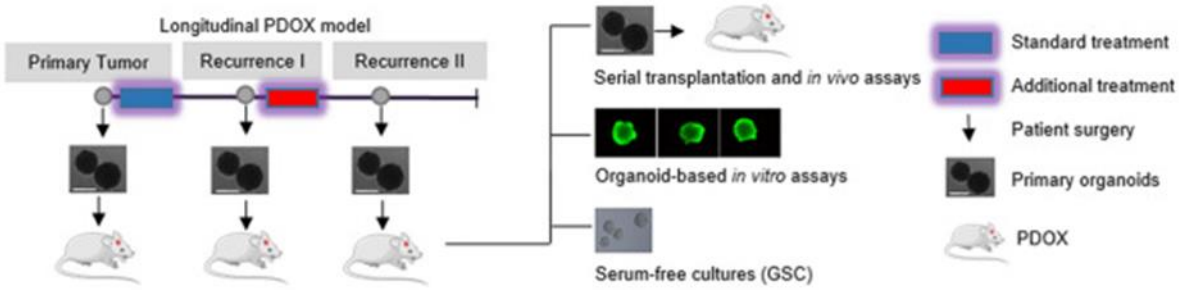

Figure 14. Glioma organoids and PDOX generation
Schematic representation of derivation of PDOXs, organoids and patient-derived cells from primary and recurrent patient gliomas. Longitudinal PDOX model refers to different mice orthotopic implantation of primary organoids from same patient during different stages of tumor development (primary tumor, recurrence I and recurrence II), treatment refers to patients. PDOX models can be kept in the laboratory via serial transplantations to perform *in vivo* assays. Primary organoids can be preserved in culture for short-term *in vitro* assays. Some organoids can also be kept for long-term *in vitro* manipulation in serum-free medium as glioma stem-like cell (GSC) spheres. Used from (Golebiewska et al., 2020).

The specific purpose of the study will be decisive for the choice of the most appropriate IDHm glioma model. E.g. when aiming to understand the specific metabolic behavior of IDHm gliomas, the selection of the model plays a critical role, most often requiring to preserve or mimic the metabolic environment of the tumor as best as possible. While genetic blueprints may remain relatively stable, cellular metabolism is a process in motion, rapidly responding to external conditions and stimuli.

3. Principles of metabolism in health and cancer

Metabolism, which encompasses more than 8,700 reactions and 16,000 metabolites, can be defined as all biochemical processes involving organic compounds which either produce or consume energy in living organisms (DeBerardinis and Thompson, 2012). Metabolism represents the essential event of life in which macronutrients obtained from food are decomposed in building blocks which are processed for energy production and recycled for biosynthesis of new compounds. In cancer, the metabolic behavior of tumors depend on the constant communication and competition of malignant cells with its environment, what allows them to proliferate and invade neighboring tissues. These intricate metabolic interactions are possible due to adaptive mechanisms that may be conserved in different cancer types, but may also be specifically determined by the physiological scenario of each tumor.

In section 2.2, we discussed the repercussions in epigenetic reprogramming and tumorigenesis linked to D-2HG accumulation. In section 4 we will analyze how IDH mutation alters the specific metabolic landscape of glioma cells. To understand the specific metabolic pathways altered in IDHm gliomas, we will first review the general principles of metabolism in health and cancer, including: the basic metabolic regulation in normal cells, the specificities of brain metabolism and the general hallmarks of cancer metabolism.

3.1. Basics of cellular metabolism

In general terms, all biochemical pathways participating in cellular metabolism can be classified in four groups: 1) Nutrient uptake from the extracellular space towards the cell; 2) Anabolism: the synthesis or polymerization of molecules, which requires energy; 3) Catabolism: the degradation of molecules, which releases energy; 4) Waste disposal: the elimination of toxic compounds derived from the previous reactions (DeBerardinis and Thompson, 2012). Nutrients delivered via blood supply from food digestion are essentially

carbohydrates, amino acids and fatty acids. These nutrients are the building blocks for the anabolism of macromolecules, which will serve either as energy storage (lipids and polysaccharides) or to promote cellular growth (proteins, nucleic acids and lipids), but they can also be re-catabolized back to building blocks. This represents a continuous loop driven by energy availability where micronutrients and macronutrients are constantly interconverted. Catabolism of building blocks promotes energy release. At the same time, secondary metabolites are formed which can be either re-utilized as metabolic intermediates (such as pyruvate or acetyl-CoA) or might be waste to be removed (such as CO_2 or NH_3). Thousands of intermediary metabolites shape the overall landscape of metabolic regulation, and although some are directly related with molecular recycling or energy production, others bear their own cellular functions such as signaling molecules, vitamins, neurotransmitters or enzymatic cofactors (DeBerardinis and Thompson, 2012) (**Figure 15**).

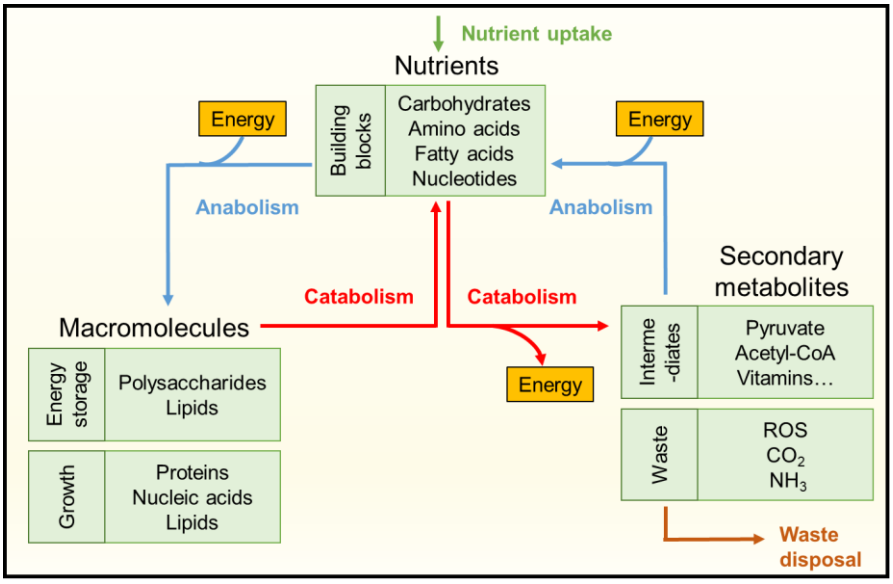

Figure 15. Overview of cellular metabolism regulation.
Schematic representation of the different processes involved in cellular metabolism as well as the most important compound groups involved.

Energy is the primal force that drives life against entropy. As mentioned, anabolic metabolism requires energy whereas catabolic reactions generate it. Adenosine triphosphate (ATP) is the

"molecular currency" which stores and transports chemical energy obtained from catabolic reactions (Nelson et al., 2009). When required, ATP will be used as energy boost to allow anabolic synthesis. Moreover, all metabolic reactions will require the action of specific catalysts that force reactivity of substrates: enzymes. In order to catalyze specific reactions, enzymes need particular cofactors. These are organic (e.g. NADH) or inorganic (e.g. metal ions such as Fe^{2+}) molecules and atoms, that interact with the enzyme triggering the reaction catalysis. Finally, all these reactions will be influenced by the electron charge carried by each compound. Therefore, the pH of the cell and the electronegativity of certain molecules will create the need of electron donors and acceptors (e.g. NAD(P)H and $NAD(P)^+$ respectively) which will promote reductions and oxidations in order to preserve the pathway flow. These reduction and oxidation (redox) reactions are essential in multiple metabolic events, such as oxidative phosphorylation and ATP synthesis or anabolic pathways such as biosynthesis of fatty acids (He et al., 2017). Taking into account the different principles aforementioned, in the present section we will review cellular metabolism in three different parts: 1) Intermediary metabolism: anabolic and catabolic reactions involving processing of building blocks, macromolecules and secondary metabolites thereof; 2) Energy metabolism: reactions aiming to produce energy in form of ATP; 3) Redox metabolism: reactions that lead to reduction or oxidation of compounds and the machinery of the cell to balance this process.

3.1.1. Intermediary metabolism

The physical-chemical properties of the carbon atom, makes it ideal for the generation of living organisms. Carbon erects the central skeleton of all organic compounds, and together with hydrogen, oxygen and nitrogen, they account for more than 99% of all atoms in life (Koolman and Röhm, 2013). In addition, sulfur and phosphate are also highly represented elements. Metabolites are the basic organic compounds that make life possible, by allowing energy production and growth. Intermediary metabolism is the field that attempts to understand how all metabolites organize. The magnitude of interconnectivity and multi-functionality of the

thousands of different metabolites is yet unfathomable and although much is already known, the field of intermediary metabolism is still under constant investigation. Between the 1920s-1960s most of today's known metabolic networks have been defined. These networks are mainly related to nutrient utilization and energy production, such as glycolysis (Embden, Meyerhof and Parnas), the TCA cycle (Krebs), or respiration (Warburg). Nowadays, with the advance of mass-spectrometry metabolomics techniques and *in silico* simulations, different public databases (e.g. KEGG or Expasy) have considerably improved the classification and understanding of the intricate metabolic organization (Okuda et al., 2008, Gasteiger et al., 2003). In brief, all intermediary metabolism revolves around the processing of the four base building blocks: sugars, amino acids, fatty acids and nucleotides.

Sugars. The carbohydrates are a group of carbonyl compounds (aldehydes or ketones), containing several hydroxyl groups (**Figure 16A**). Monosaccharides, or sugars, are the simplest unit of this group, which may polymerize into oligosaccharides or polysaccharides. In nature, monosaccharides are found in cyclic conformation due to the reactivity of one of the hydroxyl groups with the aldehyde. Glucose is the most common sugar, an aldehyde with six carbons (i.e. aldohexose), which lies at the core of intermediary and energy metabolism. Most monosaccharides have a similar configuration as glucose, there exist many sugar derivatives or metabolic intermediates. Within the cell, glucose is rapidly phosphorylated into glucose-6-phosphate (Glc-6-P), which is the starting point or endpoint of many metabolic pathways (Nelson et al., 2009). Besides biosynthesis of metabolic intermediates, the main function of glucose metabolism is chemical energy production in form of ATP. In this process, glucose is consumed into pyruvate via glycolysis, which in the presence of O_2 will enter the mitochondrion to be metabolized into acetyl-CoA to generate ATP through the TCA cycle. Glycolysis alone gives ATP, although in a much limited amount than within the complete mitochondrial respiration. In the absence of oxygen, glycolysis can still promote ATP formation due to positive feedback of pyruvate-derived lactate, a process known as anaerobic glycolysis or lactic fermentation. In cases of deficiency, glucose can be synthesized *de novo* from glucogenic

amino acids (e.g. alanine or glutamine), and also lactate and glycerol, a process known as gluconeogenesis. In cases of excess of glucose, it can be polymerized into long monomeric chains known as glycogens, which serve as energy reserve. The PPP (pentose phosphate pathway) is another important metabolic route of glucose which lead to the generation of nucleotide precursors, as well as electron donors in form of NADPH (Koolman and Röhm, 2013).

Amino acids. Amino acids are compounds containing amino and carboxyl groups alongside another specific chemical group which will confer them different polarities (**Figure 16B**). Their characteristic amino group (NH_2) makes amino acids an essential source of nitrogen. The most commonly known amino acids serve as building blocks for proteins (i.e proteinogenic, e.g. cysteine or glutamine), however many are non-proteinogenic and participate in the synthesis and breakdown of other proteinogenic amino acids or as intermediates in different metabolic pathways (e.g. homocysteine or ornithine) (Nelson et al., 2009). Proteins can be classified into distinct groups, such as transport, regulatory or structural proteins, however in terms of metabolism, catalytic proteins or enzymes are the most relevant ones, since they drive the flow of all different pathways. Besides protein synthesis, amino acids are pivotal in diverse metabolic events. TCA anaplerosis is the alternative pathway to fuel TCA cycle independently of glycolysis. This serves as a glucose-independent alternative to promote synthesis of intermediates and/or ATP. Directly or indirectly, several amino acids such as glutamate, glutamine, aspartate or proline may perform TCA anaplerosis. On the other hand, certain amino acids serve as precursors for acetyl-CoA and synthesis of lipids (ketogenic amino acids, e.g. glutamine, leucine and lysine). Amino acids can as well be grouped as essential (i.e. they cannot be synthesized by animal cells, e.g. arginine or methionine), and nonessential (i.e. they can be synthesized, e.g. serine or cysteine). Glutamate is a key precursor in the synthesis of several other amino acids via transamination (e.g. alanine, arginine, proline or aspartate). Other similarly structured amino acids, such as glycine, serine and cysteine, can as well be interconverted (Koolman and Röhm, 2013).

Fatty acids. Fatty acids are carboxylic acids with unbranched hydrocarbon chains of 3-24 carbons (**Figure 16C**). Lipids represent a heterogeneous group of hydrophobic compounds, made up of fatty acids. In most cases, fatty acids are esterified with alcohols (e.g. glycerol, sphingosine). Fat, for instance, which is the main energy storage in animals, is formed as esters of glycerol with three fatty acids, also known as triacylglycerols (fatty acid residue = acyl group). On the other hand, fat or glycerolipids can as well be linked to a phosphate group, forming phospholipids. This phosphate group confers phospholipids an amphipathic potential (both hydrophobic and hydrophilic potential), making them the ideal constituent of biological membranes (Nelson et al., 2009). In order to be broken down or incorporated into other molecules, fatty acids are linked to coenzyme A (CoA), forming the more reactive derivative acyl-CoA in a process known as fatty acid activation. The degradation of acyl-CoA promotes the synthesis of acetyl-CoA in a process called β-oxidation which takes place within the mitochondrion. Through this process, acetyl-CoA can enter the TCA cycle for ATP synthesis independently of glucose, thereby making lipids an important source of energy. Inversely, when fatty acids are scarce, they can be synthetized from acetyl-CoA coming from different sources such as mitochondrial citrate from TCA cycle or cytosolic citrate derived from a multi-step process of glutaminolysis, where IDH is involved. Other important pathways such as lipogenesis (i.e. synthesis of fats), cholesterol and steroid hormone synthesis, and ketone body processing, play as well key roles in lipid metabolism (Koolman and Röhm, 2013).

Nucleotides. The nucleotides are organic compounds formed by a pentose, a phosphate residue and a nucleobase (**Figure 16D**). Nucleobases or nitrogenous bases, are aromatic heterocyclic molecules which can be classified as purines or pyrimidines. Polymerizing sequences of nucleotides form the nucleic acids, such as deoxyribonucleic acid (DNA) and ribonucleic acid (RNA) (Koolman and Röhm, 2013). Besides generation of nucleic acids, nucleotides may have independent functions such as enzymatic cofactors or signaling molecules. In fact, the most important function of a nucleotide within metabolism is the storage of chemical energy, when adenosine is conjugated to three phosphate residues forms

adenosine triphosphate, i.e. ATP. Moreover, pyridine nucleotides NAD and NADP are the most common redox cofactors in the cell. Carbohydrate and amino acid metabolism is directly linked to the synthesis of nucleotides, either in order to produce pentoses (via PPP), or for synthesis of purines and pyrimidines. For instance, aspartate and glutamine are important precursors of pyrimidines (Koolman and Röhm, 2013).

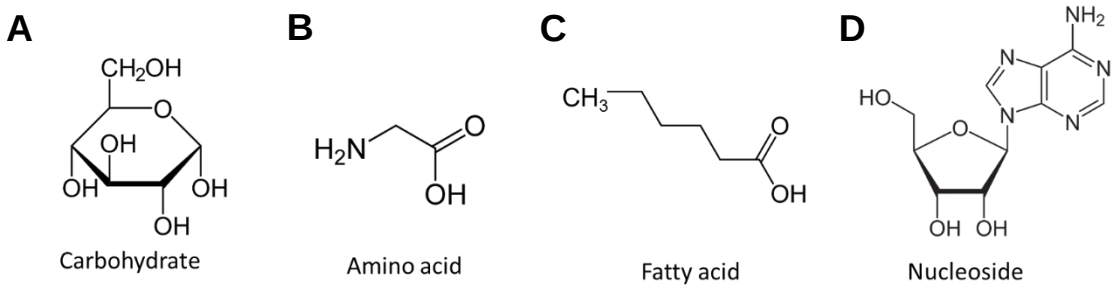

Figure 16. Building blocks
A. Chemical structure (represented as Haworth projection) of the carbohydrate monosaccharide glucose. **B.** Chemical structure of the amino acid glycine. **C**. Structure of the fatty acid hexanoic acid. **D.** Structure of the nucleoside adenosine.

In summary, intermediary metabolism is composed by a network of pathways involving synthesis and break down of building blocks, macromolecules and their derivatives. All these pathways interconnect since in many cases some metabolites can enter different routes depending on the cellular requirements. Intermediary metabolism supplies the cell with the organic compounds that it needs to undergo growth and division. In order to cope with the amount of energy needed to maintain metabolic functioning, the animal cells produce ATP in a multi-pathway process in which redox homeostasis gets altered.

3.1.2. Energy metabolism

The energy system in the cell is organized as an energetic coupling. This means all biochemical reactions that require energy (endergonic), are coupled to another reaction that releases energy (exergonic). As mentioned previously, the nucleotide coenzyme ATP is the

most important chemical energy storage in cells. ATP acts as an energy supplier molecule for endergonic reactions (e.g. biosynthesis, movement and transport processes) since its cleavage is strongly exergonic. Synthesis of ATP is essential for living cells to maintain their metabolic machinery in motion (Nelson et al., 2009). Animals are chemoheterotrophic organisms, which means they need to ingest organic compounds from the diet and catabolize them in order to synthesize ATP. Although they can produce ATP independently of O_2, animal cells rely mostly on O_2 to drive energetic metabolism, in a process known as oxidative phosphorylation or cellular respiration, taking place in the mitochondria. In brief, during oxidative phosphorylation, electrons obtained from degradation of organic compounds within the TCA cycle, are transferred from electron donors (e.g. NADH) onto an oxygen molecule. Due to the wide difference in redox potential between the electron donor, NADH, and the acceptor, oxygen, this reaction is strongly exergonic. The energy released then is used to establish a proton gradient across the mitochondrial membrane which enables the synthesis of ATP (Koolman and Röhm, 2013).

The process of cellular respiration starts with acetyl-CoA. This molecule will fuel the TCA cycle, within mitochondria (**Figure 17**). In this pathway, tricarboxylic acid compounds (such as isocitrate) are oxidized releasing CO_2. Coupled to each oxidation there is a reduction of an electron acceptor (i.e. NAD^+) to produce a reducing equivalent (i.e. NADH). All the NADH molecules produced within the cycle will then serve as electron donors within the respiratory chain. This, also known as electron transport chain (ETC), is a sequence of large protein complexes (complex I, II and III as well as ubiquinone and cytochrome c, and the ATP synthase) that are embedded within the inner mitochondrial membrane. Since mitochondria possess a double membrane, these ETC complexes tunnel between the mitochondrial matrix and the intermembrane space (**Figure 17**). Electrons coming from NADH are transferred alongside the mitochondrial membrane via ETC complexes attracted by the high redox potential against the oxygen molecule located at the end of the chain, in the complex IV. When the electrons reach the oxygen molecule, H_2O is produced after coupling with free H^+. During

the process of electron transfer, each of the ETC complexes pump H^+ from the mitochondrial matrix, generating a cumulus of H^+ within the intermembrane space. Finally, the ATP synthase pumps all H^+ accumulated in the intermembrane space back into the mitochondrial matrix. This drastic change in the proton charge from both sides of the membrane releases enough free energy to promote the highly endergonic addition of a phosphate residue into an ADP molecule, and ATP is produced (**Figure 17**) (Nelson et al., 2009). This complex multi-step process is a highly efficient source of ATP. Although glycolysis alone leads to ATP synthesis, this is far less productive than cellular respiration. Only 2 molecules of ATP per molecule of glucose are gained during glycolysis whereas oxidative phosphorylation has a yield of 36 ATPs per glucose (Vander Heiden et al., 2009) (Nelson et al., 2009).

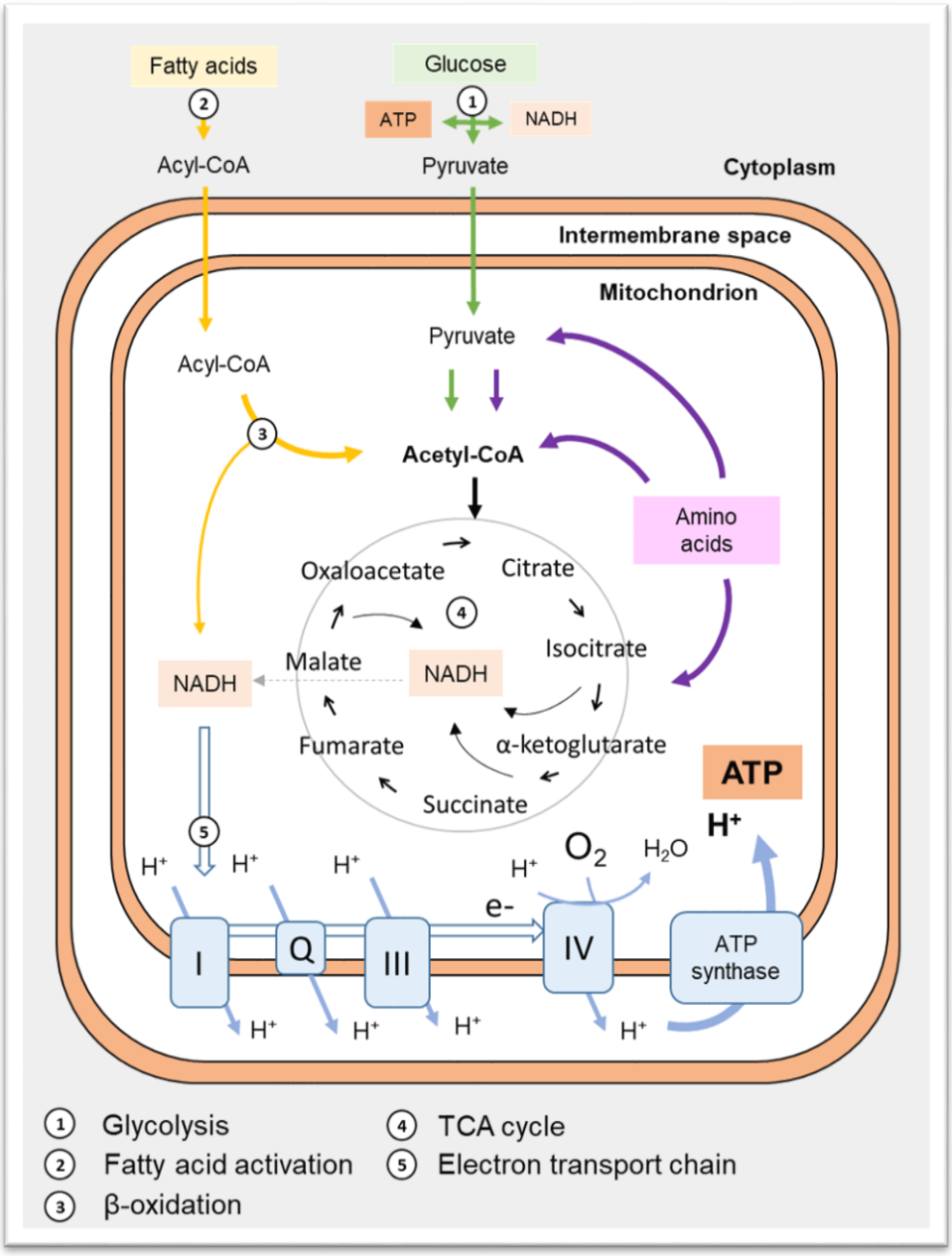

Figure 17. Cellular respiration.
Scheme of main metabolic pathways involved in cellular respiration.
ATP: Adenosine triphosphate; NADH: nicotinamide adenine dinucleotide; I: complex I; Q: cytochrome Q; III: complex III; IV: complex IV, e^-: electron; H^+: proton.

3.1.3. Redox metabolism

The presence of electron donors and acceptors is essential to maintain the flow of reduction-oxidation (redox) metabolism. As we have seen previously, these redox reactions are common in diverse metabolic pathways: in cellular respiration NADH acts as electron donor for O_2, generating the force that drives ATP synthesis. Apart from NADH, NADPH is another common electron donor, which is mostly used during biosynthesis reactions, but also plays an essential role in the production of antioxidants and the defense against excessive oxidation within cell structures (oxidative stress) (Koolman and Röhm, 2013).

Redox reactions are chemical processes in which electrons are transferred from one reactant to the other. This reactions always involve pairs of compounds. Each pair is known as a redox system, in which one component is richer in electrons (i.e. reduced) than the other (i.e. oxidized). The redox potential of a system determines the capacity to transfer electrons. Therefore, in redox reactions, the reduced form from one system donates electrons to the oxidized form of the other system and vice versa. At the end of the reaction, the reducing agents become oxidized and the oxidizing agents are reduced (Koolman and Röhm, 2013). Within the cell the majority of redox reactions are catalyzed by enzymes known as oxidoreductases, which require specific redox cofactors. Indeed, the redox cofactors are the other member of the pair in the redox system in order to perform a specific reduction or oxidation of a molecule (and therefore acting as electron donors or acceptors). The most common redox cofactors are the pyridine nucleotides NAD and NADP, which transfer hydride ions (H^-). In their oxidized form, they are electron acceptors represented as NAD^+ and $NADP^+$ and in their reduced form they are electron donors represented as NADH and NADPH. Whereas NAD(H) is commonly used in catabolic pathways such as the ones leading to the respiratory chain, NADP(H) is essential during anabolic pathways such as biosynthesis (e.g. fatty acids, cholesterol) or biotransformation. There are other redox cofactors such as flavin coenzymes or ubiquinone (Koolman and Röhm, 2013).

O_2 contains two unpaired electrons (i.e. diradical). Due to the high electronegativity of the oxygen atom, O_2 tend to accept instead of donating electrons, therefore oxidizing other molecules (hence the term “oxidation”). If the molecule takes up extra electrons generates reactive oxygen species (ROS) such as superoxide radical (O_2^-) or hydrogen peroxide (H_2O_2) (Koolman and Röhm, 2013). ROS, also known as free radicals, are highly reactive molecules that interact with chemical compounds of biological structures (e.g. lipids, DNA, proteins) forcing their degradation, a process commonly known as oxidative stress. Therefore, excessive exposure to oxygen can be toxic to the cell. During oxidative phosphorylation the electron charged oxygen ion (O^{2-}) gets neutralized by addition of protons giving rise to H_2O. However, the higher the activity of this process the higher the chances to generate more ROS. In fact, besides directly degrading biological structures, ROS can also act as signaling molecules that can trigger a wide variety of physiological events, such as apoptosis or cell cycle arrest (D'Autréaux and Toledano, 2007). Increasing evidence supports a role for other sources of reactive species, such as reactive nitrogen species (RNS, e.g. NO) or reactive sulfur species (RSS, e.g. H_2S), all molecules containing highly electronegative atoms. However the specific impact of RNS and RSS in human physiology is still under investigation (Cortese-Krott et al., 2017).

In order to combat the serious hazard promoted by oxidative stress, the cells generate antioxidants. These are specific reducing agents that react readily with those oxidizing agents thereby preventing damage against more important molecules. There exist different types of antioxidants: either enzymatic, such as thioredoxin (Trx), superoxide dismutase (SOD) and catalase (CAT); or non-enzymatic, such as ascorbic acid (AA or vitamin C) or reduced glutathione (GSH) (He et al., 2017). The glutathione system is also composed of various enzymes that reinforce the antioxidant capacity of this molecule, making it the most important antioxidant in humans (Forman et al., 2009). The antioxidant mechanism of glutathione consists of a redox reaction in which the reduced form (i.e. GSH) interacts with a ROS. Through the catalysis of GSH peroxidases (GPx), the ROS will be reduced into unreactive products,

while oxidizing GSH into its oxidizing form, glutathione disulfide (GSSG) (**Figure 18**). Besides ROS, GSH has also the ability to conjugate with xenobiotic molecules via a glutathione s-transferase (GST) reaction. The importance of GSH relies in its versatility but also in its reusability, and GSSG can be recycled back to GSH by glutathione reductase (GR), using NADPH as reducing power (Forman et al., 2009) (**Figure 18**). The chemical advantage that makes GSH an excellent antioxidant lies in its free thiol group (SH), which interacts with the different ROS. GSSG, is created by assembling two oxidized GSH molecules by their thiol groups, generating a disulfide bond (S-S) that masks the reactivity of the molecule (**Figure 18**). Hence, NADPH plays a pivotal role maintaining the pool of GSH and securing redox homeostasis, thus protecting cells against ROS and oxidative stress.

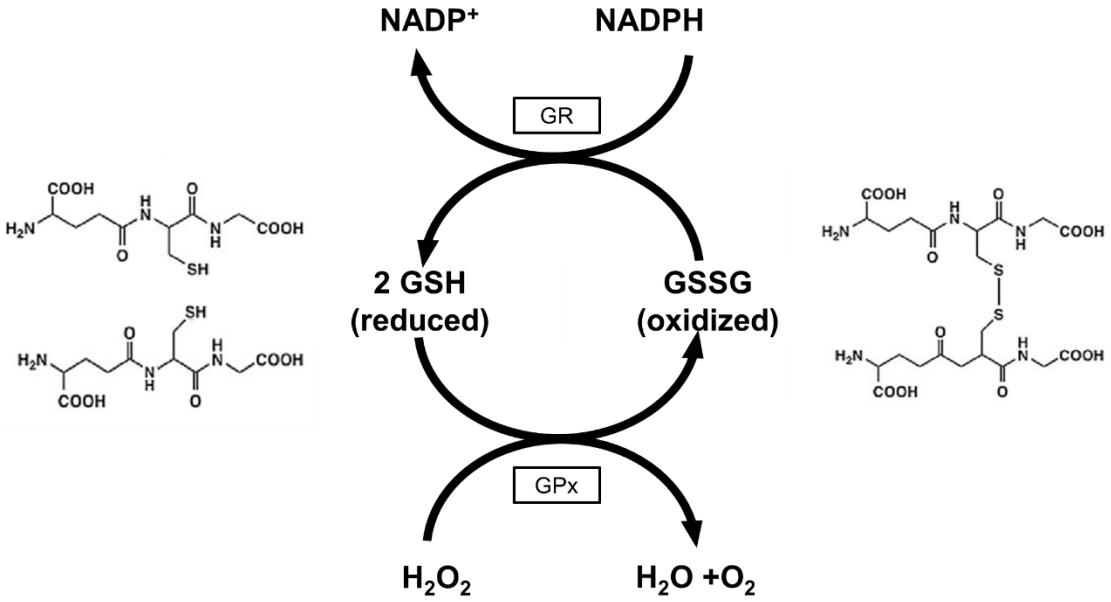

Figure 18. Glutathione redox reactions.
Glutathione peroxidase (GPx) catalyzes the oxidation of reduced glutathione (GSH) into oxidized glutathione (GSSG) what neutralizes reactive oxygen species (ROS). For instance, this reaction will lead to H_2O_2 (i.e. a common ROS) conversion into H_2O and O_2. Every two molecules of GSH will oxidize into one molecule of GSSG. Glutathione reductase (GR), will be in charge of the reduction of GSSG into two recycled GSH molecules, a reaction that requires NADPH as reducing power.

3.2. Specificities of brain metabolism

Due to the specific physiological compartmentalization of the brain, its metabolic regulation represents a specifically exclusive process within the human body. The most important substrate that will mediate the metabolic activity of the brain is glucose. This molecule lies at the apex of central carbon metabolism and will be key to sustain the energetic needs of the brain, but as we saw previously, it will as well trigger the synthesis of a wide range of metabolic intermediates important in many different pathways. In principle, neurometabolism is essentially oxidative, thus both glucose and oxygen are crucial substrates that must be administrated via blood irrigation. About 20% of oxygen and 25% of glucose consumed by the human body are dedicated to cerebral functions, yet the brain represents only 2% of the total body mass (Alle et al., 2009). Other metabolic substrates can compensate energetic needs in the brain during particular situations, such as ketone bodies during development and starvation (Belanger et al., 2011) or lactate during periods of intense physical activity (van Hall et al., 2009). In fact, it has been observed that there is a high metabolic plasticity in the brain, been able to switch between anaerobic glycolysis and oxidative metabolism depending on the momentary cellular needs. Constant maintenance of synaptic and action potentials together with synthesis and recycling of neurotransmitters and building blocks contribute to the high brain energy demand (Belanger et al., 2011).

CNS barriers. The exclusivity of neurological tissue, forces the brain to be semi-isolated from the rest of the body, being the blood stream that enters the brain permanently filtered by the blood-brain barrier (BBB). Together with the blood influx, another fluid with a less restrictive brain contact covers the organ, the cerebrospinal fluid (CSF). The CSF is secreted by ependymal cells from the choroid plexus to then travel around the spinal cord and the subarachnoid space that covers the brain (**Figure 19A**). This fluid provides mechanical protection and different molecular factors that enhance brain homeostasis, complementing those provided by blood. Moreover, CSF allows the removal of waste products from the brain, to be then absorbed through the arachnoid granulations into the blood stream and the rest of

the body (Huff et al., 2020) (**Figure 19A**). CSF can be extracted and analyzed and may serve as a good indicator of brain metabolic composition.

The highly selective semi-permeability of the BBB prevents solutes in the circulating blood crossing into the interstitial fluid of the brain and CNS. This barrier is formed by blood capillary endothelial cells, pericytes and astrocytes (**Figure 19B**). This cellular complex restricts the passage of pathogens and diffusion of solutes and large or hydrophilic compounds (such as proteins), while allowing passive diffusion of hydrophobic molecules (e.g. O_2, CO_2, hormones) and small polar molecules. Specific proteins across the barrier actively mediate the selective transport of essential ions and metabolites, such as glucose. On the other hand, CSF and brain extracellular fluid are separated by a thin layer of ependymal cells. Finally, in addition to the BBB, a blood-CSF barrier (BSCFB) also prevents the flow of large or hydrophilic molecules from blood to CSF. This BCSFB is formed by ependymal cells, some pericytes and the endothelial layer of the blood capillary. (D'Agata et al., 2017) (**Figure 19B**). In brief, blood molecular supply is tightly restricted into the brain and into the CSF, but this restriction is mild between brain and CSF.

The presence of these different barriers creates the necessity to have an internal source of metabolic production within the brain. Astrocytes are the main cell type in charge of brain metabolism regulation, on one hand uptaking filtered compounds through the BBB, and on the other hand providing neurons with the necessary factors for them to function and endure. Thus, the key of brain metabolism lies at the center of astrocyte-neuron communication. As we introduced in section 1.2 astrocytes are the most abundant glial cell in the CNS. In fact, astrocytes outnumber even neurons in the human brain (Nedergaard et al., 2003). They carry numerous functions such as ion and water homeostasis, neurotransmitter and nutrient regulation, antioxidant defense, energy production, tissue repair and synapse maintenance (Bélanger and Magistretti, 2009). These cells are able to dynamically respond to changes in their microenvironment in order to assist neurons in their synaptic activity. They are star-shaped cells with many processes (neurocellular arms) (**Figure 5A**) that envelope blood

vessels in order to uptake necessary nutrients, and ensheath neuronal synapses to provide neurons with their metabolic demands (Iadecola and Nedergaard, 2007) (**Figure 19B**).

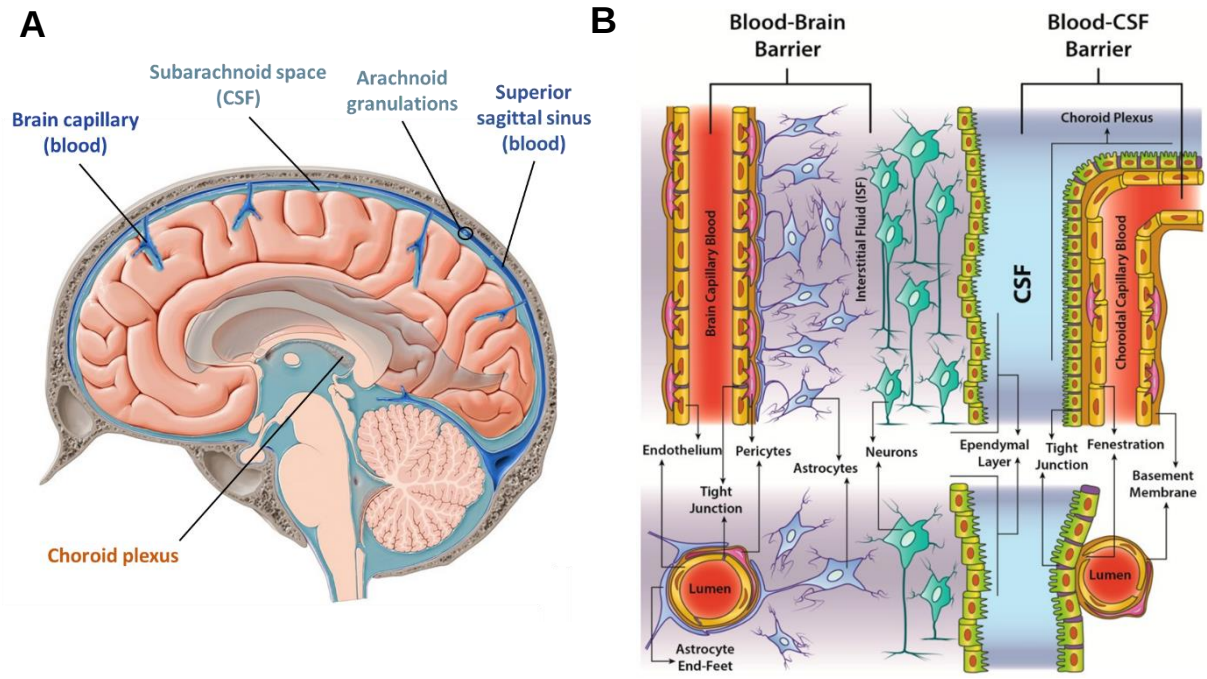

Figure 19. Physiological and cellular distribution of fluids within the brain.
A. Cerebrospinal fluid secreted by the ependymal cells of the choroid plexus travels around the brain through the subarachnoid space. On the other hand, the blood stream enters into the brain through capillary innervations. CSF carrying neuronal waste is absorbed at the arachnoid granulations, drained out into the superior sagittal sinus and returned to venous circulation. Adapted from kenhub.com.
B. BBB is formed by endothelial cells of the capillary walls closely linked by tight junctions, as well as pericytes embedded to the capillary and the end-feet of astrocytes from the brain interstitial fluid ensheathing all. CSF and brain extracellular fluid are separated by a layer ependymal cells with no tight junctions. The BCSFB is formed by tightly linked ependymal cells, some pericytes and the endothelial layer of the capillary, with fenestrations or space among cells. Used from (D'Agata et al., 2017).

Glucose supply. Cerebral metabolism is mainly oxidative due to the high energetic requirements of neurons to sustain the synaptic transmission (Lebon et al., 2002). It has been observed that neurons display a low glycolytic rate, due to the low expression of key enzymes such as the phosphofructo-kinase Pfkfb3, in charge of fructose-2,6-biphosphate formation (Almeida et al., 2004). They therefore lack not only the capacity of producing their own pyruvate for TCA cycle and oxidative phosphorylation (Bolaños et al., 2010). These deficiencies make them largely dependent on the external supply from astrocytes. Astrocytes, on the contrary, are highly glycolytic cells overexpressing Pfkfb3 (Berkich et al., 2007, Itoh et al., 2003), but

display a disrupted TCA cycle, due to downregulation of pyruvate dehydrogenase (PDH) (Laughton et al., 2007). Thereby, both cell types complement energetically: astrocytes obtain glucose from the blood through glucose transporter 1 (GLUT1), and metabolize it into lactate due to their increased glycolytic rate, they then release the excessive lactate and neurons uptake it via monocarboxylate transporters (MCTs) (Magistretti and Allaman, 2015, Allaman et al., 2011). Within their cytosol, neurons are able to convert lactate to pyruvate to then carry on with oxidative phosphorylation and ATP production. This process is commonly termed the astrocyte-neuron lactate shuttle (ANLS) (Belanger et al., 2011) (**Figure 20**). Neurons also have the possibility to uptake glucose from the extracellular fluid with their specific transporter GLUT3. Nevertheless, it has been proven that the astrocyte specific transporter GLUT1 is essential for brain cells to survive, since its absence results in severe neurological phenotype (Wang et al., 2006), whereas GLUT3 inhibition do not represent any neurological or brain metabolism abnormalities (Schmidt et al., 2008). In order to maintain a pool of rapidly accessible glucose, astrocytes store deposits of glycogen in their cytosol. Experimental increase of astrocytic glycogen storage have been proven to preserve neuronal function and viability during limited energy supply, such as hypoglycemia (Brown, 2004). In fact, the machinery to trigger glycogen synthesis and breakdown is inactive in neurons, and glycogen deposition induced in cultured neurons caused apoptosis (Vilchez et al., 2007). Therefore, astrocytic glycogen pool is thought to be an essential energy store to maintain the metabolic demands of the different cerebral functions (**Figure 20**).

Ketone bodies. Fatty acids may as well be used as energy source during certain specific circumstances, such as brain development, starvation periods or during high-fat diets. Although still partially understood, increasing evidence suggests as well an astrocyte-neuron interaction for fatty acid metabolism. With this regard, astrocytes may use different fatty acids to generate water-soluble ketone bodies (e.g. β-ketobutyrate, acetoacetate) that can be released to the interstitial fluid and uptaken by neurons via MCTs (Le Foll and Levin, 2016, Nehlig, 2004). Within neurons, ketone bodies may be transported into the mitochondria as

precursors for acetyl-CoA, to finally enter into the TCA cycle and promote ATP synthesis (Nehlig, 2004) (**Figure 20**). In addition, astrocytes have been shown to be responsible of phospholipid regulation, interestingly, via IDH1-mediated reductive carboxylation (Bogdanovic et al., 2014).

Glutamate-glutamine shuttle. Another well studied process in which astrocyte's assistance is essential is the removal of excessive glutamate molecules within the synaptic cleft. Glutamate is the primary excitatory neurotransmitter in the brain and overstimulation of glutamate receptors is highly toxic in neurons (excitotoxicity). To avoid this, astrocytes uptake glutamate through specific excitatory amino acid transporters (EAATs) (Bak et al., 2006), in an ATP-dependent mechanism. In fact, this ATP consumption in astrocytes is a positive regulator of glycolysis and lactate production, what stimulate the ANLS (Bélanger and Magistretti, 2009). When required, astrocytes release glutamate in form of glutamine, after previous conversion via glutamine synthetase (GS), to be then uptaken by neurons and deaminated back into glutamate by glutaminase (GLS), a process known as glutamate-glutamine cycle (Belanger et al., 2011) (**Figure 20**). It is worth mentioning that neurons rely entirely on astrocytes for *de novo* synthesized glutamate, as they are the only neural cell type that express pyruvate carboxylase (PC), being able to produce glutamate from glucose (Belanger et al., 2011, Bak et al., 2006, Gamberino et al., 1997). However, the deficient astrocytic PDH activity aforementioned may limit this de novo glutamate production.

GSH synthesis. One of the most important roles of astrocytes is to provide neurons with the required antioxidant products. Being highly oxidative, neurons are subjected to the toxic effect derived from increased ROS. Yet, these cells lack the metabolic substrates to synthesize important redox compounds, such as glutathione GSH, the most relevant antioxidant in the brain (Bélanger and Magistretti, 2009, Paul et al., 2018). Indeed, astrocytes have proved to be the mayor provider of these substrates, and co-culture of neurons with astrocytes rescues the damage caused by oxidative agents (e.g. H_2O_2, NO) (Calkins et al., 2009). GSH (or γ-L-glutamyl-L-cysteinglycine) is formed by assembling of three different amino acids: glutamate,

glycine and cysteine. As we previously described, astrocytes sustain neurons with glutamate through the glutamate-glutamine cycle. In order for them to provide with glycine and cysteine, the limiting metabolite for GSH production, astrocytes release GSH to the extracellular space. GSH, instead of been directly absorbed by neurons, is cleaved into L-cysteineglycine and subsequently to both cysteine and glycine to be used as GSH precursors by neurons when required (Paul et al., 2018, Dringen, 2000, Aoyama et al., 2008) (**Figure 20**). The highly oxidative landscape of the brain forces it to maintain a stable GSH pool. To do so, NADPH is indispensable as reducing power to maintain a constant recycling of GSH. Interestingly, it has been shown that IDH is the main source of NADPH in the human brain (Atai et al., 2011). Although not yet confirmed, considering their main role as metabolic suppliers, astrocytes are most probably in charge of this function. Another antioxidant that can be provided by astrocytes to neurons is ascorbic acid (AA), a metabolite that requires GSH oxidation (into its disulfide form GSSG) to be formed and once in the neuron, favors lactate metabolism over glucose via MCTs stimulation (Castro et al., 2009) (**Figure 20**). Brain susceptibility to oxidative damage is observed in different neuropathological conditions such as stroke, traumatic brain injury or neurodegenerative diseases, what highlights the importance of astrocytes in neuroprotection (Dringen, 2000).

Besides what it has been discussed above, there are other relevant astrocyte-neuron interactions. The release of H^+ and Na^+ from astrocytes enables MCTs shuttling activity and pH buffering. In addition, astrocytic K^+ buffering after neuronal activity alleviates its accumulation in the extracellular space (Allaman et al., 2011) (**Figure 20**).

Blood nutrient supply. A factor noteworthy to consider with regard to brain amino acid and small molecule supply is the balance between blood uptake and biosynthesis via astrocytes. The exact ratio of income of each amino acid from either blood or astrocytes still remains elusive, however, some studies suggest that the importance of each source will depend on the grade of auxotrophy for each molecule. Therefore, generally, all non-essential amino acids that might be biosynthesized are preferentially produced by astrocytes through their required

precursors. On the other hand, all the essential molecules that may not be generated *de novo* are transported from blood supply (Banos et al., 1975, Cakir et al., 2007). For instance, serine may be synthesized via glucose via PHGDH reaction. Moreover methionine and serine might be combined to produce cysteine, via transsulfuration pathway, which has been shown to be an important cysteine source in astrocytes, especially during increased antioxidant demands (McBean, 2018). However, neither glucose nor methionine are *de novo* synthesizable within the brain.

In summary, there is a wide set of mechanisms that make astrocytes crucial support cells, complementing neurons in a constant symbiosis. Astrocytes act as the perfect engines that enable the motion of neuronal machinery. The biology of these cells is essential to study glioma metabolic behavior, not only because allows to understand general brain metabolism, but also because the majority of IDHm gliomas arise from this specific cell type (e.g. astrocytomas or secondary GBMs). In section 4 we will analyze all the specific metabolic pathways that had been found altered in IDHm gliomas, however, first we will present an introductory section on the basics of cancer metabolism.

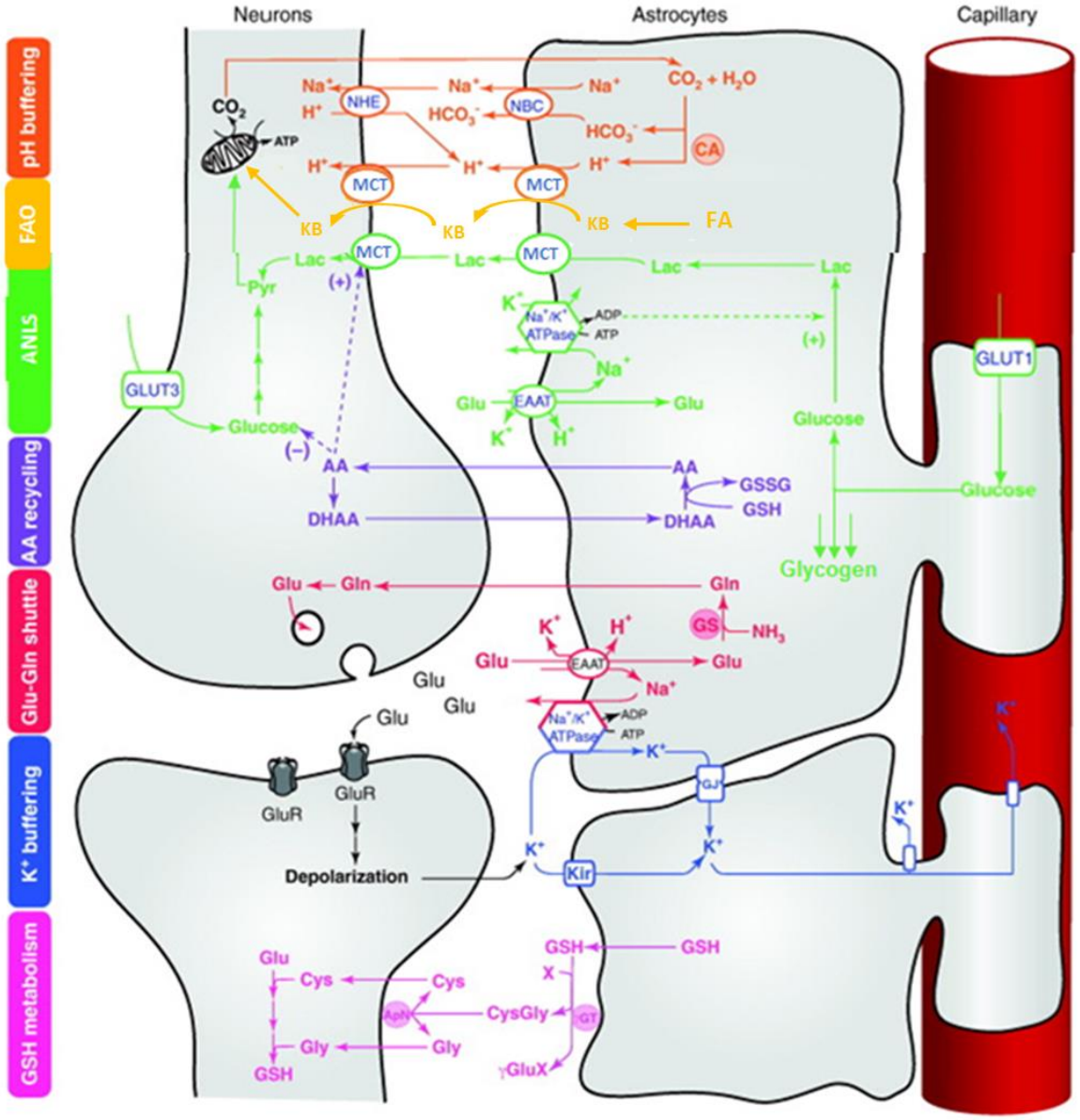

Figure 20. Schematic representation of astrocyte-neuron metabolic interactions.
(I) pH buffering (orange). NHE, sodium-hydrogen exchange; NBC, sodium-bicarbonate (HCO_3^-) co-transporter; MCTs, monocarboxylate transporters; CA, carbonic anhydrase. (II) FAO (Yellow). FAO, Fatty acid oxidation; KB, ketone bodies; FA, fatty acids. (III) ANLS (green). ANLS, astrocyte-neuron lactate shuttle; GLUT3, glucose transporter 3; EAAT, excitatory amino acid transporter; GLUT 1, glucose transporter 1. (IV) AA recycling (purple). AA, ascorbic acid; DHAA, dehydroascorbic acid. (V) Glu-Gln shuttle (red). Glu, glutamate; Gln, glutamine; GS, glutamine synthetase; GluR, glutaminergic receptors. (VI) K^+ buffering (blue). Kir, inwardly rectifying K^+ channels, GJ, gap junctions. (VII) GSH metabolism (pink). Cys, cysteine; Gly, glycine; ApN, ectopeptidase aminopeptidase N; CysGly, cysteine-glycine dipeptide; γGT, γ-glutamyl transpeptidase; X, potential γ-glutamyl acceptor; γGluX, complex of γ-glutamyl and X.
Dashed arrows represent positive (+) or negative (-) stimulation. Adapted from (Allaman et al., 2011).

3.3. Introduction to cancer metabolism

The discovery of aberrant metabolic pathways has unveiled a new paradigm in the study of cancer. Their altered role might have a great impact in the malignancy of the disease since it can trigger a metabolic rewiring that promotes the proliferation of malignant cells, either by increasing macromolecule synthesis (anabolism), energy production (catabolism) or antioxidant defense. However, mutations in metabolic enzymes not always are advantageous for the tumor but may lead to certain metabolic constraints and thus revealing new therapeutic strategies.

The underlying meaning of cancer metabolism lies on the idea that in order to maintain their uncontrolled proliferation, cancer cells reprogram their metabolic activity, thus fueling cell growth and division. In fact, reprogramming cancer metabolism is nowadays considered one of the emerging hallmarks of cancer overall (Hanahan and Weinberg, 2011). Although the new advances in cancer metabolism have nowadays considerably widen this hallmark, its initial conception was entirely sustained by the seminal discovery of Otto Warburg, which occurred nearly a century ago, and gained him the Nobel Prize of Medicine in 1931. Warburg, who is generally credited to be the “father” of cancer metabolism, observed an anomalous characteristic of cancer cell energy production. Under aerobic conditions, normal differentiated tissue (i.e. non-proliferating cells) process glycolytic-derived pyruvate in the TCA cycle within the mitochondria for ATP production. In anaerobiosis, the absence of oxygen constrains respiration, forcing the cells to redirect glycolytic pyruvate into lactate synthesis, what favors more glycolytic activity. This anaerobic glycolysis is a bacterial mechanism yet conserved in eukaryotes that leads to ATP production, although minimal when compared to the highly evolved oxidative phosphorylation. Warburg observed that cancer cells tend to convert glucose to lactate regardless the cellular oxygen levels, a state that has been termed “aerobic glycolysis” (Warburg et al., 1927). In fact, it has been observed that normal proliferative cells, such as many embryonic tissues, share this mechanism. Both cancerous and normal

proliferative cells, continue using some cellular respiration in a small extent, since their mitochondria remains functional. However, this aerobic glycolysis is still very inefficient when compared to oxidative phosphorylation for ATP production (**Figure 21**).

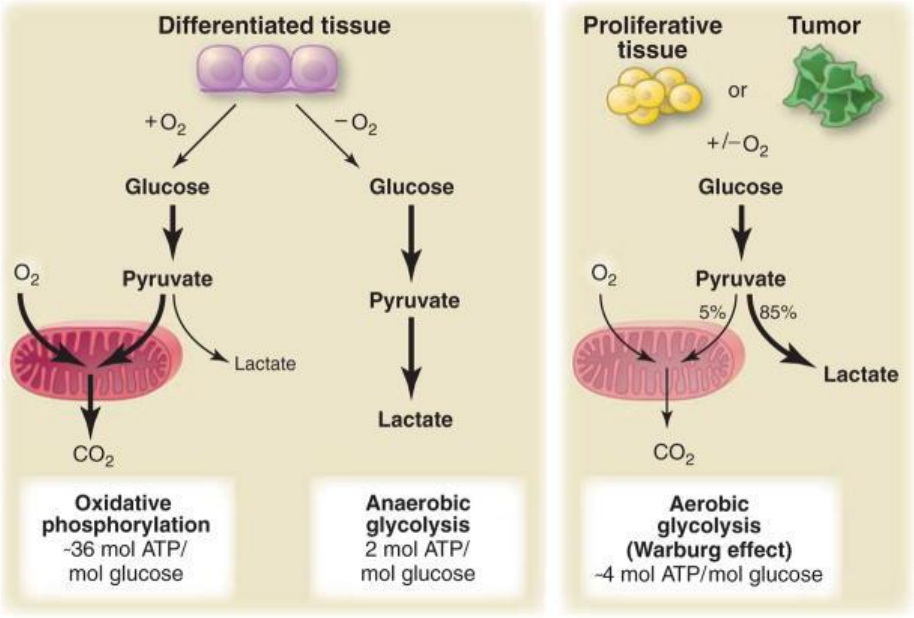

Figure 21. Modes of ATP production of differentiated and proliferative cells.
Schematic representation of the differences among oxidative phosphorylation, anaerobic glycolysis and aerobic glycolysis (Warburg effect). Used from (Vander Heiden et al., 2009).

Such glycolytic switch is seemingly unproductive, and cancer cells must compensate the lower ATP efficiency relative to mitochondrial oxidative phosphorylation. It has been shown that cancer cells indeed upregulate glucose transporters such as GLUT1, thus increasing the glucose uptake into the cytoplasm (DeBerardinis et al., 2008, Hsu and Sabatini, 2008). Moreover, such a short pathway as glycolysis might occur in a much faster way than the multistep process of cellular respiration, therefore by the time one molecule of glucose is completely metabolized to produce ATPs in the mitochondria, the same number of ATPs might have been produced by the overactive aerobic glycolysis. Yet, a robust explanation for the preference of aerobic glycolysis by proliferative cells has been elusive. The most established hypothesis, states that increased glycolysis allows the diversion of its intermediate metabolites into different biosynthetic pathways, including those generating nucleotides and amino acids.

This effect may enhance the formation of the macromolecules required for active cell growth and proliferation (Potter, 1958, Vander Heiden et al., 2009).

Boosted by the advances in biochemical and molecular biological tools, cancer metabolism has gained renewed interest in the past decades expanding our understanding of the mechanisms behind tumor-associated metabolic alterations. Thus, nowadays reprogramming metabolism is understood as a set of different key mechanisms that go beyond energy production. Inspired by the initial work of Hanahan and Weinberg (Hanahan and Weinberg, 2011), a more recent publication exposed and organized known cancer-associated metabolic changes into six hallmarks of cancer metabolism: (1) deregulated uptake of glucose and amino acids, (2) use of opportunistic modes of nutrient acquisition, (3) use of glycolysis/TCA intermediates for biosynthesis and NADPH production, (4) increased demand for nitrogen, (5) alterations in metabolite-driven gene regulation, (6) metabolic interactions with the microenvironment (Pavlova and Thompson, 2016). Based on the cellular metabolism stage, these hallmarks can be sub-divided in three different groups. The first two hallmarks would correspond to (a) altered nutrient uptake. The next two hallmarks would be part of (b) reprogramming intracellular metabolism. The last two hallmarks would exert (c) changes in cell behavior and function (**Figure 22**).

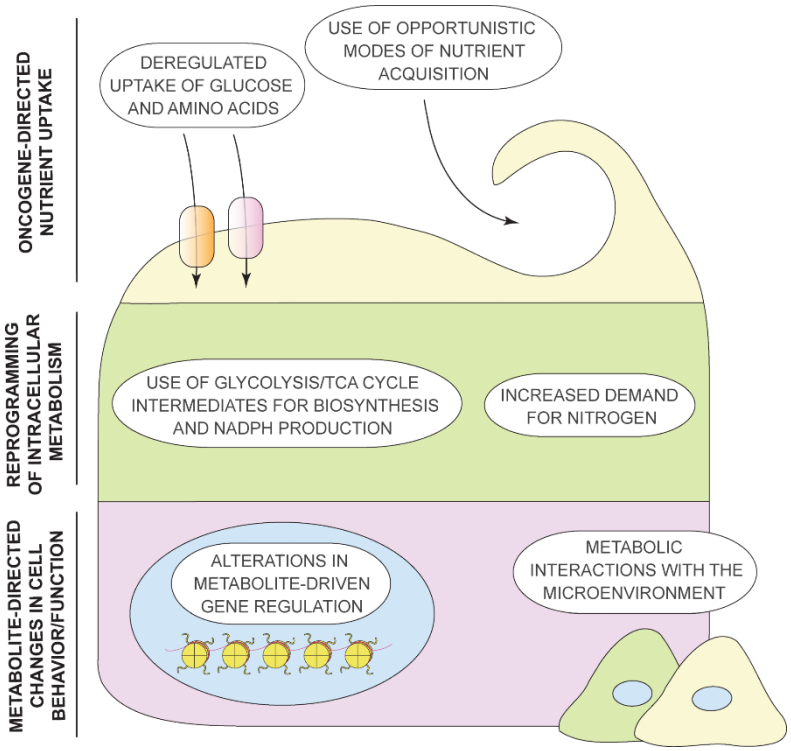

Figure 22. The hallmarks of cancer metabolism.
Six emerging hallmarks of cancer metabolism, subdivided in three layers of cell-metabolite interaction, all of which become reprogrammed in cancer. Used from (Pavlova and Thompson, 2016).

Deregulated uptake of glucose and amino acids. It has been reported that tumors bear a high consumption rate not only of glucose but also of glutamine, compared to normal tissue (Som et al., 1980, Almuhaideb et al., 2011). Catabolism of these metabolites is key to maintain pools of diverse carbon and nitrogen intermediates, such as nucleotides and amino acids, but also to capture reducing power either for ATP production (NADH) or for redox maintenance (NADPH) (Pavlova and Thompson, 2016). It has been shown how these increased nutrient uptake is strictly regulated by growth factor signaling and interactions with extracellular matrix (Lindsten et al., 2003, Grassian et al., 2011). Moreover, the accumulation of different oncogenic alterations such as PI3k/Akt signaling or c-*myc*, can as well induce high nutrient uptake in the absence of those external requirements (Pavlova and Thompson, 2016).

Use of opportunistic modes of nutrient acquisition. Due to the increased rates of consumption, cancer cell environment often experience situations of nutrient shortage. In this scenario, malignant cells are able to activate certain mutations that trigger alternative ways of nutrient

acquisition. The mutation of RAS or c-Src have been shown to enhance the capacity of cells to recover amino acids via lysosomal degradation of extracellular proteins (Commisso et al., 2013). In addition, free amino acids can be as well obtained by entosis: the engulfment and digestion of entire living cells; or by phagocytosis of apoptotic cellular corpses (Krajcovic et al., 2013, Stolzing and Grune, 2004). Thus, mutations that lead to these alternative nutrient procurements, may not only be an advantage but a direct threat over neighbor cells, creating a competition that leads to more aggressive cell populations.

Use of glycolysis/TCA intermediates for biosynthesis and NADPH production. Metabolic reprogramming not only leads to an increased nutrient uptake but also to a change in the way nutrients are used. This metabolite rewiring, will depend on the specific cellular demands. While quiescent tumor cells still conduct their glycolysis and TCA derivatives for oxidative phosphorylation, proliferating cells use these intermediaries for biosynthesis of a diverse array of compounds. Moreover, this reprogramming in central carbon metabolism also permits production of NADPH for most biosynthetic reactions and antioxidant defense (Vander Heiden et al., 2009). Glycolytic-derived glucose-6-phosphate can be redirected into the pentose PPP, one of the main sources of NADPH and ribose-5-phosphate, a structural component of nucleotides (Wang et al., 2011) (**Figure 23**). Other glycolytic intermediates such fructose-6-phosphate or dihydroxyacetone phosphate (DHAP) are crucial precursors of hexosamines (which regulate the stability of certain oncogenic proteins such as c-*myc*) and phospholipids respectively (Itkonen et al., 2013, Pavlova and Thompson, 2016). Moreover, 3-phosphoglycerate, plays a key role in biosynthesis of serine and glycine (**Figure 23**). Around 50% of all cancer cell-serine is derived from glucose (Locasale et al., 2011). Subsequently, serine is the major substrate for one-carbon metabolism or folate cycle, where one-carbon-tetrahydrofolate (THF) species are precursors for purines, thymidines and NADPH production (Fan et al., 2014). Moreover, the redirection of pyruvate from excess glycolytic flux, into lactate helps maintaining NAD^+ levels to sustain glycolysis (Pavlova and Thompson, 2016). However, glycolysis is not the sole epicenter of carbon metabolism, and TCA cycle intermediates are

also used by cancer cells to keep their high biosynthetic rate. The pyruvate that enters TCA cycle may be as well converted into citrate and subsequently secreted into the cytosol to be re-turned into acetyl-CoA for lipid biosynthesis (Bauer et al., 2005). TCA cycle also provides with precursors of several non-essential amino acids such as aspartate or asparagine.

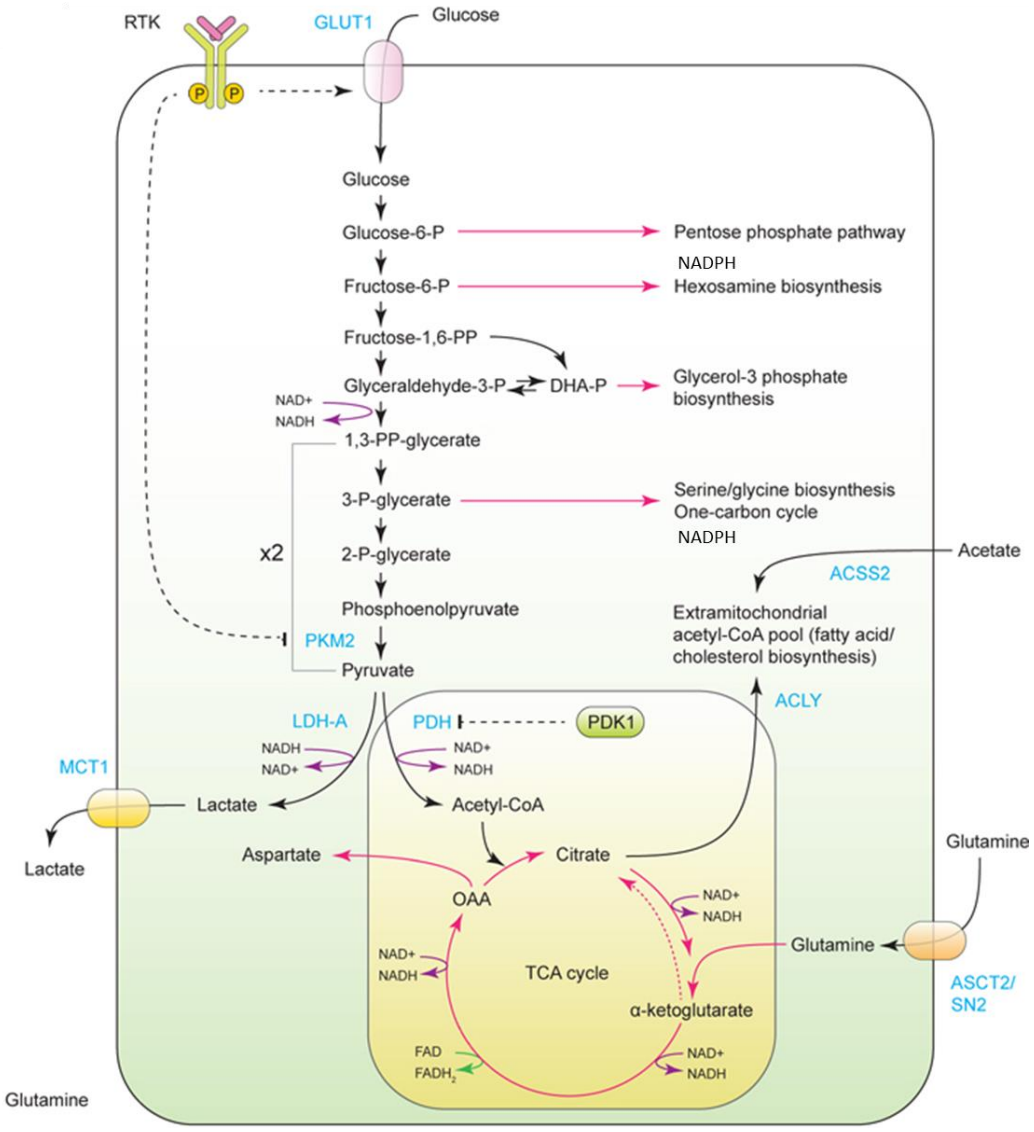

Figure 23. Use of glycolysis/TCA cycle intermediates for biosynthesis and NADPH production. Diverse metabolite regulation of central carbon metabolism. RTK, receptor tyrosine kinase; GLUT1, glucose transporter 1; PKM2, pyruvate kinase M2; ACSS2, acetyl-CoA synthetase 2; LDH-A, lactate dehydrogenase A; PDH, pyruvate dehydrogenase; PDK1, pyruvate dehydrogenase kinase 1; ACLY, ATP-citrate lyase; MCT1, monocarboxylate transporter 1; ASCT2/SN2, glutamine transporter. Adapted from (Pavlova and Thompson, 2016)

To maintain TCA cycle active independently of glucose, cancer cells use anaplerotic influx into the cycle. This anaplerotic influx can be derived from different sources such as glutamine and glutamate but also glucose-independent pyruvate or aspartate (DeBerardinis et al., 2007) (**Figure 23**).

Increased demand for nitrogen. Besides carbon metabolism, increasing evidence points to the importance of nitrogen regulation in tumorigenesis. One of the main nitrogen sources in cancer cells is glutamine, which amine group is crucial for synthesis of nucleotides, as well as glutamate and other non-essential amino acids via transamination (Gaglio et al., 2009). Arginine, can also be important for a wide variety of nitrogen compounds such as creatine, proline and polyamines, which accumulation have been shown to inhibit apoptosis and promote tumor invasion (Casero and Marton, 2007). Elevated synthesis of proline have been observed in different tumors, and its accumulation is thought to facilitate collagen production and new extracellular matrix deposition, enabling tumor invasion (Phang et al., 2008).

Alterations in metabolite-driven gene regulation. Certain metabolic network alterations not only influence direct nutrient regulation, but may as well drive genomic reprogramming by deposition and removal of epigenetic marks on chromatin. We already discussed in section 2.2 how the production of D-2HG by IDHm leads to competitive inhibition of α-KG-dependent dioxygenases what leads to an increase in DNA and histone methylation. However, it has been found that succinate and fumarate accumulation may as well lead to dioxygenases inhibition and subsequent increase in methylation. Different cancer types show these effect due to succinate dehydrogenase (SDH) or fumarate hydratase (FH) mutation (Janeway et al., 2011, Tomlinson et al., 2002). Moreover, recent reports have shown that S-adenosylmethionine (SAM), a product of the one-carbon metabolism mediated by serine, acts as an important methyl group donor directly influencing the levels of histone and DNA methylation (Chiang et al., 2009). In addition, recent studies demonstrate that when cells metabolize more glucose than needed, acetyl-CoA will serve as substrate for histone acetylation, a process that unlike

methylation, leads to an increased accessibility of genomic DNA for assembly of transcription factors (Cai et al., 2011).

Metabolic interactions with the microenvironment. The metabolic state of a cell not only affects its own fate but may as well influence the microenvironment to assist tumor growth and invasion. In this sense, lactate secretion during aerobic glycolysis, may play a central role. It has been observed that increased extracellular lactate levels promote immunosuppression by attenuating the activity of dendritic cells, T cells, macrophages or monocytes (Fischer et al., 2007, Goetze et al., 2011, Gottfried et al., 2006, Colegio et al., 2014). Besides, lactate secretion together with the hypoxic environment of certain tumor areas, may promote stabilization of HIF1α and activation of vascular endothelial growth factor (VEGF), facilitating the surge of angiogenesis (Constant et al., 2000). In addition, the extracellular acidification due to high lactate levels stimulates the proteolytic activity of matrix metalloproteinases (MMPs), leading to degradation of extracellular matrix and enhancing tumor invasion (Rothberg et al., 2013).

In conclusion, cancer metabolism may be composed of a wide variety of mechanisms, either intrinsic or extrinsic, that provide cells with the raw materials needed to sustain their invasive and uncontrolled growth. For this reason, the specific physiological context where each tumor originates will be fundamental for its progression. In the case of glioma, the brain acts as a semi-closed system with a particular metabolic landscape, essential to address the vulnerabilities that determine brain tumor fate.

4. Metabolic alterations of IDH mutant gliomas

Isocitrate dehydrogenases 1 and 2 (IDH1 and IDH2) are the metabolic enzymes most frequently mutated in cancer, being commonly observed in gliomas, acute myeloid leukemia (AML) and chondrosarcoma. Other important metabolic enzymes, central in the fueling of the TCA cycle such as succinate dehydrogenase (SDH) or fumarate hydratase (FH), have also shown to be mutated in different cancers e.g. paraganglioma, renal carcinoma or T-cell leukemia among others (Sciacovelli and Frezza, 2016). The essential difference between these mutations, is that they represent loss-of-function mutations whereas in the case of IDH it constitutes a gain of function mutation. This leads to a neomorphic reaction that produces the oncometabolite D-2HG.

Besides D-2HG production, various metabolic pathway alterations in IDHm tumors may be triggered by the stoichiometric imbalance of IDH reaction after the mutation. Hence, the impair of normal enzymatic conversion of isocitrate to α-KG and NADPH generation, may have profound impacts in cellular metabolism by altering metabolic flux of α-KG, depleting NADPH and impairing canonical biosynthetic pathways that require wild type IDH activity. In this section we will review some of the most important metabolic routes that are affected by IDH mutation.

4.1. Glucose metabolism

As we addressed previously, cancer cells predominantly upregulate their glycolytic flux, and these may be induced through a diverse number of signaling pathways. One of these pathways is PI3K/Akt cascade, which contributes to growth and aggressiveness in gliomas (Bleau et al., 2009, Bai et al., 2016). This cascade is commonly downregulated in IDHm gliomas what suggests a potential vulnerability in glucose metabolism. Specifically, this pathway stimulates metabolic biosynthesis and glycolysis by favoring the expression of nutrients transporters, such as GLUT1, and boosting the activity of glycolytic enzymes such as Pfkfb3 (DeBerardinis et al., 2008, Vander Heiden et al., 2009). Interestingly, different studies showed that isogenic

glioblastoma cells bearing the IDH1 mutation promote a decrease in Akt expression both from genetic and protein perspective, as well as decreased phosphorylation-derived activation (Bralten et al., 2011, Birner et al., 2014). Moreover, *in vivo* inhibition of PI3K pathway has shown to not only increase survival, but also lead to a reduced D-2HG production of IDHm tumor cells (Batsios et al., 2019). This suggests that IDH mutation interacts with PI3K/Akt pathway and may attenuate the glycolytic impact in the cell. Indeed, some of the top downregulated genes in IDH mutant tumors are proteins directly linked with PI3k/Akt activation (e.g. PDPN1 and RBP1) (Noushmehr et al., 2010). However, it has been found that IDH1m oligodendroglioma tumors, exhibit high PI3K/Akt activation (Parker and Metallo, 2015). Thus, the exact mechanism by which IDH mutation affects Akt activity in either oligodendrogliomas or astrocytomas remains unclear, especially taking into account that normal astrocytes are indeed highly glycolytic and overexpress Pfkfb3 (Belanger et al., 2011). It has been shown, however, that D-2HG may activate mTOR, a downstream factor of Akt, independently of this pathway (Carbonneau et al., 2016). Therefore, this would be a compensatory mechanism by which IDH mutant cells undergo glycolysis despite low PI3k/Akt activation (Cheng et al., 2014). Yet, it has been proven that IDHm tumors display an overall low glucose turnover into TCA cycle intermediaries and an overall low ATP production (Fack et al., 2017).

Another common feature of glycolytic cancer cells is the upregulation of lactate dehydrogenase A (LDHA), which is indeed a critical enzyme for GBM aggressiveness (Daniele et al., 2015). This enzyme is in charge of the final step of glycolytic metabolism leading to the transformation of pyruvate into lactate, and maintaining glycolysis via NAD^+ regeneration (Metallo and Vander Heiden, 2013). This is also a common pathway used by normal astrocytes (Belanger et al., 2011), however, in line with the low PI3k/Akt activity, IDH1m gliomas show decreased levels of LDHA when compared to IDH wild type (Parker and Metallo, 2015). Indeed, it has been observed that both IDH1m glioma and brain tumor-derived stem cells silence LDHA expression through promoter hypermethylation (Chesnelong et al., 2014). In addition, IDHm AML patients show as well lower levels of LDH activity when compared with their IDHwt counterparts,

suggesting a common phenotype between IDH mutant tumors (Chou et al., 2011). LDHA expression is commonly regulated by HIF1-α (Keith et al., 2011), however, its role in IDHm tumors is not clear due to the contradictory findings with regard to D-2HG-dependent HIF1- α stabilization (Zhao et al., 2009) or degradation (Koivunen et al., 2012). Studies that support the hypothesis of a HIF1-α degradation in IDHm gliomas, have found upregulated gene expression of factor inhibiting HIF1 (FIH-1) in these tumors (Mustafa et al., 2014). Moreover, it has been observed that LDHB, is increased in glioma cells with IDH mutation when compared with IDHwt gliomas or normal brain tissue (Mustafa et al., 2014). LDHB is a HIF1-α-independent enzyme that, although capable to convert pyruvate to lactate, it has shown to be more sensitive to substrate inhibition, been able to perform the reverse reaction and convert lactate to pyruvate (Dang, 2013) (**Figure 24**). Taking into account the metabolic scenario of the brain, it is possible that glioma cells uptake the lactate secreted by astrocytes, converting it into pyruvate via LDHB.

The canonical entry into the TCA cycle requires the conversion of glucose-derived pyruvate into acetyl-CoA via pyruvate dehydrogenase (PDH) (Pavlova and Thompson, 2016). Interestingly, the activity of this enzyme is mediated as well by HIF1-α, which stimulates the expression of PDK1 that displays the inactivating phosphorylation of PDH (Kim et al., 2006). The altered activity of HIF1- α in IDHm tumors, may be therefore directly related with changes in flux of pyruvate-derived acetyl-CoA into the mitochondria (Parker and Metallo, 2015). Thus, in the scenario where IDH mutant gliomas express high HIF1- α (Xu et al., 2011b), PDH activity would be expected to be attenuated. Different anaplerotic entries into the TCA cycle may be also active in these tumors, such as oxaloacetate income via pyruvate carboxylase (PC) or α-KG entry via glutaminolysis (Cheng et al., 2011). Whereas IDHwt GBM activate both PDH and PC (Marin-Valencia et al., 2012), it has been shown that overexpression of IDH mutant enzyme in normal astrocytes leads to and increased flux through PC as well as its increased gene expression (Izquierdo-Garcia et al., 2014). This implies that PC activity is important for IDH mutant cells to maintain TCA cycle pace (Laughton et al., 2007, Bak et al., 2006) (**Figure 24**).

As we will forthcoming address, the other alternative entry into the TCA cycle via gluaminolysis-derived α-KG, plays a critical role in the overall IDH mutant regulatory metabolism.

4.2. Glutaminolysis, reductive carboxylation and acetyl-CoA

Glutamine is an important contributor to TCA metabolism in cancer, entering as α-KG after previous conversion into glutamate, a process commonly denominated glutaminolysis (Maus and Peters, 2017). Moreover, glutamate is also important to direct biosynthesis of different molecules such as nucleotides, hexosamines or asparagine (Gaglio et al., 2011). During glutaminolysis two enzymes play crucial roles; glutaminase (GLS) performs the conversion of glutamine to glutamate, and glutamate dehydrogenase (GDH or GLUD) converts glutamate to α-KG (**Figure 24**). During the hypoxic conditions at the core of most solid tumors, the normal glucose oxidation for TCA metabolism gets restricted, and glutaminolysis serves then as a compensatory mechanism against this effect (Fan et al., 2013). Furthermore, as we have previously discussed, the canonical entry into TCA cycle through PDH activity may be altered in IDHm gliomas, what makes glutaminolysis flux especially necessary. In addition, the presence of IDH mutation restricts the α-KG availability for either mitochondrial TCA cycle or cytosolic usage (i.e. dioxygenases activation or glutamate and lipid biosynthesis) (Maus and Peters, 2017). Whether the mutation occurs in IDH1 (cytosolic) or IDH2 (mitochondrial) will tilt the balance to either pathway. Yet, IDH mutation rarely occurs in both isoforms at the same time, and the wild type isoenzyme can attempt to compensate the imbalance generated by the mutant one.

Different studies highlight the importance of glutaminolysis in IDHm tumors. Indeed, high extent of the D-2HG produced by IDH1 mutant cells is derived from glutamine, suggesting that glutaminolysis may as well serve as source of α-KG, besides the IDHwt monomer of the IDHm/wt heterodimer (Grassian et al., 2014). In fact, IDHm glioma cells may possibly uptake the glutamine secreted by astrocytes in the brain interstitial fluid during the glutamate-

glutamine cycle, in order to satisfy their high glutaminolysis rate. IDHm-transfected GBM cells and astrocytes have showed to be especially sensitive to GLS inhibition (Seltzer et al., 2010). Moreover, it has been observed that IDH1m gliomas overexpress both GDH1 and GDH2, and GDH1/2 knockdowns of IDH1m glioma *in vivo* models, showed decreased tumor growth (Chen et al., 2014). In addition, IDHm-transfected GBM cells and astrocytes showed to be especially sensitive to GLS inhibition (Seltzer et al., 2010).

During normoxic conditions, healthy cells favor the IDH oxidative decarboxylation of isocitrate to α-KG. However, under conditions of hypoxia or mitochondrial dysfunction, IDH catalyzes the reductive carboxylation of α-KG to isocitrate. This reverse reaction, which entails NADPH consumption, will further favor synthesis of citrate and acetyl-CoA, a basic source of fatty acids, phospholipids, cholesterol or amino acids (Metallo et al., 2011, Kaelin and McKnight, 2013) (**Figure 24**). Whereas the reverse IDH2 reaction may serve as a switch in the directionality of TCA cycle, in IDH1 this reverse reaction has a key biosynthetic role. Therefore, the biosynthesis requirements during hypoxia may be fulfilled by cytosolic IDH1 reverse activity. This is at the same time associated with a higher flux of glutaminolysis towards α-KG, facilitating these biosynthetic reactions (Metallo et al., 2011). As we described in section 2.2, IDHm cells express a heterodimeric enzyme formed by the complex of an IDHm monomer with an IDHwt one. It has been shown that the reductive carboxylation reaction is inactive upon these IDH1 or 2 mutant/wild type heterodimers (Leonardi et al., 2012). Thus, only IDH wildtype cells expressing the normal IDH homodimer are able to perform both forward and reverse reactions. The inefficiency of IDHm cells to produce isocitrate may rely in the preference of IDHm monomer for α-KG consumption and D-2HG synthesis. This aberrant hoarding of IDHm enzyme for α-KG, would explain as well the high levels of glutamine-derived D-2HG, and subsequent low glutaminolysis-derived citrate and acetyl-CoA synthesis during hypoxic conditions (Grassian et al., 2014). Indeed it has been shown that not only IDHwt but also IDH2m cells show a higher activation of glutamine reductive metabolism when compared to

IDH1m cells, suggesting the importance of cytosolic IDH for this pathway (Parker and Metallo, 2015) (**Figure 24**).

Due to their defective glycolytic machinery (e.g. low PI3K/Akt signaling), IDHm cells are thought to be rather oxidative. In fact, it has been observed that during hypoxic conditions, these cells increased their cellular respiration but decrease cell growth (Grassian et al., 2014). This suggests that, due to their inactive reductive carboxylation, IDHm cells focus in the use of their scarce acetyl-CoA to gain ATP by oxidative phosphorylation to detriment of their biosynthetic metabolism, what decelerates cell growth. The dependence of these cells on oxidative phosphorylation is seconded by their observed sensitivity to ETC/respiration inhibitors and changes in oxygen consumption rates under hypoxia (Grassian et al., 2014). Moreover, it has been shown that D-2HG can additionally inhibit complex IV of the ETC, increasing their energetic limitations (Chan et al., 2015).

Acetyl-CoA is an essential metabolite which production directly affects the synthesis of lipids but also of acetylated amino acids (Kaelin and McKnight, 2013). It has been reported that certain N-acetylated amino acids including N-acetyl-aspartyl-glutamate (NAAG) and N-acetyl-aspartate (NAA) are decreased in IDH1m glioma cells (Reitman et al., 2011). These may be directly linked with the restricted flux fueling acetyl-CoA pools, due to defects in reductive carboxylation or PDH activity. IDH1m tumors show as well dysregulated phospholipid profile when compared to IDHwt tumors (Fack et al., 2017), especially pools of phospholipid metabolites such as phosphoethanolamine and glycerophosphocholine (Esmaeili et al., 2014). Interestingly, the dysregulated lipid metabolism in IDHm gliomas may be as well altered by PI3k/Akt oncogenic signaling pathway. For instance, ATP-citrate lyase (ACL or ACLY), the enzyme in charge of synthesis of acetyl-CoA from citrate, is a major Akt substrate (Berwick et al., 2002). In addition, Akt also induces the activation of other lipid and fatty acid synthesis enzymes (e.g. FAS, ACC) via mTOR and SREBP-1 (Porstmann et al., 2008). Apart from *de novo* synthesis, lipids can be as well scavenged from the extracellular fluid. LDL receptor, which supply cells with cholesterol, is also regulated by PI3K/Akt pathway via SREBP-1 (Guo

et al., 2011). In fact, IDH1 is a transcriptional target of SREBP-1, which further supports a dysregulated lipogenic environment in IDHm gliomas. Interestingly, it has been observed that the excess of ketone bodies, such as the one promoted by astrocyte release, may be used by glioma cells as an alternative acetyl-CoA source via upregulation of monocarboxylate transporters (MCTs) (De Feyter et al., 2016). However this may contradict the idea that a ketogenic diet might have a therapeutic effect in glioma (Thomas and Veznedaroglu, 2020)

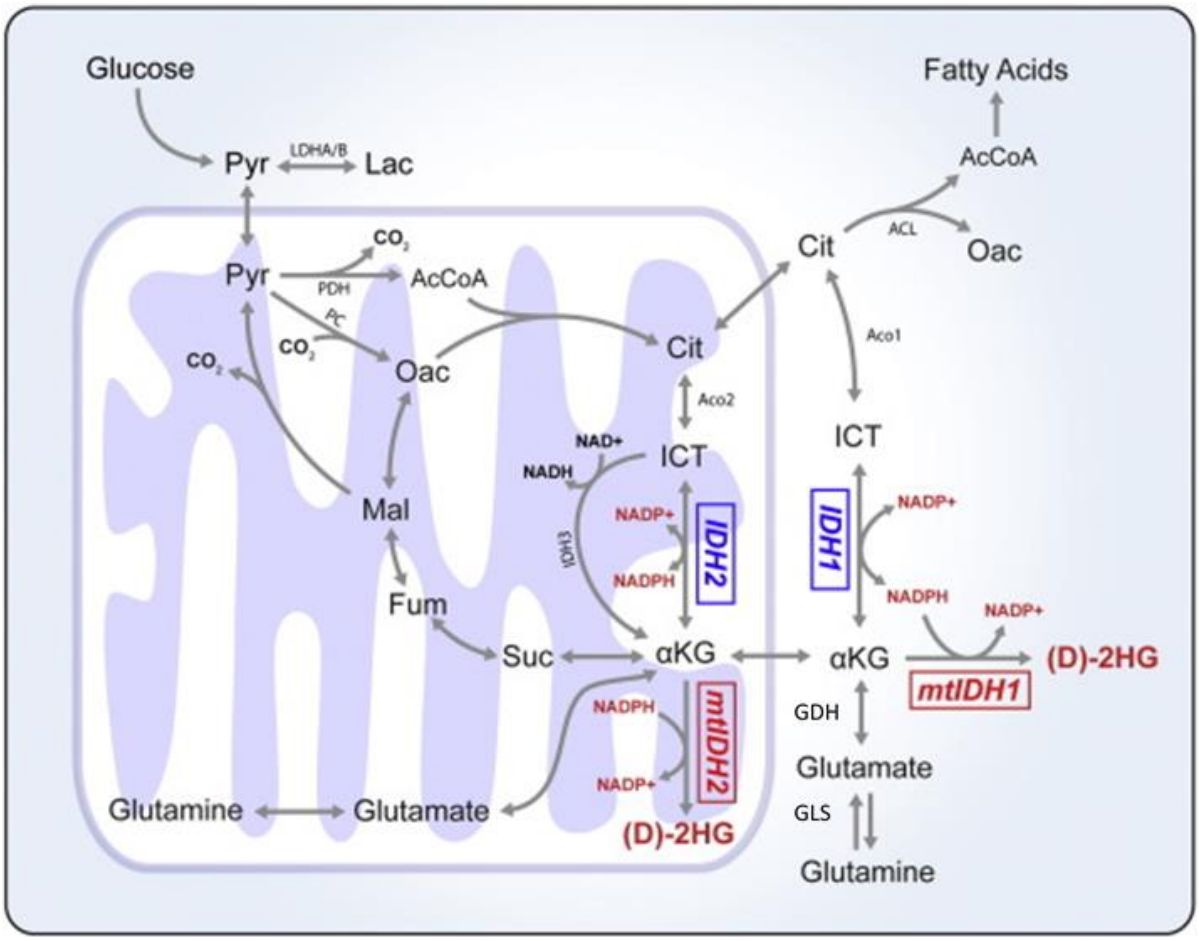

Figure 24. Biochemical pathways involved in IDHm intermediary metabolism.
The activity of lactate dehydrogenase B (LDHB) may facilitate the input of pyruvate into the mitochondrion. PC-mediated Pyruvate fueling into the TCA cycle in form of oxaloacetate may be the leading way of entry. Glutamine-derived α-KG may as well serve as anaplerotic TCA cycle fueling. In addition, DH mutation hampers the isocitrate availability as fatty acid precursor. AcCoA: acetyl-coenzyme A, ACL: ATP-citrate lyase, Aco1/2: aconitase 1/2, Cit: citrate, Fum: fumarate, ICT: isocitrate, Lac: lactate, Mal: malate, Oac: oxaloacetate, Pyr: pyruvate, Suc: succinate. Used from (Parker and Metallo, 2015).

4.3. Antioxidant defense

The main similarity between IDH1 and IDH2 is the NADP(H) dependency, unlike IDH3 which is NAD(H) dependent. Both NAD and NADP are essential electron donors (at their reduced state; NADPH, NADH) or acceptors (at their oxidized state; $NADP^+$, NAD^+) in biochemical reduction or oxidation reactions respectively (section 3.1.3). Generally, NAD(H) cofactor is preferentially used during catabolic energy-producing reactions (e.g. TCA cycle-derived ATP production), whereas NADP(H) is more common in biosynthetic reactions (e.g. lipids synthesis) and redox homeostasis (e.g. antioxidants recycling) (Al-Khallaf, 2017). Indeed, the ratio $NADP^+$/NADPH has a critical impact in cellular physiology (Pollak et al., 2007). In cancer, NADPH pool is rapidly replenished. In 20 minutes can be completely regenerated, a much higher pace than in normal tissue (Fan et al., 2014). Although initially it was thought that the PPP was the main source of NADPH, recent evidence suggests that several other enzymes are also important contributors. IDH is among them, as well as malic enzymes (ME), aldehyde dehydrogenases (ALDH) or methylene tretrahydrofolate dehydrogenases (MTHFD) (Pollak et al., 2007, Fan et al., 2014, Lunt and Vander Heiden, 2011). In fact, the preference for each enzyme is tissue-dependent. Interestingly, IDH has been shown to be the main contributor of NADPH in human brain, however this mechanism is not reproduced in rodents, suggesting the exclusive complexity of human brain metabolism (Atai et al., 2011). Moreover, NADP(H) cannot be directly transported across organelle membranes, therefore the maintenance of this cofactor is independently regulated in each subcellular compartment (Parker and Metallo, 2015). This suggests that whereas IDHwt isoform can replenish metabolite imbalances generated by the IDHm one (e.g. α-KG transport), this is not the case with regard to NADPH compensation.

As expected, the presence of the IDHm heterodimer, not only hoards most of the α-KG available, but also the NADPH, required for D-2HG generation. Therefore, IDH mutation de-activates the NADPH-producing capacity of these enzymes, and IDHm cells may require to reroute flux through compensatory pathways to avoid an $NADP^+$/NADPH imbalance (Han et

al., 2020). The direct consequence of this type of imbalance is, on one hand, an alteration of NADPH-dependent biosynthetic reactions, but most importantly a dysregulated redox homeostasis. This redox homeostasis is reached in normal cells when the ROS are properly neutralized. The uncontrolled proliferation and growth of cancer cells make them highly susceptible to oxidative stress. In fact, the therapeutic effect of certain strategies, such as radiation, is based on inflicting oxidative damage in the tumor (Perillo et al., 2020). For this reason, due to the relevance of IDH in the production of NADPH and maintenance of antioxidant defense, various groups are studying the potential redox vulnerabilities of IDHm tumors. Moreover, the highly oxidative metabolism of the brain make gliomas especially interesting targets for redox-based therapeutic strategies (Han et al., 2020). As a matter of fact, IDHm gliomas have been proved to be highly sensitive to oxidative stress-inducing radiotherapy or chemotherapy (Juratli et al., 2015, Mohrenz et al., 2013, Li et al., 2013).

GSH synthesis. As explained in section 3.1.3, GSH is the most important antioxidant in animal cells, due to its abundance and its potent mechanism of action. Increasing efforts are been directed to determine the precise impact of IDH mutation in NADPH, GSH and ROS production, however, the lack of appropriate models carrying the endogenous IDH mutation and the reactive nature of redox compounds, makes it an elusive challenge. Different studies carried out with *in vitro* (Shi et al., 2014) and *in vivo (Sasaki et al., 2012)* models as well as patient cohorts (Bleeker et al., 2010), show how IDH mutant tumors display lower NADPH levels, as well as lower GSH and/or higher ROS generation. However, some studies show that, although IDH1m gliomas exhibited increased $NADP^+$/NADPH ratio, decreased GSH and decreased ascorbic acid in the brain, intracellular ROS were significantly lower when compared to IDH1wt (Sasaki et al., 2012). More recent studies continue exposing unexpected data. Whereas some appreciate no differences in NADPH in IDHm gliomas despite a decrease in GSH, (McBrayer et al., 2018), others observe the inverse effect (Fack et al., 2017). Several factors may be driving these contradictory results. Due the complexity of redox metabolism, it is possible that other unconsidered molecular variables are interplaying.

Recently, novel perspectives are studying alternative routes by which IDHm gliomas maintain their GSH storage, overcoming their potential imbalance of reducing power. Indeed, before been able to recycle their antioxidant pool, cells need to acquire GSH in order to store it for the first time. As we explained in section 3.2, in the particular metabolic landscape of the brain, astrocytes are the main suppliers of GSH precursors (cysteine, glutamate and glycine) (Belanger et al., 2011). Therefore, in order to create a sufficient GSH pool, glioma cells may uptake GSH precursors released by astrocytes in the extracellular fluid in order to synthesize their own GSH *de novo* in a NADPH-independent manner. This would explain how, despite bearing IDH mutation, these tumors could keep their GSH storage full. Interestingly, astrocytic gliomas may even have the intrinsic machinery to produce their own GSH precursors. In the process of GSH (γ-L-glutamyl-L-cysteineglycine) synthesis, a cysteine and a glutamate molecules are first combined via glutamate-cysteine ligase (GCL) to form γ-glutamylcysteine. Subsequently, glycine and γ-glutamylcysteine are condensed by glutathione synthetase (GSS) to produce GSH (Forman et al., 2009) (**Figure 25**). Therefore, the amount of GSH that will be able to be newly synthesized will depend on the availability of the cysteine, glutamate and glycine. Some recent studies in IDHm gliomas, propose to stop GSH biosynthesis by blocking the source of its precursor amino acids. In one study carried out with *in vitro* and *in vivo* models transfected with or without IDH1m overexpressing vectors, it was observed that D-2HG directly inhibits the activity of branch chain amino acid transaminase 1 and 2 (BCAT1/2). These enzymes are in charge of the production of glutamate via branch chain amino acids (BCAA, i.e. valine, leucine and isoleucine). This study defended that IDHm gliomas are restricted to use glutamine as their only source of glutamate and subsequently of GSH. Thus, they observed that inhibition of GLS with CB-839 sensitized IDHm glioma cells to oxidative stress, due to GSH depletion. Moreover, the specificity of the approach was lost when used the GCL inhibitor buthionine-sulfoximine (BSO), which was highly toxic for both IDHm and IDHwt cells (McBrayer et al., 2018). A more recent study observed that IDHm glioma cells were vulnerable as well to the block of NRF2 signaling pathway, in charge of transcriptional regulation of GSH synthesis under oxidative stress stimulus (Tang et al., 2020).

Cysteine availability. Yet, among the three amino acids required for synthesis of GSH, the least abundant of them is cysteine, which represents the limiting factor for the production of the antioxidant (Griffith, 1999). Indeed, cysteine contains the thiol group that will confer GSH its particularly high reactivity against ROS. Cysteine, as a free amino acid in the extracellular fluid, is very unstable and tend to oxidize into its dimeric form cystine, by forming disulfide bonds from the thiol groups of every two molecules (Forman et al., 2009). The supply of cysteine is very restricted in the brain, where it is ~ 100 times less concentrated than in blood (Engelborghs et al., 2003). Cells may uptake it from extracellular sources in form of cystine through the cystine/glutamate antiporter (xCT) or synthesize it de novo via transsulfuration pathway (Paul et al., 2018). The use of xCT to acquire cysteine may be counterproductive when aiming to generate GSH, since by using this antiporter glutamate will be released out of the cell. Moreover, in order to reduce cystine into cysteine, additional reducing power would be required. Thus, in an oxidative stress scenario where extra cysteine is required for GSH production, astrocytic transsulfuration pathway (TP) is thought to be highly active in the brain (McBean, 2012, McBean, 2017). The TP consists of a number of different reactions where the thiol group from methionine will be transferred into various intermediate metabolites (such as homocysteine or cystathionine) to finally result in cysteine formation (Sbodio et al., 2019). Serine will as well play here a key role. On one hand because will be required in the TP for the synthesis of cystathionine, and on the other hand because it can be interconverted into glycine by the action of serine hydroxymethyltransferase (SHMT) (Locasale, 2013). As aforementioned, besides glutamate and cysteine, glycine is the other precursor amino acid for GSH synthesis. In addition, cysteine can also be catabolize to produce taurine, which may have an important role in the CNS as neurotransmitter, as a trophic factor during development (Wu and Prentice, 2010) (**Figure 25**). A recent publication suggests that TP may be an essential source of cysteine from GSH in IDHm gliomas (Fack et al., 2017). In this study, performed in patient derived xenografts, cystathionine, the substrate for cysteine synthesis, showed to be decreased in IDHm gliomas when compared to IDHwt, suggesting higher consumption rate. Moreover, it was observed that CBS, one of the main mediators of TP, was

genetically upregulated in IDHm glioma patients according to The Cancer Genome Atlas (TCGA) database (Fack et al., 2017). These findings open the door to a new therapeutic perspective for IDHm gliomas, in which cysteine production could be blocked by targeting some of the main mediators of TP, thus depleting the GSH pool.

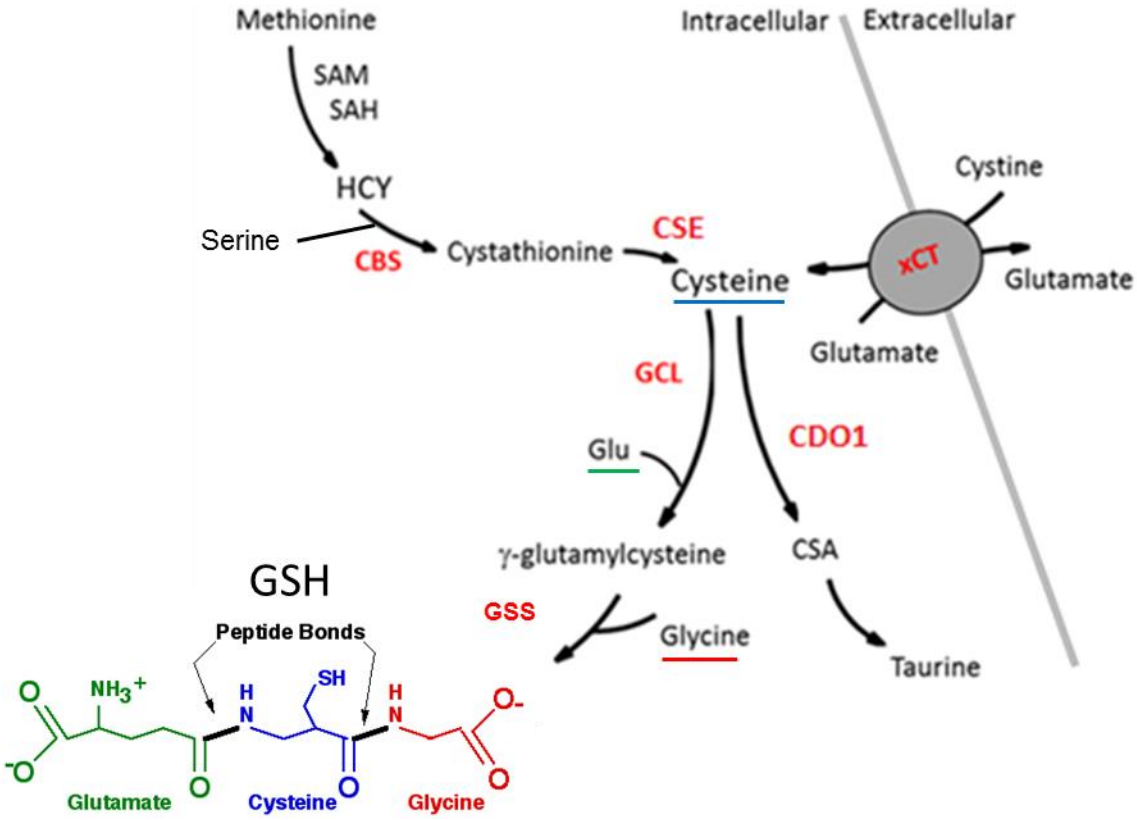

Figure 25. Cysteine metabolism and *de novo* GSH synthesis.
Cysteine can be synthesized via transsulfuration pathway, in which methionine and serine are key substrate metabolites. In addition, cysteine may be uptaken via xCT antiporter, which incorporates oxidized cysteine (cystine) in the cell and releases glutamate to the extracellular fluid. Cysteine (blue) may be used as substrate for taurine, or for GSH de novo synthesis, being the limiting factor in the assembling with glutamate (green) and glycine (red) for GSH formation. CBS: cystathionine β-synthase, CDO1: cysteine dioxygenase 1, CSA: cysteine sulfinate, CSE: cystathionine γ-lyase, GCL: glutamate-cysteine ligase, GSS: glutathione synthetase, SAH: S-adenosyl homocysteine, SAM: S-adenosyl methionine, xCT: cystine/glutamate antiporter. Adapted from (Fack et al., 2017).

Overall, the field of redox metabolism encompasses a broad spectrum of chemical reactions which is nowadays yet under elucidation. Despite the recent advances in the area, there is still room for vast improvement in the understanding of redox metabolism of IDHm gliomas. Yet,

wide amount of evidence point to oxidative damage as a key approach that could be therapeutically harnessed for the improvement of patient prognosis of such a deadly and elusive disease. Before addressing the specific strategic perspectives in line with these ideas of the present PhD, we will review the different therapeutic approaches against IDHm gliomas that are currently in and pre-clinical studies.

5. Therapeutic strategies targeting IDH mutant gliomas

The high prevalence of IDH mutations in gliomas and other tumors has led to intensive research efforts to identify small-molecule inhibitors of IDHm or related downstream targets. Moreover, the advances in the field of immunotherapy has disclosed new medical opportunities. Ongoing pre-clinical and early clinical studies of potential therapies in the context of IDHm gliomas, highlight a promising development for anti-cancer therapy. Prior to any other chemical approach, surgical resection represents the therapeutic strategy that currently bears a more favorable outcome for IDHm glioma patients, especially in astrocytomas (Beiko et al., 2014, Kawaguchi et al., 2016). The development of non-invasive imaging techniques to detect D-2HG as a method to discriminate between IDHm and IDHwt tumors, may have significant clinical implications (Andronesi et al., 2013, Emir et al., 2016). In addition, radiotherapy also represents an important therapeutic tool, likely enhanced by the potential sensitivity of IDHm tumors against the oxidative damage generated by this type of treatment (Juratli et al., 2015, Li et al., 2013).

IDHm inhibitors. Due to the wide variety of malignant aberrations linked to IDH mutation and its neomorphic activity, the direct targeting of this mutant enzyme has been laboriously studied (**Figure 26**). Some promising results were achieved by the use of the pan-inhibitor BAY1436032. This inhibitor has shown to efficiently inhibit both IDH1 and IDH2 mutant isoenzymes and lower considerably the D-2HG production in both an *in vitro* and *in vivo* set up (Pusch et al., 2017). The inhibition lead to a certain increase in xenograft mice survival after a bi-daily dose of 75mg/kg of the drug, although this has so far not been reproduced in other models (Pusch et al., 2017). Other tested IDHm inhibitors also did not show very satisfactory results. A study carried out with MRK-A $IDH1^{R132H/WT}$ inhibitor showed no alteration in tumor growth or survival of patient derived-GB10 glioma xenografts. However, the same MRK-A dose prolonged survival in BT142 xenografts (Kopinja et al., 2017). It is noteworthy to mention that BT142 xenografts are derived from an IDHm heterozygous cell line that has already been reported to commonly undergo loss of heterozygosity after time, thus becoming IDHm

homozygous (Luchman et al., 2013). This might be an effect to consider when analyzing the outcome generated by MRK-A inhibitor. Regarding IDHm inhibitors, Agios pharmaceuticals© was the first company to commercialize active compounds. The $IDH1^{R132H/WT}$ inhibitor, AGI-5198 has been extensively studied, although showing contradictory results by inducing increased viability in several IDH1m glioma patient-derived cell lines (Tateishi et al., 2015). Moreover, AGI-5198 did not show improvements in survival of SCID mice bearing patient-derived intracranial IDH1m GBM xenografts. In fact, it was reported that incubation of glioma cell lines with AGI-5198 prior intracranial implantation into mice, shortened the latency period of the tumor and decreased median survival (Tateishi et al., 2015). This suggests that this IDH1m inhibitor may cause the xenograft to be even more aggressive. Due to the role of IDH1 mutation in sensitizing cells to oxidative stress due to the NADPH imbalance, it is possible that in cases where there is an increased oxidative activity, these inhibitors may have a counterproductive effect (Molenaar et al., 2015). Some studies attempt to augment the oxidative dependency of these tumors. It has been observed that IDH1m gliomas display a downregulation of nicotinate phosphoribosyltransferase 1 (NAPRT1) in charge of NAD^+ generation. Treatment of IDH1m cells with inhibitors of the alternative NAD^+ producer, nicotinamide phosphoribosyltransferase (NAMPT) decreased viability of these cells (Tateishi et al., 2015) (**Figure 26**). IDH1m gliomas may be sensitive to NAD+ blockade due to their dependence for this molecule as substrate for oxidative energy production.

GLS and GDH inhibitors. Other strategies focus in targeting IDH1m-derived metabolic liabilities. One of the most commonly investigated is the effect of GLS inhibition (**Figure 26**). Studies carried out with bis-2-(5-phenylacetomido-1,2,4-thiadiazol-2-yl)ethyl sulfide (BPTES), showed how GLS inhibition blocks cell growth in both IDHm GBM and AML cells (Emadi et al., 2014, Seltzer et al., 2010). In fact, the GLS inhibitor CB-839, is being currently assessed in clinical trials for several clinical indications including IDHm myeloid malignances. As explained in section 4.3, the therapeutic effect of GLS inhibition may lie in its potential to block GSH synthesis thus increasing the oxidative damage in these tumors (McBrayer et al., 2018). From

another perspective, increasing research is investigating the potential of GDH2 inhibition in IDHm tumors, which is expected to cut their TCA cycle fueling (**Figure 26**). As it has been demonstrated, GDH2 is crucial in IDHm gliomas as anaplerotic input into the TCA cycle (Chen et al., 2014). It has been recently reported that the role of GDH2 is hominid-specific due to a late evolved amino acid substitution in the allosteric domain (Waitkus et al., 2018b).

Inhibitors of epigenetic modulators. Other therapeutic strategies focus in targeting tertiary oncogenic alterations linked to IDH mutation. For instance, proliferation of IDHm cell lines harboring *MYCN* amplification can be blocked by treatment with BET inhibitor JQ1, which suppresses n-Myc overexpression (Puissant et al., 2013) (**Figure 26**). In addition, it has been observed that inhibition the BCL-2 apoptotic regulator promotes a lethal phenotype in IDH1m glioma cells (Karpel-Massler et al., 2017) (**Figure 26**). The concept of inhibiting D-2HG-derived methylation has as well been experimentally exploited. DNA methyltransferase 1 (DNMT1) inhibitor showed to suppress IDH1m cell proliferation both *in vitro* and *in vivo* (Turcan et al., 2013). Similarly, azacytidine, a molecule that compromises the activity of DNA methyltransferases, was shown to reduce growth of IDHm glioma xenografts (Borodovsky et al., 2013) (**Figure 26**).

Immunotherapy. Promising evidence suggests that IDH mutation and D-2HG may play critical roles in shaping the immunological scenario of the tumor, revealing the potential of immunotherapy in these types of cancer (Amankulor et al., 2017). It has been reported that IDHm gliomas has decreased tumor-infiltrating lymphocytes and low programmed death-ligand 1 (PDL1) expression (Berghoff et al., 2017). Moreover, these tumors suppress expression of the ligands ULBP1 and ULBP3 which may trigger a mechanism for evading NK cell surveillance (Zhang et al., 2016). Additional studies with *in vitro*, *in vivo* and patient material, show that D-2HG attenuates T cell accumulation by downregulating T lymphocyte-associated genes and cytokines (Kohanbash et al., 2017, Bunse et al., 2018). This strongly suggests that D-2HG contributes to immune suppression, raising the possibility of sensitizing IDHm gliomas to immnunotherapeutic agents by IDHm inhibition. Indeed, it has been reported that IDH1m

inhibition enhanced the activity of peptide vaccines, specific for glioma, in mice intracranial xenografts. Moreover, since the IDHm is specific to cancer cells, it represents a tumor-specific neoantigen that may be exploited for vaccine or other targeted approaches. In this regard, the neo-epitope generated by IDH mutant enzyme is currently used in clinical trials with peptide- and RNA-based vaccines (Schumacher et al., 2014, Platten et al., 2018, Weller et al., 2017). A study carried out with transgenic IDH1m MHC-devoid mice, showed that peptide vaccination elicited specific anti-tumor responses, correlating with an increased survival, and apparent curative responses in 25% of treated mice (Pellegatta et al., 2015). Overall, these data suggest that IDH mutation may alter the production of immunogenic cytokines and receptors facilitating immunosuppression. Although, the specific mechanism by which IDHm and/or D-2HG mediate this response is still under investigation, this supposes a promising strategy in the future of IDHm glioma therapies.

In summary, besides the arduous and extensive efforts dedicated to stop the aggressive and highly elusive IDHm gliomas, there is still lack of a clear and effective treatment that can considerably improve patient prognosis. The present PhD dissertation is a comprehensive study of IDHm glioma malignant behavior with the aim to identify and target its aberrant metabolic escape mechanisms. In this chapter we have widely exposed the theoretical background encompassing IDHm glioma research, especially within the field of metabolism. This has served us as the groundwork to present the specific strategy and findings of this PhD project investigations, in which we wish to contribute in the understanding and fighting against such deadly disease.

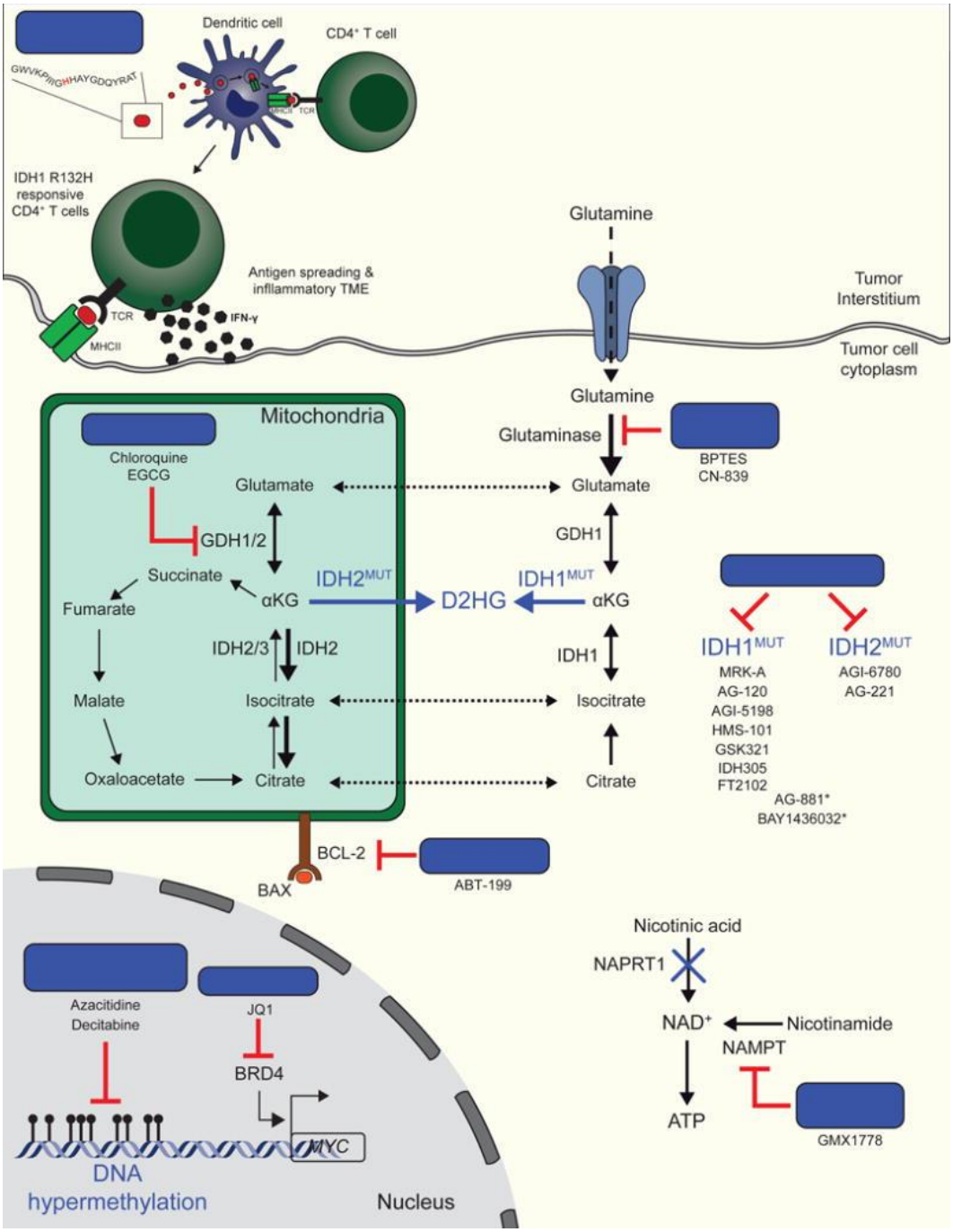

Figure 26. Therapeutic strategies against IDHm gliomas.
Inhibitors of IDHm 1 and 2 as well as IDHm derived altered enzymes and pathways, are currently under per-clinical and early clinical investigation, aiming to block the tumorigenic and invasive potential of these tumors, and improve the clinical outcome of IDHm glioma patients. In addition, increasing evidence suggests immunotherapy as a promising novel therapeutic approach. * Pan-inhibitors of both IDH1 and IDH2 mutant isoforms. Used from (Waitkus et al., 2018a).

CHAPTER II. SCOPE AND AIMS

Diffuse gliomas are still one of the most deadly cancer types. Although displaying a disparate average life expectancy among tumor sub-types, ranging from 1 year for GBM to about 7 years for lower grade gliomas, no curative treatments are currently available (Ostrom et al., 2019). With the advance in molecular diagnosis, it has been found that the presence of a point mutation in isocitrate dehydrogenase (*IDH*) gene, delineates the classification of glioma tumors. IDH mutation is present in most of low grade gliomas (LGG) and secondary glioblastomas (GBM), tumors arising in younger patient population (<50 years) (Ostrom et al., 2019). IDH mutant (IDHm) malignancies are also found in other cancer types such as acute myeloid leukemia (AML), chondrosarcomas or cholangiocarcinomas (Han et al., 2020).

Increasing research focus is directed to understand the impact of this mutation in cancer malignancy. IDHm tumors display a gain-of-function mutation that leads to the synthesis of the oncometabolite D-2HG. The epigenetic reprogramming derived from this neomorphic activity has being extensively studied, e.g. the role in histone and DNA methylation or HIF1-α regulation (Turcan et al., 2012, Zhao et al., 2009). Yet, IDH being an important metabolic enzyme, the consequences of this mutation in cellular metabolism are yet to be fully elucidated. Increasing evidence suggests that IDHm tumors may have a relevant impact on glutamine metabolism and lipid synthesis (Metallo et al., 2011). In addition, it has been suggested that IDH mutation might be detrimental for GSH synthesis and cellular redox homeostasis, due to the limited NADPH production, characteristic of the wild type reaction (Shi et al., 2015).

One of the biggest impediments that has hampered the collection of metabolic data is the availability of adequate IDHm glioma models. The slow-growing nature of IDHm cells hinders both *in vitro* and *in vivo* handling. To overcome this difficulty, many research groups have focused on the use of highly proliferative IDHm transgenic GBM cells and xenografts, an easier experimental set-up that eludes the tedious work with original LGG IDHm models. This approach obviates the tumor-specific genetic background that may be crucially influencing the metabolic organization of the cells. Thus, in our group we chose to use patient-derived cell lines and animal models carrying the endogenous IDH mutation, despite their sharp growth

lag. In a recent publication from our group, in-house patient-derived orthotopic xenografts of both DHm and IDHwt gliomas were used to investigate the metabolic disparities between these tumor-types (Fack et al., 2017). Via different metabolomic techniques, such as liquid chromatography mass spectrometry (LC-MS) or matrix-assisted laser desorption/ionization (MALDI) imaging, it was observed that IDHm glioma tumors displayed a dysregulated phospholipid regulation as well as a slower energetic rate. In addition, both *in vivo* metabolite detection and clinical gene expression analysis from public datasets, suggested that IDHm gliomas upregulate cysteine synthesis through transsulfuration pathway (TP) in order to generate GSH independently of NADPH. In fact, TP has been shown to be readily active in normal astrocytes, leading to increased GSH production (McBean, 2012). Further investigation yet awaits to confirm this mechanism in gliomas.

Today there is still lack of a clear and effective treatment against diffuse gliomas. The high sensitivity of IDHm tumors to oxidative stress-inducing radiation suggests they display a deficient antioxidant defense. Based on what has been proposed by our group (Fack et al., 2017), the hypothesis of this PhD project proposed that IDHm gliomas rely on *de novo* synthesis of cysteine via TP in order to produce GSH, regardless of their defective NADPH production. Therefore, this would uncover an IDHm-specific vulnerability in which blocking TP would leave these tumors openly exposed against oxidative insults. In order to explore our hypothesis, in this project we dispose of patient-derived glioma cell lines with and without the endogenous IDH mutation, orthotopic xenografts derived thereof and patient material clinically provided after surgical resection. Making use of these models we aimed to:

- Characterize the general metabolic behavior of IDHm gliomas, through an integrative and LC-MS-based metabolomics and proteomics analyses, including cell, animal and patient material, as well as consulting public genomic datasets.
- Evaluate the potential of novel targets observed in the IDHm metabolism characterization.

- Address whether glutathione synthesis relies on an increased transsulfuration pathway in IDHm gliomas through metabolomic flux analysis.
- Analyze the effect of genetic and chemical blockade of TP and/or GSH de novo synthesis, on cell viability, ROS and metabolite regulation, in glioma cells and xenograft tumors.

Based on our study, our prospective goal is to design a novel therapeutic strategy, to our knowledge not yet exploited, that could improve the clinical outcome of IDHm glioma patients by combining oxidative stress-inducing agents with inhibition of GSH synthesis in the tumor.

CHAPTER III. METHODOLOGY

1. Clinical samples

Clinical samples for LC-MS analysis were obtained from 22 patients (10 IDHwt glioblastomas; 8 IDH1m astrocytomas; 4 IDH1m oligodendrogliomas) from the Haukeland Hospital, Bergen, Norway. Tissue fragments were stereotactically sampled (25mg) during the operation and snap-frozen. Diagnosis was first determined by classical histopathology, followed by molecular diagnosis through DNA methylation profiling (Infinium® MethylationEPIC, Illumina) as described (Golebiewska et al., 2020). In brief, genomic DNA was extracted using the QIAamp Blood & Tissue Kit. Bisulfite conversion was done using up to 250ng of extracted gDNA. DNA methylation-based glioma classification was performed by referencing data to the dataset of over 2800 neuropathological tumors at https://www.molecularneuropathology.org/mnp as described previously (Capper et al., 2018) . For samples where methylation profiling was not possible due to limited sample amount, IDH status was confirmed by droplet digital PCR (ddPCR) as previously described (Golebiewska et al., 2020). Patient characteristics are shown at **Chapter IV-2 Supplementary Table 1**. Patient sample collection was approved by the local ethics committee (Haukeland University Hospital, Bergen (REK 2010/130-2) and in line with the Declaration of Helsinki.

2. Patient-derived glioma cell lines and xenografts

Patient-derived cell lines were generated in the laboratory of Dr Christel Herold-Mende and grown as 3D spheres under serum-free conditions (**Chapter IV-2 Figure S1A**). These glioma stem-like cells (GSCs) have been previously used in other studies (Trong et al., 2020, Dao Trong et al., 2018, Dettling et al., 2018, Bougnaud et al., 2016a). NCH644, NCH601 and NCH421k correspond to patients with IDH1wt Glioblastoma. NCH1681 and NCH551b were from patients with IDH1m astrocytoma; NCH612 from a patient with an IDH1m Oligodendroglioma. All IDH1m cells were slow growing and sensitive to culture conditions. For routine culture, all cells were grown as non-adherent spheres in DMEM-F12 medium (Lonza,

BE04-687F/U1) supplemented with 20% BIT100 (Provitro), 2mM L-Glutamine, 30 U/ ml Pen-Strep, 1U/ml Heparin (Sigma), 20 ng/ml bFGF (Miltenyi, 130-093-041), and 20ng/ml EGF (Provitro, 1325950500). Cells were incubated under standard normoxic conditions at 37°C and 5% CO_2 and were regularly tested for mycoplasma. The presence of the IDH mutation was regularly validated by Western blot. Glioma patient-derived orthotopic xenografts (PDOX) generated in NOD/Scid mice (male or female, at least 2 months of age) were described previously (Bougnaud et al., 2016b, Golebiewska et al., 2020).

3. Western blot

Cells were lysed in RIPA extraction buffer supplemented with protease inhibitor cocktail (Roche). Protein quantification was performed with 2D-Quant (GE Healthcare). Protein lysates were resolved in NuPage 4-12 % BisTris gels (ThermoFisher), and blotted onto a PVDF membrane. Membranes were blocked with TBST buffer in 2% milk. Blots were incubated with primary antibodies at 4°C overnight with: anti-IDH1m R132H (DIANOVA DIA-H09), anti-Cystathionase (Abcam ab189916), anti-GAPDH (Cell Signaling 5174S) and anti-LaminB1 (Abcam ab16048). Secondary antibodies anti-mouse and anti-rabbit (Jackson ImmunoResearch) were applied, and blots were developed with a chemiluminescent substrate (ThermoFisher) using ImageQuant analyzer (GE Healthcare).

4. Seahorse XF analyzer

Cells were seeded in Seahorse XFe96 plates (Agilent) at 5 x 10^4 cells per well using 200 µl of our DMEM-F12 medium (Lonza, BE04-687F/U1) supplemented as aforementioned. The plates were previously coated with 20 µg/ml of laminin in 200 µl per well, left during 2 hours at 37º. After the 2 hours the laminin solution was removed before starting the cell seeding. Cells were incubated overnight at 37º and 5% CO_2. Then, the medium was substituted by Seahorse XF

Base Medium (Agilent) supplemented with 2mM Glutamine (pH=7.4) and cells were incubated for 30 minutes at 37º and no CO_s. Oxygen consumption rate (OCR) and extracellular acidification (ECAR) was recorded using Seahorse XFe96 Extracellular Flux Analyzer (Agilent) at baseline. InCucyte was used to normalize the data with cell density (IncuCyte ZOOM 2018A software). Raw density data was taken from Phase Object Confluence (POC), which measures the percentage of the phase contrast image area that is occupied by objects (cells).

5. CRISPR/Cas9-mediated IDH1m knock-in GBM cell line

Our strategy consisted in the binding and double strand break (DSB) of a single guide RNA (sgRNA)-Cas9 complex into *IDH* gene, followed by homologous directed repair (HDR) with a donor plasmid containing the IDH1 R132H mutation (adapted from (Brabetz et al., 2017)). In order to do so, we selected a sgRNA with predicted minimal off-target activity that recognized *IDH* gene 3' of exon 4 (Sulkowski et al., 2017). This sgRNA was cloned in a vector expressing Cas9 as well as GFP reporter. We tested sgRNA efficiency after transfection of the sgRNA plasmid into HEK293T cells by T7 endonuclease assay. We fused a reporter gene (mCherry) to the IDH1 cDNA sequence via a P2A self-cleaving peptide. Therefore, random genomic integration or out of frame integration of the donor plasmid are not expected to result in mCherry expression. In order to avoid recutting of the target site after HDR, the guide recognition sequence was omitted from the 3'HDR sequence of the donor plasmid.

The donor plasmid was then transfected together with the sgRNA-Cas9 plasmid into NCH644 GBM cell line via electroporation. In order to obtain clonal lines with integration of the donor plasmid, mCherry positive cells were single cell sorted and allowed to recover. Clonal lines were later analyzed on for correct integration of the donor construct by PCR and sequencing of the 5' and 3' HDR borders. Selected heterozygote and homozygous clonal lines were further analyzed for IDH1R132H expression by Western Blot and by Sanger sequencing of cDNA as well as for 2-HG content by LC/MS analysis.

6. Quantitative RT-PCR

RNA was isolated following the Trizol protocol (ThermoFisher) and cDNA was synthesized using iScript Reverse Transcriptase (BioRad). cDNA was applied for real-time PCR reactions in a Via7 instrument using Fast SYBR Green (Applied Biosystems). Relative gene expression levels were normalized against elongation factor 1 alpha (EF1α) housekeeping gene, and calculated using the ΔCT method. Reactions were performed in triplicates. Specific primers used were: CSE (Fw: GGCCTGGTGTCTGTTAATTGT, Rv: GCCATTCCGTTTTTGAAATGCT), CBS (Fw: GGCCAAGTGTGAGTTCTTCAA, Rv: GGCTCGATAATCGTGTCCCC), EF1 α (Fw: TTGTCGTCATTGGACACGTAG, Rv: TGCCACCGCATTTATAGATCAG), EZRIN (Fw: TGCCCCACGTCTGAGAATC, Rv: CGGCGCATATACAACTCATGG) (Eurogentec).

7. TCGA analysis

Gene expression data from glioma patients was obtained from The Cancer Genome Atlas (TCGA) dataset via the GlioVis data portal (Bowman et al., 2017).

8. Untargeted proteomics analysis by LC-MS/MS

For the proteomic analysis, all cell lines were extracted by two different preparation methods for a total of two replicates per cell line. In the first preparation, proteins were extracted using methanol/chloroform and protein pellets were dissolved in 8M urea buffer, while in the 2nd preparation the cells were lysed with 1% sodium deoxycholate detergent (SDC). Protein concentrations were determined by EZQ assay (Invitrogen, cat#R33200). Equal amounts of proteins were used for the analysis. Samples were reduced with 5 mM dithiothreitol for 1 h at 37°C and alkylated with 15 mM iodoacetamide for 30 min at RT followed by a two-step

sequential protein digestion with Lys-C (Wako, cat#125-05061) for 3 h at 37°C, and trypsin (Promega, cat#V5111) at 37°C overnight. Tryptic peptides were desalted on C18 SPE (Sep Pak tC18, 25 mg, Waters) and dried using a vacuum centrifuge. Peptides were analyzed on a Q-Exactive HF mass spectrometer (Thermo Scientific) coupled with a Dionex Ultimate 3000 RSLC chromatography system operated in column switching mode. Peptides were trapped on a 75 µm x 2 cm pre-column (C_{18} pepmap 100, 3 µm) and separated onto a 75 µm × 50 cm column (C_{18} pepmap 100, 2 µm) by a 240 min linear gradient starting from 2 % solvent A (0.1% formic acid in water) to 35% solvent B (0.1% formic acid in 100 % acetonitrile) at a flow rate of 300 µl/minute. The mass spectrometer was operated in a data-dependent acquisition mode with a survey scan acquired at a resolving power of 120,000 at 200m/z. The 12 most intense multiple-charged ions ($z \geq 2$) were isolated and fragmented at normalized collision energy of 28 and the resulting fragment ions acquired at a resolution of 15,000 at 200 m/z. Fragmented precursors m/z were excluded for another fragmentation for 20 s. MS files were analyzed in the MaxQuant (Cox and Mann, 2008) software version 1.6.7.0. MS/MS spectra were searched by the Andromeda search engine (Cox et al., 2011) against the TrEMBL UniProt Homo sapiens (February 2019, 73,928 entries). Cysteine carbamidomethylation was set as a fixed modification and methionine oxidation and N-terminal protein acetylation as variable modifications. For protein quantification, label-free quantitation (LFQ) was performed with a minimum ratio count of 2 (Cox et al., 2014) with match between runs activated. The FDR cut-off for peptide and protein identifications was set to 1%. Bioinformatic analysis was performed in the Perseus platform version 1.6.2.1 (Tyanova et al, 2016). Two-sample Student's t-test was used to determine the significantly changed proteins between IDH1wildtype and IDH1mutant cell lines with a permutation-based FDR of 0.05 for multiple testing correction. Results were filtered to have both a significant FDR-corrected P-value and a minimum fold change of 2.

9. Generation of stable shRNA-mediated knockdown cell lines

Since patient-derived glioma cells were not amenable to standard transfection procedures, all gene knockdown (KD) experiments were performed with lentiviral vectors to establish stably transduced KD lines. To target the CSE gene in NCH1681 cells, two different shRNA variants were used: shCSE1 (ATAGCTTTAGGTTCTTGAG; Code: V2LHS_151012) and shCSE2 (ATGAAAGATAATGAGGTGC; Code: V2LHS_151015), and one non-targeting scrambled shRNA was used as control: shCTR (CTTACTCTCGCCCAAGCGAGAG; Code: RHS4346) (Dharmacon). Plasmids containing shRNAs and GFP (pGIPZ-shRNA-targets and pGIPZ-shRNA-scramble) were amplified by midi-prep (Machery-Nagel). Lentiviral particle production was done in HEK293T ($5x10^5$ cells in 5ml of DMEM 2% FBS) using the core packaging construct pCMVR8.74 and envelope protein vector pMD2.G. The supernatant containing viral particles was harvested and 1ml was used to transfect NCH1681 ($8x10^5$ cells in 3ml of DMF12 specific medium for IDH1m cells). After lentiviral transduction, cells were passaged five times in the presence of 1ug/ml puromycin as selection marker to obtain stable GFP-positive KD cells.

10. Cysteine titration in medium

The optimal culture medium for IDH1m cell lines is based on DMEMF12 (Lonza, BE04-687F/U1) (containing 100 µM cysteine and 100 µM of its oxidized dimer cystine) supplemented with 20% BIT100 (containing 600 µM cysteine), thus the final cysteine concentration (combining both cysteine and cystine) in the medium being 360 µM. With cysteine-free DMEMF12 (see below) plus 20% BIT the final cysteine concentration was still at 120 µM. Since BIT contains essential hormones for cell growth (transferrin, insulin and BSA), completely eliminating BIT was too deleterious for the sensitive IDHm cells. Therefore to further decrease the concentration of cysteine we applied serial BIT dilutions, at 10% BIT (60 µM cysteine) and 5% BIT (30 µM cysteine) (**Chapter IV-2 Supplementary table 2**). We confirmed that the toxic

effect of PAG in low BIT/cysteine medium was due to the lack of cysteine by rescuing the cells with extracellular cysteine (**Chapter IV-2 Figure S4D**). The cysteine-free medium consisted of DMEM high glucose, no glutamine, no methionine, no cysteine (ThermoFisher, 21013024), supplemented with an amino acid mix to reach these final concentrations: 115 µM methionine, 250 µM glycine, 50 µM alanine, 50 µM asparagine, 50 µM aspartic acid, 50 µM glutamic acid, 50 µM proline, RPMI 1640 Vitamins Solution 1X (Sigma, R7256), 2mM L-Glutamine, 30 U/ml Pen-Strep, 1 U/ml Heparin (Sigma), 20 ng/ml bEGF (Miltenyi, 130-093-041), 20 ng/ml EGF (Provitro, 1325950500).

11. Sphere size measurement

Sphere growth assays were performed in an IncuCyte imaging incubator. Cells ($1x10^3$ cells/well) were seeded in a 384 well plate in 75 µl. The plate was briefly centrifuged (3 min, 300 rpm) and placed in the incubator at 37ºC to allow sphere formation. Twelve hours later, once the spheres were properly formed, each single sphere per well was imaged every 4 hours during 7 days. For quantification of sphere size a specific mask was applied (IncuCyte ZOOM 2018A software) and raw data was taken from Phase Object Confluence (POC), which measures the percentage of the phase contrast image area that is occupied by objects (cells).

12. GFP fluorescence as a proxy for cell viability

GFP fluorescence was measured in an IncuCyte imaging incubator. Cells ($1x10^3$ cells/well) were seeded in a 384 well plate in 50 µl. The plate was briefly centrifuged (3 min, 300 rpm) and placed in the incubator at 37ºC to allow sphere formation. Twelve hours later, the spheres were properly formed and each single sphere per well was imaged every day during 6 days. Raw data was taken from mean green fluorescent values from IncuCyte ZOOM 2018A software. (Trong et al., 2020)

13. Toxicity assay

Toxicity was determined with the CellTox Green Cytotoxicity assay® (Promega). The CellTox working solution consists of a compound that emits green fluorescence after reacting with free extracellular DNA. Cells ($1x10^3$ cells/well) were seeded in a 384 well plate in 75 µl of the desired medium, the plate was briefly centrifuged (3 min, 300 rpm) and 25 µl of CellTox working solution were added. The plate was then placed in the incubator under normoxia at 37ºC. Twelve hours later, green fluorescence was measured in a CLARIOstar Plus microplate reader (BMG LABTECH) and again every day for up to 4 days.

14. ROS measurement

$1.5x10^5$ cells/ml/well were seeded in a 12 well plate. Each well contained a specific cysteine concentration medium (360, 60, 30 µM cysteine). The plate was placed in the incubator under normoxia at 37ºC for 3 days to allow ROS formation. After 4 days, 2′,7′-Dichlorofluorescin diacetate (DCFDA) probe was applied at 10 µM. After 30 minutes, cells were washed, harvested in PBS and seeded in 8 replicates in a 96-well plate ($3x10^4$ cells/well in 100 µl). Green fluorescence was determined in a CLARIOstar Plus microplate reader (BMG LABTECH).

15. *In vivo* experiment in orthotopic xenografts

$3x10^5$ NCH1681 cells were stereotactically injected into the frontal cortex of NSG mice (NOD.Cg-Prkdc^{scid} Il2rg^{tm1Wjl}/SzJ) (n=20). Tumor growth was monitored by MRI (FSE-T2 sequence, 3T MRI system, MR Solutions) as described previously (Golebiewska et al., 2020). MRI data was analyzed by ImageJ and the tumor volume (mm^3) was determined by tumor delineation in each slice and multiplying by slice thickness (1mm). Two months after implantation, mice with tumors (size range 2-10 mm^3) were selected and randomized in 2

groups (8 mice per group). The experimental group received intraperitoneal injections of PAG (35mg/kg), 5 times/week during 3 months, while the control group received saline injections. The treatment dose was based on previous reports (Cho et al., 1991). Tumor growth rate (GR) was calculated using the tumor volume (TV) measurement at 2 different time points as GR = 100 * log (TVf/TV0) / (tf-t0), where TVf and TV0 are the tumor volumes at the last and first time points respectively, and tf-t0 is the difference in days between the time points (Mehrara et al., 2007). Mice were observed daily, about two months after treatment start, mice from the control group started to present neurological symptoms and body weight loss. The experiment was halted 3 months post-treatment after two control mice had died.

For in vivo flux analysis, 130mg/kg/h of L-serine (U-13C3, 99%) (CLM-1574-H-0.1 Eurisotop) was intravenously (tail vein) infused in 2 mice of each group during 4 hours, as well as in 2 healthy mice without tumors (healthy brain controls). Mice were maintained anesthetized with 2.5% of isoflurane during the infusion. The 4 hours and 130mg/kg concentration of serine tracer infusion which was based on (Ducker et al., 2016), was confirmed in our pilot experiment where metabolite steady state in the brain was reached after 4 hours (**Chapter IV-2 Figure S5A**). After infusion brain, liver, kidney and heart were dissected and flash frozen in isopentane at -80ºC LC-MS analysis

All procedures were approved by the animal welfare structure of LIH and the national authorities responsible for animal experiments in Luxembourg under the reference LUPA.

16. Metabolite and flux analysis in cell lines and tissues

Cell lines ($5x10^5$ cells/well) were seeded in triplicates in 12 well plates in a total volume of 2ml at 30 µM cysteine. For the tracing experiments 400 µM of L-serine (U-13C3, 99%) (CLM-1574-H-0.1 Eurisotop) was added to the culture medium which already contained 400 µM natural serine (ThermoFisher, 21013024) (ratio ^{13}C3-Serine/Serine 1:1). After 4 days, cells were washed in PBS and transferred to 1.5ml Eppendorf tubes. Cell lysis was done in 300 µl of cold

metabolite extraction solvent (30% Acetonitril 50% MeOH 20%H2O). Samples were put on a shaker (1000 rpm at 4ºC for 5 minutes) and centrifuged at 4ºC for 10 minutes. 150 µl of supernatant was collected and stored at -80ºC for downstream LC-MS. The cell pellets were kept for protein quantification using the Lowry method for sample normalization.

Frozen tissue of human or mouse samples were cut with a scalpel on dry ice and weighed to obtain pieces of 15-25mg. Mouse tumor samples were carefully collected by cryomicrotome sectioning of the frozen brains. 25 µl/mg tissue of metabolite extraction buffer (30% Acetonitril 50% MeOH 20%H_2O) was added and samples were homogenized via bead-mill (Qiagen Tissuelyzer) mechanical disruption with 5 mm beads (2 times x 20 seconds shake at 20 Hz frequency). Samples were shaken at 1400 rpm (12 minutes at 4ºC) and centrifuged at 16000 g (15 minutes at 4ºC). Metabolite extracts in the supernatant were recovered and stored at -80ºC until LC-MS analysis was performed.

A pilot GC-MS-based approach to determine steady state levels of $^{13}C_3$-serine in different mice tissues (**Chapter IV-2 Figure S5A**) was performed as described in (Meiser et al., 2016). LC-MS analysis was performed as previously described (Vande Voorde et. al 2019 Science Advances). Briefly, analysis was carried out on an Ultimate 3000 HPLC coupled to Q Exactive Orbitrap mass spectrometer with electrospray (ESI) ionization (Thermo Scientific, Waltham, MA, USA). Metabolite extracts (5µl) were separated on ZIC-pHILIC column (SeQuant, 150 x 2.1mm, 5µm, Merck KGaA, Darmstadt, Germany) held at 45°C. The gradient started at 20% A (20mM ammonium carbonate, pH 9.2) and 80% B (acetonitrile), decreasing to 20% B at a flow rate of 200µL/min over 15 minutes. Data was acquired using Thermo Xcalibur software over a mass range of 75-1000 m/z at a resolution of 35,000 (at 200m/z) with polarity switching. Data analysis was carried out in TraceFinder (v4.0, Thermo Scientific) software. Metabolites were identified using an in-house library of exact mass and known retention time generated using commercial standards on the same LC-MS system.

17. Statistical analysis

All statistical analyses were performed using GraphPad Prism 8 software. Statistical comparisons were based on two-tailed Student's t-test between the corresponding groups, except where otherwise stated. Number of replicate experiments (n), errors and p-values are indicated in each corresponding figure legend.

CHAPTER IV. EXPERIMENTAL DATA

1. Integrative characterization of IDH1 mutant gliomas discloses alterations in central carbon metabolism and GSH synthesis

Andrés Cano-Galiano[1], Elena Martinez-Garcia[2], Fred Fack[1], Maria-Francesca Allega[3,4], David Sumpton[3], Anais Oudin[1], Monika Dieterle[1], Sabrina Fritah[1], Saverio Tardito[3,4*], Gunnar Dittmar[2], Rolf Bjerkvig[1,6] and Simone P. Niclou[1,6]

[1]NORLUX Neuro-Oncology Laboratory, Department of Oncology, Luxembourg Institute of Health, Luxembourg; [2]Quantitative biology unit, Luxembourg Institute of Health, Luxembourg; [3]Cancer Research UK Beatson Institute, Glasgow, UK; [4]Institute of Cancer Sciences, University of Glasgow, Glasgow, UK; [5]Department of Neurosurgery, University of Heidelberg, Germany; [6]Department of Biomedicine, University of Bergen, Norway; [7]Cancer Metabolism Group, Department of Oncology, Luxembourg Institute of Health, Luxembourg

ABSTRACT

Isocitrate dehydrogenase 1 or 2 (IDH1/2) mutations determine diffuse glioma subtypes. This mutation leads to a gain-of-function synthesis of D-2-hydroxyglutarate (D-2HG) that impacts tumor epigenetics and metabolism. IDH are central metabolic enzymes participating in various intermediary pathways such as tricarboxylic acid (TCA) cycle, redox or lipid metabolism, yet the specific implications of this mutation are only partially understood. Here, we make use of patient material with and without IDH1 mutation as well as patient-derived cell lines and xenografts, and CRISPR/Cas9 generated IDH1m isogenic *in vitro* models. We performed an integrative characterization of the metabolic regulation in these models by mass spectrometry-based proteomics and metabolomics analysis combined with energy metabolic reading via Seahorse analyzer. We found that IDH1m gliomas have a decreased energetic yield although they upregulate master regulators of central carbon metabolism, especially within glucose and glutamate processing pathways as well as GSH synthesis. Our data suggests that IDH1 mutation leads to an increased production of glucose derivatives for nucleotide, lipid and amino acid synthesis, whereas they upregulate anaplerotic input into the TCA cycle via glutamate or glucose-independent pyruvate to cope with their vast D-2HG production. Moreover, we propose that these tumors upregulate *de novo* synthesis of GSH in order to maintain their antioxidant pool from a NADPH-independent manner. Thus, here we show a comprehensive and integrative characterization of potential metabolic vulnerabilities of IDH1m gliomas.

1.1. Introduction

Mutations in isocitrate dehydrogenase 1 and 2 (*IDH1/2*) are frequent in various cancer types, especially in gliomas, defining their classification. Low grade astrocytic and oligodendroglial tumors are IDH mutant (IDHm), whereas glioblastomas (GBM) are IDH wild type (IDHwt) (Louis et al., 2016b). Wild type IDH catalyzes the oxidative decarboxylation of isocitrate to α-ketoglutarate (α-KG) generating NADPH, an important reducing agent in various metabolic pathways. The IDH mutation (R132H), most often affects the cytosolic isoform IDH1 and leads to the neomorphic consumption of α-KG and NADPH, to generate the oncometabolite D-2HG (Dang et al., 2009a). Competitive inhibition of α-KG-dependent dioxygenases by D-2HG, triggers epigenetic reprogramming, e.g. DNA and histone methylation and HIF1-α stabilization (Xu et al., 2011b, Turcan et al., 2012).

Diverse studies show that IDHm tumors may alter different metabolic pathways. It has been observed that tricarboxylic acid (TCA) cycle anaplerosis via glutamine and glutamate is altered in these tumors. Indeed, α-KG from IDHwt reaction is not the only source of D-2HG, since much of this metabolite is derived from glutamine (Grassian et al., 2014). TCA cycle alterations has shown to restrict oxidative metabolism in these tumors, sensitizing them to electron transport chain (ETC) inhibitors (Grassian et al., 2014, Reitman et al., 2011). Mutations in IDH has also been found to alter redox metabolism, due to reduced $NADP^+$-dependent IDH activity (Bleeker et al., 2010). This decrease in reducing agents may impact the glutathione (GSH) availability and oxidative damage of these cells (Shi et al., 2015). In addition, phospholipid production has also been found altered by IDH mutation (Esmaeili et al., 2014). In our group, we have studied the metabolic landscape of IDHm gliomas in patient derived orthotopic xenografts (PDOX), and we also reported a dysregulated phospholipid metabolism as well as low energetic yield and a potential redox vulnerability (Fack et al., 2017). Recent studies have performed untargeted proteomic analyses, in order to characterize the overall metabolic regulation in IDHm and IDHwt gliomas (Oh et al., 2020, Doll et al., 2017, Dekker et al., 2020). Significant changes in glycolytic, TCA cycle and glutamate metabolism enzyme abundance,

suggested IDH1m metabolism may be rewired by an increased input of lactate and glutamate to preserve TCA-cycle activity (Dekker et al., 2020). Moreover, IDH mutant tumors showed decreased oxidative-phosphorylation proteins, suggesting a constrained respiration capacity (Oh et al., 2020). Overall, these latest findings suggest an impaired TCA cycle and oxidative-derived energy production in IDHm gliomas. There is still a need of comprehensive studies which combine metabolomics and proteomics regulation, and it remains to further investigation the metabolic vulnerabilities thereof and the specific targetable proteins to explore them.

In the present study, we profiled IDHm glioma metabolic environment through an integrative approach which combined proteomics, genomics and metabolomics as well as functional assays (e.g. Seahorse). This comprehensive analysis was conducted in a varied range of glioma models, including glioma patient samples obtained from surgical resection, patient derived cell lines expressing the endogenous IDH1 mutation and orthotopic xenografts thereof, as well as CRISPR/Cas9-generetad IDH1m knock-in GBM cells. Collectively, we observed that IDHm tumors display a significant dysregulation in key protein and metabolite intermediaries of central carbon metabolism, especially in those pathways derived from glucose and glutamate processing. In addition, we observed mayor differences in GSH redox system, fatty acid and phospholipid regulation. Overall we present a comprehensive study and data resource of the metabolic blueprint of IDHm gliomas, from which potential targets for future investigations are proposed. We expect to enlarge our understanding of glioma biology, providing a clearer perspective of the metabolic vulnerabilities of this elusive disease.

1.2. Results

Metabolomics dysregulation of central carbon intermediates in IDH1m gliomas

In order to first address the differential metabolic regulation of IDH1m and IDHwt gliomas, we performed liquid chromatography-mass spectrometry (LC-MS)-based metabolomics analysis. We used a cohort of clinical samples obtained from 22 glioma patients (12 IDH1m and 10

IDHwt) (**Chapter IV-2; Supplementary Table 1**). These samples were kindly provided by Haukeland Hospital in Bergen, Norway. For this study we made use of TraceFinder software where we created a compound database of ~ 100 metabolites that are considered important in the overall intermediary metabolism. Moreover, as a complementary validation, the metabolomics analysis was performed in four patient-derived cell lines (PDCs). Two of these cell lines correspond to IDHwt GBM (NCH644, NCH421k), Two correspond to IDH1m astrocytomas (NCH1681, NCH551b). The IDH1m lines are glioma stem-like (GSC) cells which grow as neurospheres and have already been reported (Trong et al., 2020, Dao Trong et al., 2018). Moreover, we analyzed as well metabolomics regulation in an IDH1m mouse xenograft model generated by orthotopic implantation of one IDH1m cell line (NCH1681), and compared metabolite levels with control mice without the disease. In line with what shown by previous studies, we observed significant dysregulation of key metabolites within glucose, glutamate, GSH and lipid metabolism. In addition to patient sample analysis (**Figure 1**), metabolomics analysis in cells (**Figure S1**) but also in xenografts (**Figure S2**), complemented our patient data with additional metabolites that largely matched within the same metabolic pathways.

Interestingly, the central glycolytic metabolites, glucose, glucose 6-phosphate and fructose 1,6-biphosphate were significantly increased in IDH1m gliomas (**Figure 1A**). As products of secondary catabolism of glucose, we found that different nucleotides or nucleosides were increased in IDH1m gliomas, such as GMP or adenosine (**Figure 1B**). On the other hand there was a significant decrease of glutamate in IDH1m patients, which we previously reported (Fack et al., 2017), as well as the expected upregulation of D-2HG. Moreover, leucine, a branch chain amino acid (BCAA) which may serve as precursor of glutamate, was also significantly decreased in IDH1m patients (**Figure 1C**). Glutamine and α-ketoglutarate (α-KG) were not differential in patients. With regard to GSH metabolism certain precursors of *de novo* synthesis of this antioxidant were also differential in IDH1m gliomas, such as S-adenosyilmethionine (SAM) and α-ketobutyrate (**Figure 1D**). However, as we previously reported (Fack et al., 2017), we did not appreciate significant differences in GSH. Regarding lipid metabolism glycerol 3-

phosphate, which acts as phospholipid precursor, was found increased in IDH1m gliomas, as well as hexanoic acid, a common short chain fatty acid (**Figure 1E**).

Overall, here we confirmed that IDH1m gliomas display differences in intermediaries of central metabolic pathways compared to IDHwt GBM. Specifically, it appears that glucose catabolism may be dysregulated. It is not clear whether increase in glucose intermediates means a faster or slower pathway activity. Further functional assays should be performed to address this. The observed shortage in glutamate, may suggest an increased consumption for the generation of α-KG to fuel TCA cycle or catalyze D-2HG production. Glutamine and α-KG were indeed significantly upregulated in IDH1m cell lines, as well as glutamate and other glutamate derivatives such as GABA (**Figure S1C**). Disparity of results between *in vitro* and patients with regard to glutamine-glutamate intermediates might be explained by the high glutamine concentration (2 mM) supplemented in the culture medium. The increase in GSH precursors may indicate a higher de novo synthesis flux to cope with GSH demands in a NADPH-independent manner. The observed increase in glycerol 3-P confirms a potential imbalance in synthesis of phospholipids in IDH1m tumors (Fack et al., 2017). Accumulation of the short chain fatty acid hexanoic acid suggests an altered fatty acid processing.

Proteomics analysis reveals altered metabolic processes in IDH1m gliomas

To combine the observed metabolomics dysregulation with the differential enzymatic abundance derived from IDH mutation, we performed a label-free quantitative (LFQ) LC-MS proteomic comparison. For the proteomics analysis we added to the aforementioned patient cohort another cohort of 13 patients (6 IDH1m and 7 IDHwt) which was previously reported (Fack et al., 2017). Hence we analyzed a total of 33 patient samples (16 IDH1m and 17 IDHwt). In addition, we also analyzed proteomics differences in six PDCs, three IDHwt (NCH644, NCH601, NCH421k) and three IDH1m (NCH1681, NCH551b (astrocytomas), NCH612 (oligodendroglioma)). In order to eliminate patient specific differences, we generated an isogenic model by inserting the IDH1 mutation in an IDHwt GBM cell line (NCH644), via

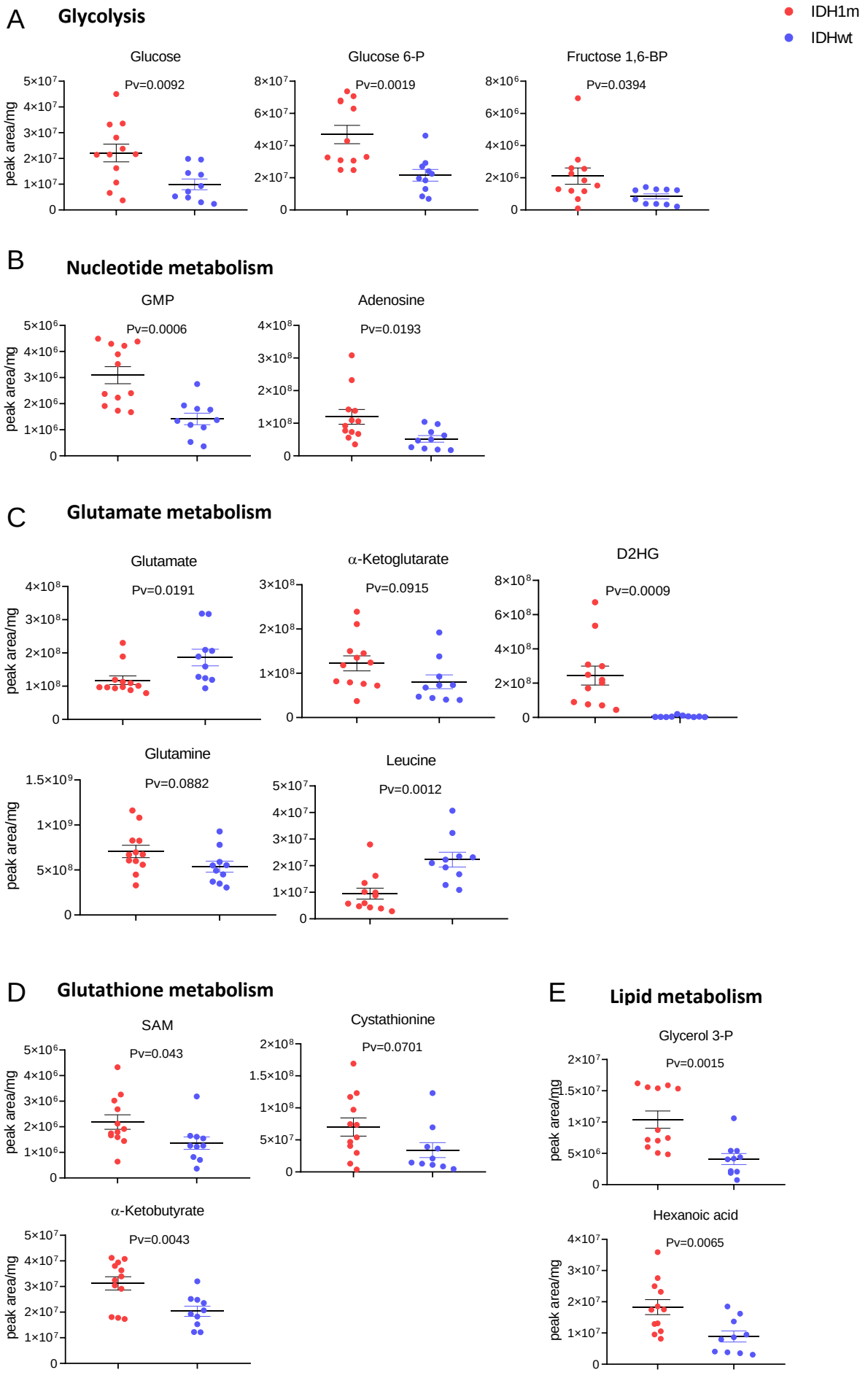
A
Glycolysis
IDH1m
IDHwt
Glucose
Pv=0.0092
Glucose 6-P
Pv=0.0019
Fructose 1,6-BP
Pv=0.0394
peak area/mg
B
Nucleotide metabolism
GMP
Pv=0.0006
Adenosine
Pv=0.0193
C
Glutamate metabolism
Glutamate
Pv=0.0191
α-Ketoglutarate
Pv=0.0915
D2HG
Pv=0.0009
Glutamine
Pv=0.0882
Leucine
Pv=0.0012
D
Glutathione metabolism
SAM
Pv=0.043
Cystathionine
Pv=0.0701
α-Ketobutyrate
Pv=0.0043
E
Lipid metabolism
Glycerol 3-P
Pv=0.0015
Hexanoic acid
Pv=0.0065

Figure 1. Metabolite distribution of central carbon intermediates in IDH1m gliomas.
LC-MS-based detection of differentially regulated metabolites in IDHwt and IDH1m glioma patients corresponding to the specific metabolic pathways revealed by proteomic analysis, (A), (B), (C) and (D). Each dot of the charts corresponds to one independent tumor. IDHwt (n=10), IDH1m (n=12). Data presented as means ± S

CRISPR/Cas9 technology. Therefore, the proteomics comparison was performed between the IDH1m knock-in (KI) model (i.e. NCH644 sgIDH1m) and its isogenic counterpart, NCH644 (i.e. NCH644wt). Based on the different proteomics analyses we found a total of 808 proteins differentially expressed between IDH1m and IDHwt patients, 590 in the cell lines, and 250 in the KI model. These proteins presented a fold change (FC) >1.5 and a false discovery rate (FDR) <0.05 (**Figure 2A**). We primarily aimed to uncover all differential metabolic proteins in IDH1m glioma patients. In addition, we combined this with the proteomics analysis in PDCs and KI models as complementary validation. Most of the proteins upregulated in IDH1m gliomas patients were related to metabolic pathways. However, significantly downregulated proteins in these tumors were rarely metabolic, and most commonly related with other pathways such as growth factor transport and uptake, extracellular matrix organization or protein translation and post-translation processing. Since the aim of our study was to address the metabolic vulnerabilities of IDH1m gliomas, we focused in the metabolic enzymes, mostly upregulated in our proteomics analysis.

We found four proteins that were significantly increased in IDH1m entities from the three different models: patients, PDCs and KI (**Figure 2B**). Of those four, two of them are directly linked to metabolism, glutathione S-transferase 2 and 3 (GSTM2 and GSTM3), which are in charge of detoxification of xenobiotic agents using GSH as redox cofactor. The higher expression of GSTM1/2 may be the consequence of an increased demand for antioxidant protection that may be caused by an IDHm-dependent redox vulnerability. The other two enzymes, dystrobrevin alpha (DTNA) and guanine nucleotide-binding protein G subunit gamma-7 (GNG7) are specific modulators of molecular signaling within the brain and CNS. In order to identify common biological processes we analyzed the Gene Ontology Biological Process (GOBP) enrichment. Proteins upregulated in IDH1m subsets of each biological model

were often participating in metabolic processes, e.g. small molecule catabolic process, monocarboxylic acid metabolic process, or organic acid catabolic process (**Figure 2C**). In order to get more insightful in the specific metabolic pathways involved in these processes, we performed a pathway analysis from different databases such as KEGG pathways, Canonical pathways and Reactome Gene Sets (source: metascape.org) of the differentially expressed proteins in IDH1m models. All three models pointed to a dysregulation of pathways related to cellular metabolism, which could be classified in 3 major metabolic groups: 1) Central carbon metabolism, 2) GSH metabolism, 3) lipid and fatty acid metabolism (**Figure S3**).

Although most of pathways associated with upregulated proteins in IDH1m patients were related with metabolism, in the *in vitro* models (PDCs and KI cells) downregulated proteins were also associated with metabolic pathways. This might be explained by the differential nutrient supply encountered within culture conditions. However, as observed in patient material similar metabolic pathways related with glucose, glutamate, TCA or GSH metabolism were found differential as well in the *in vitro* models.

Integrative characterization of IDH1m differential metabolism

For visualization of dysregulated pathways we merged our proteomics and metabolomics studies of IDH1m vs IDHwt glioma patients. *In vitro* and *in vivo* models were checked for complementary validation. To do so, we made use of the Cytoscape© software, an open access platform for visualization of complex biological networks (i.e. genomic, proteomic, metabolomics), based on public databases. Specifically, we utilized KEGG metabolomics dataset (Okuda et al., 2008) in order to integrate the specific proteins and metabolites revealed by our study. As mentioned, metabolic enzymes and metabolites of IDH1m glioma patients are most often upregulated when compared to IDHwt tumors. Although increased enzyme abundance suggest a higher pathway activity, higher metabolite levels could mean either increased production or decreased consumption rates. In order to quantify pathway activity

A

	Patients	PDCs	Isogenic cells
Total differntial proteins	808	590	250
Upregulated proteins IDH1m	336	280	110
Downregulated proteins IDH1m	472	310	140

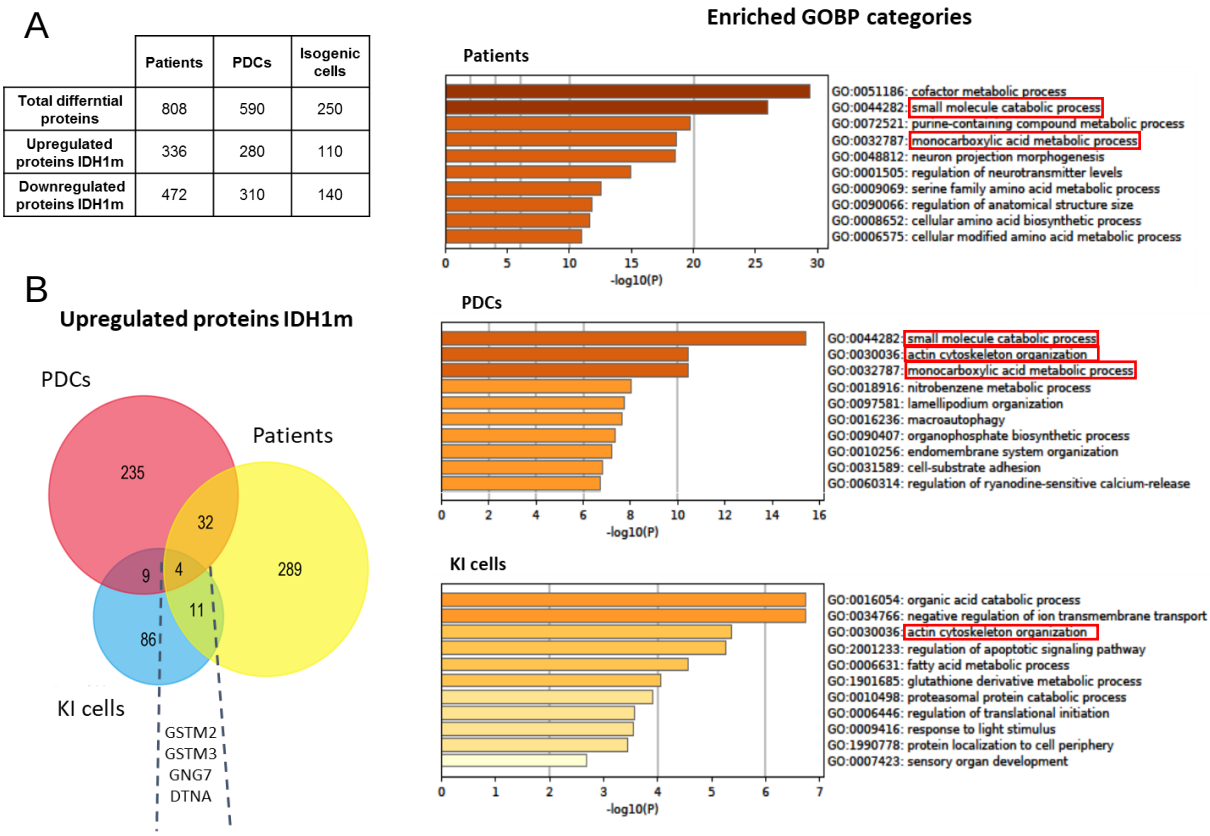

Figure 2. Proteomics analysis reveals altered metabolic processes in IDH1m gliomas
Label-free quantitative (LFQ) LC-MS proteomic comparison on three different glioma models: patient samples (IDH1m n=16 IDHwt n=17), patient-derived cell lines (PDCs) (IDHwt: NCH644 (n=4), NCH601 (n=4), NCH421k (n=4); IDH1m: NCH1681 (n=6), NCH551b (n=4), NCH612 (n=4)) and IDH1m knock-in (KI) cells (sgIDH1m NCH644 (n=4) and IDHwt NCH644 (n=4)) (A) Number of differentially expressed proteins detected in the different models (B) Venn diagram of the upregulated proteins among the three different settings. Four proteins were shared between all conditions: GSTM2, GSTM3, GNG7 and DTNA (C) Top 10 Enriched Gene Ontology Biological Processes (GOBP) from upregulated proteins in IDH1m samples in each model. Processes shared in >1 model are highlighted in red.

levels, further functional validation should be applied, e.g. tracing flux studies. Yet, our integrative analysis aids to understand relevant metabolic pathways and specific reactions that might be decisive in IDH1m gliomas.

Visualization of glycolysis pathway suggests that glucose derivatives may be used to generate precursors for nucleotides and lipids through glucose 6P and glycerol 3P respectively. Glucose 6P is as well the precursor for the pentose phosphate pathway (PPP), one of the main sources of cytosolic NADPH besides IDHwt reaction. Amino acids, such as serine can as well be synthesized *de novo* from glucose intermediate 3P glycerate via PHGDH reaction (**Figure 3**).

In addition, several glucose-independent pyruvate synthesis enzymes were found increased, such as LDHB and MPST, suggesting alternative TCA cycle influx. Besides, ACSS1 (acetyl-CoA synthase 1) catalyzes the synthesis of acetyl-CoA through other metabolites instead of pyruvate (e.g. ethanol, acetate) (**Figure 3**).

We observed certain TCA cycle enzymes to be upregulated in IDH1m tumors, including IDH3, ACO2 (aconitase hydratase), SUCLA2 (succinate-CoA ligase) (**Figure S4**). However, our previously reported low glucose turnover into TCA intermediates (Fack et al., 2017) suggests this pathway may be fueled by anaplerotic input, such as the aforementioned glucose-indepenedent pyruvate production. Moreover, our study showed glutamate metabolism may also play a crucial role in anaplerotic influx into the TCA cycle. Glutamate was in fact, one of the only metabolites significantly decreased in IDH1m tumors. The high levels of glutamate to α-ketoglutarate catabolic enzyme, GLUD1, suggests that IDH1m tumors may increase α-ketoglutarate pool through glutamate in order to cope with its vast D-2HG production (**Figure S4**). Moreover, high levels of glutamine conversion via glutamate via GLUL higlights the limiting availability of glutamate in these cells. In addition, we found BCAT1 to be downregulated as well as leucine, which participate in the production of glutamate (**Figure S4**). Finally, as previously mentioned glutamate transporter SLC1A2 or EAAT2 was found increased in IDH1 mutants (**Figure S4**).

The other major metabolic route found significantly increased in IDH1m gliomas was GSH *de novo* synthesis (**Figure S5**). The transsulfuration pathway is a multistep route, key for GSH synthesis, where methionine is metabolized to cysteine. We found central enzymes of transsulfuration pathway to be upregulated such as AHCYL1/2, CBS and GCLC (**Figure S5**). Different metabolites were also found increased here such as S-adenosymethionine (SAM) or α-ketobutyrate. SAM is the methyl donor in cytosine methylation, which is a key epigenetic regulatory process, thus higher SAM levels may be linked to the hypermethylated status associated to IDH1m gliomas. In addition, certain enzymes related with GSH synthesis and

transsulfuration pathway may be also linked to lipid metabolism such as CRAT, but also CKMT1A or CKB (**Figure S5**). Finally, as aforementioned, GSTM enzymes were consistently

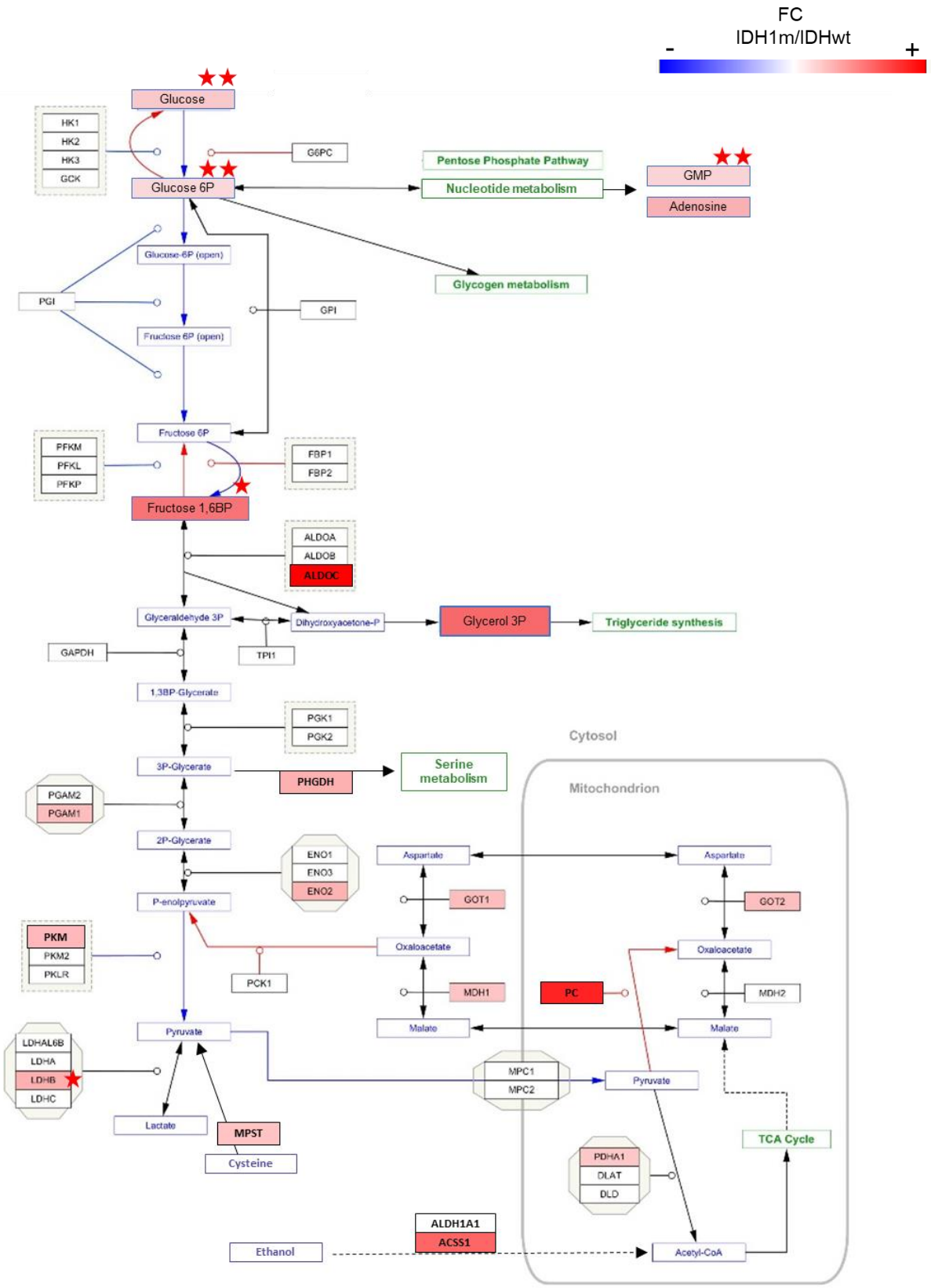

Figure 3. IDH1m metabolic regulation of glucose derivatives
Cytoscape representation of glycolysis pathway regulation in IDH1m glioma patients (Source: KEGG database). Proteins and metabolites that were found differentially expressed from our analysis are colored. The coloring pattern determines the fold change (FC) of IDH1m/IDHwt ranging from red to blue. Each star next to a protein or metabolite indicates that it was also found significantly differential in other complementary model: PDCs and isogenic IDH1m models for proteins; PDCs and xenografts for metabolites.

upregulated in IDH1m gliomas, not only in patients but in all models analyzed, highlighting the capital importance of GSH utilization in these tumors (**Figure S5**).

Overall, we present a metabolic network visualization of IDH1m glioma displaying aberrant regulation in important intermediary pathways such as central carbon metabolism or GSH synthesis. Thus, our study highlights the importance of these pathways as potential targetable vulnerabilities against IDH1m gliomas.

Central enzymes in intermediary metabolism as potential therapeutic targets for IDH1m gliomas

After our integrative analysis we listed a number of different enzymes that could be promising therapeutic targets for IDH1m gliomas due to its central relevance in intermediary metabolism (**Figure 4**). We confirmed the upregulation of these sets of metabolic enzymes by consulting gene expression data from a different patient cohort (source: TCGA database, GlioVis (Bowman et al., 2017)). In concordance to the proteomics data from our patient samples, the genes encoding for those proteins were found to be upregulated in IDH1m patients in the TCGA dataset (**Figure S6**).

Among glucose metabolism enzymes, we found the following to be upregulated in IDH1m gliomas: ALDOC, PDHA1, PC, LDHB and PHGDH (**Figure 4A**). Fructose-biphosphate aldolase (ALDOC) was the most significantly upregulated in IDH1 mutant samples. This enzyme mediates glycolytic flux through conversion of fructose 1,6-BP into glyceraldehyde 3-P. On the other hand, 3-phosphoglycerate dehydrogenase (PHGDH) plays a key role in

alternative processing of glucose for serine synthesis, and is upregulated in many cancers (Mattaini et al., 2016). PDHA1 belongs to the pyruvate dehydrogenase (PDH) enzymatic complex which mediates the conversion of pyruvate into acetyl-CoA thereby linking glycolysis to the TCA cycle. Pyruvate carboxylase (PC), on the other hand, catalyzes the synthesis of the TCA intermediate oxaloacetate from pyruvate, as anaplerotic influx into the TCA cycle. Lactate dehydrogenase B (LDHB) isoform, unlike LDHA, has higher affinity for lactate to pyruvate conversion, thus sustaining cells with alternative sources of pyruvate to the detriment of lactate. We previously reported a lower energetic yield in IDH1m gliomas (Fack et al., 2017). Then, the high abundance of glycolytic enzymes observed here suggests that IDH1m cells may redirect glucose derivatives for biosynthesis of different metabolites such as nucleotides, phospholipids or amino acids. The targeting of some of these enzymes might compromise the capacity of these cells to perform metabolic biosynthesis.

With regard to glutamate metabolism, IDH1m patients showed high levels of different glutamate synthesis and catabolism enzymes including: SLC1A2, GLUD1, GOT1 and GLUL (**Figure 4B**). SLC1A2 gene encodes EAAT2 (excitatory amino acid transporter 2), which is the main transporter mediating the uptake of glutamate into the cell. GLUD1 (Glutamate dehydrogenase 1), catalyzes the conversion of glutamate into α-KG, an anaplerotic influx into the TCA cycle. This might act as α-KG source in IDH1m cells. GOT1, performs the reverse reaction, combining α-KG and aspartate to synthesize glutamate. Finally, glutamine synthase (GLUL), is the enzyme in charge of glutamate to glutamine conversion. The activity of these enzymes together with the low levels of glutamate highlights the importance of glutamate metabolism in IDH1m cells. Besides its role as source for α-KG, glutamate is a limiting metabolite for anaplerosis of the TCA cycle, synthesis of glutathione or synaptic signaling. This suggests that inhibition of glutamate synthesis or transport via some of these enzymes might accentuate the g of IDH1m cells to glutamate dependence.

In addition, several enzymes upregulated in IDH1m patients are important mediators of GSH metabolism, such as CBSL, GCLC, AHCYL1 and GSTM2 (**Figure 4C**). CBSL (Cystathionine

β-synthase like protein), GCLC (Glutamate-cysteine ligase catalytic subunit) and AHCYL1 (S-adenosylhomocysteine hydrolase 1 like protein) participate in *de novo* synthesis of GSH through transsulfuration pathway. We did not detect CSE (i.e. CTH) which is a key enzyme in transsulfuration pathway synthesizing cysteine *de novo*. However, according to parallel investigations currently under process of publication, we have observed that CSE is specifically upregulated in IDH1m astrocytomas and not in IDH1m oligodendrogliomas (**Chapter IV-2**). As aforementioned, GSTM enzymes were significantly upregulated as well in IDH1m patients, participating in GSH-dependent detoxification. NADPH is required as reducing agent for recycling of GSH. As we previously reported we did not observe differences in GSH levels in IDH1m cells although the mutation compromises their NADPH production. The higher activity of transsulfuration pathway enzymes suggests that IDH1m cells rely on de novo synthesis of GSH due to their lack of NADPH production derived from IDH mutation. Overall, this uncovers a redox vulnerability of IDH1m cells which could be harnessed by targeting transsulfuration pathway enzymes, or GSTM2 isoform.

Finally, important enzymes involved in fatty acid metabolism were increased in IDH1m patients including PCCA, ACOT1 and CRAT (**Figure 4D**). PCCA (Propionyl-CoA carboxylase A) mediates catabolism of fatty acids, and ACTO1 (acyl-CoA thioesterase) converts acyl-CoA into free fatty acids. CRAT (Carnitine O-acetyltransferase) regulates the availability of acyl-CoA. Due to the defect in reductive carboxylation of IDH during the mutation, there is a restricted availability of isocitrate, a key substrate for fatty acids. This suggests, some of these enzymes compensate this deficiency in IDH1m cells, therefore its targeting could compromise their fatty acid availability.

IDH1m glioma cells display a low energy metabolism

Besides the observed increase in central carbon metabolism intermediaries, we have previously reported that IDH1m gliomas harbor a low ATP production when compared to IDHwt tumors (Fack et al., 2017).

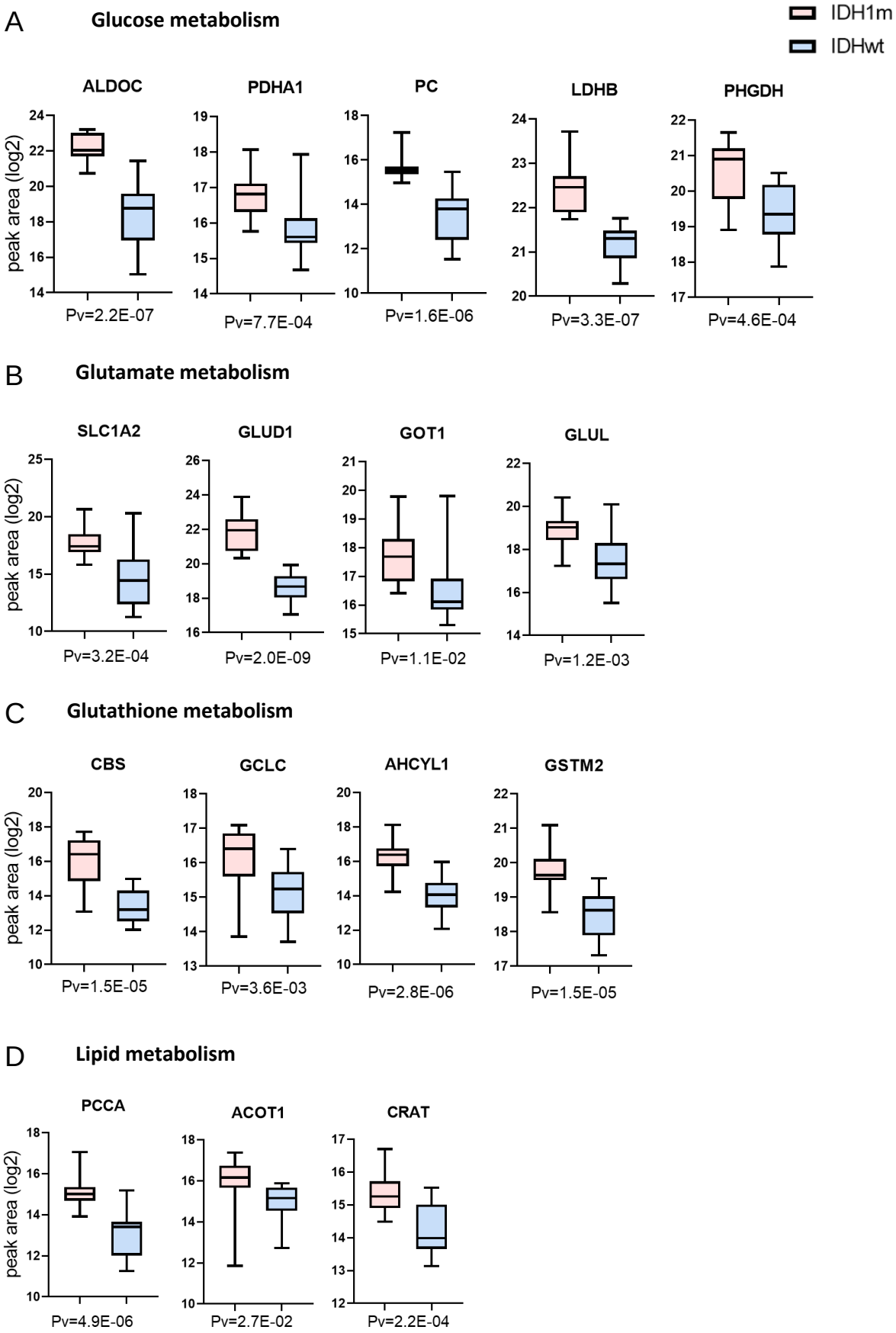
A
Glucose metabolism
IDH1m
IDHwt
ALDOC
PDHA1
PC
LDHB
PHGDH
peak area (log2)
Pv=2.2E-07
Pv=7.7E-04
Pv=1.6E-06
Pv=3.3E-07
Pv=4.6E-04
B
Glutamate metabolism
SLC1A2
GLUD1
GOT1
GLUL
peak area (log2)
Pv=3.2E-04
Pv=2.0E-09
Pv=1.1E-02
Pv=1.2E-03
C
Glutathione metabolism
CBS
GCLC
AHCYL1
GSTM2
peak area (log2)
Pv=1.5E-05
Pv=3.6E-03
Pv=2.8E-06
Pv=1.5E-05
D
Lipid metabolism
PCCA
ACOT1
CRAT
peak area (log2)
Pv=4.9E-06
Pv=2.7E-02
Pv=2.2E-04

Figure 4. IDH1m glioma patients upregulate central enzymes of the intermediary metabolism
Significantly upregulated proteins in IDH1m glioma patients (IDH1m n=16, IDHwt n=17) revealed by the LC-MS-based untargeted proteomics comparison grouped in (A) glucose metabolism, (B) glutamate metabolism, (C) glutathione and (D) lipid metabolism.

However, we hypothesize that IDH1m cells rewire their central carbon metabolism to perform alternative biosynthesis of metabolites. To confirm the low energetic capacity of IDHm cells from a functional perspective, we measured extracellular acidification rate (ECAR) and oxygen consumption rate (OCR) in the PDCs as a proxy of their glycolytic and respiratory capacity respectively. IDH1m cells showed stable levels of the mutant protein (**Figure 5A**). However, IDH1m allele frequency was especially high in astrocytomas, reaching ~100% (**Figure 5B**). This suggests a loss of the heterozygosity normally associated with IDH1m tumors. The tendency to develop an IDH1m homozygosity *in vitro* has been already reported by others (Luchman et al., 2013). Despite the observed loss of heterozygosity, these models yet present active production of D2HG, therefore are still used as correct models to study IDH1 mutation (**Figure S1**). However the mechanism by which the cells are able to produce D2HG despite their IDH1m homozygous status remains unclear. These PDCs grow as 3D spheres in serum-free medium, and are not easily amenable to assays where cells need to be coated on the assay plate. NCH421k and NCH551b were especially reluctant to attach and tended to end up as big sphere clusters (**Figure 5C**). We observed both a significantly decreased basal respiratory capacity and a significantly decreased basal glycolytic capacity in IDH1m cells when compared to IDHwt (**Figure 5D**). This is in line with the reduction of ATP previously reported in IDH1m gliomas and may explain the relatively low proliferation rate compared to GBM tumors.

1.3. Discussion

Mutations in genes encoding IDH1/2 enzymes, are commonly observed in different cancer types, and especially in gliomas (Louis et al., 2016b). Although IDH1m-derived epigenetic

alterations have been well studied due to the advance of genomic profiling technologies (Ceccarelli et al., 2016, Turcan et al., 2012), the metabolic repercussions associated to this mutation are yet poorly understood. Increasing evidence suggests an imbalance of glucose,

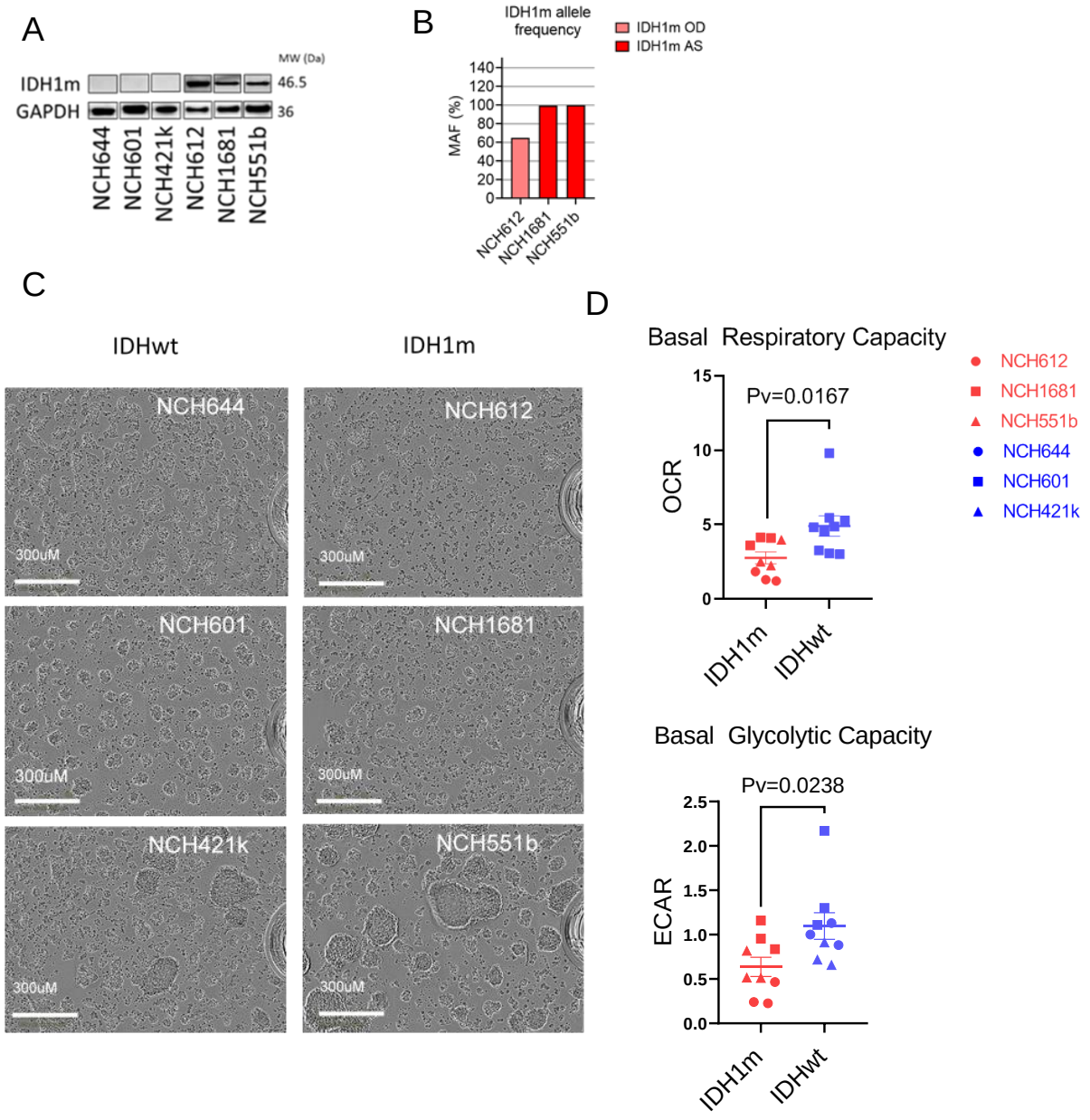

Figure 5. IDH1m glioma cell lines display a low energetic metabolism

(A) Western blot for IDH1m (R132H) and GAPDH in the six glioma patient derived cell (PDC) lines. NCH644, NCH601 and NCH421k correspond to patients with IDH1wt primary glioblastoma (GBM); NCH1681 and NCH551b correspond to patients with IDH1m astrocytoma; NCH612 correspond to a patient with IDH1m oligodendroglioma. (B) Percentage of IDH1 mutant allele frequency (MAF) observed by digital PCR in all IDH1m cell lines, including astrocytomas (AS) and oligodendroglioma (OD). MAF and 95% confidence interval (CI) for each cell line were: NCH612 MAF=64.85%, CI= 61.196% -- 68.65%; NCH1681 MAF= 99.45%, CI= 93.223% -- 106%; NCH551b MAF= 99.98%, CI= 94.808% -- 105.33%. Digital PCR procedure was performed as described in1. Error bars correspond to 95%

confidence intervals (CI) of MAF estimation. One cell stock replicate for each line (n=1)..(C) Phase contrast microscope imaging of PDCs coated to assay plate. (D) Basal respiratory capacity and basal glycolytic capacity based on oxygen consumption rate (OCR) and extracellular acidification rate (ECAR) respectively, in IHDwt and IDH1m cell lines. Each different symbol corresponds to a different cell line and each repeated symbol correspond to one biological replicate. The statistical analysis was performed between all the biological replicates of IDHwt and IDH1m cell lines (n=9). Data normalized to cell density and presented as means ± SEM.

glutaminolysis, lipid biosynthesis and redox metabolism in IDH1m gliomas (Parker and Metallo, 2015), however, the lack of a complete metabolics characterization of these tumors has hampered the deeper understanding.

Some recent mass spectrometry (MS)-based metabolomics studies have attempted to characterize IDHm gliomas, however, data obtained in engineered IDHm GBM cell lines, has not been completely reproduced in PDCs and patient material (Garrett et al., 2018, Miyata et al., 2019). Here we present a comprehensive characterization of IDH1m glioma metabolism through the combination of proteomics, metabolomics and functional assays and making use of *in vitro*, *in vivo* and patient material harboring the mutation. We observed that IDH1m tumors dysregulate essential metabolic pathways such as glucose/glutamate central carbon metabolism and GSH synthesis and utilization. This study reveals new insights, to our knowledge not yet exploited, that may instruct future investigations within the field of IDHm glioma metabolism.

Overall, we observed higher metabolite and metabolic enzyme abundance in IDH1m gliomas when compared to IDHwt. It is not clear whether the high metabolite levels means a high production or otherwise an accumulation due to low consumption, while increased enzyme levels suggest increased pathway activity. In order to confirm this, further tracing flux studies should be applied as functional validation.

We previously reported that IDHm gliomas show decreased ATP levels and reduced energy charge index when compared to IDHwt tumors (Fack et al., 2017). This was confirmed here by our observation that IDH1m PDCs display a decreased basal respiratory and glycolytic capacity (**Figure 5**), suggesting a reduced glucose consumption. However, by combining

proteo-metabolomics analysis in patients and *in vitro* models, we found interestingly that glycolytic and TCA cycle mediators were upregulated in IDH1m gliomas. We previously shown by ^{13}C glucose tracing experiments *in vivo*, that IDH1m gliomas have a decreased glucose turnover into TCA intermediates, especially α-KG (Fack et al., 2017). This suggests that the observed high levels of glycolytic mediators such as glucose, glucose 6P or fructose 1,6BP may be dedicated to fuel other intermediary metabolism routes, instead of the TCA cycle. Indeed, we observed high levels of enzymes mediating glucose derived amino acid production (i.e. PHGDH) or glucose derivatives important in nucleotide metabolism (i.e. GMP, adenosine) and phospholipid synthesis (i.e. glycerol 3P) (**Figure 3**). On the other hand we observe higher expression of LDHB in IDH1m tumors which may also contribute to a decreased glycolytic capacity. LDHB is considered to have higher affinity for lactate to pyruvate reaction (Dang, 2013), what would mean that IDH1m tumors consume lactate in order to increase their pyruvate production, explaining the low ECAR levels we observe. High expression of LDHB has been already reported in IDH1m gliomas (Mustafa et al., 2014).

We found upregulation of certain TCA cycle enzymes including IDH3, ACO2, SUCL2 and SUCLG1. High TCA cycle activity may be directed to increase α-KG availability. IDH1 mutant enzyme consists of a heterodimer formed by an IDH1wt monomer and an IDH1m one. Due to the vast production of D-2HG by the mutant enzyme (FC>40 IDH1m/IDHwt in patients; **Figure 1**), IDH1wt monomer might not be a sufficient source of α-KG. This would specially match with the increased levels of IDH3 (**Figure S4**). However, our previously reported low glucose turnover into TCA intermediates (Fack et al., 2017) suggests an anaplerotic input into this pathway. We observed different enzymatic mediators that regulate pyruvate synthesis independent of glucose, such as PC, MPST, or enzymes that fuel the TCA cycle via other glucose-independent anaplerosis (e.g. via oxaloacetate, malate, acetyl-CoA), such as GOT1/2, MDH1, ACSS1 (**Figure 3**). We also observed high levels of PKM which synthesizes pyruvate from phosphoenolpyruvate, which can be generated from glycolysis but also from oxaloacetate. Indeed we found also high expression of enzymes capable of oxaloacetate

production such as GOT1 and MDH1 (**Figure 3**). Yet, although through anaplerotic sources, TCA cycle would be highly active in IDH1m gliomas, which *a priori* may not explain the low OCR we observed by Seahorse analyzer. It has been reported that D-2HG inhibits complex IV of the electron transport chain (ETC) (Chan et al., 2015, da Silva et al., 2002, Latini et al., 2005). This would explain low OCR levels, meaning that even bearing an active TCA cycle, cellular respiration is yet defective in IDH1m tumors.

Other important anaplerotic sources are glutamate and glutamine (i.e. glutaminolysis). Our data suggests glutamate is limiting in IDH1m gliomas due to high conversion into α-KG via GLUD1 (**Figure S4**). In fact, GLUD1/2 (also known as GDH1/2) have already been shown to promote growth in IDH1m gliomas (Chen et al., 2014). Other sources may attempt to compensate the lack of glutamate, such as glutamate transporter SLC1A2 (i.e. EAAT2), yet glutamate levels are significantly lower in IDH1m gliomas. We also observed that branched-chain amino acid aminotransferase 1 (BCAT1) is downregulated in IDH1m gliomas, as well as the branched-chain amino acid (BCAA) leucine (**Figure S4**). BCATs are enzymes in charge of the synthesis of glutamate through BCAAs. Indeed, it has been shown that D-2HG inhibits BCAT enzymes, further constraining glutamate availability in IDH1m gliomas (McBrayer et al., 2018). Currently glutaminase inhibitors are being tested in clinical trials as potential treatment against IDH1m myeloid malignancies by preventing glutamate synthesis through glutamine (Waitkus et al., 2018a).

Finally, we observed many mediators of GSH metabolism increased in IDH1m gliomas (**Figure S5**). In fact, redox homeostasis is one of the most important metabolic routes thought to be altered in these tumors because of the major role of IDHwt to generate the cytosolic reducing equivalent NADPH, crucial for GSH recycling (Parker and Metallo, 2015, Shi et al., 2015, Fan et al., 2014). Since the IDHm isoform consumes NADPH to produce the oncometabolite D-2HG, it is expected that NADPH is reduced in IDHm gliomas. This is supported by preliminary reports (Bleeker et al., 2010), however due to the difficulty to accurately measure NADP/NADPH, this remains an open question. Here we confirm our previous observation that

certain transsulfuration pathway enzymes, including CBS and GCLC, are upregulated in IDH1m gliomas, suggesting a compensatory pathway to produce GSH independently of NADPH (Fack et al., 2017). Moreover, the consistent upregulation of GSTM enzymes suggests that IDH1m gliomas strictly depend on GSH utilization to be defended against xenobiotic agents. Overall this highlights the potential of targeting GSH synthesis as therapeutic strategy against IDH1m gliomas. On the other hand, NADPH can as well be produced through PPP. We observed that IDH1m gliomas have high levels of glucose 6P (**Figure S5**), which is a precursor for PPP. This could mean that this tumors upregulate the synthesis of NADPH through this pathway to compensate their imbalance generated by IDH mutation.

To conclude, in this study we observed that IDH1 mutation in gliomas leads to a significant dysregulation in diverse enzymes and metabolites within central carbon and GSH metabolism. To fully elucidate the exact implications that upregulation of these pathways have in IDH1m gliomas, it would be interesting to perform additional functional and metabolic flux analyses. Yet, here we show an integrative metabolic characterization of IDH1m gliomas, to our knowledge not yet reported, linking the presence of IDH mutation to the dysregulation of intermediary, energetic and redox metabolism. Moreover we present different enzymatic targets to further investigate their therapeutic potential in IDH1m glioma models Therefore, we expect to provide here with the basis of future investigations that may be of help to comprehend and address promising metabolic vulnerabilities in these tumors.

1.4. Supplementary material

Figure S1

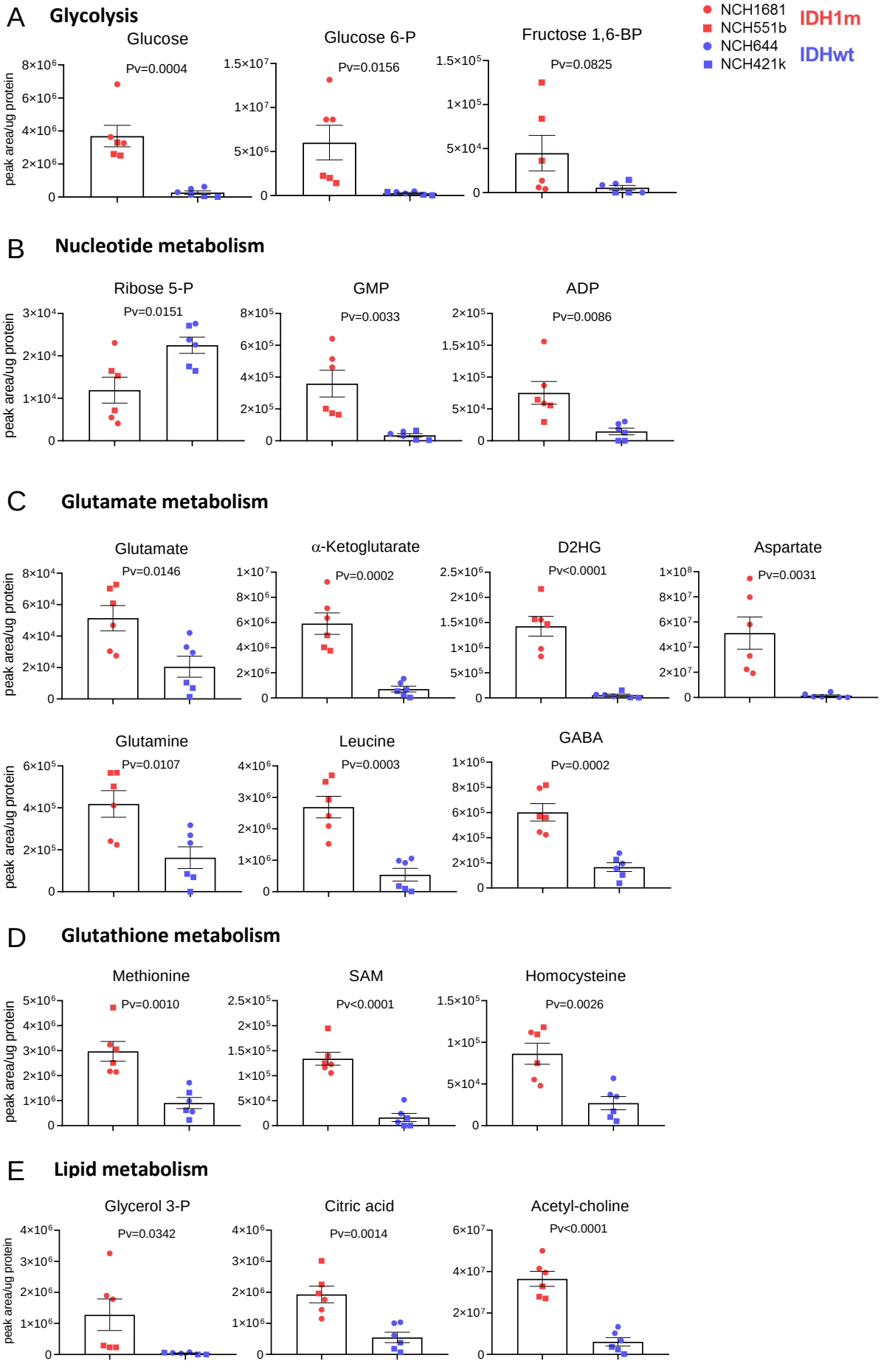
A Glycolysis
Glucose
Pv=0.0004
Glucose 6-P
Pv=0.0156
Fructose 1,6-BP
Pv=0.0825
peak area/ug protein
NCH1681
NCH551b
NCH644
NCH421k
IDH1m
IDHwt
B Nucleotide metabolism
Ribose 5-P
Pv=0.0151
GMP
Pv=0.0033
ADP
Pv=0.0086
C Glutamate metabolism
Glutamate
Pv=0.0146
α-Ketoglutarate
Pv=0.0002
D2HG
Pv<0.0001
Aspartate
Pv=0.0031
Glutamine
Pv=0.0107
Leucine
Pv=0.0003
GABA
Pv=0.0002
D Glutathione metabolism
Methionine
Pv=0.0010
SAM
Pv<0.0001
Homocysteine
Pv=0.0026
E Lipid metabolism
Glycerol 3-P
Pv=0.0342
Citric acid
Pv=0.0014
Acetyl-choline
Pv<0.0001

Figure S1. Metabole analysis in IDH1m patient-derived cell lines
LC-MS-based detection of differentially regulated metabolites in IDHwt (NCH644 (n=3), NCH421k (n=3)) and IDH1m (NCH1681 (n=3), NCH551b (n=3)) cell lines corresponding to the specific metabolic pathways revealed by proteomic analysis, (A), (B), (C) and (D). Each dot of the bar charts corresponds to one independent experiment (n=3). Statistical comparison was applied against NCH644 IDHwt reference sample. Data presented as means ± SEM.*

Figure S2

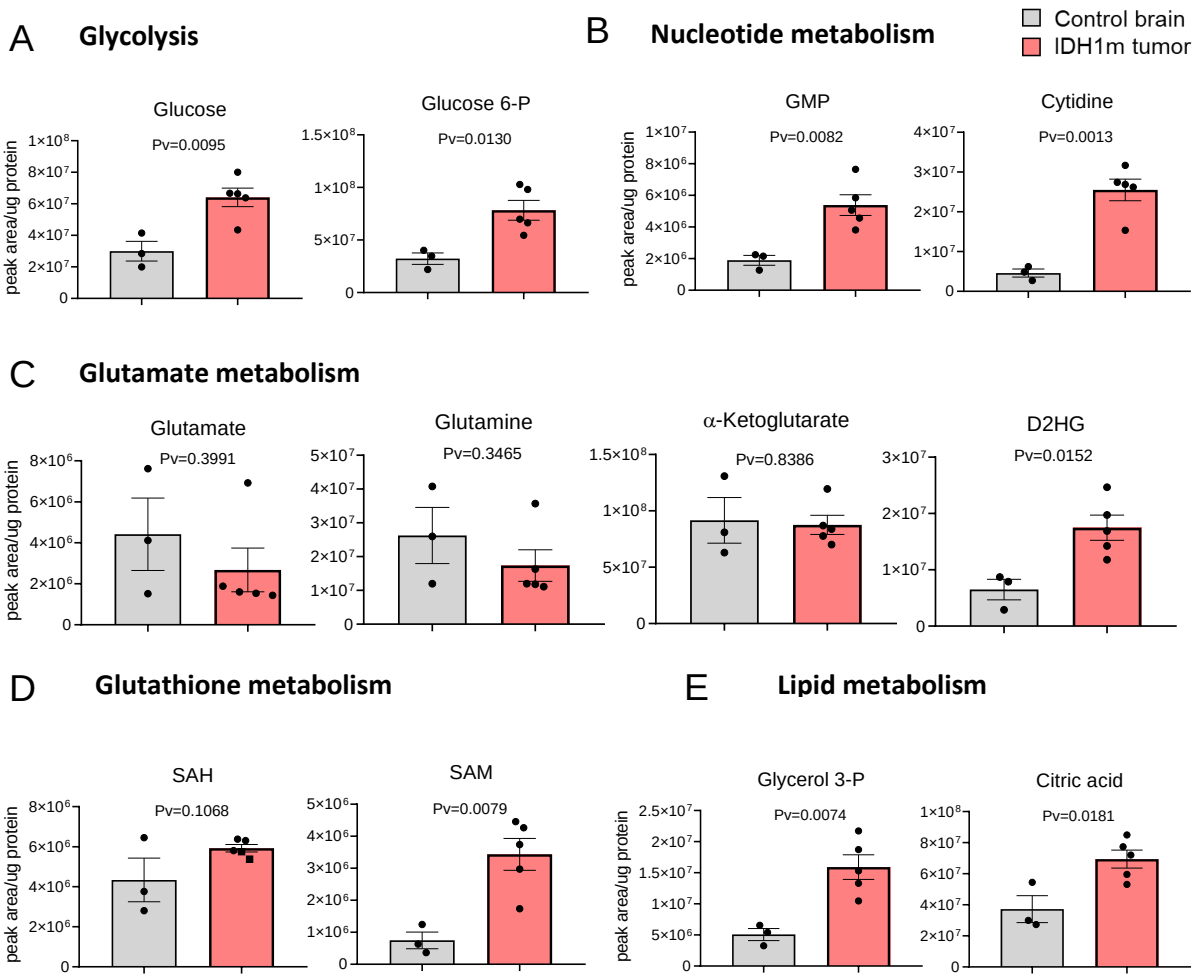

Figure S2. Metabolite analysis in IDH1m xenograft tumors compared to healthy brain tissue
LC-MS-based detection of differentially regulated metabolites in healthy mouse brain and IDH1m glioma xenograft (orthotopic implantation of NCH1681 PDC), corresponding to the specific metabolic pathways revealed by proteomic analysis, (A), (B), (C) and (D). Each dot of the charts corresponds to one independent tumor. Healthy brain (n=3), IDH1m tumors (n=5). Data presented as means ± SEM.

Figure S3

Patients

Up/down proteins	Metabolic group	Pathway	Detected/ Total
Up	Central carbon metabolism	Carbon metabolism	22/114
		Pyruvate metabolism	11/39
		Pyruvate metabolism and Citric Acid (TCA) cycle,	10/55
		Citrate cycle (TCA cycle)	7/30
		Alanine, aspartate and glutamate metabolism	7/35
		Glycine, serine and threonine metabolism	7/40
	GSH metabolism	Cysteine and methionine metabolism	15/56
	Lipid metabolism	Fatty acid metabolism	14/177
Down	Others	Asparagine N-linked glycosylation	25/304
		Diseases associated with glycosaminoglycan metabolism	9/41

PDCs

Up/down proteins	Metabolic group	Pathway	Detected/ Total
Up	Central carbon metabolism	Amino sugar and nucleotide sugar metabolism	5/48
	GSH metabolism	Glutathione metabolism	7/54
	Lipid metabolism	Metabolism of lipids	23/739
Down	Central carbon metabolism	Pyrimidine metabolism	10/109
		The citric acid (TCA) cycle and respiratory electron transport	11/175
		Central carbon metabolism in cancer	6/65
		Metabolism of nucleotides	7/101
		Valine, leucine and isoleucine degradation	5/52
		Glucose metabolism	6/91
		Nucleobase biosynthesis	3/15
		Glycolysis / Gluconeogenesis	5/67
	GSH metabolism	Cysteine and methionine metabolism	7/45

KI cells

Up/down proteins	Metabolic group	Pathway	Detected/ Total
Up	Central carbon metabolism	Pyruvate metabolism	3/39
		Glycine, serine and threonine metabolism	3/40
	GSH metabolism	Glutathione metabolism	4/54
		Biological oxidations	6/222
	Lipid metabolism	Fatty acid metabolism	5/177
Down	Central carbon metabolism	Amino sugar and nucleotide sugar metabolism	5/48
		Carbon metabolism	4/114
	Lipid metabolism	Sphingolipid signaling pathway	4/118

Figure S3. Metabolic pathways dysregulated in IDH1m glioma models

Each table represents the different pathways to which the dysregulated proteins in the proteomics analysis belong, in each of the three different models: Patient samples, patient derived cells (PDCs) and IDH+m knock-in (KI) cells. These are grouped in pathways of upregulated proteins (Up) and downregulated proteins (Down). Pathways are grouped within 3 major metabolic groups: Central carbon metabolism, GSH metabolism and lipid metabolism. “Other” refers to pathways not classified within these three groups. Detected/Total refers to the number of proteins found differential in our analysis over the total proteins listed in the pathway. The pathways were obtained from KEGG, Canonical pathways and Reactom Gene Sets datasets (source: metascape.org). Non-metabolic pathways were not shown.

Figure S4

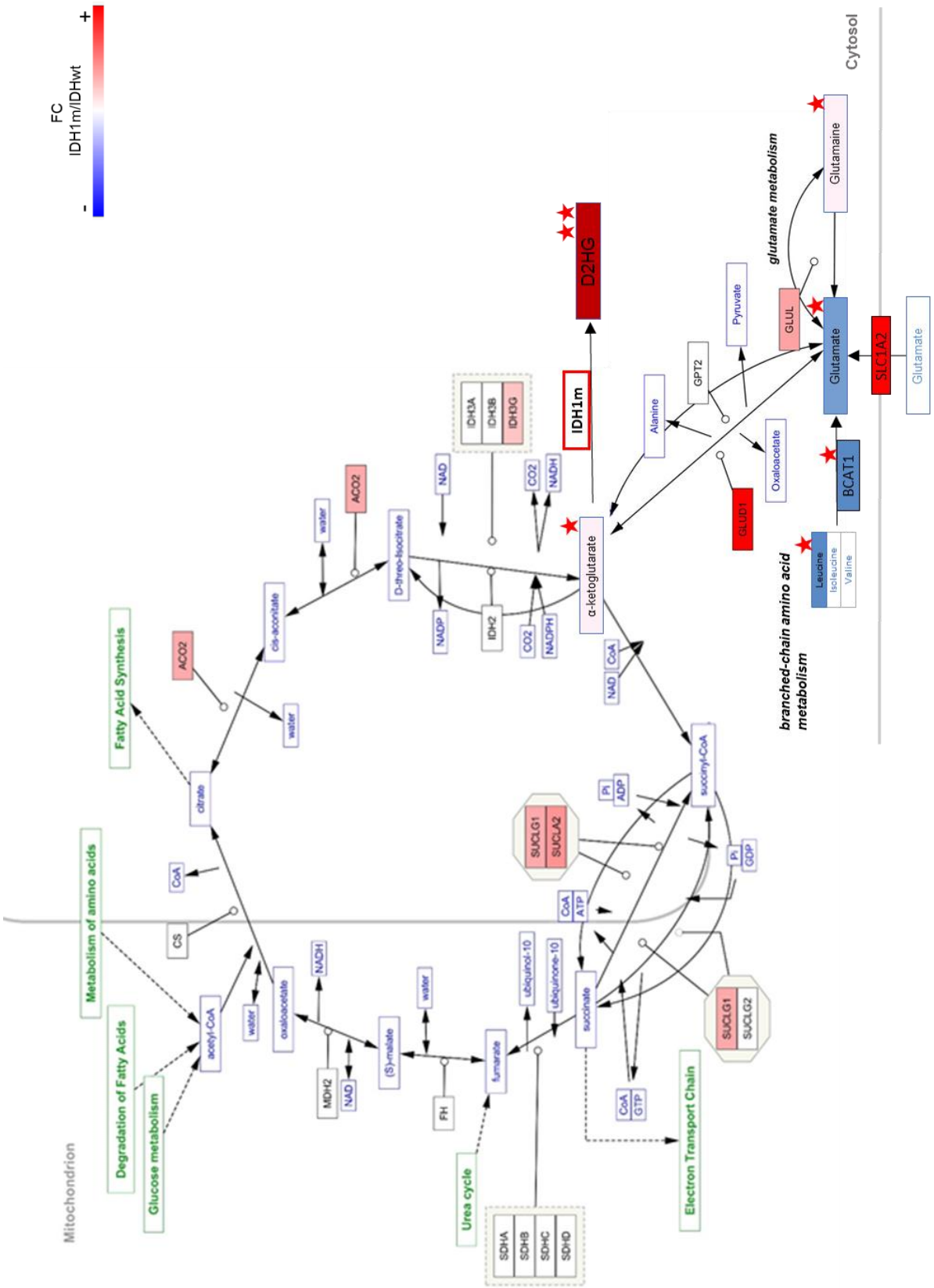
FC
IDH1m/IDHwt
+
-
Cytosol
Mitochondrion
D2HG
IDH1m
Glutamaine
Glutamate
Glutamate
SLC1A2
GLUL
glutamate metabolism
Pyruvate
GPT2
Alanine
Oxaloacetate
GLUD1
BCAT1
Leucine
Isoleucine
Valine
branched-chain amino acid metabolism
α-ketoglutarate
IDH3A
IDH3B
IDH3G
IDH2
NAD
NADP
CO2
NADH
NADPH
D-threo-Isocitrate
ACO2
water
cis-aconitate
citrate
CS
CoA
acetyl-CoA
oxaloacetate
MDH2
(S)-malate
FH
fumarate
SDHA
SDHB
SDHC
SDHD
ubiquinol-10
ubiquinone-10
succinate
SUCLG1
SUCLA2
SUCLG2
succinyl-CoA
Pi
ADP
GDP
ATP
GTP
Metabolism of amino acids
Fatty Acid Synthesis
Degradation of Fatty Acids
Glucose metabolism
Urea cycle
Electron Transport Chain

Figure S4. TCA cycle and glutamate regulation in IDH1m gliomas

Cytoscape representation of TCA cycle and glutamate metabolism in IDH1m glioma patients (Source: KEGG database). All proteins and metabolites that were found differentially expressed from our analysis are colored. The coloring pattern determines the fold change (FC) of IDH1m/IDHwt ranging from red to blue being red the most upregulated in IDH1m gliomas and red the most downregulated. Each star next to a protein or metabolite indicates that it was also found significantly differential in other complementary model: PDCs and isogenic IDH1m models for proteins; PDCs and xenografts for metabolites.

Figure S5

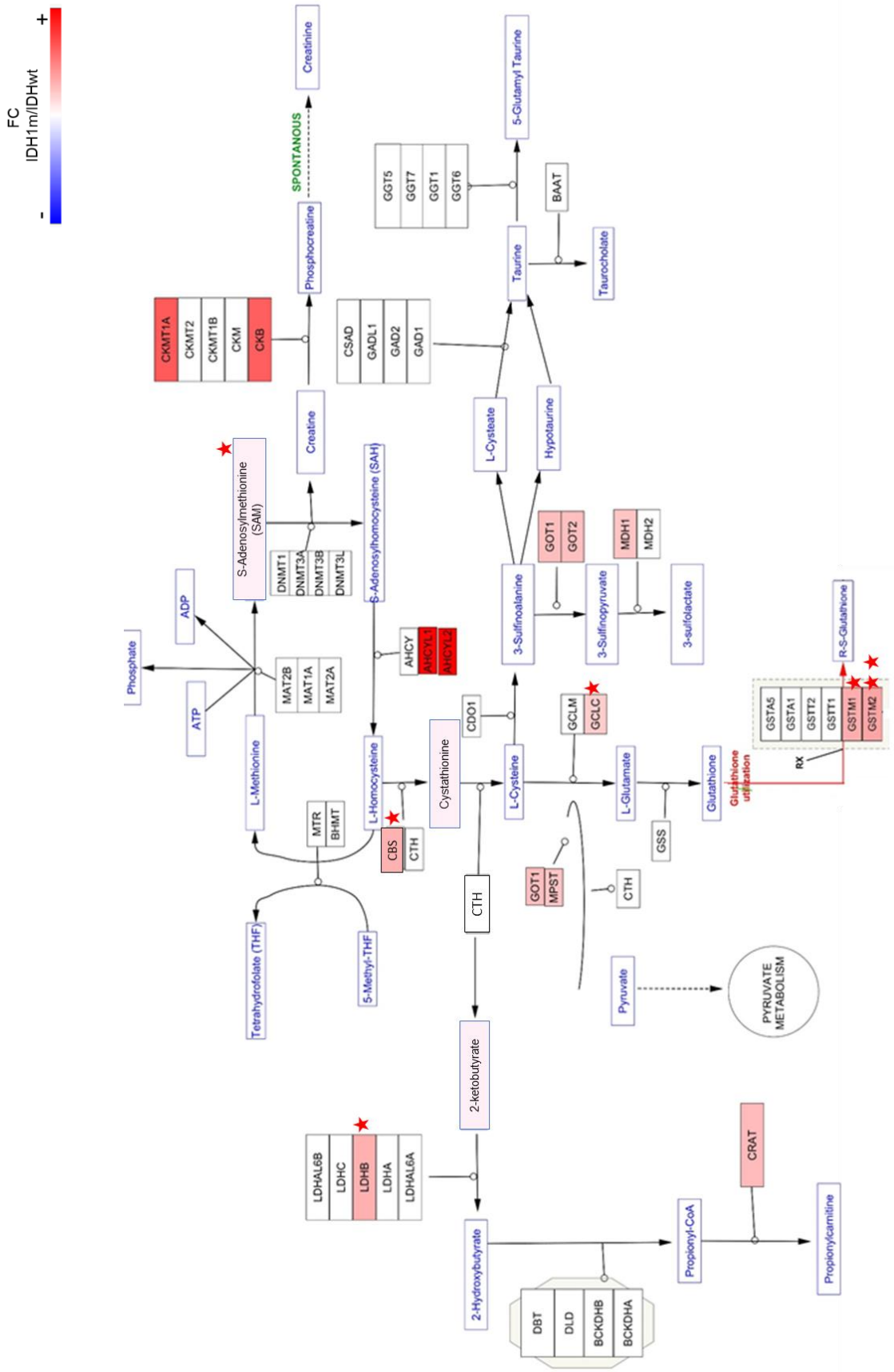
FC
IDH1m/IDHwt
+
-
Creatinine
SPONTANOUS
Phosphocreatine
5-Glutamyl Taurine
GGT5
GGT7
GGT1
GGT6
BAAT
Taurine
Taurocholate
CKMT1A
CKMT2
CKMT1B
CKM
CKB
CSAD
GADL1
GAD2
GAD1
Creatine
L-Cysteate
Hypotaurine
S-Adenosylmethionine (SAM)
S-Adenosylhomocysteine (SAH)
DNMT1
DNMT3A
DNMT3B
DNMT3L
GOT1
GOT2
MDH1
MDH2
ADP
Phosphate
ATP
MAT2B
MAT1A
MAT2A
AHCY
AHCYL1
AHCYL2
3-Sulfinoalanine
3-Sulfinopyruvate
3-sulfolactate
R-S-Glutathione
GSTA5
GSTA1
GSTT2
GSTT1
GSTM1
GSTM2
RX
Glutathione conjugation
L-Methionine
L-Homocysteine
Cystathionine
CDO1
GCLM
GCLC
L-Cysteine
L-Glutamate
Glutathione
MTR
BHMT
CBS
CTH
GSS
GOT1
MPST
CTH
Tetrahydrofolate (THF)
5-Methyl-THF
CTH
Pyruvate
PYRUVATE METABOLISM
2-ketobutyrate
LDHAL6B
LDHC
LDHB
LDHA
LDHAL6A
CRAT
2-Hydroxybutyrate
Propionyl-CoA
Propionylcarnitine
DBT
DLD
BCKDHB
BCKDHA

Figure S5. GSH and transulfuration pathway regulation of IDHm gliomas

Cytoscape representation of GSH metabolism and transsulfuration pathway in IDH1m glioma patients (Source: KEGG database). All proteins and metabolites that were found differentially expressed from our analysis are colored. The coloring pattern determines the fold change (FC) of IDH1m/IDHwt ranging from red to blue being red the most upregulated in IDH1m gliomas and red the most downregulated. Each star next to a protein or metabolite indicates that it was also found significantly differential in other complementary model: PDCs and isogenic IDH1m models for proteins; PDCs and xenografts for metabolites.

Figure S6

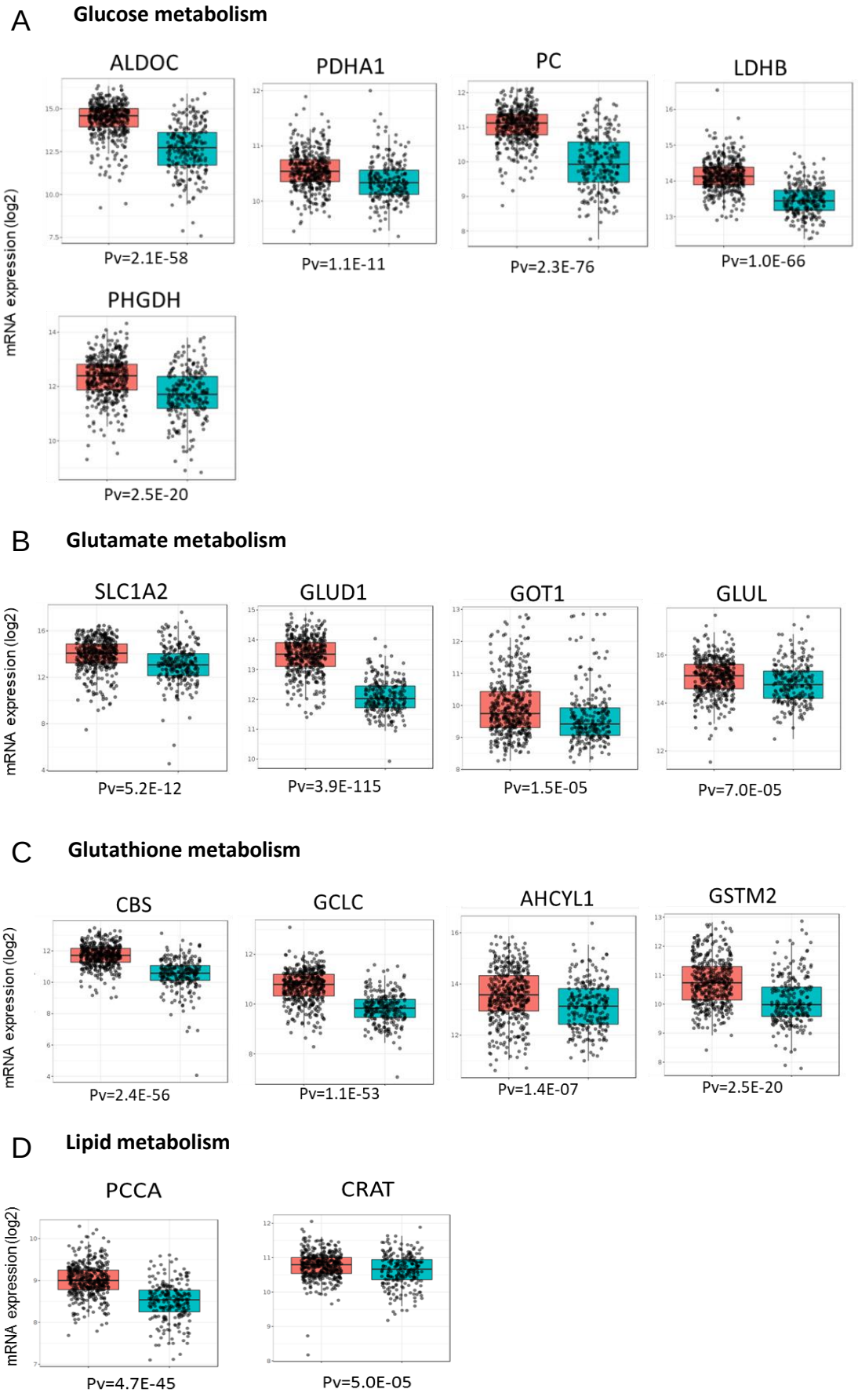
A
Glucose metabolism
ALDOC
PDHA1
PC
LDHB
mRNA expression (log2)
Pv=2.1E-58
Pv=1.1E-11
Pv=2.3E-76
Pv=1.0E-66
PHGDH
Pv=2.5E-20
B
Glutamate metabolism
SLC1A2
GLUD1
GOT1
GLUL
mRNA expression (log2)
Pv=5.2E-12
Pv=3.9E-115
Pv=1.5E-05
Pv=7.0E-05
C
Glutathione metabolism
CBS
GCLC
AHCYL1
GSTM2
mRNA expression (log2)
Pv=2.4E-56
Pv=1.1E-53
Pv=1.4E-07
Pv=2.5E-20
D
Lipid metabolism
PCCA
CRAT
mRNA expression (log2)
Pv=4.7E-45
Pv=5.0E-05

Figure S6. TCGA patient dataset confirms upregulation of specific metabolic genes
IDH1m vs IDHwt glioma significantly differential genes corresponding to the dysregulated metabolic proteins from our proteomic comparison, according to The Cancer Genome Atlas (TCGA), which displays patient gene expression data. TCGA_GBMLGG adult glioma dataset. Pairwise t tests. Pairwise comparisons between group levels with corrections for multiple testing (p-values with Bonferroni correction). (Bowman et al., 2017).

2. Cystathionine-γ-lyase drives antioxidant defense in cysteine-restricted IDH1 mutant astrocytomas

Andrés Cano-Galiano[1], Anais Oudin[1], Fred Fack[1], Maria-Francesca Allega[3,4], David Sumpton[3,] Elena Martinez-Garcia[2], Gunnar Dittmar[2], Ann-Christin Hau[1]; Alfonso De Falco[5], Christel Herold-Mende[6], Rolf Bjerkvig[7,1]; Johannes Meiser[8*], Saverio Tardito[3,4*] and Simone P. Niclou[1,7]

[1]NORLUX Neuro-Oncology Laboratory, Department of Oncology, Luxembourg Institute of Health, Luxembourg;

[2]Quantitative biology unit, Luxembourg Institute of Health, Luxembourg;

[3]Cancer Research UK Beatson Institute, Glasgow, UK;

[4]Institute of Cancer Sciences, University of Glasgow, Glasgow, UK;

[5]National Center of Genetics, Laboratoire national de santé, Dudelange, Luxembourg;

[6]Department of Neurosurgery, University of Heidelberg, Germany;

[7]Department of Biomedicine, University of Bergen, Norway;

[8]Cancer Metabolism Group, Department of Oncology, Luxembourg Institute of Health, Luxembourg

* equal contribution

ABSTRACT

Background. Mutations in isocitrate dehydrogenase 1 or 2 (*IDH1/2*) define glioma subtypes and are considered primary events in gliomagenesis, impacting tumor epigenetics and metabolism. IDH enzyme activity is crucial for the generation of reducing potential in normal cells, yet the impact of the mutation on the cellular antioxidant system in glioma is not understood. The aim of this study was to determine how glutathione (GSH), the main antioxidant in the brain, is maintained in IDH1 mutant gliomas, despite an altered NADPH/NADP balance.

Methods. Proteomics, metabolomics, metabolic tracer studies, genetic silencing and drug targeting approaches *in vitro* and *in vivo* were applied. Analyses were done in clinical specimen of different glioma subtypes, in glioma patient-derived cell lines carrying the endogenous IDH1 mutation and corresponding orthotopic xenografts in mice.

Results. We find that cystathionine-γ-lyase (CSE), the enzyme responsible for cysteine production upstream of GSH biosynthesis, is specifically upregulated in IDH1 mutant astrocytomas. CSE inhibition sensitized these cells to cysteine depletion, an effect not observed in IDH1 wild-type gliomas. This correlated with an increase in reactive oxygen species and reduced GSH synthesis. Propargylglycine (PAG), a brain-penetrant drug specifically targeting CSE, led to delayed tumor growth in mice.

Conclusions. We show that IDH1 mutant astrocytic gliomas critically rely on NADPH-independent *de novo* GSH synthesis via CSE to maintain the antioxidant defense, which highlights a novel metabolic vulnerability that may be therapeutically exploited.

KEY WORDS

IDH mutation, glioma, glutathione, transsulfuration pathway, antioxidant defense, cysteine

2.1. Introduction

The identification of a point mutation in the enzymes isocitrate dehydrogenase 1 or 2 (IDH1, IDH2) has dramatically improved our understanding of glioma genesis (Parsons et al., 2008) and led to a better delineation of glioma subtypes. Whereas primary glioblastomas (GBM) harbour the wild-type enzyme (IDHwt), mutated IDH (IDHm) defines lower grade gliomas, which are further subdivided based on codeletion of chromosomal arms 1p and 19q (1p19q codel) for oligodendrogliomas (OD) and mutations in *TP53* and *ATRX* for astrocytomas (AS) (Louis et al., 2016b). While both IDH1 and IDH2 can be mutated in cancer, gliomas most often display the R132H mutation in IDH1. IDH1 is a cytoplasmic enzyme that β-decarboxylates isocitrate to α-ketoglutarate (αKG) thereby generating NADPH and CO_2, while the mutant enzyme converts αKG into D-2-hydroxyglutarate (D2HG) and oxidizing NADPH (Dang et al., 2009b). D2HG competitively inhibits αKG-dependent TET dioxygenases and JmjC histone demethylases (Xu et al., 2011a, Losman and Kaelin, 2013) leading to hypermethylation of CpG islands and histones H3 and H4 respectively (Turcan et al., 2012, Duncan et al., 2012). Wild-type IDH1 is one of the main contributors of cytosolic NADPH, which is crucial for anabolic processes and redox homeostasis via GSH recycling (Jiang et al., 2016). It has been shown that up to 65% of total NADPH comes from this reaction in IDH1wt GBM, whereas this contribution is decreased in IDH1m gliomas (Bleeker et al., 2010). Moreover, several reports suggest that the IDH1 mutation enhances chemo-radiosensitivity through GSH depletion and ROS generation (Shi et al., 2015, Juratli et al., 2015, Li et al., 2017, Reitman et al., 2011).

We previously reported metabolic aberrations in phospholipids, energy and oxidative stress regulation in IDH1m glioma patients and derived orthotopic xenografts (Fack et al., 2017). Notably, despite a drop in the NADPH/NADP ratio, we detected high levels of GSH in IDH1m tumors, while enzymes related to cysteine metabolism and *de novo* GSH production such as cystathionine-β-synthase (CBS) and Glutamate-cysteine ligase catalytic subunit (GCLC) showed increased gene expression in IDH1m gliomas, suggesting that *de novo* GSH synthesis might be active in these tumors (Fack et al., 2017).

A major limitation in the study of metabolic adaptations of IDH1m gliomas is the lack of appropriate cell culture and animal models. The notorious difficulty of growing glioma cells carrying the endogenous IDH mutation has led various research groups to use GBM cell lines engineered to overexpress the mutant enzyme (Zhu et al., 2017, Li et al., 2017, Reitman et al., 2011, McBrayer et al., 2018). Although a practical cellular set up, such models lack the phenotype and genetic background of astrocytoma or oligodendroglioma subtypes. Here we were able to use clinical material of different glioma types as well as unique patient-derived cell lines with and without the endogenous IDH1 mutation and corresponding orthotopic xenografts to interrogate GSH and cysteine metabolism in IDH1m gliomas. Using proteomics, metabolomics, tracer studies and genetic silencing approaches, we report that IDH1m astrocytomas specifically rely on cystathionine-γ-lyase (CSE, also known as cystathionase encoded by the *CTH* gene) to increase their cysteine pool for *de novo* GSH synthesis. Furthermore, we show that the CSE inhibitor propargylglycine (PAG) leads to increased reactive oxygen species (ROS) and cytotoxicity at low cysteine levels *in vitro*, and decreases tumor growth *in vivo.* Our data provide a rationale for therapeutically targeting CSE in IDH1m astrocytoma patients.

2.2. Results

IDH1m astrocytomas upregulate cystathionine-γ-lyase (CSE)

We previously reported the upregulation of CBS and GCLC in IDHm gliomas, suggesting an activation of the transsulfuration pathway **(Figure 1a)** in these tumors(Fack et al., 2017), an important source of cysteine for GSH synthesis in astrocytes(McBean, 2012, McBean, 2017). To corroborate this at the metabolite level, we analyzed specimen from 22 glioma patients including IDHwt GBM (n=10), IDH1m OD (n=4) and IDH1m AS (n=8) (**Supplementary Table 1**). As expected, IDHm gliomas showed high D2HG and reduced αKG levels compared to IDHwt GBM (**Figure 1b**). Interestingly, while GSH levels were similar, we observed a decrease

in glutamate and an increase in glucose and cystathionine in IDHm gliomas, supporting activation of the transsulfuration pathway (**Figure 1b**).

To address this in a model amenable to experimental manipulation, we turned to patient-derived glioma stem-like cells (GSCs) carrying the endogenous IDH1 mutation (NCH1681, NCH551b, NCH612) and control cells of IDHwt GBM (NCH644, NCH601, NCH421k) (**Figure S1a**). IDH1m GSCs exhibited D2HG levels comparable to patients and display low proliferation rates(Trong et al., 2020, Dao Trong et al., 2018, Dettling et al., 2018). We confirmed the presence of the mutation at the genetic (**Figure S1b**) and protein level **(Figure 1c)** and a more than 20 fold increase in D2HG (**Figure S1c**). IDH1m allele frequency reached almost 100% in astrocytic cell lines (**Figure S1b**), suggesting a loss of heterozygosity over time. The tendency to develop an IDH1m homozygosity *in vitro* has already been reported by others(Luchman et al., 2013). Next we investigated the expression of the main mediators of GSH production, CBS and cystathionine-γ-lyase (CSE) at the protein level. CSE is central to this pathway and the only known enzyme capable to synthesize cysteine, the limiting metabolite for GSH production(Berg et al., 2012). CSE generates cysteine, α-ketobutyrate and ammonia through the breakdown of cystathionine which is provided by CBS in the transsulfuration pathway (**Figure 1a**). While CBS showed similar expression in all tumor types, we found that CSE was upregulated in IDH1m cells both at the protein and mRNA level, **(Figure 1c-e).** Among glioma subtypes, the upregulation of CSE was mainly seen in the IDH1m AS cell lines (NCH1681, NCH551b) (**Figure 1c-e**). This was confirmed *in vivo* in a panel of patient-derived orthotopic xenografts, while there was variable expression in IDHwt xenografts (**Figure S1d-f**). We further validated these data interrogating our clinical material, which showed increased CSE protein in IDH1m tumors compared to IDHwt, with highest expression in AS (**Figure S1g,h**). Gene expression data from public databases using the GlioVis portal, further confirmed these observations (Bowman et al., 2017) (**Figure S1i**).

To obtain a more comprehensive view of protein deregulation in IDH1m gliomas, we performed label-free quantitative (LFQ) MS-based proteomics and identified a total of 6.265 proteins **(Figure 1f)**. Principal component analysis (PCA) clearly separated two distinct populations

based on IDH1 status (**Figure S1j**). From the identified proteins, 575 were differentially expressed between IDH1wt and IDH1m cell lines (FDR<0.05) (**Figure 1f** and **Supplementary table 3**), with 127 proteins upregulated and 258 downregulated in IDH1m cells (FDR <0.05, fold change (FC) >2) (**Figure 1g**). Further analysis between AS and OD was not possible because only 1 OD sample was available. Of note, CSE was the most upregulated protein in IDH1m cells (FC=37). In concordance with the above, this increase in CSE was mainly seen in AS cells (FC=71). By gene ontology interrogation, we found that the top 10 processes of IDH1m upregulated proteins were linked to metabolism (**Figure S1k**), while ribosome and RNA related processes were downregulated in IDH1m cells (**Figure S1k**), in line with the low proliferative phenotype of these tumors. Among the metabolic processes upregulated is the oxidation-reduction process including several proteins involved in redox regulation: glutathione S-transferase Mu 2 (GSTM2) in charge of GSH conjugation and dehydrogenase/reductase SDR family member 4 (DHRS4) an important NADPH producer (**Figure 1g**). In summary, we found that cystathionine accumulates in IDHm gliomas and identify its converting enzyme CSE and related partners to be specifically upregulated in IDH1m AS, suggesting an increased activity of the transsulfuration pathway in this glioma type.

Loss of CSE reduces viability in IDH1m astrocytoma cells under cysteine depletion

To investigate the role of CSE in IDH1m AS, we established stable CSE knockdown (KD) lines in NCH1681 cells (IDH1m AS) using two different shRNAs. Both KD clones (shCSE1 and shCSE2) showed a strong drop in CSE protein (**Figure 2a,b**), yet we did not observe a significant difference in sphere size over time (**Figure 2c**) compared to control (shCTR), indicating that the proliferation capacity of these cells was unaltered under standard culture conditions. We argued that CSE may not be required if sufficient cysteine is provided from extracellular sources. In standard culture medium the concentration of cysteine (360 µM combined cysteine and its oxidized dimer cystine; see **Supplementary Methods**) is higher

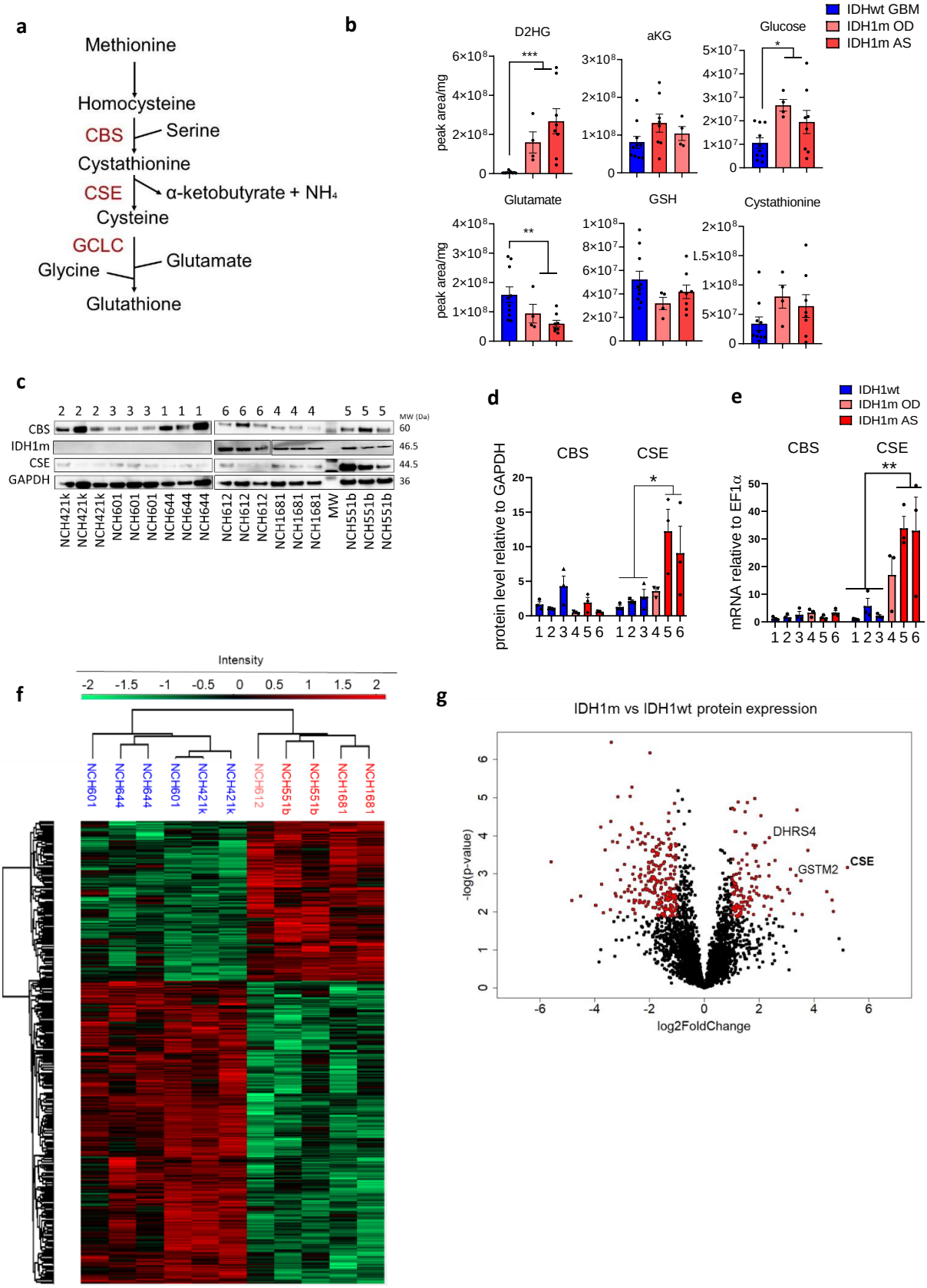
a
Methionine
Homocysteine
CBS
Serine
Cystathionine
CSE
α-ketobutyrate + NH4
Cysteine
GCLC
Glycine
Glutamate
Glutathione
b
IDHwt GBM
IDH1m OD
IDH1m AS
D2HG
aKG
Glucose
Glutamate
GSH
Cystathionine
peak area/mg
c
CBS
IDH1m
CSE
GAPDH
MW (Da)
60
46.5
44.5
36
NCH421k
NCH601
NCH644
NCH612
NCH1681
NCH551b
MW
d
CBS
CSE
protein level relative to GAPDH
e
IDH1wt
IDH1m OD
IDH1m AS
mRNA relative to EF1α
f
Intensity
g
IDH1m vs IDH1wt protein expression
DHRS4
GSTM2
CSE
-log(p-value)
log2FoldChange

Figure 1. CSE is specifically upregulated in IDH1m astrocytomas
(a) Schematic of GSH *de novo* synthesis through the transsulfuration pathway. (b) Total levels of metabolites in 22 clinical samples, presented as peak area relative to mg of tissue. IDHwt (n=10), IDH1m OD (n=4) and IDH1m AS patients (n=8). (c) Western blot for CBS, IDH1m, CSE and GAPDH in IDH1wt and IDH1m cell lines. MW (Da) indicates specific molecular weight of each protein. (d) Quantification relative to GAPDH (n=3). (e) *CSE* gene expression relative to *EF1α* determined by qPCR (n=3). (f) Untargeted proteomic analysis of 3 IDH1wt and 3 IDH1m cell lines. Heat map representation of 575 differentially expressed proteins (false discovery rate (FDR) <0.05). 127 proteins upregulated and 258 downregulated in IDH1m glioma cells (n=2 /cell line, except for NCH612 where n=1). (g) Volcano plot of all 6,265 detected proteins (in red differential proteins with FDR<0.05, FC>2). CSE, GSTM2 and DHRS4 are highlighted. For complete protein list see Supplementary Data 1.
D2HG: D2-hydroxyglutarate; αKG: α-ketoglutarate; GSH: glutathione; CSE: cystathionine-γ-lyase; CBS: cystathionine-β-synthase; GAPDH: Glyceraldehyde 3-phosphate dehydrogenase. IDH1wt: isocitrate dehydrogenase wild type; IDH1m: IDH1 mutant, AS: Astrocytoma; OD: Oligodendroglioma. Each independent dot of the bar charts corresponds to one biological replicate (n). Data presented as means ± SEM. * p<0.05; ** p<0.01; *** p<0.001.

than in human blood (80-180 µM)(Psychogios et al., 2011) (source: HMDB). In contrast, in cerebrospinal fluid (CSF), a reference for nutrient values in the brain, cysteine is one of the lowest amino acids with values below 1 µM(Engelborghs et al., 2003) (source: HMDB). To reach a concentration more relevant to neural tissue, cysteine was serially diluted in cysteine-free DMEM. This led to a gradual loss of sphere viability (based on GFP fluorescence) in CSE KD cells (**Figure 2d, e)**. Control cells only were affected upon complete cysteine withdrawal. The selective impact on CSE KD cells was most prominent at 30 µM cysteine, where the decrease in viability was already observed after 2 days of culture further increasing over time (**Figure 2f**). Taken together, these data provide evidence that under physiological cysteine concentrations, CSE is required to maintain viability of IDH1m AS cells.

CSE directs GSH biosynthesis upon cysteine starvation

We next asked whether CSE was required to maintain the cysteine pool for GSH production and whether the observed loss of viability was caused by a decrease in GSH levels. We determined the contribution of CSE to the overall GSH pool, by quantifying metabolites in cultures with 30 µM cysteine at different time points. After a 3 day incubation, no effects of metabolites were observed (**Figure S2a**), in line with the cell viability results (**Figure 2f**).

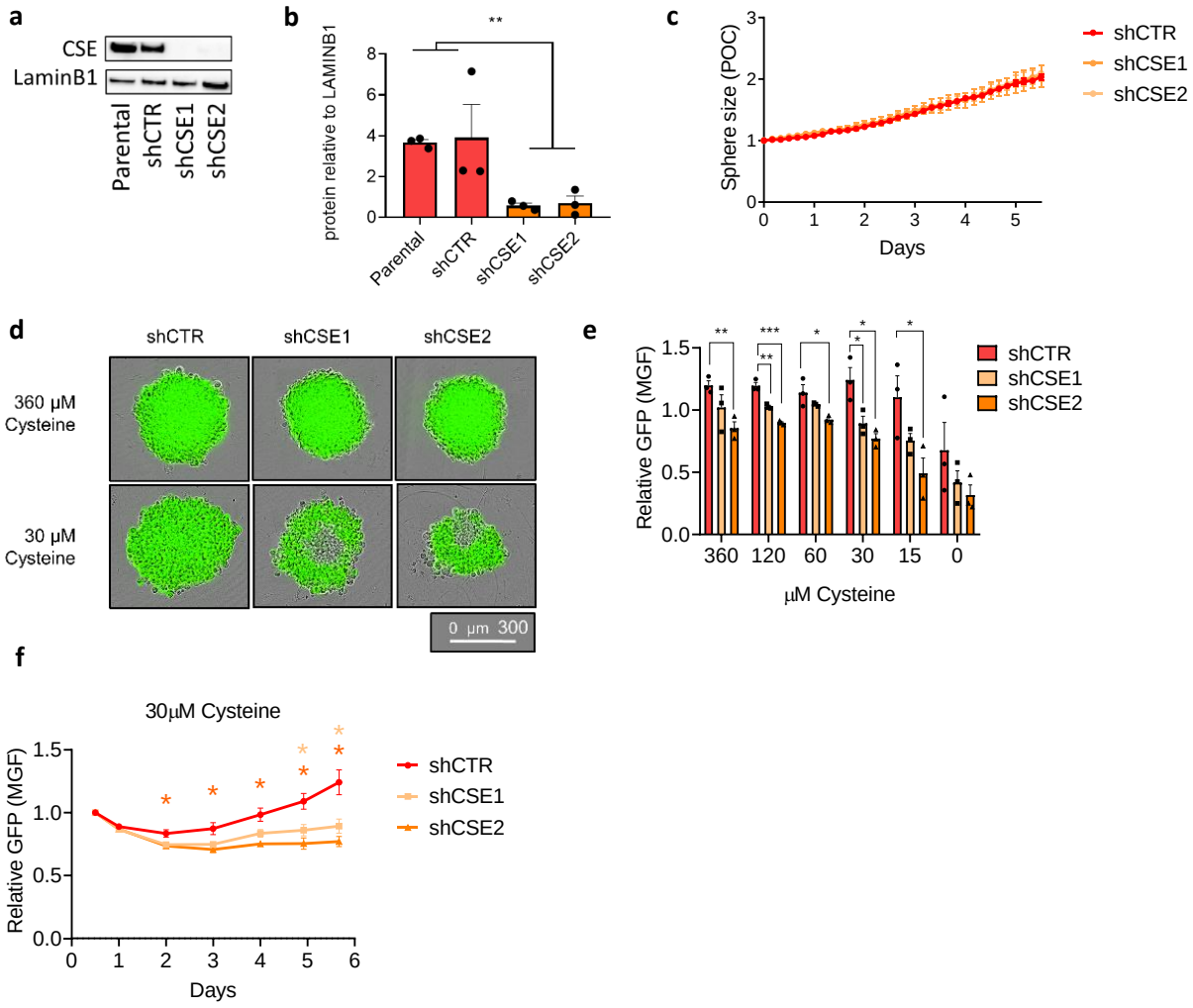

Figure 2. CSE is required to maintain viability of IDH1m astrocytoma cells under cysteine depletion.

(a) CSE western blot analysis and (b) quantification relative to LaminB1 in IDH1m AS cells (NCH1681) with two CSE KD clones (shCSE1, shCSE2) compared to the parental and scramble control (shCTR) (n=3). (c) Relative sphere size under standard culture conditions (360 µM cysteine). Data presented as fold change of phase object confluence (POC) of each cell line relative to day 0. (n=3 with 5 spheres per experiment). (d) Representative fluorescent images of spheres after 6 days. (e) Relative GFP signal in CSE KD cells at decreasing cysteine concentrations (day 6). Measurements expressed as fold change of mean green fluorescence (MGF) of each cell line relative to starting point (360 µM cysteine at day 0.5 once the sphere was formed). (n=3 with 5 spheres per experiment). (f) Time course of GFP signal of spheres at 30 µM cysteine. All data presented as means ± SEM. * p<0.05, ** p<0.01; *** p<0.001.

However, at 4 days, we found a decrease of total GSH level in the CSE KD cells (**Figure 3a**). Presumably all remaining cysteine had been used up which was also reflected in cell viability. This was confirmed in a 2nd experiment (**Figure S2b**). Unfortunately because of the gradual exhaustion of cysteine, many cells were vulnerable at day 4 and not all datapoints could be recovered in these experiments. Interestingly, there was a tendency for decreased serine, glycine, glutamate and glucose in CSE KD cells, along with a slight accumulation in cystathionine (**Figure 3a, S2b**), suggesting an attempt of the cells to compensate for the loss of GSH. Taken together, these data support the premise that GSH biosynthesis depends at least in part on CSE activity upon cysteine depletion.

To confirm that the drop in GSH in CSE knockdown cells was due to a decrease of *de novo* GSH synthesis, we traced $^{13}C_3$-serine in cells cultured with 30 µM cysteine for 4 days (ratio $^{13}C_3$-serine/natural serine = 1:1) (**Figure 3b**). As aforementioned, the limiting culture conditions prevented to recover sufficient biological replicates to perform statistical analysis (**Figure 3c** and **Figure S2c** respectively). Comparable levels of $^{13}C_3$-serine were observed in all cells (**Figure 3c, S2c**), whereas the natural serine isotopologue was reduced in the KDs (**Figure S2d**). This drop in natural serine together with the decrease in total glucose (**Figure 3a**) suggests a preference for glucose-derived serine when there is a high demand for this metabolite. In fact, the enrichment of heavy carbon labelled serine did not exceed 10% of the total pool (**Figure S2e**). Despite the low serine tracer incorporation, there was a tendency for lower $^{13}C_2$-glycine in CSE KD cells (**Figure 3c, S2c**) suggesting reduced serine-to-glycine conversion. In addition, shCSE cells tended towards increased levels of $^{13}C_3$-cystathionine and a consistent decrease in $^{13}C_3$-GSH (**Figure 3c, S2c**). The ratios GSH m+3/Serine m+3 (**Figure S2f**) was significantly lower in the CSE KDs. These data support the notion that under cysteine deprivation CSE is essential to generate cysteine, preferentially via the transsulfuration pathway using glucose-derived serine to sustain GSH biosynthesis.

4 days culture at 30 µM cysteine

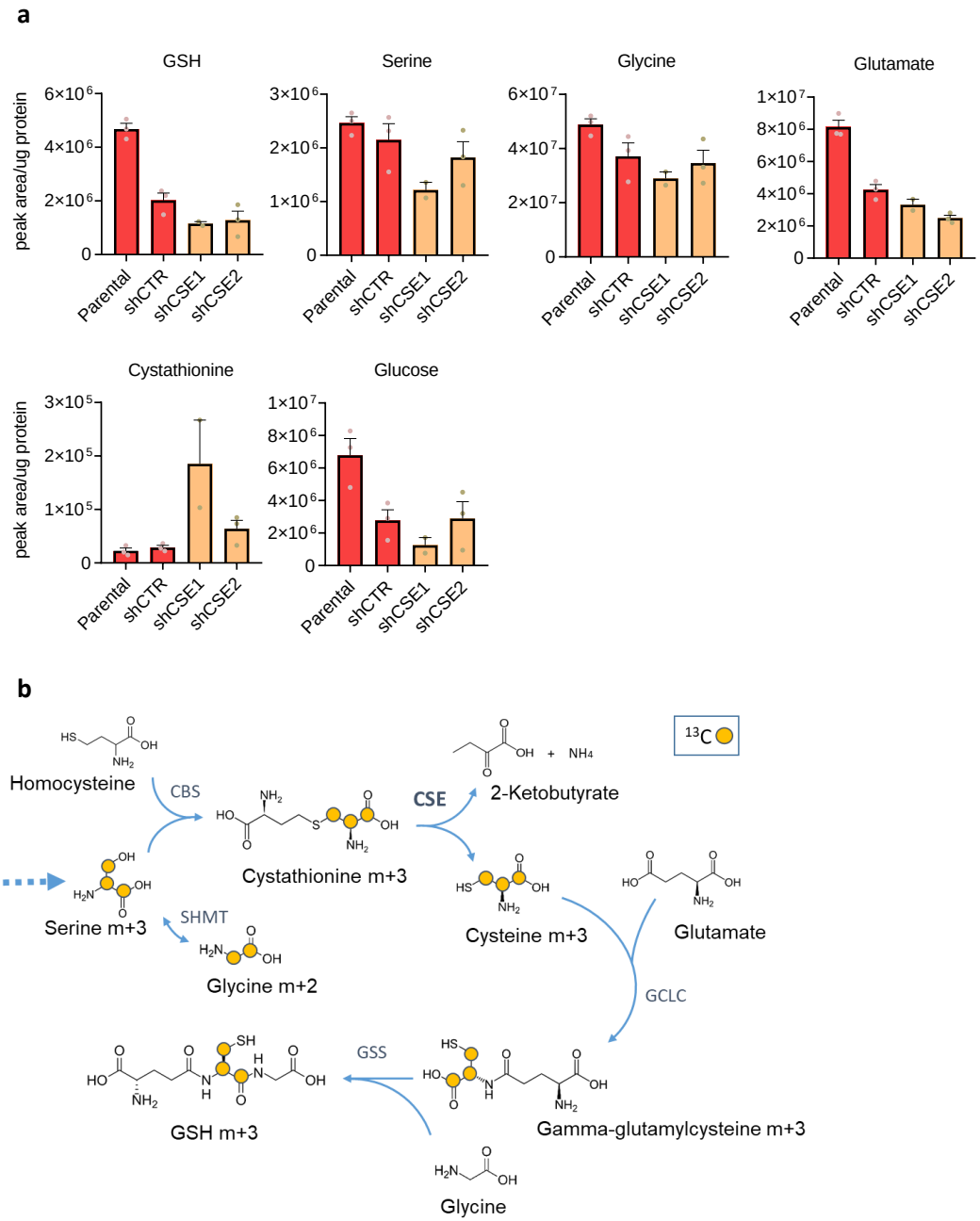

Figure 3. CSE directs GSH biosynthesis upon cysteine starvation
(a) Total metabolite level represented as normalized peak areas at 4 days in 30 µM cysteine. (b) Schematic of $^{13}C_3$-serine metabolite flux towards GSH synthesis. (c) Isotopologues (normalized peak area) after $^{13}C_3$-serine tracing at 4 days in 30µM cysteine. (n=1 with 3 technical replicates in (a) and (c), no statistical analysis). CBS: cystathionine β-synthase; SHMT: Serine hydroxymethyltransferase; CSE: cystathionine-γ-lyase; GCLC: Glutamate-cysteine ligase catalytic subunit; GSS: glutathione synthetase.

IDH1m astrocytoma cells are selectively sensitive to CSE inhibition

Next we wished to evaluate the therapeutic potential of CSE inhibition in glioma using available chemical inhibitors of CSE. Propargylglycine (PAG) (**Figure S3a**) is a non-proteinogenic amino acid that irreversibly blocks CSE through the double interaction with CSE and its cofactor pyridoxal 5-phosphate, which confers strong specificity to the PAG-CSE bond (Sun et al., 2009, Szabo and Papapetropoulos, 2017). We first performed a time course experiment in two IDH1m AS cell lines (NCH1681, NCH551b) with different concentrations of the inhibitor (10, 4, 2, 1, 0 mM) and of cysteine (360, 60, 30 µM) (**Figure S3b**). At 360 µM cysteine, glioma cells were insensitive to PAG even at the highest concentration tested (10 mM), excluding significant off-target effects of the compound. Toxicity increased over time under cysteine-low conditions (60-30 µM) in line with the CSE KD experiments (**Figure S3b**). Interestingly, the cytotoxic effect of PAG was specific to IDHm AS cells, and no significant toxicity was observed in PAG-treated IDHwt GBM cells (NCH644 and NCH421k) **(Figure 4a).** Again the effect was limited to low cysteine (≤ 60 µM) (**Figure 4b**).

To test if the dependency of IDH1m AS cells on CSE activity was related to their antioxidant capacity, we measured ROS levels in IDH1m and IDHwt cells. In line with the cytotoxicity, ROS increased in one of the PAG treated IDH1m AS cells, although this was not robust in the 2nd cell line (**Figure S3d**). Taken together these data provide evidence that CSE inhibition under limited cysteine selectively affects IDH1m AS, possibly mediated by increased oxidative stress.

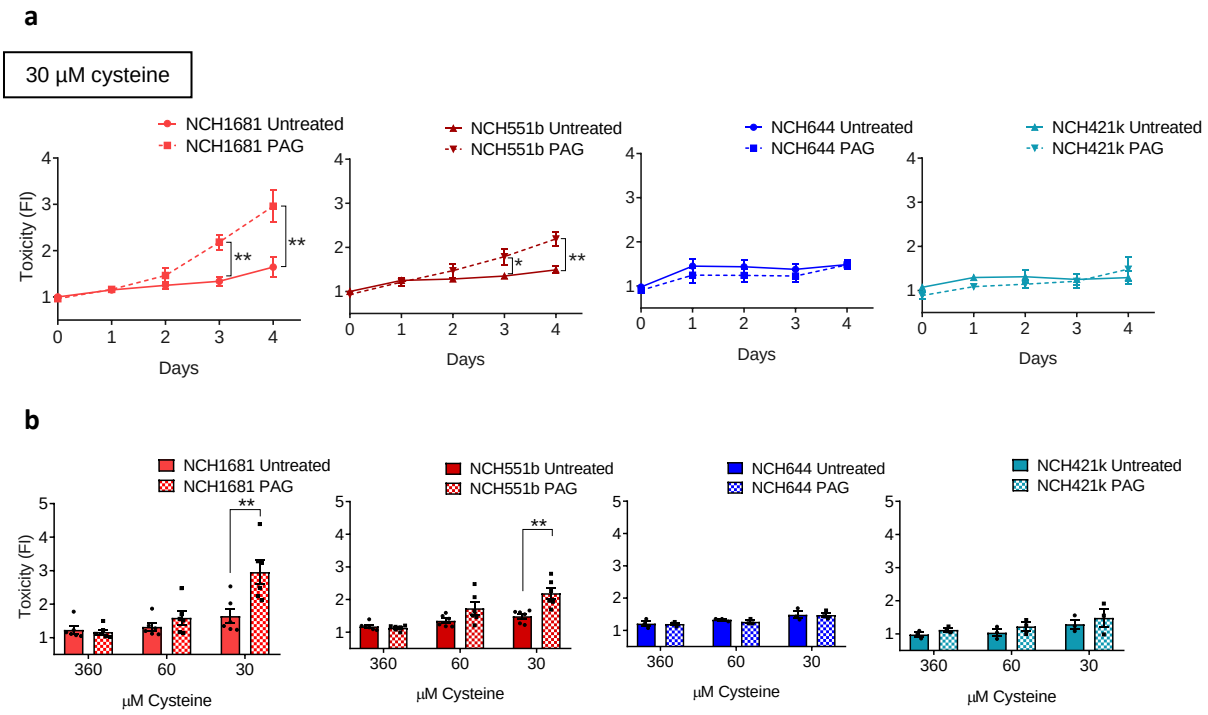

Figure 4. CSE inhibition selectively targets IDH1m astrocytoma cells under cysteine depletion
(a) Toxicity over time in IDH1m AS (NCH1681, NCH551b, in red, n=6). and IDH1wt GBM (NCH644, NCH421k, in blue, n=3) cells following PAG (10mM) at 30µM cysteine. Data presented as fold change of celltox (Promega®) probe fluorescence intensity (FI) relative to normal medium untreated (360 µM cysteine) at day 0. (b) Toxicity of PAG (10mM) upon decreasing cysteine. Data presented as fold change relative to normal medium (360µM cysteine) at day 0. IDH1m AS (n=6). IDH1wt GBM (n=3). Data presented as means ± SEM. * p<0.05; ** p<0.01

CSE inhibition delays tumor growth *in vivo*

To evaluate the efficacy of CSE inhibition on tumor growth *in vivo*, we implanted IDH1m AS cells (NCH1681) into the brain of mice. After two months, tumors were detectable by MRI (around 5 mm^3), mice were randomized into saline and PAG (35mg/kg, 5 times/ week) treated groups **(Figure 5a).** Treatment continued for 3 months and tumor size was monitored by bi-weekly MRIs. Within the first two months of treatment we found a significant decrease in tumor growth rate in PAG treated mice (n=8) (**Figure 5b**). A relative difference in tumor size was observed between both groups over time, which became pronounced, though not significant at the end of the 3rd month (**Figure 5c d**). The experiment was stopped when two mice of the control group reached clinical endpoint (**Figure S4a**).

To determine the effect of PAG at the metabolite level, labelled $^{13}C_3$-serine (130 mg/kg) was terminally infused in the tail vein (n=2/group) (**Figure 5a**), reaching steady state at 4-6 hours in the circulation and in the brain (**Figure S4b**). Consistent with the CSE KD experiment, PAG treated brain tumors showed a slight decrease in serine and glycine when compared to the control group (**Figure 5e**). Moreover the total level of cystathionine was considerably increased in PAG-treated tumors (**Figure 5e**), demonstrating target engagement *in vivo*. This was accompanied by some decrease of methionine and a significant decrease of homocysteine (**Figure 5e**), both precursors of cystathionine. In line with the KD results, GSH and glucose levels were reduced in PAG-treated tumors (**Figure 5e**). A clear accumulation of cystathionine in PAG treated mice was also observed in the liver, where *de novo* GSH biosynthesis normally occurs (Mosharov et al., 2000), while most other metabolic differences appeared to be tumor-specific (**Figure S4c).** The isotopologue distribution revealed that unlabeled serine decreased in treated tumors, whereas $^{13}C_3$-serine (M+3) showed a significant increase (**Figure S4d**). Again, labeled serine only accounted for ~10% of the total pool, reflected in the small amount of labeled cystathionine (M+3) in contrast to the strong accumulation of unlabeled one (M+0) (**Figure S4d**), suggesting preferential use of compensatory glucose-derived serine of IDH1m AS tumors also *in vivo*. In summary, we show that PAG inhibits CSE activity in IDH1m AS brain tumors which causes a significant delay in tumor growth, providing a rationale for a therapeutic potential of CSE inhibitors in IDH1m astrocytomas.

2.3. Discussion

Due to the central role of IDH1 in NADPH recycling (Fan et al., 2014, Jiang et al., 2016), several research groups including ours, have suggested that IDH1m tumors may display specific vulnerabilities in redox metabolism and GSH production that might be therapeutically harnessed (Fack et al., 2017, Shi et al., 2015, Bleeker et al., 2010). Nevertheless, to date there

Due to the central role of IDH1 in NADPH recycling (Fan et al., 2014, Jiang et al., 2016), several research groups including ours, have suggested that IDH1m tumors may display specific

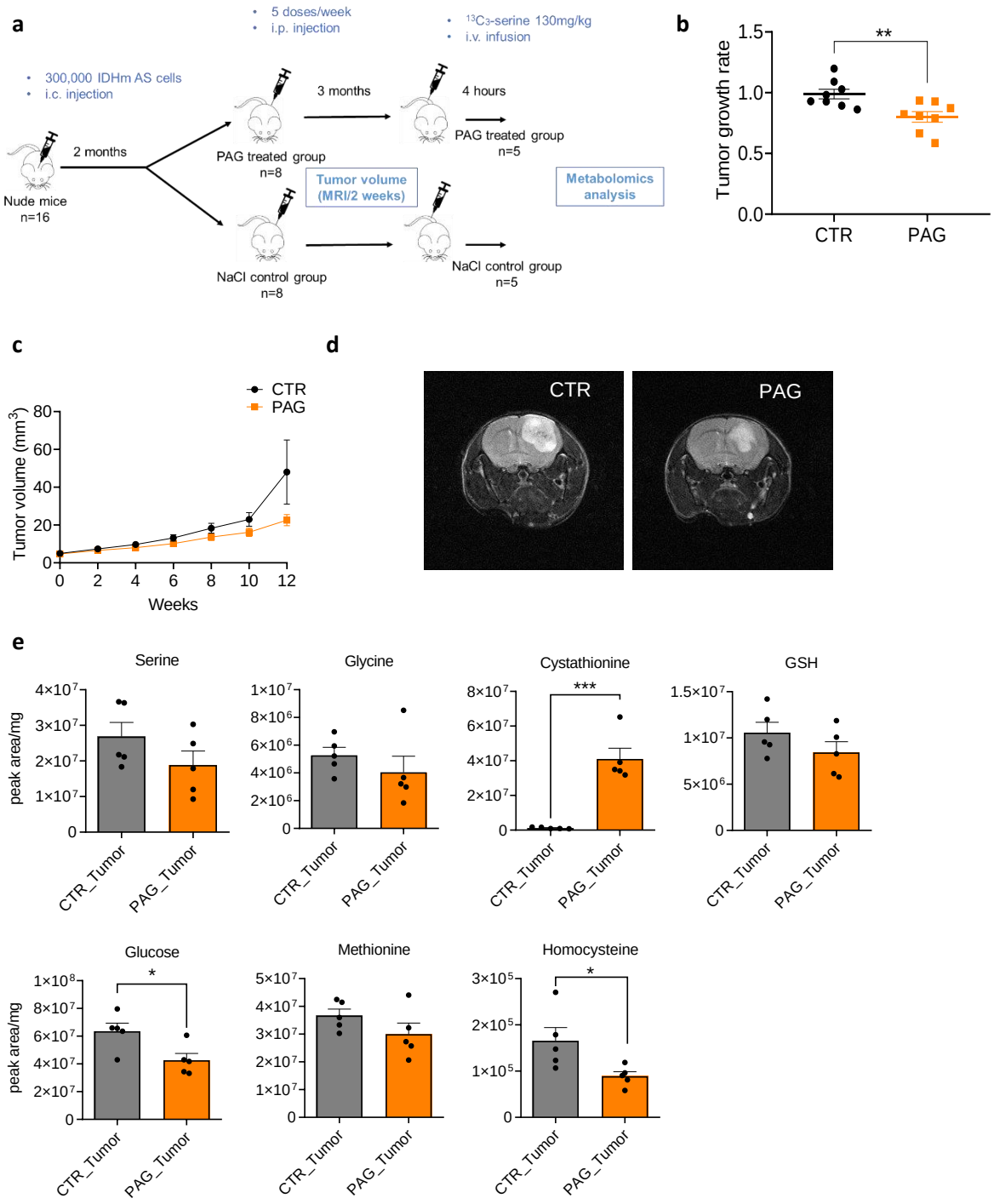

Figure 5. CSE inhibition delays tumor growth *in vivo*

(a) Setup of *in vivo* experiment. (b) Tumor growth rate of CTR and PAG treated mice during the first 8 weeks of treatment (n=8). (c) Tumor volume over time during the 3 months treatment period as determined by MRI (n=8; except for CTR where n=7 at weeks 8/10 and n=6 at week 12). Tendency to reduced volume at week 12 (not significant). Note that 2 CTR mice died after week 8. (d) Representative MRI pictures at week 12. (e) Total metabolite levels represented as normalized peak area in CTR and PAG treated tumors after 12 weeks of treatment (n=5). Each dot in charts B and F correspond to different mice. Data presented as means ± SEM. *p<0.05; **p<0.01; ***p<0.001.

vulnerabilities in redox metabolism and GSH production that might be therapeutically harnessed (Fack et al., 2017, Shi et al., 2015, Bleeker et al., 2010). Nevertheless, to date there is still limited understanding of this pathway in IDHm gliomas in part due to the difficulties of establishing IDHm cellular and animal models relevant to the human disease. The results presented in this study were generated in patient-derived astrocytic and oligodendroglial cells and tumors that carry the endogenous IDH mutation. We show that CSE, the only known enzyme capable of synthesizing cysteine, is specifically upregulated in IDH1m astrocytomas and it is essential to maintain GSH production under limited cysteine availability *in vitro* and *in vivo* in this specific glioma subtype (**Figure 6**). To our knowledge, we show for the first time that inhibition of CSE reduces astrocytoma tumor growth in the brain of mice, thus uncovering a novel metabolic vulnerability in this aggressive glioma subtype.

A key finding of our study is the upregulation of CSE in IDH1m astrocytomas compared to IDH1m oligodendrogliomas and IDHwt GBM. The importance of CSE as a source of cysteine for GSH production is well established in astrocytes (McBean, 2012, McBean, 2017). An early study in C6 glioma cells showed that CSE expression increases when GSH is experimentally depleted (Kandil et al., 2010). While the upregulation of CSE in astrocytomas over oligodendrogliomas was clear in all samples analyzed, the expression in GBM was more variable, suggesting that GBM are more adaptable to cysteine shortage. This was consistent with the specific vulnerability to CSE inhibition observed in IDHm AS cells compared to IDHwt GBM. The loss of the chromosomal arm 1p, where *CTH* is located, in IDH1m ODs, likely explains the drop in CSE expression in this glioma subtype. In line with this, a recent study reported that cystathionine, the substrate of CSE, accumulates in IDH1m ODs (Branzoli et al., 2019).

In addition, our proteomics analysis uncovered a list of 575 novel proteins dysregulated in IDH1m tumors involved in a number of different biochemical pathways. Among the total of 127 upregulated proteins, one interesting target in the context of redox metabolism is DHRS4. This enzyme could bear a specific role in NADPH production as a compensatory source of reducing

power in IDH1m gliomas. The detailed evaluation of all dysregulated proteins and pathways revealed by our proteomics study could open different promising future investigations. On the other hand, this untargeted proteomics analysis confirmed the importance of CSE in IDH1m astrocytomas as the most significantly upregulated protein of all. A possible mechanism by which astrocytomas upregulate CSE could be through mTOR signaling, which was recently described to control the transsulfuration pathway in yeast (Lyu et al., 2019). The amino-acid sensing GCN2-ATF4 pathway has also been implicated in regulating the expression of *CBS* and *CTH* in various cancer cell lines (Zhu et al., 2019). However, the exact mechanism behind the CSE regulation in IDHm AS remains to be elucidated.

We found that in addition to the IDH mutational status, the availability of extracellular cysteine determines the susceptibility to CSE inhibition. This is in agreement with recent data obtained in established cell lines, where the expression of CBS was shown to support cell growth during cysteine depletion (Zhu et al., 2019). In the microenvironment of gliomas, where the uptake of amino acids is regulated by the blood brain barrier (BBB), the cysteine concentration is reportedly very low (Engelborghs et al., 2003). Interestingly, the neuroprotective role of astrocytes depends on their capacity to exchange cysteine and GSH precursors with neurons (Belanger et al., 2011), highlighting the importance of the transsulfuration pathway for astrocytic function (Paul et al., 2018, McBean, 2017, Cakir et al., 2007, Wang and Cynader, 2000, Banos et al., 1975).

Mammalian cells have two ways to acquire cysteine: via CSE-dependent synthesis or by uptake from the extracellular environment. A key player in the supply of cysteine is the xCT antiporter, which exchanges glutamate for cystine, the oxidized form of cysteine. We previously showed that in glioma patients, the expression of *SLC7A11,* the gene encoding for xCT, does not differ between IDHwt and IDHm tumors, nor between IDHm AS and ODs (Fack et al., 2017). Nevertheless, several studies suggested a role for xCT to counteract ROS in IDHwt GBM (Singer et al., 2015, Chen et al., 2015, Polewski et al., 2016) and xCT inhibition has been explored in clinical trials against GBM (Takeuchi et al., 2014, Robe et al., 2006). In IDHm gliomas xCT activity is likely to be hampered by the IDHm-dependent consumption of α-KG, a

precursor for glutamate synthesis. Consistently, we have shown (and confirmed here Fig. 1B) that glutamate levels are lower in IDHm than in IDHwt gliomas (Fack et al., 2017). Importantly, xCT selectively transports cystine but not cysteine and the conversion of cystine to cysteine requires reducing equivalents (Paul et al., 2018). Hence the antioxidant power of xCT is expected to be blunted in NADPH-scarce tumors, such as IDHm gliomas (**Figure 6**).

CSE inhibition *in vitro* and *in vivo*, led to a significant decrease in natural serine (m+0) with no differences in the heavy carbon labelled isotopologues **(Figure 3C, S3B, S5C**). In parallel, the observed reduction in total glucose after CSE blockade, indicates that during CSE inhibition tumor cells deplete glucose-derived serine rather than the labeled one in their attempt to generate GSH (**Figure 6**). Indeed, in the brain serine may rather be synthesized from glucose which readily enters the brain rather than being taken up from the circulation (Belanger et al., 2011). Moreover, we observed in our clinical samples how IDH1m gliomas have higher levels of glucose, which may thus result in the preference for glucose-derived serine in this tumor type. To further investigate the role of glucose in the redox defense of IDH1m gliomas it would be interesting to perform a glucose flux analysis.

IDHm astrocytoma patients are known to benefit from radiotherapy (Juratli et al., 2015), suggesting a vulnerability to the oxidative damage caused by radiation. Therefore, it is tempting to speculate that the addition of PAG might increase the anticancer effects of radiation therapy. This is in line with a recent study, where the combination of radiotherapy with a glutaminase inhibitor (CB-839) led to increased mouse survival (McBrayer et al., 2018). It would be interesting to probe the anti-tumor effects of CSE inhibition in combination with a dietary restriction of cysteine. Indeed, this combinatorial approach was shown to be tolerated and even more effective in depleting GSH in the brain of healthy rats compared to PAG alone (Cho et al., 1991). Furthermore a study in prostate and breast cancer models elegantly showed how the enzyme cyst(e)inase efficiently degrades cysteine in the circulation, thereby significantly increasing oxidative damage and decreasing tumor cell proliferation (Cramer et al., 2017). On these bases, it would be appropriate to test the tolerability of a therapeutic regimen based on

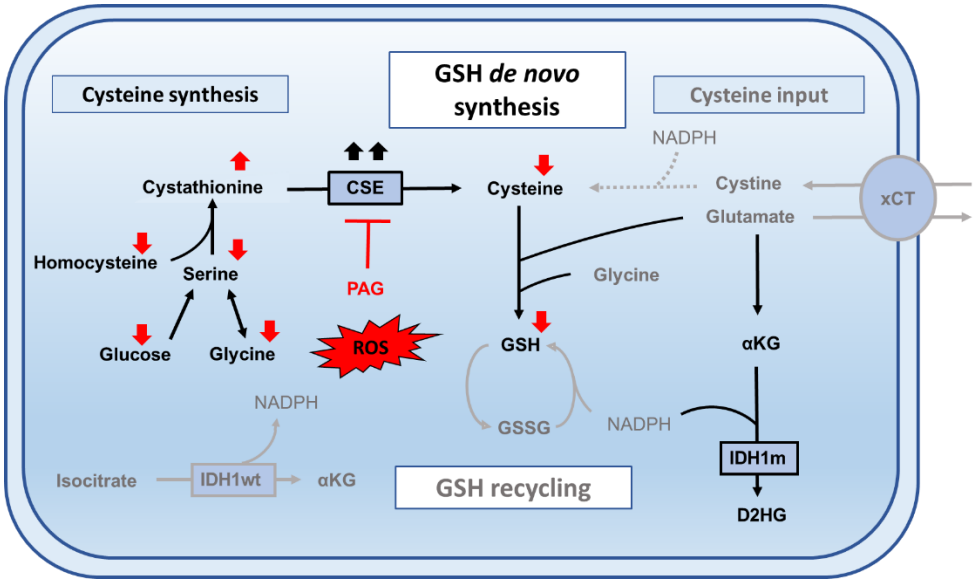

Figure 6. IDH1 mutant astrocytoma critically depend on CSE for GSH synthesis to counteract ROS

Schematic summary showing how IDH1 mutant astrocytomas increase de novo GSH synthesis through CSE upregulation leading to increased cysteine from cystathionine. This pathway compensates the lack of NADPH for GSH recycling due to the IDH1 mutation. Cysteine input from xCT may not be efficient in astrocytomas because of limited cysteine availability in the brain and/or limited intracellular glutamate which is consumed for 2HG production. CSE knockdown or chemical inhibition through PAG hampers the cysteine availability for GSH synthesis thus increasing ROS and subsequent cell death.

the combination of cyst(e)inase and PAG, aiming to block exogenous and endogenous cysteine supply to the tumor.

In conclusion, here we identified a specific metabolic vulnerability of IDH1m astrocytomas that in a cysteine-restricted microenvironment depend on CSE activity to maintain their antioxidant homeostasis, and are selectively susceptible to pharmacological inhibition of CSE *in vivo*.

LIMITATIONS OF STUDY

(1) Patient-derived glioma cells with the endogenous IDH mutation are slow growing cells and poorly adapted to culture conditions. This restricts the experimental procedures possible (e.g. high sensitivity to transfection/infection protocols and depletion of extracellular cysteine) and the amount of material recoverable e.g. for metabolite analysis. Despite this limitation, we were able to confirm a decrease in viability and a clear drop in total GSH in our CSE knockdown

models under low cysteine supply. Similarly the slow *in vivo* growth required extended treatment periods (3 months) and an even longer time would probably have been required to observe a significant difference in tumor volume. Nevertheless cystathionine accumulation was observed in tumors in the brain, supporting a role for CSE in GSH production also *in vivo*.

(2) Our serine tracing studies *in vitro* clearly show that CSE knockdown led to an accumulation of cystathionine concomitant with GSH depletion, both in total levels as well as the m+3 isotopologues (**Figure 3A-B**). The percentage of $^{13}C_3$-serine detected in cells was low (<10% of the total) (**Figure S3B**) which may explain the subsequent low level of GSH isotopologue m+3 (<1%) and the lack of detectable GSH m+5 (m+3 from cysteine and m+2 from glycine) (**Figure S3B**). Yet a significant decrease in GSH m+3 percentage was observed (**Figure S3C**). A complementary approach would be to trace methionine as an alternative substrate for the transsulfuration pathway.

(3) Similarly after CSE inhibition *in vivo*, there was a significant decrease in natural serine isotope (m+0), followed by a drastic accumulation of cystathionine m+0 and a subsequent decrease of GSH m+0 (**Figure S5C**). Moreover the observed reduction in glucose after PAG treatment, indicates that during CSE inhibition tumor cells consume glucose-derived serine rather than the labeled one in their attempt to generate GSH. A possible explanation to this effect could be a limited transport of serine through the BBB and/or a time delay in available labeled serine passing the extracellular matrix to the tumor cells. Indeed the MID percentage of labeled serine detected in the brain was much lower than in the liver and other organs (**Figure S5A, S5D**), where some cystathionine m+3, GSH m+3 and GSH m+5 were detectable after PAG treatment (**Figure S5C**). Thus in the brain serine may rather be synthesized from glucose which readily enters the brain rather than being taken up from the circulation (Belanger et al., 2011), suggesting that a glucose tracing might be more efficient to follow GSH production from serine in the brain.

2.4. Supplementary material

REFERENCES

Figure S1

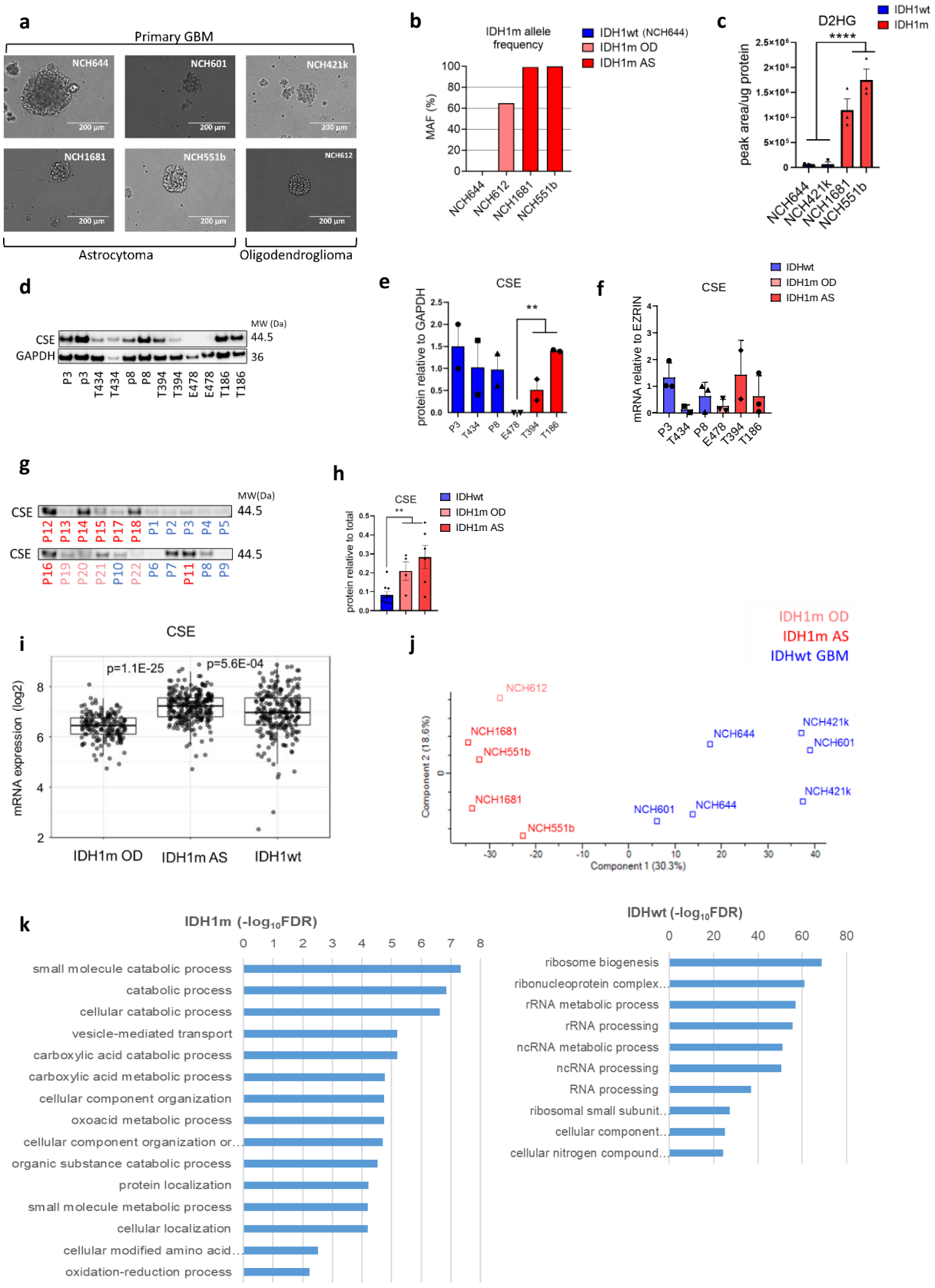
a
Primary GBM
NCH644
NCH601
NCH421k
NCH1681
NCH551b
NCH612
200 µm
Astrocytoma
Oligodendroglioma
b
IDH1m allele frequency
IDH1wt (NCH644)
IDH1m OD
IDH1m AS
MAF (%)
NCH644
NCH612
NCH1681
NCH551b
c
D2HG
IDH1wt
IDH1m
****
peak area/ug protein
NCH644
NCH421k
NCH1681
NCH551b
d
MW (Da)
CSE
GAPDH
44.5
36
P3
p3
T434
T434
p8
P8
T394
T394
E478
E478
T186
T186
e
CSE
**
protein relative to GAPDH
P3
T434
P8
E478
T394
T186
f
CSE
IDHwt
IDH1m OD
IDH1m AS
mRNA relative to EZRIN
P3
T434
P8
E478
T394
T186
g
MW(Da)
CSE
44.5
P12
P13
P14
P15
P17
P18
P1
P2
P3
P4
P5
CSE
44.5
P16
P19
P20
P21
P10
P22
P6
P7
P11
P8
P9
h
CSE
**
IDHwt
IDH1m OD
IDH1m AS
protein relative to total
i
CSE
p=1.1E-25
p=5.6E-04
mRNA expression (log2)
IDH1m OD
IDH1m AS
IDH1wt
j
IDH1m OD
IDH1m AS
IDHwt GBM
NCH612
NCH1681
NCH551b
NCH644
NCH421k
NCH601
NCH421k
NCH1681
NCH601
NCH644
NCH551b
Component 2 (18.6%)
Component 1 (30.3%)
k
IDH1m (-log10FDR)
small molecule catabolic process
catabolic process
cellular catabolic process
vesicle-mediated transport
carboxylic acid catabolic process
carboxylic acid metabolic process
cellular component organization
oxoacid metabolic process
cellular component organization or...
organic substance catabolic process
protein localization
small molecule metabolic process
cellular localization
cellular modified amino acid...
oxidation-reduction process
IDHwt (-log10FDR)
ribosome biogenesis
ribonucleoprotein complex...
rRNA metabolic process
rRNA processing
ncRNA metabolic process
ncRNA processing
RNA processing
ribosomal small subunit...
cellular component...
cellular nitrogen compound...

Figure S1. Relative to Figure 1

(a) Phase contrast microscope imaging of the six patient derived glioma cell lines. NCH644, NCH601 and NCH421k correspond to patients with IDH1wt primary glioblastoma (GBM); NCH1681 and NCH551b correspond to patients with IDH1m astrocytoma; NCH612 correspond to a patient with IDH1m oligodendroglioma.
(b) Percentage of IDH1 mutant allele frequency (MAF) observed by digital PCR in all IDH1m cell lines, including astrocytomas (AS) (NCH551b, NCH1681) and oligodendroglioma (OD) (NCH612) and one of the IDHwt cell lines (NCH644). MAF and 95% confidence interval (CI) for each cell line were: NCH644 MAF= 0.00032%, CI= 8.59E-3% -- 0.117%; NCH612 MAF= 64.85%, CI= 61.196% -- 68.65%; NCH1681 MAF= 99.45%, CI= 93.223% -- 106%; NCH551b MAF= 99.98%, CI= 94.808% -- 105.33%. Digital PCR procedure was performed as described in(Golebiewska et al., 2020). Error bars correspond to 95% confidence intervals (CI) of MAF estimation. One cell stock replicate for each line (n=1).
(c) D2HG and GSH levels in patient-derived IDH1wt glioblastoma and IDH1m astrocytoma cell lines as determined by LC-MS. Each biological replicate (n) correspond to an independent cell culture stock of each cell line (n=3).
(d) Western blot of CSE in patient-derived orthotopic xenografts: IDH1wt GBM (P3, T434, P8), IDH1m OD (E478) and IDHm AS (T394, T186). MW (Da) represents the specific molecular weights of each protein. (e) Quantification thereof relative to GAPDH. Each biological replicate (n) correspond to an indepenedent xenograft tumor (n=2). Original blots are shown in Figure 1SC.
(f) *CSE* gene expression in patient-derived orthotopic xenografts relative to *EZRIN* determined by qPCR. Each biological replicate (n) correspond to an independent xenograft tumor (n=3, except for T434 and T394 where n=2).
(g) Western blot of clinical samples for CSE. IDHwt (blue; P1-P10), IDH1m AS (red; P11-P18) and IDH1m OD (pink; P19-P22). (h) Quantification thereof relative to total protein amount. Each biological replicate (n) correspond to an independent patient tumor, IDHwt (n=10), IDH1m AS (n=6) and IDH1m OD (n=4).
(i) *CSE* gene expression in glioma patients (source: Gliovis (Bowman et al., 2017)). IDH1m OD (169; 25.76%), IDH1m AS (258; 39.33%), IDH1wt (229; 34.91%). TCGA_GBMLGG adult glioma dataset. Pairwise t tests. Pairwise comparisons between group levels with corrections for multiple testing (p-values with Bonferroni correction).
(j) Principal Component Analysis (PCA) of the untargeted proteomics comparison between IDH1m AS (red) IDH1m OD (pink) and IDHwt GBM (blue) cell lines
GBM: Glioblastoma; OD: Oligodendroglioma; AS: Astrocytoma
(k) Gene Ontology Biological Process (GOBP) terms representation of the top 10 terms (IDHwt) and top 15 (IDH1m) terms, based on STRING database analysis (Szklarczyk et al., 2019).
Data in A and F presented as means ± SEM. ** $p<0.01$; **** $p<0.0001$.

Figure S2

3 days culture at 30 µM cysteine

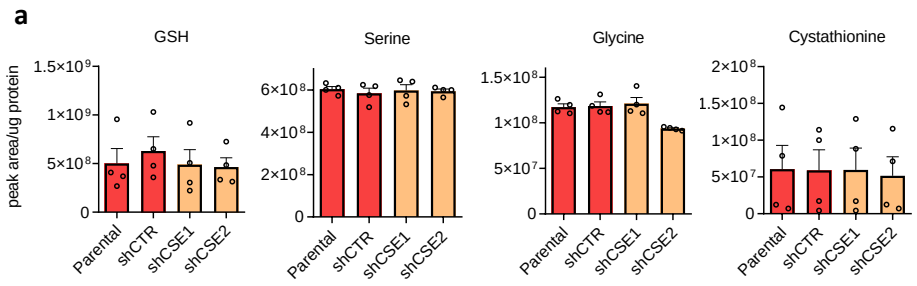

4 days culture at 30 µM cysteine

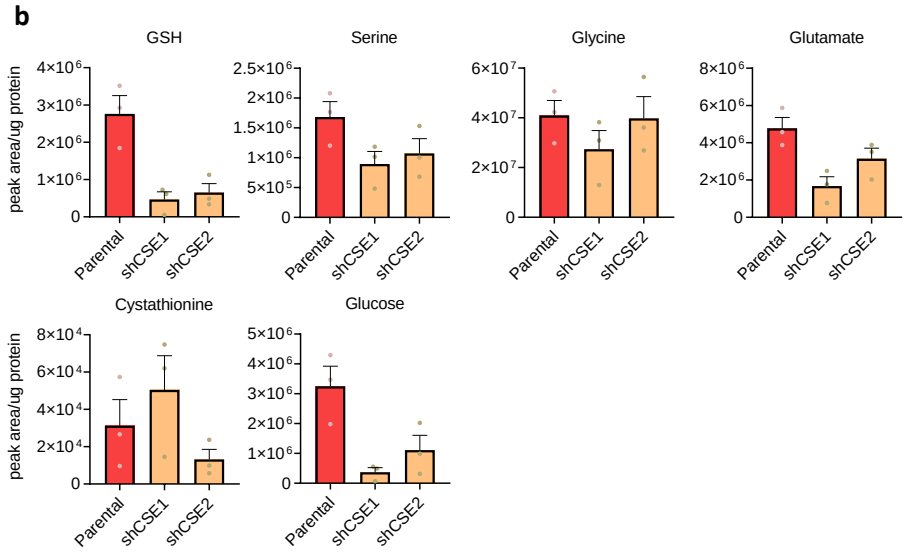

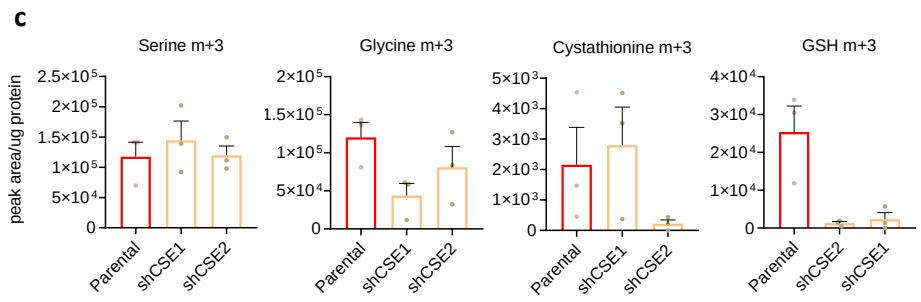

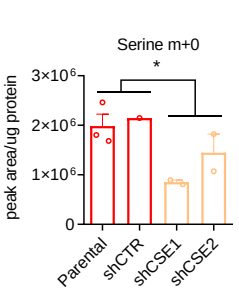

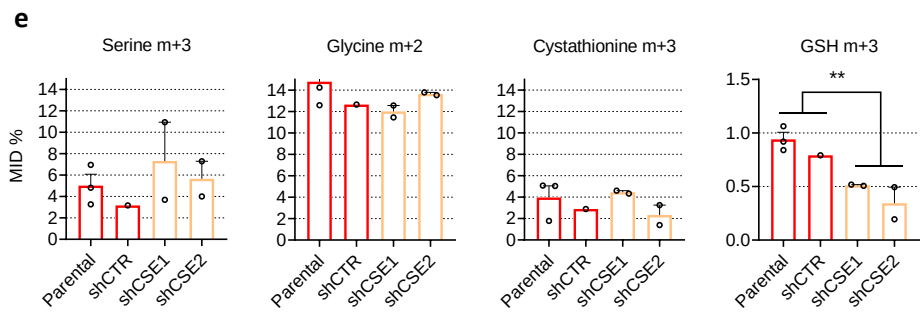

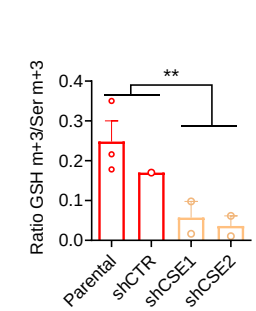

Figure S2. **Relative to Figure 3**

(a) Total GSH, serine, glycine and cystathionine levels in parental, shCTR, shCSE1 and shCSE2. Cells were incubated during 3 days at 30 µM cysteine. Each dot of the bar charts correspond to an independent experiment (n=4).
(b) Total GSH, serine, glycine, glutamate cystathionine and glucose levels in parental, shCSE1 and shCSE2. Cells were incubated during 4 days at 30 µM cysteine.
(c) Isotopologue levels of GSH, serine, glycine and cystathionine after $^{13}C_3$-serine tracing (ratio 1:1 natural L-Serine and L-Serine13C3) in parental, shCSE1 and shCSE2. One independent experiment represented in (b) and (c) (n=1). Each dot corresponds to a technical replicate. Three technical replicates in each group. No statistical analysis was applied due to the lack of biological replicates
(d) Natural serine (m+0) levels of parental, shCTR, shCSE1 and shCSE2 cells incubated during 4 days with 30 µM cysteine and $^{13}C_3$-serine tracing. Each dot of the bar charts correspond to an independent experiment (n). Parental (n=3), shCTR (n=1), shCSE1 (n=2) and shCSE2 (n=2).
(e) Mass Isotopologue Distribution (MID) percentages of serine m+3, glycine m+2, cystathionine m+3 and GSH m+3in CSE knockdown and control cells. Cells were incubated during 4 days at 30 µM cysteine. Each dot of the bar charts correspond to an independent experiment (n). Parental (n=3), shCTR (n=1), shCSE1 (n=2) and shCSE2 (n=2). (f) GSH m+3/Ser m+3 ratio of same cells as in (d).
Data presented as means ± SEM.* $p<0.05$ ** $p<0.01$

Figure S3

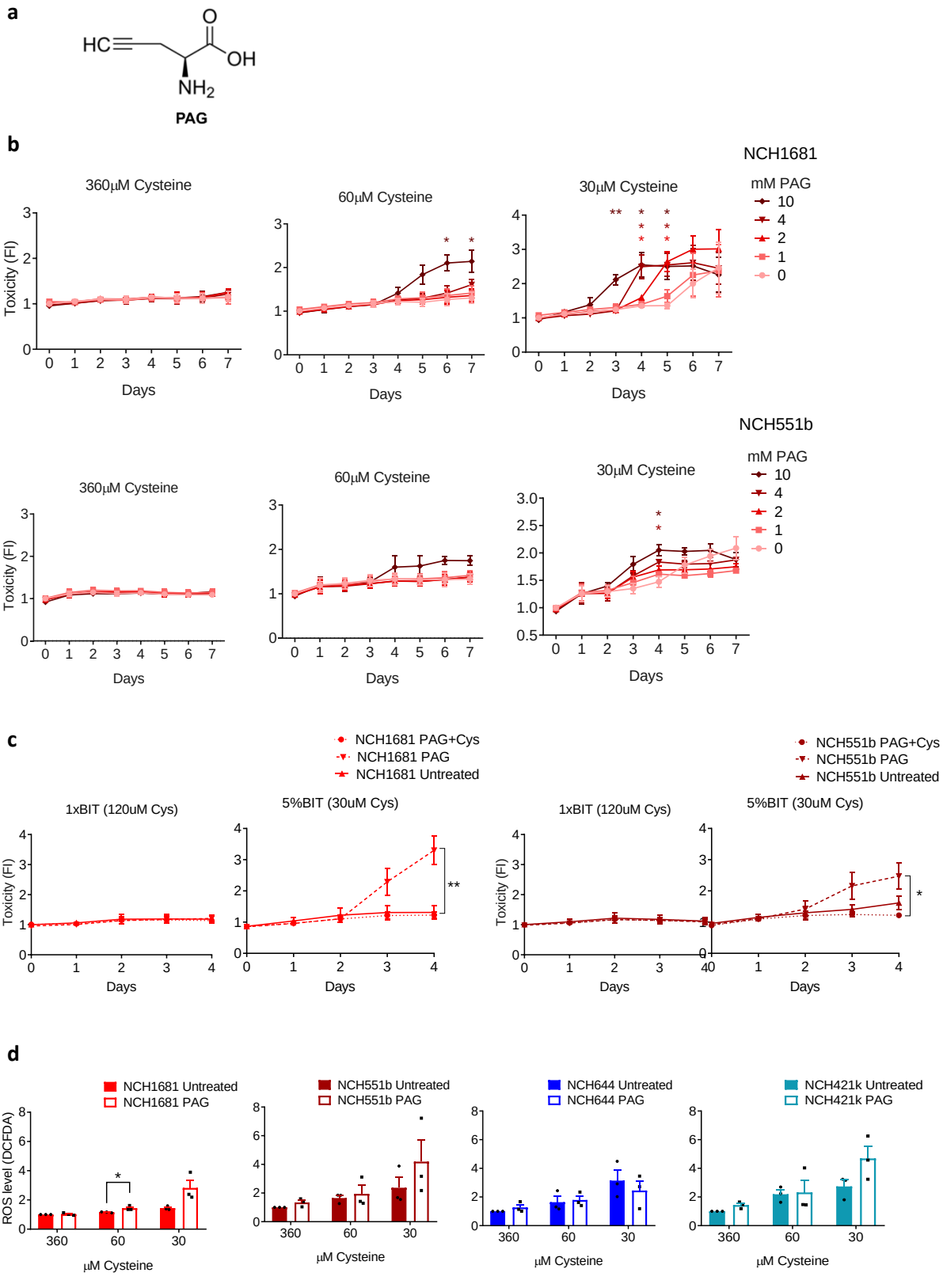
a
HC
O
OH
NH2
PAG
b
NCH1681
mM PAG
10
4
2
1
0
360μM Cysteine
60μM Cysteine
30μM Cysteine
Toxicity (FI)
Days
NCH551b
c
NCH1681 PAG+Cys
NCH1681 PAG
NCH1681 Untreated
NCH551b PAG+Cys
NCH551b PAG
NCH551b Untreated
1xBIT (120uM Cys)
5%BIT (30uM Cys)
d
NCH1681 Untreated
NCH1681 PAG
NCH551b Untreated
NCH551b PAG
NCH644 Untreated
NCH644 PAG
NCH421k Untreated
NCH421k PAG
ROS level (DCFDA)
μM Cysteine

Figure S3. Relative to Figure 4

(a) Chemical structure of PAG.
(b) Toxicity of IDH1m astrocytoma cell lines (NCH1681 and NCH551b) incubated with different cysteine concentrations (360, 60 and 30 µM respectively) and with different PAG concentrations (0, 1, 2, 4 and 10 mM) over time. Data of toxicity presented as fold change relative to 360 µM cysteine medium, day 0 untreated (n=3).
(c) Validation of *in vitro* cysteine titration via BSA Insulin Transferring (BIT) supplement dilution (Detailed explanation in methods section "Cysteine titration mediums"). Toxicity of IDH1m astrocytoma cell lines (NCH1681 and NCH551b) incubated with 20% and 5%BIT expecting to obtain 120 µM and 30 µM cysteine respectively. The toxicity of CSE inhibitor PAG at 5%BIT is rescued by addition of extra cysteine up to 120 µM, which matches with the lack of toxicity at 20%BIT and the expected 120 µM cysteine. Data presented as fold change relative to 20% BIT (120µM) at day 0 untreated (n=3).
(d) ROS production upon PAG (10mM) and at different cysteine concentrations, presented as fold change of DCFDA fluorescence intensity (FI) relative to control cells (untreated, 360µM cysteine) (n=3). N represents one independent experiment. Data presented as means ± SEM. * $p<0.05$; ** $p<0.01$

Figure S4

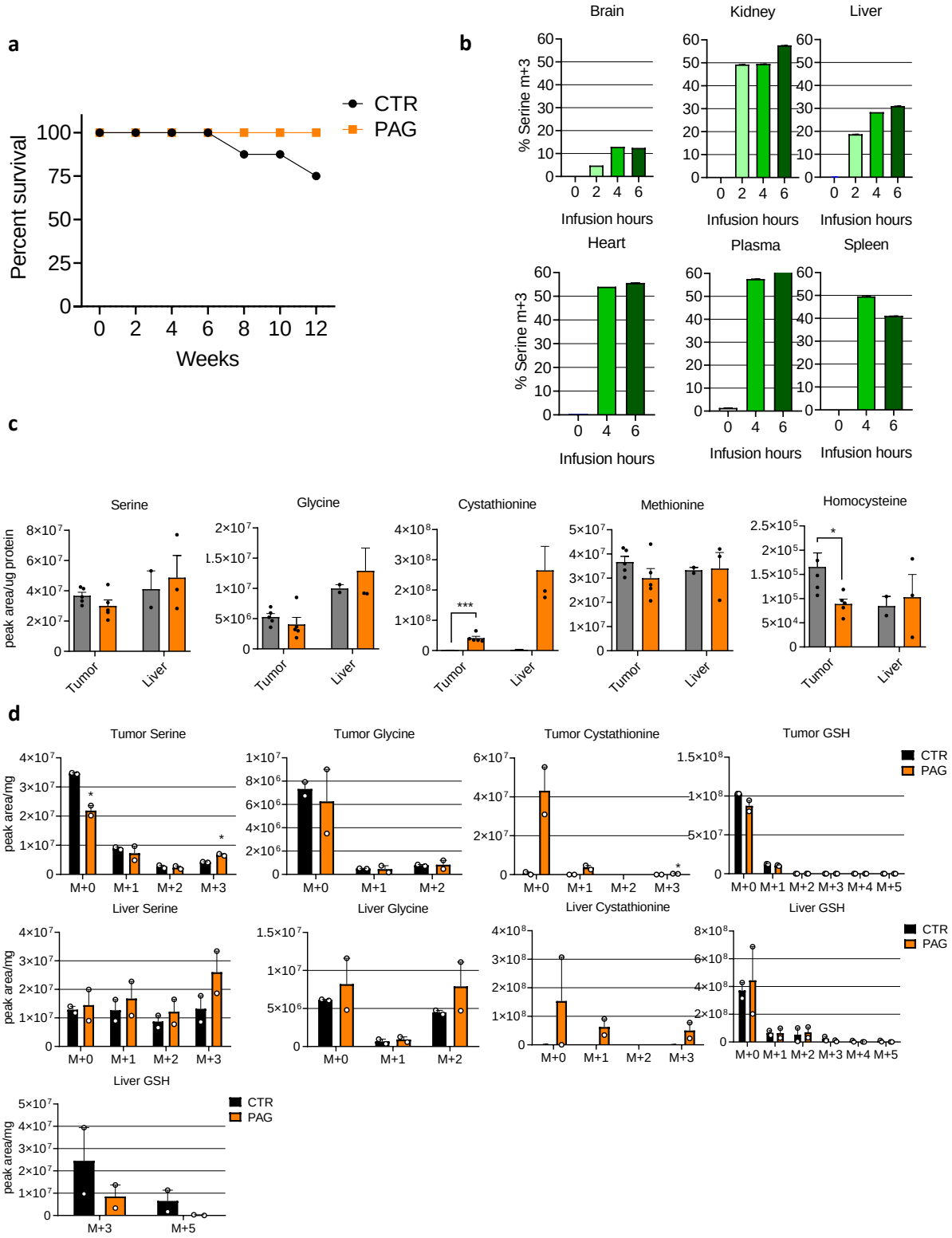
a
CTR
PAG
Percent survival
Weeks
b
Brain
Kidney
Liver
Heart
Plasma
Spleen
% Serine m+3
Infusion hours
c
Serine
Glycine
Cystathionine
Methionine
Homocysteine
peak area/ug protein
Tumor
Liver
d
Tumor Serine
Tumor Glycine
Tumor Cystathionine
Tumor GSH
Liver Serine
Liver Glycine
Liver Cystathionine
Liver GSH
peak area/mg
M+0
M+1
M+2
M+3
M+4
M+5

Figure S4. Relative to Figure 5

(a) Mass Isotopologue Distribution (MID) percentage of heavy labelled $^{13}C_3$-serine (serine m+3) incorporated in different tissues after tracer infusion over time (n=1).
(b) Total serine, glycine, cystathionine, GSH, glucose, methionine and homocysteine levels in tumor and liver with and without PAG treatment (tumor CTR (n=5), tumor PAG (n=5), liver CTR (n=2), liver PAG (n=3)). Data presented as means ± SEM.
(c) Total isotopologue levels of serine, glycine, cystathionine and GSH in tumor and in liver with and without PAG treatement (n=2). Data presented as means ± SEM. * $p<0.05$; ** $p<0.01$

Supplementary Table 1. Clinical sample characteristics and glioma classification.

NA: not available. * IDH status of samples which methylation diagnosis was not available, were determined by ddPCR

Glioma group	Patient	Age	Gender	Histopathological diagnosis	Molecular diagnosis-Methylation Class	IDH status
IDH wt	P1	38	Male	GBM	NA	IDHwt*
	P2	65	Male	GBM	GBM, mesenchymal	IDHwt
	P3	56	Male	GBM	NA	IDHwt*
	P4	71	Female	GBM	GBM, RTK II	IDHwt
	P5	51	Male	GBM	GBM, RTK I	IDHwt
	P6	69	Male	GBM	GBM, mesenchymal	IDHwt
	P7	73	Male	GBM	NA	IDHwt*
	P8	72	Male	GBM	GBM, mesenchymal	IDHwt
	P9	68	Female	GBM	NA	IDHwt*
	P10	26	Female	Oligodendroglioma	NA	IDHwt*
IDHm AS	P11	31	Male	GBM	High grade astrocytoma	IDH1m
	P12	37	Male	Astrocytic glioma	High grade astrocytoma	IDH1m
	P13	41	Male	Astrocytic glioma	High grade astrocytoma	IDH1m
	P14	23	Male	Astrocytic glioma	Astrocytoma	IDH1m
	P15	34	Male	Astrocytic glioma	Astrocytoma	IDH1m
	P16	37	Male	Oligodendroglioma	Astrocytoma	IDH1m
	P17	NA	NA	Astrocytic glioma	NA	NA
	P18	NA	NA	Astrocytic glioma	NA	NA
IDHm OD	P19	47	Male	Oligodendroglioma	NA	IDH1m*
	P20	47	Female	Oligodendroglioma	Oligodendroglioma 1p/19q codeleted	IDH1m
	P21	36	Male	Oligodendroglioma	NA	IDH1m*
	P22	51	Male	Oligodendroglioma	NA	IDH1m*

Supplementary Table 2. Cell culture media with different cysteine concentrations

* Cys concentrations refer to the combination of both cysteine (oxidized) and cystine (reduced). DMEMF12: 300 µM cys = 100 µM oxidized and 100 µM reduced. BIT100: 600 µM cys = 300 µM reduced. **Percentage in volume over the total volume of the mix

Culture medium	DMEMF12 (300 µM cys) *	DMEM cys-free	BIT100 (600 µM cys) *	Extra 30mM cys	Final [cys]
Normal NCH cells	80%**	-	20%	-	360 µM
Cysteine titration mediums	-	80%	20%	1%	360 µM
	-	80%	20%	-	120 µM
	-	90%	10%	-	60 µM
	-	95%	5%	-	30 µM

CHAPTER V. CONCLUSIONS AND PERSPECTIVES

As stated in the dissertation's title, this PhD project aimed to "identify and target metabolic vulnerabilities in IDH mutant gliomas". To explore this objective we analyzed *in vitro* and *in vivo* glioma models as well as clinical material carrying wild type IDH and IDH mutation. Via proteomics, metabolomics and genetic editing approaches we identified the dysregulation of central metabolic pathways derived from IDH1 mutation, highlighting potential strategies that could interrupt tumor progression. Specifically, our data reveal alterations in glucose metabolism, glutamate/glutamine metabolism, lipid processing and glutathione (GSH) regulation. Additionally, we specifically targeted one of these vulnerabilties, evidencing the dependence of IDH1m astrocytomas on cystathionine γ-lyase (CSE) for *de novo* cysteine synthesis and GSH production, and disclosing a novel oxidative stress vulnerability for these tumors.

In chapter IV-1 we showed the impact of the IDH1 mutation in the dysregulation of central carbon metabolism and GSH metabolism, and we proposed potential therapeutic targets that could be further investigated. We observed that IDH1m gliomas have a particularly high storage of glucose. Being the most abundant metabolite in the brain (Allaman et al., 2011), glucose plays a pivotal role in energy production but also as source of intermediates for biosynthesis of amino acids, nucleotides, reducing power or phospholipids (Metallo and Vander Heiden, 2013). We previously reported a tendency towards low glucose turnover to TCA cycle intermediates as well as a reduced ATP production in IDHm tumors (Fack et al., 2017). However, here we observed that IDH1m tumors upregulate glycolytic and TCA metabolite and enzymatic mediators. Yet we also report high expression of glucose-independent pyruvate synthesis enzymes, and enzymes in charge of anaplerotic entry into TCA cycle, suggesting that IDH1m tumors upregulate glycolysis to fuel alternative biosynthetic pathways, and activate TCA cycle through secondary inputs. In fact, our observed high pyruvate carboxylase (PC) level, matches with previous observations that this enzyme is critical for IDHm cells to maintain TCA activity (Izquierdo-Garcia et al., 2014). Moreover, it has

been shown that D-2HG readily inhibits the complex IV of electron transport chain (ETC) which may explain the especially low energetic capacity of IDH1m cells (da Silva et al., 2002, Latini et al., 2005). This deficient ATP production in IDH1m gliomas may be an explanation for the decreased aggressiveness of these tumors when compared to IDHwt glioblastomas (Brat et al., 2015). Based on the critical energy constraints that IDH1m cells have, as a future perspective it would be interesting to observe the sensitivity of IDH1m cells against respiration inhibitors such as rotenone or phenformin, an approach previously addressed (Grassian et al., 2014), in combination with inhibitors of some of the upregulated enzymes fueling TCA observed in our study, such as PKM, PC, LDHB or ACSS1.

We found that glutamate is a limiting metabolite in IDH1m tumors, likely due to its increased consumption to satisfy high D-2HG production, via GLUD1, and due to the inhibition in these tumors of glutamate synthesis through branched-chain amino acids (BCAAs), as previously reported (McBrayer et al., 2018). Indeed, it has been shown that GLUD1/2 knockdowns in *in vivo* IDH1m gliomas develop a decreased tumor growth (Chen et al., 2014). Moreover, there seems to be upregulation of alternative production of glutamate as an attempt to compensate this deficiency, through increased extracellular glutamate uptake. Glutaminolysis has been reported to be especially important in cancer cell growth (Cheng et al., 2011), thus representing a potential IDH1m metabolic vulnerability. Indeed glutaminase inhibitors have been already extensively tested against IDHm glioma cells, showing promising results (Seltzer et al., 2010, McBrayer et al., 2018). It would be interesting to address the effect of combining GLS inhibitors with inhibitors of transporters of glutamate (SLC1A2) or glutamine synthase, since these were proteins revealed upregulated in IDH1m tumors in our study.

Glutathione (GSH) is thought to be the most important antioxidant in the human body due to its evolutionary conserved enzymatic organization which enables it not only to counteract the effect of reactive oxygen species (ROS) but also to neutralize xenobiotic agents (Forman et al., 2009). Our study served us to confirm the hypothesis stating that IDHm gliomas bear an altered GSH production due to their defective NADPH synthesis (Shi et al., 2015, Fack et al.,

2017). In line with this, the efficacy of blocking GSH through glutaminase inhibition in IDH1m gliomas has been reported (McBrayer et al., 2018). Here we observed several intermediates of the transsulfuration pathway and *de novo* GSH synthesis to be upregulated in IDH1m models, as well as enzymes directly in charge of GSH mediated detoxification such as glutathione S-transferases (GSTMs). Indeed, to our knowledge there are no reports testing the effect of GSTM inhibition in IDH1m gliomas, which could be an interesting study to approach. The antioxidant machinery of these tumors is an attractive area of study due to the specific vulnerability of IDHm gliomas to oxidative stress induced by radio-chemotherapy (Juratli et al., 2015). Thus, here we consistently show that IDH1m tumors display an altered biosynthesis and regulation of GSH, what served us as preliminary data for the next experimental strategy conducted in this PhD project, based on targeting GSH-dependent specific vulnerability of IDH1m gliomas.

In chapter IV-2, we further analyzed via functional approaches the relevance of GSH biosynthesis in IDH1m glioma cells, and proposed a potential therapeutic strategy that would combine the depletion of this antioxidant with conventional therapeutic agents which inflict oxidative damage in the tumor.

Here we observed that cystathionine γ-lyase (CSE), a central mediator of the TP and the only enzyme in charge of cysteine *de novo* synthesis, was significantly increased in IDH1m astrocytomas, an effect to our knowledge undiscovered as of today. In fact, CSE is located in the chromosome arm 1p, what explains our observed low expression of this enzyme in IDH1m 1p/19q co-deleted oligodendrogliomas. Indeed, a recent study observed an increased accumulation of cystathionine, the direct substrate of the CSE reaction, in oligodendroglioma patients when compared to IDHm astrocytomas or IDHwt GBM (Branzoli et al., 2019). CSE upregulation may be an astrocytoma-specific compensatory mechanism to cope with the IDH1m-derived NADPH deficiency. The lack of this opportunity in oligodendrogliomas could

explain the better patient prognosis of these tumors with respect to astrocytomas and GBM (Brat et al., 2015), as aspect that would be interesting to further study.

We found CSE activity to be critical upon cysteine restriction in culture, a metabolic state that resembles the physiological scenario in the brain (Engelborghs et al., 2003). Indeed, we observed that CSE was the main source of cysteine which was at the same time the limiting factor for GSH *de novo* synthesis in IDH1m AS cells. Thus, inhibition of CSE under limiting cysteine conditions promoted an oxidative stress-dependent cell toxicity. This toxic effect showed to be exclusive in IDH1m AS, since the same conditions were harmless in IDHwt glioblastoma cells. Yet, the specific transcriptional signal that mediates overexpression of CSE in IDH1m AS is still unknown, and would be an interesting mechanism to determine in future investigations. According to recent evidence, it is possible that GSH biosynthesis via TP is activated through NRF2 and mTOR signaling pathways (Tang et al., 2020, Zhu et al., 2019, Gureev et al., 2020).

Interestingly, we observed that CSE inhibition via propargylglycine (PAG) effectively delayed IDH1m AS tumor growth *in vivo*, via relative decrease of GSH. These data suggest a potential therapeutic strategy to combine conventional oxidative stress agents with CSE inhibition. Although there was a clear tendency towards an increasing difference in tumor growth and survival over time in PAG treated vs control xenografts, the slow growth of IDH1m AS would have required longer treatment and follow up times. In fact, the slow-growing nature of these tumors considerably hampered the *in vitro* experimentation as well, e.g. metabolomics. Thus it would be very interesting to follow the effect of PAG treatment *in vivo* during longer time points. Moreover, the use of oxidative stress inducing agents in combination of CSE inhibition could be a strategy to consider in the future in order to increase the toxic effect of the treatment. In addition, it has been already shown that the combination of the CSE inhibitor PAG with cysteine-free diets increased the GSH blocking effect, without presenting side effects in healthy rats (Cho et al., 1991). Thus, dietary restriction in combination with CSE blockade could potentially increase the anti-tumor effect of the treatment in IDHm AS tumors.

Although the serine tracing experiments demonstrated the importance of TP *in vitro*, the incorporation and processing rate of heavy label serine in the brain was lower than expected, harnessing the TP flux analysis *in vivo*. Indeed, according to our data, we believe that IDHm AS, instead of incorporating extracellular serine may rather synthesize it *de novo* via glucose, which is highly abundant in the brain. For this reason, it will be worthwhile to trace in the future the fate of glucose towards serine, cysteine and GSH synthesis.

Generally, the use of inhibitors of transsulfuration pathway enzymes such as PAG focused on the regulation of hydrogen sulfide (H_2S), a gasotransmitter that has been suggested as an important modulator of tumor cell proliferation, with roles in oxidative stress, VEGF induction and HIF-1α stabilization, among others (Szabo and Papapetropoulos, 2017). Depending on the amino acid availability, CSE can also be in charge of cysteine degradation producing H_2S. In fact CSE, CBS and 3-mercaptopyruvate sulfurtransferase (3-MST) are the only enzymes in charge of H_2S production. Here we show that CSE inhibitor PAG is selectively toxic in IDHm AS cells inducing tumor growth delay *in vivo*, although its role in ROS is not yet conclusive. Whether H_2S modulation via CSE inhibition has an additive toxic impact in IDH1m AS would be an interesting future topic to study.

In conclusion, in this PhD project we characterized IDH1m gliomas from an integrative approach, generating a comprehensive perspective of the exclusive metabolic regulation that uncovers a specific vulnerability in these tumors. In addition, we identified CSE inhibition as a novel therapeutic strategy that affects tumor cell viability via GSH depletion and oxidative damage, an approach that could serve as the basis for clinical investigations to improve IDH1m astrocytoma patient prognosis.

References

AL-KHALLAF, H. 2017. Isocitrate dehydrogenases in physiology and cancer: biochemical and molecular insight. *Cell Biosci,* 7**,** 37.

ALLAMAN, I., BÉLANGER, M. & MAGISTRETTI, P. J. 2011. Astrocyte-neuron metabolic relationships: for better and for worse. *Trends Neurosci,* 34**,** 76-87.

ALLE, H., ROTH, A. & GEIGER, J. R. 2009. Energy-efficient action potentials in hippocampal mossy fibers. *Science,* 325**,** 1405-8.

ALMEIDA, A., MONCADA, S. & BOLAÑOS, J. P. 2004. Nitric oxide switches on glycolysis through the AMP protein kinase and 6-phosphofructo-2-kinase pathway. *Nat Cell Biol,* 6**,** 45-51.

ALMUHAIDEB, A., PAPATHANASIOU, N. & BOMANJI, J. 2011. 18F-FDG PET/CT imaging in oncology. *Ann Saudi Med,* 31**,** 3-13.

AMANKULOR, N. M., KIM, Y., ARORA, S., KARGL, J., SZULZEWSKY, F., HANKE, M., MARGINEANTU, D. H., RAO, A., BOLOURI, H., DELROW, J., HOCKENBERY, D., HOUGHTON, A. M. & HOLLAND, E. C. 2017. Mutant IDH1 regulates the tumor-associated immune system in gliomas. *Genes Dev,* 31**,** 774-786.

ANDRONESI, O. C., RAPALINO, O., GERSTNER, E., CHI, A., BATCHELOR, T. T., CAHILL, D. P., SORENSEN, A. G. & ROSEN, B. R. 2013. Detection of oncogenic IDH1 mutations using magnetic resonance spectroscopy of 2-hydroxyglutarate. *J Clin Invest,* 123**,** 3659-63.

AOYAMA, K., WATABE, M. & NAKAKI, T. 2008. Regulation of neuronal glutathione synthesis. *J Pharmacol Sci,* 108**,** 227-38.

ATAI, N. A., RENKEMA-MILLS, N. A., BOSMAN, J., SCHMIDT, N., RIJKEBOER, D., TIGCHELAAR, W., BOSCH, K. S., TROOST, D., JONKER, A., BLEEKER, F. E., MILETIC, H., BJERKVIG, R., DE WITT HAMER, P. C. & VAN NOORDEN, C. J. 2011. Differential activity of NADPH-producing dehydrogenases renders rodents unsuitable models to study IDH1R132 mutation effects in human glioblastoma. *J Histochem Cytochem,* 59**,** 489-503.

BADUR, M. G., MUTHUSAMY, T., PARKER, S. J., MA, S., MCBRAYER, S. K., CORDES, T., MAGANA, J. H., GUAN, K. L. & METALLO, C. M. 2018. Oncogenic R132 IDH1 Mutations Limit NADPH for De Novo Lipogenesis through (D)2-Hydroxyglutarate Production in Fibrosarcoma Cells. *Cell Rep,* 25**,** 1680.

BAI, H., HARMANCı, A. S., ERSON-OMAY, E. Z., LI, J., COŞKUN, S., SIMON, M., KRISCHEK, B., ÖZDUMAN, K., OMAY, S. B., SORENSEN, E. A., TURCAN, Ş., BAKıRCıĞLU, M., CARRIÓN-GRANT, G., MURRAY, P. B., CLARK, V. E., ERCAN-SENCICEK, A. G., KNIGHT, J., SENCAR, L., ALTıNOK, S., KAULEN, L. D., GÜLEZ, B., TIMMER, M., SCHRAMM, J., MISHRA-GORUR, K., HENEGARIU, O., MOLITERNO, J., LOUVI, A., CHAN, T. A., TANNHEIMER, S. L., PAMIR, M. N., VORTMEYER, A. O., BILGUVAR, K., YASUNO, K. & GÜNEL, M. 2016. Integrated genomic characterization of IDH1-mutant glioma malignant progression. *Nat Genet,* 48**,** 59-66.

BAK, L. K., SCHOUSBOE, A. & WAAGEPETERSEN, H. S. 2006. The glutamate/GABA-glutamine cycle: aspects of transport, neurotransmitter homeostasis and ammonia transfer. *J Neurochem,* 98**,** 641-53.

BANOS, G., DANIEL, P. M., MOORHOUSE, S. R. & PRATT, O. E. 1975. The requirements of the brain for some amino acids. *J Physiol,* 246**,** 539-48.

BATSIOS, G., VISWANATH, P., SUBRAMANI, E., NAJAC, C., GILLESPIE, A. M., SANTOS, R. D., MOLLOY, A. R., PIEPER, R. O. & RONEN, S. M. 2019. PI3K/mTOR inhibition of IDH1 mutant glioma leads to reduced 2HG production that is associated with increased survival. *Sci Rep,* 9**,** 10521.

BAUER, D. E., HATZIVASSILIOU, G., ZHAO, F., ANDREADIS, C. & THOMPSON, C. B. 2005. ATP citrate lyase is an important component of cell growth and transformation. *Oncogene,* 24**,** 6314-22.

BAUMANN, N. & PHAM-DINH, D. 2001. Biology of oligodendrocyte and myelin in the mammalian central nervous system. *Physiol Rev,* 81**,** 871-927.

BEIKO, J., SUKI, D., HESS, K. R., FOX, B. D., CHEUNG, V., CABRAL, M., SHONKA, N., GILBERT, M. R., SAWAYA, R., PRABHU, S. S., WEINBERG, J., LANG, F. F., ALDAPE, K. D., SULMAN, E. P., RAO, G., MCCUTCHEON, I. E. & CAHILL, D. P. 2014. IDH1 mutant malignant astrocytomas are more amenable to surgical resection and have a survival benefit associated with maximal surgical resection. *Neuro Oncol,* 16**,** 81-91.

BELANGER, M., ALLAMAN, I. & MAGISTRETTI, P. J. 2011. Brain energy metabolism: focus on astrocyte-neuron metabolic cooperation. *Cell Metab,* 14**,** 724-38.

BÉLANGER, M. & MAGISTRETTI, P. J. 2009. The role of astroglia in neuroprotection. *Dialogues Clin Neurosci,* 11**,** 281-95.

BERG, J. M., TYMOCZKO, J. L. & STRYER, L. 2012. Biochemistry/Jeremy M. Berg, John L. Tymoczko, Lubert Stryer; with Gregory J. Gatto, Jr. New York: WH Freeman.

BERGHOFF, A. S., KIESEL, B., WIDHALM, G., WILHELM, D., RAJKY, O., KURSCHEID, S., KRESL, P., WÖHRER, A., MAROSI, C., HEGI, M. E. & PREUSSER, M. 2017. Correlation of immune phenotype with IDH mutation in diffuse glioma. *Neuro Oncol,* 19**,** 1460-1468.

BERKICH, D. A., OLA, M. S., COLE, J., SWEATT, A. J., HUTSON, S. M. & LANOUE, K. F. 2007. Mitochondrial transport proteins of the brain. *J Neurosci Res,* 85**,** 3367-77.

BERWICK, D. C., HERS, I., HEESOM, K. J., MOULE, S. K. & TAVARE, J. M. 2002. The identification of ATP-citrate lyase as a protein kinase B (Akt) substrate in primary adipocytes. *J Biol Chem,* 277**,** 33895-900.

BIRNER, P., PUSCH, S., CHRISTOV, C., MIHAYLOVA, S., TOUMANGELOVA-UZEIR, K., NATCHEV, S., SCHOPPMANN, S. F., TCHORBANOV, A., STREUBEL, B., TUETTENBERG, J. & GUENTCHEV, M. 2014. Mutant IDH1 inhibits PI3K/Akt signaling in human glioma. *Cancer,* 120**,** 2440-7.

BLEAU, A. M., HAMBARDZUMYAN, D., OZAWA, T., FOMCHENKO, E. I., HUSE, J. T., BRENNAN, C. W. & HOLLAND, E. C. 2009. PTEN/PI3K/Akt pathway regulates the side population phenotype and ABCG2 activity in glioma tumor stem-like cells. *Cell Stem Cell,* 4**,** 226-35.

BLEEKER, F. E., ATAI, N. A., LAMBA, S., JONKER, A., RIJKEBOER, D., BOSCH, K. S., TIGCHELAAR, W., TROOST, D., VANDERTOP, W. P., BARDELLI, A. & VAN NOORDEN, C. J. 2010. The prognostic IDH1(R132) mutation is associated with reduced NADP+-dependent IDH activity in glioblastoma. *Acta Neuropathol,* 119**,** 487-94.

BOGDANOVIC, E., SADRI, A. R., CATAPANO, M., VANCE, J. E. & JESCHKE, M. G. 2014. IDH1 regulates phospholipid metabolism in developing astrocytes. *Neurosci Lett,* 582**,** 87-92.

BÖGLER, O., HUANG, H. J., KLEIHUES, P. & CAVENEE, W. K. 1995. The p53 gene and its role in human brain tumors. *Glia,* 15**,** 308-27.

BOLAÑOS, J. P., ALMEIDA, A. & MONCADA, S. 2010. Glycolysis: a bioenergetic or a survival pathway? *Trends Biochem Sci,* 35**,** 145-9.

BORODOVSKY, A., SALMASI, V., TURCAN, S., FABIUS, A. W., BAIA, G. S., EBERHART, C. G., WEINGART, J. D., GALLIA, G. L., BAYLIN, S. B., CHAN, T. A. & RIGGINS, G. J. 2013. 5-azacytidine reduces methylation, promotes differentiation and induces tumor regression in a patient-derived IDH1 mutant glioma xenograft. *Oncotarget,* 4**,** 1737-47.

BOUGNAUD, S., GOLEBIEWSKA, A., OUDIN, A., KEUNEN, O., HARTER, P. N., MADER, L., AZUAJE, F., FRITAH, S., STIEBER, D., KAOMA, T., VALLAR, L., BRONS, N. H., DAUBON, T., MILETIC, H., SUNDSTROM, T., HEROLD-MENDE, C., MITTELBRONN, M., BJERKVIG, R. & NICLOU, S. P. 2016a. Molecular crosstalk between tumour and brain parenchyma instructs histopathological features in glioblastoma. *Oncotarget,* 7**,** 31955-71.

BOUGNAUD, S., GOLEBIEWSKA, A., OUDIN, A., KEUNEN, O., HARTER, P. N., MÄDER, L., AZUAJE, F., FRITAH, S., STIEBER, D., KAOMA, T., VALLAR, L., BRONS, N. H., DAUBON, T., MILETIC, H., SUNDSTRØM, T., HEROLD-MENDE, C., MITTELBRONN, M., BJERKVIG, R. & NICLOU, S. P. 2016b. Molecular crosstalk between tumour and brain parenchyma instructs histopathological features in glioblastoma. *Oncotarget,* 7**,** 31955-71.

BOWMAN, R. L., WANG, Q., CARRO, A., VERHAAK, R. G. & SQUATRITO, M. 2017. GlioVis data portal for visualization and analysis of brain tumor expression datasets. *Neuro Oncol,* 19**,** 139-141.

BRABETZ, O., ALLA, V., ANGENENDT, L., SCHLIEMANN, C., BERDEL, W. E., ARTEAGA, M. F. & MIKESCH, J. H. 2017. RNA-Guided CRISPR-Cas9 System-Mediated Engineering of Acute Myeloid Leukemia Mutations. *Mol Ther Nucleic Acids,* 6**,** 243-248.

BRALTEN, L. B., KLOOSTERHOF, N. K., BALVERS, R., SACCHETTI, A., LAPRE, L., LAMFERS, M., LEENSTRA, S., DE JONGE, H., KROS, J. M., JANSEN, E. E., STRUYS, E. A., JAKOBS, C., SALOMONS, G. S., DIKS, S. H., PEPPELENBOSCH, M., KREMER, A., HOOGENRAAD, C. C., SMITT, P. A. & FRENCH, P. J. 2011. IDH1 R132H decreases proliferation of glioma cell lines in vitro and in vivo. *Ann Neurol,* 69**,** 455-63.

BRANZOLI, F., PONTOIZEAU, C., TCHARA, L., DI STEFANO, A. L., KAMOUN, A., DEELCHAND, D. K., VALABREGUE, R., LEHERICY, S., SANSON, M., OTTOLENGHI, C. & MARJANSKA, M. 2019. Cystathionine as a marker for 1p/19q codeleted gliomas by in vivo magnetic resonance spectroscopy. *Neuro Oncol,* 21**,** 765-774.

BRAT, D. J., VERHAAK, R. G., ALDAPE, K. D., YUNG, W. K., SALAMA, S. R., COOPER, L. A., RHEINBAY, E., MILLER, C. R., VITUCCI, M., MOROZOVA, O., ROBERTSON, A. G., NOUSHMEHR, H., LAIRD, P. W., CHERNIACK, A. D., AKBANI, R., HUSE, J. T., CIRIELLO, G., POISSON, L. M., BARNHOLTZ-SLOAN, J. S., BERGER, M. S., BRENNAN, C., COLEN, R. R., COLMAN, H., FLANDERS, A. E., GIANNINI, C., GRIFFORD, M., IAVARONE, A., JAIN, R., JOSEPH, I., KIM, J., KASAIAN, K., MIKKELSEN, T., MURRAY, B. A., O'NEILL, B. P., PACHTER, L., PARSONS, D. W., SOUGNEZ, C., SULMAN, E. P., VANDENBERG, S. R., VAN MEIR, E. G., VON DEIMLING, A., ZHANG, H., CRAIN, D., LAU, K., MALLERY, D., MORRIS, S., PAULAUSKIS, J., PENNY, R., SHELTON, T., SHERMAN, M., YENA, P., BLACK, A., BOWEN, J., DICOSTANZO, K., GASTIER-FOSTER, J., LERAAS, K. M., LICHTENBERG, T. M., PIERSON, C. R., RAMIREZ, N. C., TAYLOR, C., WEAVER, S., WISE, L., ZMUDA, E., DAVIDSEN, T., DEMCHOK, J. A., ELEY, G., FERGUSON, M. L., HUTTER, C. M., MILLS SHAW, K. R., OZENBERGER, B. A., SHETH, M., SOFIA, H. J., TARNUZZER, R., WANG, Z., YANG, L., ZENKLUSEN, J. C., AYALA, B., BABOUD, J., CHUDAMANI, S., JENSEN, M. A., LIU, J., PIHL, T., RAMAN, R., WAN, Y., WU, Y., ALLY, A., AUMAN, J. T., BALASUNDARAM, M., BALU, S., BAYLIN, S. B., BEROUKHIM, R., BOOTWALLA, M. S., BOWLBY, R., BRISTOW, C. A., BROOKS, D., BUTTERFIELD, Y., CARLSEN, R., CARTER, S., CHIN, L., CHU, A., et al. 2015. Comprehensive, Integrative Genomic Analysis of Diffuse Lower-Grade Gliomas. *N Engl J Med,* 372**,** 2481-98.

BROWN, A. M. 2004. Brain glycogen re-awakened. *J Neurochem,* 89**,** 537-52.

BUNSE, L., PUSCH, S., BUNSE, T., SAHM, F., SANGHVI, K., FRIEDRICH, M., ALANSARY, D., SONNER, J. K., GREEN, E., DEUMELANDT, K., KILIAN, M., NEFTEL, C., UHLIG, S., KESSLER, T., VON LANDENBERG, A., BERGHOFF, A. S., MARSH, K., STEADMAN, M., ZHU, D., NICOLAY, B., WIESTLER, B., BRECKWOLDT, M. O., AL-ALI, R., KARCHER-BAUSCH, S., BOZZA, M., OEZEN, I., KRAMER, M., MEYER, J., HABEL, A., EISEL, J., POSCHET, G., WELLER, M., PREUSSER, M., NADJI-OHL, M., THON, N., BURGER, M. C., HARTER, P. N., RATLIFF, M., HARBOTTLE, R., BENNER, A., SCHRIMPF, D., OKUN, J., HEROLD-MENDE, C., TURCAN, S., KAULFUSS, S., HESS-STUMPP, H., BIEBACK, K., CAHILL, D. P., PLATE, K. H., HÄNGGI, D., DORSCH, M., SUVÀ, M. L., NIEMEYER, B. A., VON DEIMLING, A., WICK, W. & PLATTEN, M. 2018. Suppression of antitumor T cell immunity by the oncometabolite (R)-2-hydroxyglutarate. *Nat Med,* 24**,** 1192-1203.

BURGER, P. C. 1995. Revising the World Health Organization (WHO) Blue Book--'Histological typing of tumours of the central nervous system'. *J Neurooncol,* 24**,** 3-7.

CAI, L., SUTTER, B. M., LI, B. & TU, B. P. 2011. Acetyl-CoA induces cell growth and proliferation by promoting the acetylation of histones at growth genes. *Mol Cell,* 42**,** 426-37.

CAKIR, T., ALSAN, S., SAYBASILI, H., AKIN, A. & ULGEN, K. O. 2007. Reconstruction and flux analysis of coupling between metabolic pathways of astrocytes and neurons: application to cerebral hypoxia. *Theor Biol Med Model,* 4**,** 48.

CALKINS, M. J., JOHNSON, D. A., TOWNSEND, J. A., VARGAS, M. R., DOWELL, J. A., WILLIAMSON, T. P., KRAFT, A. D., LEE, J. M., LI, J. & JOHNSON, J. A. 2009. The Nrf2/ARE pathway as a potential therapeutic target in neurodegenerative disease. *Antioxid Redox Signal,* 11**,** 497-508.

CAPPER, D., JONES, D. T. W., SILL, M., HOVESTADT, V., SCHRIMPF, D., STURM, D., KOELSCHE, C., SAHM, F., CHAVEZ, L., REUSS, D. E., KRATZ, A., WEFERS, A. K., HUANG, K., PAJTLER, K. W.,

SCHWEIZER, L., STICHEL, D., OLAR, A., ENGEL, N. W., LINDENBERG, K., HARTER, P. N., BRACZYNSKI, A. K., PLATE, K. H., DOHMEN, H., GARVALOV, B. K., CORAS, R., HOLSKEN, A., HEWER, E., BEWERUNGE-HUDLER, M., SCHICK, M., FISCHER, R., BESCHORNER, R., SCHITTENHELM, J., STASZEWSKI, O., WANI, K., VARLET, P., PAGES, M., TEMMING, P., LOHMANN, D., SELT, F., WITT, H., MILDE, T., WITT, O., ARONICA, E., GIANGASPERO, F., RUSHING, E., SCHEURLEN, W., GEISENBERGER, C., RODRIGUEZ, F. J., BECKER, A., PREUSSER, M., HABERLER, C., BJERKVIG, R., CRYAN, J., FARRELL, M., DECKERT, M., HENCH, J., FRANK, S., SERRANO, J., KANNAN, K., TSIRIGOS, A., BRUCK, W., HOFER, S., BREHMER, S., SEIZ-ROSENHAGEN, M., HANGGI, D., HANS, V., ROZSNOKI, S., HANSFORD, J. R., KOHLHOF, P., KRISTENSEN, B. W., LECHNER, M., LOPES, B., MAWRIN, C., KETTER, R., KULOZIK, A., KHATIB, Z., HEPPNER, F., KOCH, A., JOUVET, A., KEOHANE, C., MUHLEISEN, H., MUELLER, W., POHL, U., PRINZ, M., BENNER, A., ZAPATKA, M., GOTTARDO, N. G., DRIEVER, P. H., KRAMM, C. M., MULLER, H. L., RUTKOWSKI, S., VON HOFF, K., FRUHWALD, M. C., GNEKOW, A., FLEISCHHACK, G., TIPPELT, S., CALAMINUS, G., MONORANU, C. M., PERRY, A., JONES, C., et al. 2018. DNA methylation-based classification of central nervous system tumours. *Nature,* 555**,** 469-474.

CARBONNEAU, M., L, M. G., LALONDE, M. E., GERMAIN, M. A., MOTORINA, A., GUIOT, M. C., SECCO, B., VINCENT, E. E., TUMBER, A., HULEA, L., BERGEMAN, J., OPPERMANN, U., JONES, R. G., LAPLANTE, M., TOPISIROVIC, I., PETRECCA, K., HUOT, M. & MALLETTE, F. A. 2016. The oncometabolite 2-hydroxyglutarate activates the mTOR signalling pathway. *Nat Commun,* 7**,** 12700.

CASERO, R. A., JR. & MARTON, L. J. 2007. Targeting polyamine metabolism and function in cancer and other hyperproliferative diseases. *Nat Rev Drug Discov,* 6**,** 373-90.

CASTRO, M. A., BELTRÁN, F. A., BRAUCHI, S. & CONCHA, II 2009. A metabolic switch in brain: glucose and lactate metabolism modulation by ascorbic acid. *J Neurochem,* 110**,** 423-40.

CECCARELLI, M., BARTHEL, F. P., MALTA, T. M., SABEDOT, T. S., SALAMA, S. R., MURRAY, B. A., MOROZOVA, O., NEWTON, Y., RADENBAUGH, A., PAGNOTTA, S. M., ANJUM, S., WANG, J., MANYAM, G., ZOPPOLI, P., LING, S., RAO, A. A., GRIFFORD, M., CHERNIACK, A. D., ZHANG, H., POISSON, L., CARLOTTI, C. G., JR., TIRAPELLI, D. P., RAO, A., MIKKELSEN, T., LAU, C. C., YUNG, W. K., RABADAN, R., HUSE, J., BRAT, D. J., LEHMAN, N. L., BARNHOLTZ-SLOAN, J. S., ZHENG, S., HESS, K., RAO, G., MEYERSON, M., BEROUKHIM, R., COOPER, L., AKBANI, R., WRENSCH, M., HAUSSLER, D., ALDAPE, K. D., LAIRD, P. W., GUTMANN, D. H., NOUSHMEHR, H., IAVARONE, A. & VERHAAK, R. G. 2016. Molecular Profiling Reveals Biologically Discrete Subsets and Pathways of Progression in Diffuse Glioma. *Cell,* 164**,** 550-63.

CHAN, S. M., THOMAS, D., CORCES-ZIMMERMAN, M. R., XAVY, S., RASTOGI, S., HONG, W. J., ZHAO, F., MEDEIROS, B. C., TYVOLL, D. A. & MAJETI, R. 2015. Isocitrate dehydrogenase 1 and 2 mutations induce BCL-2 dependence in acute myeloid leukemia. *Nat Med,* 21**,** 178-84.

CHEN, L., LI, X., LIU, L., YU, B., XUE, Y. & LIU, Y. 2015. Erastin sensitizes glioblastoma cells to temozolomide by restraining xCT and cystathionine-gamma-lyase function. *Oncol Rep,* 33**,** 1465-74.

CHEN, R., NISHIMURA, M. C., KHARBANDA, S., PEALE, F., DENG, Y., DAEMEN, A., FORREST, W. F., KWONG, M., HEDEHUS, M., HATZIVASSILIOU, G., FRIEDMAN, L. S. & PHILLIPS, H. S. 2014. Hominoid-specific enzyme GLUD2 promotes growth of IDH1R132H glioma. *Proc Natl Acad Sci U S A,* 111**,** 14217-22.

CHENG, S. C., QUINTIN, J., CRAMER, R. A., SHEPARDSON, K. M., SAEED, S., KUMAR, V., GIAMARELLOS-BOURBOULIS, E. J., MARTENS, J. H., RAO, N. A., AGHAJANIREFAH, A., MANJERI, G. R., LI, Y., IFRIM, D. C., ARTS, R. J., VAN DER VEER, B. M., DEEN, P. M., LOGIE, C., O'NEILL, L. A., WILLEMS, P., VAN DE VEERDONK, F. L., VAN DER MEER, J. W., NG, A., JOOSTEN, L. A., WIJMENGA, C., STUNNENBERG, H. G., XAVIER, R. J. & NETEA, M. G. 2014. mTOR- and HIF-1α-mediated aerobic glycolysis as metabolic basis for trained immunity. *Science,* 345**,** 1250684.

CHENG, T., SUDDERTH, J., YANG, C., MULLEN, A. R., JIN, E. S., MATÉS, J. M. & DEBERARDINIS, R. J. 2011. Pyruvate carboxylase is required for glutamine-independent growth of tumor cells. *Proc Natl Acad Sci U S A,* 108**,** 8674-9.

CHESNELONG, C., CHAUMEIL, M. M., BLOUGH, M. D., AL-NAJJAR, M., STECHISHIN, O. D., CHAN, J. A., PIEPER, R. O., RONEN, S. M., WEISS, S., LUCHMAN, H. A. & CAIRNCROSS, J. G. 2014. Lactate dehydrogenase A silencing in IDH mutant gliomas. *Neuro Oncol,* 16**,** 686-95.

CHIANG, E. P., WANG, Y. C., CHEN, W. W. & TANG, F. Y. 2009. Effects of insulin and glucose on cellular metabolic fluxes in homocysteine transsulfuration, remethylation, S-adenosylmethionine synthesis, and global deoxyribonucleic acid methylation. *J Clin Endocrinol Metab,* 94**,** 1017-25.

CHO, E. S., HOVANEC-BROWN, J., TOMANEK, R. J. & STEGINK, L. D. 1991. Propargylglycine infusion effects on tissue glutathione levels, plasma amino acid concentrations and tissue morphology in parenterally-fed growing rats. *J Nutr,* 121**,** 785-94.

CHOU, W. C., LEI, W. C., KO, B. S., HOU, H. A., CHEN, C. Y., TANG, J. L., YAO, M., TSAY, W., WU, S. J., HUANG, S. Y., HSU, S. C., CHEN, Y. C., CHANG, Y. C., KUO, K. T., LEE, F. Y., LIU, M. C., LIU, C. W., TSENG, M. H., HUANG, C. F. & TIEN, H. F. 2011. The prognostic impact and stability of Isocitrate dehydrogenase 2 mutation in adult patients with acute myeloid leukemia. *Leukemia,* 25**,** 246-53.

CLAUS, E. B., WALSH, K. M., WIENCKE, J. K., MOLINARO, A. M., WIEMELS, J. L., SCHILDKRAUT, J. M., BONDY, M. L., BERGER, M., JENKINS, R. & WRENSCH, M. 2015. Survival and low-grade glioma: the emergence of genetic information. *Neurosurg Focus,* 38**,** E6.

COLEGIO, O. R., CHU, N. Q., SZABO, A. L., CHU, T., RHEBERGEN, A. M., JAIRAM, V., CYRUS, N., BROKOWSKI, C. E., EISENBARTH, S. C., PHILLIPS, G. M., CLINE, G. W., PHILLIPS, A. J. & MEDZHITOV, R. 2014. Functional polarization of tumour-associated macrophages by tumour-derived lactic acid. *Nature,* 513**,** 559-63.

COMMISSO, C., DAVIDSON, S. M., SOYDANER-AZELOGLU, R. G., PARKER, S. J., KAMPHORST, J. J., HACKETT, S., GRABOCKA, E., NOFAL, M., DREBIN, J. A., THOMPSON, C. B., RABINOWITZ, J. D., METALLO, C. M., VANDER HEIDEN, M. G. & BAR-SAGI, D. 2013. Macropinocytosis of protein is an amino acid supply route in Ras-transformed cells. *Nature,* 497**,** 633-7.

CONSTANT, J. S., FENG, J. J., ZABEL, D. D., YUAN, H., SUH, D. Y., SCHEUENSTUHL, H., HUNT, T. K. & HUSSAIN, M. Z. 2000. Lactate elicits vascular endothelial growth factor from macrophages: a possible alternative to hypoxia. *Wound Repair Regen,* 8**,** 353-60.

CORTESE-KROTT, M. M., KONING, A., KUHNLE, G. G. C., NAGY, P., BIANCO, C. L., PASCH, A., WINK, D. A., FUKUTO, J. M., JACKSON, A. A., VAN GOOR, H., OLSON, K. R. & FEELISCH, M. 2017. The Reactive Species Interactome: Evolutionary Emergence, Biological Significance, and Opportunities for Redox Metabolomics and Personalized Medicine. *Antioxid Redox Signal,* 27**,** 684-712.

COX, J., HEIN, M. Y., LUBER, C. A., PARON, I., NAGARAJ, N. & MANN, M. 2014. Accurate proteome-wide label-free quantification by delayed normalization and maximal peptide ratio extraction, termed MaxLFQ. *Mol Cell Proteomics,* 13**,** 2513-26.

COX, J. & MANN, M. 2008. MaxQuant enables high peptide identification rates, individualized p.p.b.-range mass accuracies and proteome-wide protein quantification. *Nat Biotechnol,* 26**,** 1367-72.

COX, J., NEUHAUSER, N., MICHALSKI, A., SCHELTEMA, R. A., OLSEN, J. V. & MANN, M. 2011. Andromeda: a peptide search engine integrated into the MaxQuant environment. *J Proteome Res,* 10**,** 1794-805.

CRAMER, S. L., SAHA, A., LIU, J., TADI, S., TIZIANI, S., YAN, W., TRIPLETT, K., LAMB, C., ALTERS, S. E., ROWLINSON, S., ZHANG, Y. J., KEATING, M. J., HUANG, P., DIGIOVANNI, J., GEORGIOU, G. & STONE, E. 2017. Systemic depletion of L-cyst(e)ine with cyst(e)inase increases reactive oxygen species and suppresses tumor growth. *Nat Med,* 23**,** 120-127.

D'AGATA, F., RUFFINATTI, F. A., BOSCHI, S., STURA, I., RAINERO, I., ABOLLINO, O., CAVALLI, R. & GUIOT, C. 2017. Magnetic Nanoparticles in the Central Nervous System: Targeting Principles, Applications and Safety Issues. *Molecules,* 23.

D'AUTRÉAUX, B. & TOLEDANO, M. B. 2007. ROS as signalling molecules: mechanisms that generate specificity in ROS homeostasis. *Nat Rev Mol Cell Biol,* 8**,** 813-24.

DA SILVA, C. G., RIBEIRO, C. A., LEIPNITZ, G., DUTRA-FILHO, C. S., WYSE, A. A., WANNMACHER, C. M., SARKIS, J. J., JAKOBS, C. & WAJNER, M. 2002. Inhibition of cytochrome c oxidase activity in rat cerebral cortex and human skeletal muscle by D-2-hydroxyglutaric acid in vitro. *Biochim Biophys Acta,* 1586**,** 81-91.

DANG, C. V. 2013. Role of aerobic glycolysis in genetically engineered mouse models of cancer. *BMC Biol,* 11**,** 3.

DANG, L., WHITE, D. W., GROSS, S., BENNETT, B. D., BITTINGER, M. A., DRIGGERS, E. M., FANTIN, V. R., JANG, H. G., JIN, S., KEENAN, M. C., MARKS, K. M., PRINS, R. M., WARD, P. S., YEN, K. E., LIAU, L. M., RABINOWITZ, J. D., CANTLEY, L. C., THOMPSON, C. B., VANDER HEIDEN, M. G. & SU, S. M. 2009a. Cancer-associated IDH1 mutations produce 2-hydroxyglutarate. *Nature,* 462**,** 739-44.

DANG, L., WHITE, D. W., GROSS, S., BENNETT, B. D., BITTINGER, M. A., DRIGGERS, E. M., FANTIN, V. R., JANG, H. G., JIN, S., KEENAN, M. C., MARKS, K. M., PRINS, R. M., WARD, P. S., YEN, K. E., LIAU, L. M., RABINOWITZ, J. D., CANTLEY, L. C., THOMPSON, C. B., VANDER HEIDEN, M. G. & SU, S. M. 2009b. Cancer-associated IDH1 mutations produce 2-hydroxyglutarate. *Nature,* 462**,** 739-744.

DANIELE, S., GIACOMELLI, C., ZAPPELLI, E., GRANCHI, C., TRINCAVELLI, M. L., MINUTOLO, F. & MARTINI, C. 2015. Lactate dehydrogenase-A inhibition induces human glioblastoma multiforme stem cell differentiation and death. *Sci Rep,* 5**,** 15556.

DAO TRONG, P., RÖSCH, S., MAIRBÄURL, H., PUSCH, S., UNTERBERG, A., HEROLD-MENDE, C. & WARTA, R. 2018. Identification of a Prognostic Hypoxia-Associated Gene Set in IDH-Mutant Glioma. *Int J Mol Sci,* 19.

DE FEYTER, H. M., BEHAR, K. L., RAO, J. U., MADDEN-HENNESSEY, K., IP, K. L., HYDER, F., DREWES, L. R., GESCHWIND, J. F., DE GRAAF, R. A. & ROTHMAN, D. L. 2016. A ketogenic diet increases transport and oxidation of ketone bodies in RG2 and 9L gliomas without affecting tumor growth. *Neuro Oncol,* 18**,** 1079-87.

DEBERARDINIS, R. J., LUM, J. J., HATZIVASSILIOU, G. & THOMPSON, C. B. 2008. The biology of cancer: metabolic reprogramming fuels cell growth and proliferation. *Cell Metab,* 7**,** 11-20.

DEBERARDINIS, R. J., MANCUSO, A., DAIKHIN, E., NISSIM, I., YUDKOFF, M., WEHRLI, S. & THOMPSON, C. B. 2007. Beyond aerobic glycolysis: transformed cells can engage in glutamine metabolism that exceeds the requirement for protein and nucleotide synthesis. *Proc Natl Acad Sci U S A,* 104**,** 19345-50.

DEBERARDINIS, R. J. & THOMPSON, C. B. 2012. Cellular metabolism and disease: what do metabolic outliers teach us? *Cell,* 148**,** 1132-44.

DEKKER, L. J. M., WU, S., JURRIËNS, C., MUSTAFA, D. A. N., GREVERS, F., BURGERS, P. C., SILLEVIS SMITT, P. A. E., KROS, J. M. & LUIDER, T. M. 2020. Metabolic changes related to the IDH1 mutation in gliomas preserve TCA-cycle activity: An investigation at the protein level. *Faseb j,* 34**,** 3646-3657.

DETTLING, S., STAMOVA, S., WARTA, R., SCHNÖLZER, M., RAPP, C., RATHINASAMY, A., REUSS, D., POCHA, K., ROESCH, S., JUNGK, C., WARNKEN, U., ECKSTEIN, V., GRABE, N., SCHRAMM, C., WEIGAND, M. A., VON DEIMLING, A., UNTERBERG, A., BECKHOVE, P. & HEROLD-MENDE, C. 2018. Identification of CRKII, CFL1, CNTN1, NME2, and TKT as Novel and Frequent T-Cell Targets in Human IDH-Mutant Glioma. *Clin Cancer Res,* 24**,** 2951-2962.

DICKINSON, D. A. & FORMAN, H. J. 2002. Glutathione in defense and signaling: lessons from a small thiol. *Ann N Y Acad Sci,* 973**,** 488-504.

DIRKSE, A., GOLEBIEWSKA, A., BUDER, T., NAZAROV, P. V., MULLER, A., POOVATHINGAL, S., BRONS, N. H. C., LEITE, S., SAUVAGEOT, N., SARKISJAN, D., SEYFRID, M., FRITAH, S., STIEBER, D., MICHELUCCI, A., HERTEL, F., HEROLD-MENDE, C., AZUAJE, F., SKUPIN, A., BJERKVIG, R., DEUTSCH, A., VOSS-BÖHME, A. & NICLOU, S. P. 2019. Stem cell-associated heterogeneity in Glioblastoma results from intrinsic tumor plasticity shaped by the microenvironment. *Nat Commun,* 10**,** 1787.

DOLL, S., URISMAN, A., OSES-PRIETO, J. A., ARNOTT, D. & BURLINGAME, A. L. 2017. Quantitative Proteomics Reveals Fundamental Regulatory Differences in Oncogenic HRAS and Isocitrate Dehydrogenase (IDH1) Driven Astrocytoma. *Mol Cell Proteomics,* 16**,** 39-56.

DRINGEN, R. 2000. Metabolism and functions of glutathione in brain. *Prog Neurobiol,* 62**,** 649-71.

DUCKER, G. S., CHEN, L., MORSCHER, R. J., GHERGUROVICH, J. M., ESPOSITO, M., TENG, X., KANG, Y. & RABINOWITZ, J. D. 2016. Reversal of Cytosolic One-Carbon Flux Compensates for Loss of the Mitochondrial Folate Pathway. *Cell Metab,* 23**,** 1140-1153.

DUNCAN, C. G., BARWICK, B. G., JIN, G., RAGO, C., KAPOOR-VAZIRANI, P., POWELL, D. R., CHI, J. T., BIGNER, D. D., VERTINO, P. M. & YAN, H. 2012. A heterozygous IDH1R132H/WT mutation induces genome-wide alterations in DNA methylation. *Genome Res,* 22**,** 2339-55.

EMADI, A., JUN, S. A., TSUKAMOTO, T., FATHI, A. T., MINDEN, M. D. & DANG, C. V. 2014. Inhibition of glutaminase selectively suppresses the growth of primary acute myeloid leukemia cells with IDH mutations. *Exp Hematol,* 42**,** 247-51.

EMIR, U. E., LARKIN, S. J., DE PENNINGTON, N., VOETS, N., PLAHA, P., STACEY, R., AL-QAHTANI, K., MCCULLAGH, J., SCHOFIELD, C. J., CLARE, S., JEZZARD, P., CADOUX-HUDSON, T. & ANSORGE, O. 2016. Noninvasive Quantification of 2-Hydroxyglutarate in Human Gliomas with IDH1 and IDH2 Mutations. *Cancer Res,* 76**,** 43-9.

ENGELBORGHS, S., MARESCAU, B. & DE DEYN, P. P. 2003. Amino acids and biogenic amines in cerebrospinal fluid of patients with Parkinson's disease. *Neurochem Res,* 28**,** 1145-50.

ESMAEILI, M., HAMANS, B. C., NAVIS, A. C., VAN HORSSEN, R., BATHEN, T. F., GRIBBESTAD, I. S., LEENDERS, W. P. & HEERSCHAP, A. 2014. IDH1 R132H mutation generates a distinct phospholipid metabolite profile in glioma. *Cancer Res,* 74**,** 4898-907.

FACK, F., TARDITO, S., HOCHART, G., OUDIN, A., ZHENG, L., FRITAH, S., GOLEBIEWSKA, A., NAZAROV, P. V., BERNARD, A., HAU, A. C., KEUNEN, O., LEENDERS, W., LUND-JOHANSEN, M., STAUBER, J., GOTTLIEB, E., BJERKVIG, R. & NICLOU, S. P. 2017. Altered metabolic landscape in IDH-mutant gliomas affects phospholipid, energy, and oxidative stress pathways. *EMBO Mol Med,* 9**,** 1681-1695.

FAN, J., KAMPHORST, J. J., MATHEW, R., CHUNG, M. K., WHITE, E., SHLOMI, T. & RABINOWITZ, J. D. 2013. Glutamine-driven oxidative phosphorylation is a major ATP source in transformed mammalian cells in both normoxia and hypoxia. *Mol Syst Biol,* 9**,** 712.

FAN, J., YE, J., KAMPHORST, J. J., SHLOMI, T., THOMPSON, C. B. & RABINOWITZ, J. D. 2014. Quantitative flux analysis reveals folate-dependent NADPH production. *Nature,* 510**,** 298-302.

FISCHER, K., HOFFMANN, P., VOELKL, S., MEIDENBAUER, N., AMMER, J., EDINGER, M., GOTTFRIED, E., SCHWARZ, S., ROTHE, G., HOVES, S., RENNER, K., TIMISCHL, B., MACKENSEN, A., KUNZ-SCHUGHART, L., ANDREESEN, R., KRAUSE, S. W. & KREUTZ, M. 2007. Inhibitory effect of tumor cell-derived lactic acid on human T cells. *Blood,* 109**,** 3812-9.

FORMAN, H. J., ZHANG, H. & RINNA, A. 2009. Glutathione: overview of its protective roles, measurement, and biosynthesis. *Mol Aspects Med,* 30**,** 1-12.

GABRIEL, J. L., ZERVOS, P. R. & PLAUT, G. W. 1986. Activity of purified NAD-specific isocitrate dehydrogenase at modulator and substrate concentrations approximating conditions in mitochondria. *Metabolism,* 35**,** 661-7.

GAGLIO, D., METALLO, C. M., GAMEIRO, P. A., HILLER, K., DANNA, L. S., BALESTRIERI, C., ALBERGHINA, L., STEPHANOPOULOS, G. & CHIARADONNA, F. 2011. Oncogenic K-Ras decouples glucose and glutamine metabolism to support cancer cell growth. *Mol Syst Biol,* 7**,** 523.

GAGLIO, D., SOLDATI, C., VANONI, M., ALBERGHINA, L. & CHIARADONNA, F. 2009. Glutamine deprivation induces abortive s-phase rescued by deoxyribonucleotides in k-ras transformed fibroblasts. *PLoS One,* 4**,** e4715.

GAMBERINO, W. C., BERKICH, D. A., LYNCH, C. J., XU, B. & LANOUE, K. F. 1997. Role of pyruvate carboxylase in facilitation of synthesis of glutamate and glutamine in cultured astrocytes. *J Neurochem,* 69**,** 2312-25.

GARRETT, M., SPERRY, J., BRAAS, D., YAN, W., LE, T. M., MOTTAHEDEH, J., LUDWIG, K., ESKIN, A., QIN, Y., LEVY, R., BREUNIG, J. J., PAJONK, F., GRAEBER, T. G., RADU, C. G., CHRISTOFK, H., PRINS, R. M., LAI, A., LIAU, L. M., COPPOLA, G. & KORNBLUM, H. I. 2018. Metabolic characterization of isocitrate dehydrogenase (IDH) mutant and IDH wildtype gliomaspheres uncovers cell type-specific vulnerabilities. *Cancer Metab,* 6**,** 4.

GASTEIGER, E., GATTIKER, A., HOOGLAND, C., IVANYI, I., APPEL, R. D. & BAIROCH, A. 2003. ExPASy: The proteomics server for in-depth protein knowledge and analysis. *Nucleic Acids Res,* 31**,** 3784-8.

GLASGOW, S. M., CARLSON, J. C., ZHU, W., CHABOUB, L. S., KANG, P., LEE, H. K., CLOVIS, Y. M., LOZZI, B. E., MCEVILLY, R. J., ROSENFELD, M. G., CREIGHTON, C. J., LEE, S. K., MOHILA, C. A. & DENEEN, B. 2017. Glia-specific enhancers and chromatin structure regulate NFIA expression and glioma tumorigenesis. *Nat Neurosci,* 20**,** 1520-1528.

GLASGOW, S. M., LAUG, D., BRAWLEY, V. S., ZHANG, Z., CORDER, A., YIN, Z., WONG, S. T., LI, X. N., FOSTER, A. E., AHMED, N. & DENEEN, B. 2013. The miR-223/nuclear factor I-A axis regulates glial precursor proliferation and tumorigenesis in the CNS. *J Neurosci,* 33**,** 13560-8.

GOETZE, K., WALENTA, S., KSIAZKIEWICZ, M., KUNZ-SCHUGHART, L. A. & MUELLER-KLIESER, W. 2011. Lactate enhances motility of tumor cells and inhibits monocyte migration and cytokine release. *Int J Oncol,* 39**,** 453-63.

GOLEBIEWSKA, A., HAU, A. C., OUDIN, A., STIEBER, D., YABO, Y. A., BAUS, V., BARTHELEMY, V., KLEIN, E., BOUGNAUD, S., KEUNEN, O., WANTZ, M., MICHELUCCI, A., NEIRINCKX, V., MULLER, A., KAOMA, T., NAZAROV, P. V., AZUAJE, F., DE FALCO, A., FLIES, B., RICHART, L., POOVATHINGAL, S., ARNS, T., GRZYB, K., MOCK, A., HEROLD-MENDE, C., STEINO, A., BROWN, D., MAY, P., MILETIC, H., MALTA, T. M., NOUSHMEHR, H., KWON, Y. J., JAHN, W., KLINK, B., TANNER, G., STEAD, L. F., MITTELBRONN, M., SKUPIN, A., HERTEL, F., BJERKVIG, R. & NICLOU, S. P. 2020. Patient-derived organoids and orthotopic xenografts of primary and recurrent gliomas represent relevant patient avatars for precision oncology. *Acta Neuropathol*.

GOTTFRIED, E., KUNZ-SCHUGHART, L. A., EBNER, S., MUELLER-KLIESER, W., HOVES, S., ANDREESEN, R., MACKENSEN, A. & KREUTZ, M. 2006. Tumor-derived lactic acid modulates dendritic cell activation and antigen expression. *Blood,* 107**,** 2013-21.

GRASSIAN, A. R., COLOFF, J. L. & BRUGGE, J. S. 2011. Extracellular matrix regulation of metabolism and implications for tumorigenesis. *Cold Spring Harb Symp Quant Biol,* 76**,** 313-24.

GRASSIAN, A. R., PARKER, S. J., DAVIDSON, S. M., DIVAKARUNI, A. S., GREEN, C. R., ZHANG, X., SLOCUM, K. L., PU, M., LIN, F., VICKERS, C., JOUD-CALDWELL, C., CHUNG, F., YIN, H., HANDLY, E. D., STRAUB, C., GROWNEY, J. D., VANDER HEIDEN, M. G., MURPHY, A. N., PAGLIARINI, R. & METALLO, C. M. 2014. IDH1 mutations alter citric acid cycle metabolism and increase dependence on oxidative mitochondrial metabolism. *Cancer Res,* 74**,** 3317-31.

GRIFFITH, O. W. 1999. Biologic and pharmacologic regulation of mammalian glutathione synthesis. *Free Radic Biol Med,* 27**,** 922-35.

GUO, D., REINITZ, F., YOUSSEF, M., HONG, C., NATHANSON, D., AKHAVAN, D., KUGA, D., AMZAJERDI, A. N., SOTO, H., ZHU, S., BABIC, I., TANAKA, K., DANG, J., IWANAMI, A., GINI, B., DEJESUS, J., LISIERO, D. D., HUANG, T. T., PRINS, R. M., WEN, P. Y., ROBINS, H. I., PRADOS, M. D., DEANGELIS, L. M., MELLINGHOFF, I. K., MEHTA, M. P., JAMES, C. D., CHAKRAVARTI, A., CLOUGHESY, T. F., TONTONOZ, P. & MISCHEL, P. S. 2011. An LXR agonist promotes glioblastoma cell death through inhibition of an EGFR/AKT/SREBP-1/LDLR-dependent pathway. *Cancer Discov,* 1**,** 442-56.

GUREEV, A. P., POPOV, V. N. & STARKOV, A. A. 2020. Crosstalk between the mTOR and Nrf2/ARE signaling pathways as a target in the improvement of long-term potentiation. *Exp Neurol,* 328**,** 113285.

HAN, S., LIU, Y., CAI, S. J., QIAN, M., DING, J., LARION, M., GILBERT, M. R. & YANG, C. 2020. IDH mutation in glioma: molecular mechanisms and potential therapeutic targets. *Br J Cancer,* 122**,** 1580-1589.

HANAHAN, D. & WEINBERG, R. A. 2011. Hallmarks of cancer: the next generation. *Cell,* 144**,** 646-74.

HARTMANN, C., MEYER, J., BALSS, J., CAPPER, D., MUELLER, W., CHRISTIANS, A., FELSBERG, J., WOLTER, M., MAWRIN, C., WICK, W., WELLER, M., HEROLD-MENDE, C., UNTERBERG, A., JEUKEN, J. W., WESSELING, P., REIFENBERGER, G. & VON DEIMLING, A. 2009. Type and frequency of IDH1 and IDH2 mutations are related to astrocytic and oligodendroglial differentiation and age: a study of 1,010 diffuse gliomas. *Acta Neuropathol,* 118**,** 469-74.

HE, L., HE, T., FARRAR, S., JI, L., LIU, T. & MA, X. 2017. Antioxidants Maintain Cellular Redox Homeostasis by Elimination of Reactive Oxygen Species. *Cell Physiol Biochem,* 44**,** 532-553.

HSU, P. P. & SABATINI, D. M. 2008. Cancer cell metabolism: Warburg and beyond. *Cell,* 134**,** 703-7.

HUFF, T., TADI, P. & VARACALLO, M. 2020. Neuroanatomy, Cerebrospinal Fluid. *StatPearls.* Treasure Island (FL): StatPearls Publishing

IADECOLA, C. & NEDERGAARD, M. 2007. Glial regulation of the cerebral microvasculature. *Nat Neurosci,* 10**,** 1369-76.

ITKONEN, H. M., MINNER, S., GULDVIK, I. J., SANDMANN, M. J., TSOURLAKIS, M. C., BERGE, V., SVINDLAND, A., SCHLOMM, T. & MILLS, I. G. 2013. O-GlcNAc transferase integrates metabolic pathways to regulate the stability of c-MYC in human prostate cancer cells. *Cancer Res,* 73**,** 5277-87.

ITOH, Y., ESAKI, T., SHIMOJI, K., COOK, M., LAW, M. J., KAUFMAN, E. & SOKOLOFF, L. 2003. Dichloroacetate effects on glucose and lactate oxidation by neurons and astroglia in vitro and on glucose utilization by brain in vivo. *Proc Natl Acad Sci U S A,* 100**,** 4879-84.

IVAN, M., KONDO, K., YANG, H., KIM, W., VALIANDO, J., OHH, M., SALIC, A., ASARA, J. M., LANE, W. S. & KAELIN, W. G., JR. 2001. HIFalpha targeted for VHL-mediated destruction by proline hydroxylation: implications for O2 sensing. *Science,* 292**,** 464-8.

IZQUIERDO-GARCIA, J. L., CAI, L. M., CHAUMEIL, M. M., ERIKSSON, P., ROBINSON, A. E., PIEPER, R. O., PHILLIPS, J. J. & RONEN, S. M. 2014. Glioma cells with the IDH1 mutation modulate metabolic fractional flux through pyruvate carboxylase. *PLoS One,* 9**,** e108289.

JANEWAY, K. A., KIM, S. Y., LODISH, M., NOSÉ, V., RUSTIN, P., GAAL, J., DAHIA, P. L., LIEGL, B., BALL, E. R., RAYGADA, M., LAI, A. H., KELLY, L., HORNICK, J. L., O'SULLIVAN, M., DE KRIJGER, R. R., DINJENS, W. N., DEMETRI, G. D., ANTONESCU, C. R., FLETCHER, J. A., HELMAN, L. & STRATAKIS, C. A. 2011. Defects in succinate dehydrogenase in gastrointestinal stromal tumors lacking KIT and PDGFRA mutations. *Proc Natl Acad Sci U S A,* 108**,** 314-8.

JIANG, L., SHESTOV, A. A., SWAIN, P., YANG, C., PARKER, S. J., WANG, Q. A., TERADA, L. S., ADAMS, N. D., MCCABE, M. T., PIETRAK, B., SCHMIDT, S., METALLO, C. M., DRANKA, B. P., SCHWARTZ, B. & DEBERARDINIS, R. J. 2016. Reductive carboxylation supports redox homeostasis during anchorage-independent growth. *Nature,* 532**,** 255-8.

JO, S. H., LEE, S. H., CHUN, H. S., LEE, S. M., KOH, H. J., LEE, S. E., CHUN, J. S., PARK, J. W. & HUH, T. L. 2002. Cellular defense against UVB-induced phototoxicity by cytosolic NADP(+)-dependent isocitrate dehydrogenase. *Biochem Biophys Res Commun,* 292**,** 542-9.

JURATLI, T. A., LAUTENSCHLAGER, T., GEIGER, K. D., PINZER, T., KRAUSE, M., SCHACKERT, G. & KREX, D. 2015. Radio-chemotherapy improves survival in IDH-mutant, 1p/19q non-codeleted secondary high-grade astrocytoma patients. *J Neurooncol,* 124**,** 197-205.

KAELIN, W. G., JR. & MCKNIGHT, S. L. 2013. Influence of metabolism on epigenetics and disease. *Cell,* 153**,** 56-69.

KANDIL, S., BRENNAN, L. & MCBEAN, G. J. 2010. Glutathione depletion causes a JNK and p38MAPK-mediated increase in expression of cystathionine-gamma-lyase and upregulation of the transsulfuration pathway in C6 glioma cells. *Neurochem Int,* 56**,** 611-9.

KARPEL-MASSLER, G., ISHIDA, C. T., BIANCHETTI, E., ZHANG, Y., SHU, C., TSUJIUCHI, T., BANU, M. A., GARCIA, F., ROTH, K. A., BRUCE, J. N., CANOLL, P. & SIEGELIN, M. D. 2017. Induction of synthetic lethality in IDH1-mutated gliomas through inhibition of Bcl-xL. *Nat Commun,* 8**,** 1067.

KAWAGUCHI, T., SONODA, Y., SHIBAHARA, I., SAITO, R., KANAMORI, M., KUMABE, T. & TOMINAGA, T. 2016. Impact of gross total resection in patients with WHO grade III glioma harboring the IDH 1/2 mutation without the 1p/19q co-deletion. *J Neurooncol,* 129**,** 505-514.

KEITH, B., JOHNSON, R. S. & SIMON, M. C. 2011. HIF1α and HIF2α: sibling rivalry in hypoxic tumour growth and progression. *Nat Rev Cancer,* 12**,** 9-22.

KIL, I. S., HUH, T. L., LEE, Y. S., LEE, Y. M. & PARK, J. W. 2006. Regulation of replicative senescence by NADP+ -dependent isocitrate dehydrogenase. *Free Radic Biol Med,* 40**,** 110-9.

KIM, J., KIM, J. I., JANG, H. S., PARK, J. W. & PARK, K. M. 2011. Protective role of cytosolic NADP(+)-dependent isocitrate dehydrogenase, IDH1, in ischemic pre-conditioned kidney in mice. *Free Radic Res,* 45**,** 759-66.

KIM, J., KIM, K. Y., JANG, H. S., YOSHIDA, T., TSUCHIYA, K., NITTA, K., PARK, J. W., BONVENTRE, J. V. & PARK, K. M. 2009. Role of cytosolic NADP+-dependent isocitrate dehydrogenase in ischemia-reperfusion injury in mouse kidney. *Am J Physiol Renal Physiol,* 296**,** F622-33.

KIM, J. W., TCHERNYSHYOV, I., SEMENZA, G. L. & DANG, C. V. 2006. HIF-1-mediated expression of pyruvate dehydrogenase kinase: a metabolic switch required for cellular adaptation to hypoxia. *Cell Metab,* 3**,** 177-85.

KIM, S. Y. & PARK, J. W. 2003. Cellular defense against singlet oxygen-induced oxidative damage by cytosolic NADP+-dependent isocitrate dehydrogenase. *Free Radic Res,* 37**,** 309-16.

KLEIN, E., HAU, A. C., OUDIN, A., GOLEBIEWSKA, A. & NICLOU, S. P. 2020. Glioblastoma Organoids: Pre-Clinical Applications and Challenges in the Context of Immunotherapy. *Front Oncol,* 10**,** 604121.

KOH, H. J., LEE, S. M., SON, B. G., LEE, S. H., RYOO, Z. Y., CHANG, K. T., PARK, J. W., PARK, D. C., SONG, B. J., VEECH, R. L., SONG, H. & HUH, T. L. 2004. Cytosolic NADP+-dependent isocitrate dehydrogenase plays a key role in lipid metabolism. *J Biol Chem,* 279**,** 39968-74.

KOHANBASH, G., CARRERA, D. A., SHRIVASTAV, S., AHN, B. J., JAHAN, N., MAZOR, T., CHHEDA, Z. S., DOWNEY, K. M., WATCHMAKER, P. B., BEPPLER, C., WARTA, R., AMANKULOR, N. A., HEROLD-MENDE, C., COSTELLO, J. F. & OKADA, H. 2017. Isocitrate dehydrogenase mutations suppress STAT1 and CD8+ T cell accumulation in gliomas. *J Clin Invest,* 127**,** 1425-1437.

KOIVUNEN, P., LEE, S., DUNCAN, C. G., LOPEZ, G., LU, G., RAMKISSOON, S., LOSMAN, J. A., JOENSUU, P., BERGMANN, U., GROSS, S., TRAVINS, J., WEISS, S., LOOPER, R., LIGON, K. L., VERHAAK, R. G., YAN, H. & KAELIN, W. G., JR. 2012. Transformation by the (R)-enantiomer of 2-hydroxyglutarate linked to EGLN activation. *Nature,* 483**,** 484-8.

KOOLMAN, J. & RÖHM, K.-H. 2013. *Color atlas of biochemistry,* Stuttgart, Thieme.

KOPINJA, J., SEVILLA, R. S., LEVITAN, D., DAI, D., VANKO, A., SPOONER, E., WARE, C., FORGET, R., HU, K., KRAL, A., SPACCIAPOLI, P., KENNAN, R., JAYARAMAN, L., PUCCI, V., PERERA, S., ZHANG, W., FISCHER, C. & LAM, M. H. 2017. A Brain Penetrant Mutant IDH1 Inhibitor Provides In Vivo Survival Benefit. *Sci Rep,* 7**,** 13853.

KRAJCOVIC, M., KRISHNA, S., AKKARI, L., JOYCE, J. A. & OVERHOLTZER, M. 2013. mTOR regulates phagosome and entotic vacuole fission. *Mol Biol Cell,* 24**,** 3736-45.

LANDHUIS, E. 2018. Tapping into the brain's star power. *Nature,* 563**,** 141-143.

LATINI, A., DA SILVA, C. G., FERREIRA, G. C., SCHUCK, P. F., SCUSSIATO, K., SARKIS, J. J., DUTRA FILHO, C. S., WYSE, A. T., WANNMACHER, C. M. & WAJNER, M. 2005. Mitochondrial energy metabolism is markedly impaired by D-2-hydroxyglutaric acid in rat tissues. *Mol Genet Metab,* 86**,** 188-99.

LAUG, D., GLASGOW, S. M. & DENEEN, B. 2018. A glial blueprint for gliomagenesis. *Nat Rev Neurosci,* 19**,** 393-403.

LAUGHTON, J. D., BITTAR, P., CHARNAY, Y., PELLERIN, L., KOVARI, E., MAGISTRETTI, P. J. & BOURAS, C. 2007. Metabolic compartmentalization in the human cortex and hippocampus: evidence for a cell- and region-specific localization of lactate dehydrogenase 5 and pyruvate dehydrogenase. *BMC Neurosci,* 8**,** 35.

LE FOLL, C. & LEVIN, B. E. 2016. Fatty acid-induced astrocyte ketone production and the control of food intake. *Am J Physiol Regul Integr Comp Physiol,* 310**,** R1186-92.

LEBON, V., PETERSEN, K. F., CLINE, G. W., SHEN, J., MASON, G. F., DUFOUR, S., BEHAR, K. L., SHULMAN, G. I. & ROTHMAN, D. L. 2002. Astroglial contribution to brain energy metabolism in humans revealed by 13C nuclear magnetic resonance spectroscopy: elucidation of the dominant pathway for neurotransmitter glutamate repletion and measurement of astrocytic oxidative metabolism. *J Neurosci,* 22**,** 1523-31.

LEE, S. M., KOH, H. J., PARK, D. C., SONG, B. J., HUH, T. L. & PARK, J. W. 2002. Cytosolic NADP(+)-dependent isocitrate dehydrogenase status modulates oxidative damage to cells. *Free Radic Biol Med,* 32**,** 1185-96.

LEIGHTON, F., POOLE, B., LAZAROW, P. B. & DE DUVE, C. 1969. The synthesis and turnover of rat liver peroxisomes. I. Fractionation of peroxisome proteins. *J Cell Biol,* 41**,** 521-35.

LEMONS, J. M., FENG, X. J., BENNETT, B. D., LEGESSE-MILLER, A., JOHNSON, E. L., RAITMAN, I., POLLINA, E. A., RABITZ, H. A., RABINOWITZ, J. D. & COLLER, H. A. 2010. Quiescent fibroblasts exhibit high metabolic activity. *PLoS Biol,* 8**,** e1000514.

LEONARDI, R., SUBRAMANIAN, C., JACKOWSKI, S. & ROCK, C. O. 2012. Cancer-associated isocitrate dehydrogenase mutations inactivate NADPH-dependent reductive carboxylation. *J Biol Chem,* 287**,** 14615-20.

LI, K., OUYANG, L., HE, M., LUO, M., CAI, W., TU, Y., PI, R. & LIU, A. 2017. IDH1 R132H mutation regulates glioma chemosensitivity through Nrf2 pathway. *Oncotarget,* 8**,** 28865-28879.

LI, S., CHOU, A. P., CHEN, W., CHEN, R., DENG, Y., PHILLIPS, H. S., SELFRIDGE, J., ZURAYK, M., LOU, J. J., EVERSON, R. G., WU, K. C., FAULL, K. F., CLOUGHESY, T., LIAU, L. M. & LAI, A. 2013. Overexpression of isocitrate dehydrogenase mutant proteins renders glioma cells more sensitive to radiation. *Neuro Oncol,* 15**,** 57-68.

LINDSTEN, T., GOLDEN, J. A., ZONG, W. X., MINARCIK, J., HARRIS, M. H. & THOMPSON, C. B. 2003. The proapoptotic activities of Bax and Bak limit the size of the neural stem cell pool. *J Neurosci,* 23**,** 11112-9.

LOCASALE, J. W. 2013. Serine, glycine and one-carbon units: cancer metabolism in full circle. *Nat Rev Cancer,* 13**,** 572-83.

LOCASALE, J. W., GRASSIAN, A. R., MELMAN, T., LYSSIOTIS, C. A., MATTAINI, K. R., BASS, A. J., HEFFRON, G., METALLO, C. M., MURANEN, T., SHARFI, H., SASAKI, A. T., ANASTASIOU, D., MULLARKY, E., VOKES, N. I., SASAKI, M., BEROUKHIM, R., STEPHANOPOULOS, G., LIGON, A. H., MEYERSON, M., RICHARDSON, A. L., CHIN, L., WAGNER, G., ASARA, J. M., BRUGGE, J. S., CANTLEY, L. C. & VANDER HEIDEN, M. G. 2011. Phosphoglycerate dehydrogenase diverts glycolytic flux and contributes to oncogenesis. *Nat Genet,* 43**,** 869-74.

LOSMAN, J. A. & KAELIN, W. G., JR. 2013. What a difference a hydroxyl makes: mutant IDH, (R)-2-hydroxyglutarate, and cancer. *Genes Dev,* 27**,** 836-52.

LOUIS, D. N., OHGAKI, H., WIESTLER, O. D., CAVENEE, W. K., BURGER, P. C., JOUVET, A., SCHEITHAUER, B. W. & KLEIHUES, P. 2007. The 2007 WHO Classification of Tumours of the Central Nervous System. *Acta Neuropathologica,* 114**,** 97-109.

LOUIS, D. N., PERRY, A., REIFENBERGER, G., VON DEIMLING, A., FIGARELLA-BRANGER, D., CAVENEE, W. K., OHGAKI, H., WIESTLER, O. D., KLEIHUES, P. & ELLISON, D. W. 2016a. The 2016 World Health Organization Classification of Tumors of the Central Nervous System: a summary. *Acta Neuropathol,* 131**,** 803-20.

LOUIS, D. N., PERRY, A., REIFENBERGER, G., VON DEIMLING, A., FIGARELLA-BRANGER, D., CAVENEE, W. K., OHGAKI, H., WIESTLER, O. D., KLEIHUES, P. & ELLISON, D. W. 2016b. The 2016 World Health Organization Classification of Tumors of the Central Nervous System: a summary. *Acta neuropathologica,* 131**,** 803-820.

LU, C., WARD, P. S., KAPOOR, G. S., ROHLE, D., TURCAN, S., ABDEL-WAHAB, O., EDWARDS, C. R., KHANIN, R., FIGUEROA, M. E., MELNICK, A., WELLEN, K. E., O'ROURKE, D. M., BERGER, S. L., CHAN, T. A., LEVINE, R. L., MELLINGHOFF, I. K. & THOMPSON, C. B. 2012. IDH mutation impairs histone demethylation and results in a block to cell differentiation. *Nature,* 483**,** 474-8.

LUCHMAN, H. A., CHESNELONG, C., CAIRNCROSS, J. G. & WEISS, S. 2013. Spontaneous loss of heterozygosity leading to homozygous R132H in a patient-derived IDH1 mutant cell line. *Neuro Oncol,* 15**,** 979-80.

LUNT, S. Y. & VANDER HEIDEN, M. G. 2011. Aerobic glycolysis: meeting the metabolic requirements of cell proliferation. *Annu Rev Cell Dev Biol,* 27**,** 441-64.

LYU, Z., GAO, X., WANG, W., DANG, J., YANG, L., YAN, M., ALI, S. A., LIU, Y., LIU, B., YU, M., DU, L. & LIU, K. 2019. mTORC1-Sch9 regulates hydrogen sulfide production through the transsulfuration pathway. *Aging (Albany NY),* 11**,** 8418-8432.

MACDONALD, M. J., BROWN, L. J., LONGACRE, M. J., STOKER, S. W., KENDRICK, M. A. & HASAN, N. M. 2013. Knockdown of both mitochondrial isocitrate dehydrogenase enzymes in pancreatic beta cells inhibits insulin secretion. *Biochim Biophys Acta,* 1830**,** 5104-11.

MAGISTRETTI, P. J. & ALLAMAN, I. 2015. A cellular perspective on brain energy metabolism and functional imaging. *Neuron,* 86**,** 883-901.

MARIN-VALENCIA, I., YANG, C., MASHIMO, T., CHO, S., BAEK, H., YANG, X. L., RAJAGOPALAN, K. N., MADDIE, M., VEMIREDDY, V., ZHAO, Z., CAI, L., GOOD, L., TU, B. P., HATANPAA, K. J., MICKEY, B. E., MATÉS, J. M., PASCUAL, J. M., MAHER, E. A., MALLOY, C. R., DEBERARDINIS, R. J. & BACHOO, R. M. 2012. Analysis of tumor metabolism reveals mitochondrial glucose oxidation in genetically diverse human glioblastomas in the mouse brain in vivo. *Cell Metab,* 15**,** 827-37.

MATTAINI, K. R., SULLIVAN, M. R. & VANDER HEIDEN, M. G. 2016. The importance of serine metabolism in cancer. *J Cell Biol,* 214**,** 249-57.

MAUS, A. & PETERS, G. J. 2017. Glutamate and α-ketoglutarate: key players in glioma metabolism. *Amino Acids,* 49**,** 21-32.

MCBEAN, G. J. 2012. The transsulfuration pathway: a source of cysteine for glutathione in astrocytes. *Amino Acids,* 42**,** 199-205.

MCBEAN, G. J. 2017. Cysteine, Glutathione, and Thiol Redox Balance in Astrocytes. *Antioxidants (Basel),* 6.

MCBEAN, G. J. 2018. Astrocyte Antioxidant Systems. *Antioxidants (Basel),* 7.

MCBRAYER, S. K., MAYERS, J. R., DINATALE, G. J., SHI, D. D., KHANAL, J., CHAKRABORTY, A. A., SAROSIEK, K. A., BRIGGS, K. J., ROBBINS, A. K., SEWASTIANIK, T., SHAREEF, S. J., OLENCHOCK, B. A., PARKER, S. J., TATEISHI, K., SPINELLI, J. B., ISLAM, M., HAIGIS, M. C., LOOPER, R. E., LIGON, K. L., BERNSTEIN, B. E., CARRASCO, R. D., CAHILL, D. P., ASARA, J. M., METALLO, C. M., YENNAWAR, N. H., VANDER HEIDEN, M. G. & KAELIN, W. G., JR. 2018. Transaminase Inhibition by 2-Hydroxyglutarate Impairs Glutamate Biosynthesis and Redox Homeostasis in Glioma. *Cell,* 175**,** 101-116.e25.

MCCARTHY, B. J., KRUCHKO, C. & DOLECEK, T. A. 2013. The impact of the Benign Brain Tumor Cancer Registries Amendment Act (Public Law 107-260) on non-malignant brain and central nervous system tumor incidence trends. *J Registry Manag,* 40**,** 32-5.

MEHRARA, E., FORSSELL-ARONSSON, E., AHLMAN, H. & BERNHARDT, P. 2007. Specific growth rate versus doubling time for quantitative characterization of tumor growth rate. *Cancer Res,* 67**,** 3970-5.

MEISER, J., KRÄMER, L., SAPCARIU, S. C., BATTELLO, N., GHELFI, J., D'HEROUEL, A. F., SKUPIN, A. & HILLER, K. 2016. Pro-inflammatory Macrophages Sustain Pyruvate Oxidation through Pyruvate Dehydrogenase for the Synthesis of Itaconate and to Enable Cytokine Expression. *J Biol Chem,* 291**,** 3932-46.

MELLINGHOFF, I. K., WANG, M. Y., VIVANCO, I., HAAS-KOGAN, D. A., ZHU, S., DIA, E. Q., LU, K. V., YOSHIMOTO, K., HUANG, J. H., CHUTE, D. J., RIGGS, B. L., HORVATH, S., LIAU, L. M., CAVENEE, W. K., RAO, P. N., BEROUKHIM, R., PECK, T. C., LEE, J. C., SELLERS, W. R., STOKOE, D., PRADOS, M., CLOUGHESY, T. F., SAWYERS, C. L. & MISCHEL, P. S. 2005. Molecular determinants of the response of glioblastomas to EGFR kinase inhibitors. *N Engl J Med,* 353**,** 2012-24.

METALLO, C. M., GAMEIRO, P. A., BELL, E. L., MATTAINI, K. R., YANG, J., HILLER, K., JEWELL, C. M., JOHNSON, Z. R., IRVINE, D. J., GUARENTE, L., KELLEHER, J. K., VANDER HEIDEN, M. G.,

ILIOPOULOS, O. & STEPHANOPOULOS, G. 2011. Reductive glutamine metabolism by IDH1 mediates lipogenesis under hypoxia. *Nature,* 481**,** 380-4.
METALLO, C. M. & VANDER HEIDEN, M. G. 2013. Understanding metabolic regulation and its influence on cell physiology. *Mol Cell,* 49**,** 388-98.
MIYATA, S., TOMINAGA, K., SAKASHITA, E., URABE, M., ONUKI, Y., GOMI, A., YAMAGUCHI, T., MIENO, M., MIZUKAMI, H., KUME, A., OZAWA, K., WATANABE, E., KAWAI, K. & ENDO, H. 2019. Comprehensive Metabolomic Analysis of IDH1(R132H) Clinical Glioma Samples Reveals Suppression of β-oxidation Due to Carnitine Deficiency. *Sci Rep,* 9**,** 9787.
MOHRENZ, I. V., ANTONIETTI, P., PUSCH, S., CAPPER, D., BALSS, J., VOIGT, S., WEISSERT, S., MUKROWSKY, A., FRANK, J., SENFT, C., SEIFERT, V., VON DEIMLING, A. & KOGEL, D. 2013. Isocitrate dehydrogenase 1 mutant R132H sensitizes glioma cells to BCNU-induced oxidative stress and cell death. *Apoptosis,* 18**,** 1416-1425.
MOLENAAR, R. J., BOTMAN, D., SMITS, M. A., HIRA, V. V., VAN LITH, S. A., STAP, J., HENNEMAN, P., KHURSHED, M., LENTING, K., MUL, A. N., DIMITRAKOPOULOU, D., VAN DRUNEN, C. M., HOEBE, R. A., RADIVOYEVITCH, T., WILMINK, J. W., MACIEJEWSKI, J. P., VANDERTOP, W. P., LEENDERS, W. P., BLEEKER, F. E. & VAN NOORDEN, C. J. 2015. Radioprotection of IDH1-Mutated Cancer Cells by the IDH1-Mutant Inhibitor AGI-5198. *Cancer Res,* 75**,** 4790-802.
MOLOFSKY, A. V. & DENEEN, B. 2015. Astrocyte development: A Guide for the Perplexed. *Glia,* 63**,** 1320-9.
MOSHAROV, E., CRANFORD, M. R. & BANERJEE, R. 2000. The quantitatively important relationship between homocysteine metabolism and glutathione synthesis by the transsulfuration pathway and its regulation by redox changes. *Biochemistry,* 39**,** 13005-11.
MUSTAFA, D. A., SWAGEMAKERS, S. M., BUISE, L., VAN DER SPEK, P. J. & KROS, J. M. 2014. Metabolic alterations due to IDH1 mutation in glioma: opening for therapeutic opportunities? *Acta Neuropathol Commun,* 2**,** 6.
NEDERGAARD, M., RANSOM, B. & GOLDMAN, S. A. 2003. New roles for astrocytes: redefining the functional architecture of the brain. *Trends Neurosci,* 26**,** 523-30.
NEFTEL, C., LAFFY, J., FILBIN, M. G., HARA, T., SHORE, M. E., RAHME, G. J., RICHMAN, A. R., SILVERBUSH, D., SHAW, M. L., HEBERT, C. M., DEWITT, J., GRITSCH, S., PEREZ, E. M., GONZALEZ CASTRO, L. N., LAN, X., DRUCK, N., RODMAN, C., DIONNE, D., KAPLAN, A., BERTALAN, M. S., SMALL, J., PELTON, K., BECKER, S., BONAL, D., NGUYEN, Q. D., SERVIS, R. L., FUNG, J. M., MYLVAGANAM, R., MAYR, L., GOJO, J., HABERLER, C., GEYEREGGER, R., CZECH, T., SLAVC, I., NAHED, B. V., CURRY, W. T., CARTER, B. S., WAKIMOTO, H., BRASTIANOS, P. K., BATCHELOR, T. T., STEMMER-RACHAMIMOV, A., MARTINEZ-LAGE, M., FROSCH, M. P., STAMENKOVIC, I., RIGGI, N., RHEINBAY, E., MONJE, M., ROZENBLATT-ROSEN, O., CAHILL, D. P., PATEL, A. P., HUNTER, T., VERMA, I. M., LIGON, K. L., LOUIS, D. N., REGEV, A., BERNSTEIN, B. E., TIROSH, I. & SUVÀ, M. L. 2019. An Integrative Model of Cellular States, Plasticity, and Genetics for Glioblastoma. *Cell,* 178**,** 835-849.e21.
NEHLIG, A. 2004. Brain uptake and metabolism of ketone bodies in animal models. *Prostaglandins Leukot Essent Fatty Acids,* 70**,** 265-75.
NELSON, D. L., LEHNINGER, A. L., COX, M. M., OSGOOD, M. & OCORR, K. 2009. *Lehninger principles of biochemistry,* New York, W.H. Freeman.
NOUSHMEHR, H., WEISENBERGER, D. J., DIEFES, K., PHILLIPS, H. S., PUJARA, K., BERMAN, B. P., PAN, F., PELLOSKI, C. E., SULMAN, E. P., BHAT, K. P., VERHAAK, R. G., HOADLEY, K. A., HAYES, D. N., PEROU, C. M., SCHMIDT, H. K., DING, L., WILSON, R. K., VAN DEN BERG, D., SHEN, H., BENGTSSON, H., NEUVIAL, P., COPE, L. M., BUCKLEY, J., HERMAN, J. G., BAYLIN, S. B., LAIRD, P. W. & ALDAPE, K. 2010. Identification of a CpG island methylator phenotype that defines a distinct subgroup of glioma. *Cancer Cell,* 17**,** 510-22.
OH, S., YEOM, J., CHO, H. J., KIM, J. H., YOON, S. J., KIM, H., SA, J. K., JU, S., LEE, H., OH, M. J., LEE, W., KWON, Y., LI, H., CHOI, S., HAN, J. H., CHANG, J. H., CHOI, E., KIM, J., HER, N. G., KIM, S. H., KANG, S. G., PAEK, E., NAM, D. H., LEE, C. & KIM, H. S. 2020. Integrated pharmaco-

proteogenomics defines two subgroups in isocitrate dehydrogenase wild-type glioblastoma with prognostic and therapeutic opportunities. *Nat Commun,* 11**,** 3288.
OHBA, S. & HIROSE, Y. 2016. Biological Significance of Mutant Isocitrate Dehydrogenase 1 and 2 in Gliomagenesis. *Neurol Med Chir (Tokyo),* 56**,** 170-9.
OHGAKI, H. & KLEIHUES, P. 2007. Genetic pathways to primary and secondary glioblastoma. *Am J Pathol,* 170**,** 1445-53.
OHGAKI, H. & KLEIHUES, P. 2013. The definition of primary and secondary glioblastoma. *Clin Cancer Res,* 19**,** 764-72.
OKUDA, S., YAMADA, T., HAMAJIMA, M., ITOH, M., KATAYAMA, T., BORK, P., GOTO, S. & KANEHISA, M. 2008. KEGG Atlas mapping for global analysis of metabolic pathways. *Nucleic Acids Res,* 36**,** W423-6.
OSTROM, Q. T., CIOFFI, G., GITTLEMAN, H., PATIL, N., WAITE, K., KRUCHKO, C. & BARNHOLTZ-SLOAN, J. S. 2019. CBTRUS Statistical Report: Primary Brain and Other Central Nervous System Tumors Diagnosed in the United States in 2012-2016. *Neuro Oncol,* 21**,** v1-v100.
PARKER, S. J. & METALLO, C. M. 2015. Metabolic consequences of oncogenic IDH mutations. *Pharmacol Ther,* 152**,** 54-62.
PARSONS, D. W., JONES, S., ZHANG, X., LIN, J. C., LEARY, R. J., ANGENENDT, P., MANKOO, P., CARTER, H., SIU, I. M., GALLIA, G. L., OLIVI, A., MCLENDON, R., RASHEED, B. A., KEIR, S., NIKOLSKAYA, T., NIKOLSKY, Y., BUSAM, D. A., TEKLEAB, H., DIAZ, L. A., JR., HARTIGAN, J., SMITH, D. R., STRAUSBERG, R. L., MARIE, S. K., SHINJO, S. M., YAN, H., RIGGINS, G. J., BIGNER, D. D., KARCHIN, R., PAPADOPOULOS, N., PARMIGIANI, G., VOGELSTEIN, B., VELCULESCU, V. E. & KINZLER, K. W. 2008. An integrated genomic analysis of human glioblastoma multiforme. *Science,* 321**,** 1807-12.
PAUL, B. D., SBODIO, J. I. & SNYDER, S. H. 2018. Cysteine Metabolism in Neuronal Redox Homeostasis. *Trends Pharmacol Sci,* 39**,** 513-524.
PAVLOVA, N. N. & THOMPSON, C. B. 2016. The Emerging Hallmarks of Cancer Metabolism. *Cell Metab,* 23**,** 27-47.
PELLEGATTA, S., VALLETTA, L., CORBETTA, C., PATANÈ, M., ZUCCA, I., RICCARDI SIRTORI, F., BRUZZONE, M. G., FOGLIATTO, G., ISACCHI, A., POLLO, B. & FINOCCHIARO, G. 2015. Effective immuno-targeting of the IDH1 mutation R132H in a murine model of intracranial glioma. *Acta Neuropathol Commun,* 3**,** 4.
PERILLO, B., DI DONATO, M., PEZONE, A., DI ZAZZO, E., GIOVANNELLI, P., GALASSO, G., CASTORIA, G. & MIGLIACCIO, A. 2020. ROS in cancer therapy: the bright side of the moon. *Exp Mol Med,* 52**,** 192-203.
PERRY, A. & WESSELING, P. 2016. Histologic classification of gliomas. *Handb Clin Neurol,* 134**,** 71-95.
PHANG, J. M., DONALD, S. P., PANDHARE, J. & LIU, Y. 2008. The metabolism of proline, a stress substrate, modulates carcinogenic pathways. *Amino Acids,* 35**,** 681-90.
PLATTEN, M., BUNSE, L., RIEHL, D., BUNSE, T., OCHS, K. & WICK, W. 2018. Vaccine Strategies in Gliomas. *Curr Treat Options Neurol,* 20**,** 11.
POLEWSKI, M. D., REVERON-THORNTON, R. F., CHERRYHOLMES, G. A., MARINOV, G. K., CASSADY, K. & ABOODY, K. S. 2016. Increased Expression of System xc- in Glioblastoma Confers an Altered Metabolic State and Temozolomide Resistance. *Mol Cancer Res,* 14**,** 1229-1242.
POLLAK, N., DÖLLE, C. & ZIEGLER, M. 2007. The power to reduce: pyridine nucleotides--small molecules with a multitude of functions. *Biochem J,* 402**,** 205-18.
PORSTMANN, T., SANTOS, C. R., GRIFFITHS, B., CULLY, M., WU, M., LEEVERS, S., GRIFFITHS, J. R., CHUNG, Y. L. & SCHULZE, A. 2008. SREBP activity is regulated by mTORC1 and contributes to Akt-dependent cell growth. *Cell Metab,* 8**,** 224-36.
POTTER, V. R. 1958. The biochemical approach to the cancer problem. *Fed Proc,* 17**,** 691-7.
PSYCHOGIOS, N., HAU, D. D., PENG, J., GUO, A. C., MANDAL, R., BOUATRA, S., SINELNIKOV, I., KRISHNAMURTHY, R., EISNER, R., GAUTAM, B., YOUNG, N., XIA, J., KNOX, C., DONG, E., HUANG, P., HOLLANDER, Z., PEDERSEN, T. L., SMITH, S. R., BAMFORTH, F., GREINER, R.,

MCMANUS, B., NEWMAN, J. W., GOODFRIEND, T. & WISHART, D. S. 2011. The human serum metabolome. *PLoS One,* 6**,** e16957.

PUISSANT, A., FRUMM, S. M., ALEXE, G., BASSIL, C. F., QI, J., CHANTHERY, Y. H., NEKRITZ, E. A., ZEID, R., GUSTAFSON, W. C., GRENINGER, P., GARNETT, M. J., MCDERMOTT, U., BENES, C. H., KUNG, A. L., WEISS, W. A., BRADNER, J. E. & STEGMAIER, K. 2013. Targeting MYCN in neuroblastoma by BET bromodomain inhibition. *Cancer Discov,* 3**,** 308-23.

PUSCH, S., KRAUSERT, S., FISCHER, V., BALSS, J., OTT, M., SCHRIMPF, D., CAPPER, D., SAHM, F., EISEL, J., BECK, A. C., JUGOLD, M., EICHWALD, V., KAULFUSS, S., PANKNIN, O., REHWINKEL, H., ZIMMERMANN, K., HILLIG, R. C., GUENTHER, J., TOSCHI, L., NEUHAUS, R., HAEGEBART, A., HESS-STUMPP, H., BAUSER, M., WICK, W., UNTERBERG, A., HEROLD-MENDE, C., PLATTEN, M. & VON DEIMLING, A. 2017. Pan-mutant IDH1 inhibitor BAY 1436032 for effective treatment of IDH1 mutant astrocytoma in vivo. *Acta Neuropathol,* 133**,** 629-644.

RAMACHANDRAN, N. & COLMAN, R. F. 1980. Chemical characterization of distinct subunits of pig heart DPN-specific isocitrate dehydrogenase. *J Biol Chem,* 255**,** 8859-64.

REITMAN, Z. J., JIN, G., KAROLY, E. D., SPASOJEVIC, I., YANG, J., KINZLER, K. W., HE, Y., BIGNER, D. D., VOGELSTEIN, B. & YAN, H. 2011. Profiling the effects of isocitrate dehydrogenase 1 and 2 mutations on the cellular metabolome. *Proc Natl Acad Sci U S A,* 108**,** 3270-5.

ROBE, P. A., MARTIN, D., ALBERT, A., DEPREZ, M., CHARIOT, A. & BOURS, V. 2006. A phase 1-2, prospective, double blind, randomized study of the safety and efficacy of Sulfasalazine for the treatment of progressing malignant gliomas: study protocol of [ISRCTN45828668]. *BMC Cancer,* 6**,** 29.

ROHLE, D., POPOVICI-MULLER, J., PALASKAS, N., TURCAN, S., GROMMES, C., CAMPOS, C., TSOI, J., CLARK, O., OLDRINI, B., KOMISOPOULOU, E., KUNII, K., PEDRAZA, A., SCHALM, S., SILVERMAN, L., MILLER, A., WANG, F., YANG, H., CHEN, Y., KERNYTSKY, A., ROSENBLUM, M. K., LIU, W., BILLER, S. A., SU, S. M., BRENNAN, C. W., CHAN, T. A., GRAEBER, T. G., YEN, K. E. & MELLINGHOFF, I. K. 2013. An inhibitor of mutant IDH1 delays growth and promotes differentiation of glioma cells. *Science,* 340**,** 626-30.

ROTHBERG, J. M., BAILEY, K. M., WOJTKOWIAK, J. W., BEN-NUN, Y., BOGYO, M., WEBER, E., MOIN, K., BLUM, G., MATTINGLY, R. R., GILLIES, R. J. & SLOANE, B. F. 2013. Acid-mediated tumor proteolysis: contribution of cysteine cathepsins. *Neoplasia,* 15**,** 1125-37.

SASAKI, M., KNOBBE, C. B., ITSUMI, M., ELIA, A. J., HARRIS, I. S., CHIO, II, CAIRNS, R. A., MCCRACKEN, S., WAKEHAM, A., HAIGHT, J., TEN, A. Y., SNOW, B., UEDA, T., INOUE, S., YAMAMOTO, K., KO, M., RAO, A., YEN, K. E., SU, S. M. & MAK, T. W. 2012. D-2-hydroxyglutarate produced by mutant IDH1 perturbs collagen maturation and basement membrane function. *Genes Dev,* 26**,** 2038-49.

SBODIO, J. I., SNYDER, S. H. & PAUL, B. D. 2019. Regulators of the transsulfuration pathway. *Br J Pharmacol,* 176**,** 583-593.

SCHMIDT, S., RICHTER, M., MONTAG, D., SARTORIUS, T., GAWLIK, V., HENNIGE, A. M., SCHERNECK, S., HIMMELBAUER, H., LUTZ, S. Z., AUGUSTIN, R., KLUGE, R., RUTH, P., JOOST, H. G. & SCHÜRMANN, A. 2008. Neuronal functions, feeding behavior, and energy balance in Slc2a3+/- mice. *Am J Physiol Endocrinol Metab,* 295**,** E1084-94.

SCHUMACHER, T., BUNSE, L., PUSCH, S., SAHM, F., WIESTLER, B., QUANDT, J., MENN, O., OSSWALD, M., OEZEN, I., OTT, M., KEIL, M., BALß, J., RAUSCHENBACH, K., GRABOWSKA, A. K., VOGLER, I., DIEKMANN, J., TRAUTWEIN, N., EICHMÜLLER, S. B., OKUN, J., STEVANOVIĆ, S., RIEMER, A. B., SAHIN, U., FRIESE, M. A., BECKHOVE, P., VON DEIMLING, A., WICK, W. & PLATTEN, M. 2014. A vaccine targeting mutant IDH1 induces antitumour immunity. *Nature,* 512**,** 324-7.

SCIACOVELLI, M. & FREZZA, C. 2016. Oncometabolites: Unconventional triggers of oncogenic signalling cascades. *Free Radic Biol Med,* 100**,** 175-181.

SELTZER, M. J., BENNETT, B. D., JOSHI, A. D., GAO, P., THOMAS, A. G., FERRARIS, D. V., TSUKAMOTO, T., ROJAS, C. J., SLUSHER, B. S., RABINOWITZ, J. D., DANG, C. V. & RIGGINS, G. J. 2010. Inhibition of glutaminase preferentially slows growth of glioma cells with mutant IDH1. *Cancer Res,* 70**,** 8981-7.

SEMENZA, G. L. 2003. Targeting HIF-1 for cancer therapy. *Nat Rev Cancer,* 3**,** 721-32.
SHI, J., SUN, B., SHI, W., ZUO, H., CUI, D., NI, L. & CHEN, J. 2015. Decreasing GSH and increasing ROS in chemosensitivity gliomas with IDH1 mutation. *Tumour Biol,* 36**,** 655-62.
SHI, J., ZUO, H., NI, L., XIA, L., ZHAO, L., GONG, M., NIE, D., GONG, P., CUI, D., SHI, W. & CHEN, J. 2014. An IDH1 mutation inhibits growth of glioma cells via GSH depletion and ROS generation. *Neurol Sci,* 35**,** 839-45.
SINGER, E., JUDKINS, J., SALOMONIS, N., MATLAF, L., SOTEROPOULOS, P., MCALLISTER, S. & SOROCEANU, L. 2015. Reactive oxygen species-mediated therapeutic response and resistance in glioblastoma. *Cell Death Dis,* 6**,** e1601.
SOM, P., ATKINS, H. L., BANDOYPADHYAY, D., FOWLER, J. S., MACGREGOR, R. R., MATSUI, K., OSTER, Z. H., SACKER, D. F., SHIUE, C. Y., TURNER, H., WAN, C. N., WOLF, A. P. & ZABINSKI, S. V. 1980. A fluorinated glucose analog, 2-fluoro-2-deoxy-D-glucose (F-18): nontoxic tracer for rapid tumor detection. *J Nucl Med,* 21**,** 670-5.
SRERE, P. A. 1959. The citrate cleavage enzyme. I. Distribution and purification. *J Biol Chem,* 234**,** 2544-7.
STEENWEG, M. E., JAKOBS, C., ERRAMI, A., VAN DOOREN, S. J., ADEVA BARTOLOMÉ, M. T., AERSSENS, P., AUGOUSTIDES-SAVVAPOULOU, P., BARIC, I., BAUMANN, M., BONAFÉ, L., CHABROL, B., CLARKE, J. T., CLAYTON, P., COKER, M., COOPER, S., FALIK-ZACCAI, T., GORMAN, M., HAHN, A., HASANOGLU, A., KING, M. D., DE KLERK, H. B., KORMAN, S. H., LEE, C., MELDGAARD LUND, A., MEJASKI-BOSNJAK, V., PASCUAL-CASTROVIEJO, I., RAADHYAKSHA, A., ROOTWELT, T., ROUBERTIE, A., RUIZ-FALCO, M. L., SCALAIS, E., SCHIMMEL, U., SEIJO-MARTINEZ, M., SURI, M., SYKUT-CEGIELSKA, J., TREFZ, F. K., UZIEL, G., VALAYANNOPOULOS, V., VIANEY-SABAN, C., VLAHO, S., VODOPIUTZ, J., WAJNER, M., WALTER, J., WALTER-DERBORT, C., YAPICI, Z., ZAFEIRIOU, D. I., SPREEUWENBERG, M. D., CELLI, J., DEN DUNNEN, J. T., VAN DER KNAAP, M. S. & SALOMONS, G. S. 2010. An overview of L-2-hydroxyglutarate dehydrogenase gene (L2HGDH) variants: a genotype-phenotype study. *Hum Mutat,* 31**,** 380-90.
STODDARD, B. L., DEAN, A. & KOSHLAND, D. E., JR. 1993. Structure of isocitrate dehydrogenase with isocitrate, nicotinamide adenine dinucleotide phosphate, and calcium at 2.5-A resolution: a pseudo-Michaelis ternary complex. *Biochemistry,* 32**,** 9310-6.
STOLZING, A. & GRUNE, T. 2004. Neuronal apoptotic bodies: phagocytosis and degradation by primary microglial cells. *Faseb j,* 18**,** 743-5.
SULKOWSKI, P. L., CORSO, C. D., ROBINSON, N. D., SCANLON, S. E., PURSHOUSE, K. R., BAI, H., LIU, Y., SUNDARAM, R. K., HEGAN, D. C., FONS, N. R., BREUER, G. A., SONG, Y., MISHRA-GORUR, K., DE FEYTER, H. M., DE GRAAF, R. A., SUROVTSEVA, Y. V., KACHMAN, M., HALENE, S., GÜNEL, M., GLAZER, P. M. & BINDRA, R. S. 2017. 2-Hydroxyglutarate produced by neomorphic IDH mutations suppresses homologous recombination and induces PARP inhibitor sensitivity. *Sci Transl Med,* 9.
SUN, Q., COLLINS, R., HUANG, S., HOLMBERG-SCHIAVONE, L., ANAND, G. S., TAN, C.-H., VAN-DEN-BERG, S., DENG, L.-W., MOORE, P. K., KARLBERG, T. & SIVARAMAN, J. 2009. Structural basis for the inhibition mechanism of human cystathionine gamma-lyase, an enzyme responsible for the production of H(2)S. *The Journal of biological chemistry,* 284**,** 3076-3085.
SZABO, C. & PAPAPETROPOULOS, A. 2017. International Union of Basic and Clinical Pharmacology. CII: Pharmacological Modulation of H(2)S Levels: H(2)S Donors and H(2)S Biosynthesis Inhibitors. *Pharmacological reviews,* 69**,** 497-564.
SZKLARCZYK, D., GABLE, A. L., LYON, D., JUNGE, A., WYDER, S., HUERTA-CEPAS, J., SIMONOVIC, M., DONCHEVA, N. T., MORRIS, J. H., BORK, P., JENSEN, L. J. & MERING, C. V. 2019. STRING v11: protein-protein association networks with increased coverage, supporting functional discovery in genome-wide experimental datasets. *Nucleic Acids Res,* 47**,** D607-d613.
TAKEUCHI, S., WADA, K., NAGATANI, K., OTANI, N., OSADA, H. & NAWASHIRO, H. 2014. Sulfasalazine and temozolomide with radiation therapy for newly diagnosed glioblastoma. *Neurol India,* 62**,** 42-7.

TANG, X., FU, X., LIU, Y., YU, D., CAI, S. J. & YANG, C. 2020. Blockade of Glutathione Metabolism in IDH1-Mutated Glioma. *Mol Cancer Ther,* 19**,** 221-230.

TATEISHI, K., WAKIMOTO, H., IAFRATE, A. J., TANAKA, S., LOEBEL, F., LELIC, N., WIEDERSCHAIN, D., BEDEL, O., DENG, G., ZHANG, B., HE, T., SHI, X., GERSZTEN, R. E., ZHANG, Y., YEH, J. J., CURRY, W. T., ZHAO, D., SUNDARAM, S., NIGIM, F., KOERNER, M. V. A., HO, Q., FISHER, D. E., ROIDER, E. M., KEMENY, L. V., SAMUELS, Y., FLAHERTY, K. T., BATCHELOR, T. T., CHI, A. S. & CAHILL, D. P. 2015. Extreme Vulnerability of IDH1 Mutant Cancers to NAD+ Depletion. *Cancer Cell,* 28**,** 773-784.

THOMAS, J. G. & VEZNEDAROGLU, E. 2020. Ketogenic Diet for Malignant Gliomas: a Review. *Curr Nutr Rep,* 9**,** 258-263.

TOMLINSON, I. P., ALAM, N. A., ROWAN, A. J., BARCLAY, E., JAEGER, E. E., KELSELL, D., LEIGH, I., GORMAN, P., LAMLUM, H., RAHMAN, S., ROYLANCE, R. R., OLPIN, S., BEVAN, S., BARKER, K., HEARLE, N., HOULSTON, R. S., KIURU, M., LEHTONEN, R., KARHU, A., VILKKI, S., LAIHO, P., EKLUND, C., VIERIMAA, O., AITTOMÄKI, K., HIETALA, M., SISTONEN, P., PAETAU, A., SALOVAARA, R., HERVA, R., LAUNONEN, V. & AALTONEN, L. A. 2002. Germline mutations in FH predispose to dominantly inherited uterine fibroids, skin leiomyomata and papillary renal cell cancer. *Nat Genet,* 30**,** 406-10.

TRONG, P. D., JUNGWIRTH, G., YU, T., PUSCH, S., UNTERBERG, A., HEROLD-MENDE, C. & WARTA, R. 2020. Large-Scale Drug Screening in Patient-Derived IDH(mut) Glioma Stem Cells Identifies Several Efficient Drugs among FDA-Approved Antineoplastic Agents. *Cells,* 9.

TURCAN, S., FABIUS, A. W., BORODOVSKY, A., PEDRAZA, A., BRENNAN, C., HUSE, J., VIALE, A., RIGGINS, G. J. & CHAN, T. A. 2013. Efficient induction of differentiation and growth inhibition in IDH1 mutant glioma cells by the DNMT Inhibitor Decitabine. *Oncotarget,* 4**,** 1729-36.

TURCAN, S., ROHLE, D., GOENKA, A., WALSH, L. A., FANG, F., YILMAZ, E., CAMPOS, C., FABIUS, A. W., LU, C., WARD, P. S., THOMPSON, C. B., KAUFMAN, A., GURYANOVA, O., LEVINE, R., HEGUY, A., VIALE, A., MORRIS, L. G., HUSE, J. T., MELLINGHOFF, I. K. & CHAN, T. A. 2012. IDH1 mutation is sufficient to establish the glioma hypermethylator phenotype. *Nature,* 483**,** 479-83.

VAN HALL, G., STRØMSTAD, M., RASMUSSEN, P., JANS, O., ZAAR, M., GAM, C., QUISTORFF, B., SECHER, N. H. & NIELSEN, H. B. 2009. Blood lactate is an important energy source for the human brain. *J Cereb Blood Flow Metab,* 29**,** 1121-9.

VANDER HEIDEN, M. G., CANTLEY, L. C. & THOMPSON, C. B. 2009. Understanding the Warburg effect: the metabolic requirements of cell proliferation. *Science,* 324**,** 1029-33.

VILCHEZ, D., ROS, S., CIFUENTES, D., PUJADAS, L., VALLÈS, J., GARCÍA-FOJEDA, B., CRIADO-GARCÍA, O., FERNÁNDEZ-SÁNCHEZ, E., MEDRAÑO-FERNÁNDEZ, I., DOMÍNGUEZ, J., GARCÍA-ROCHA, M., SORIANO, E., RODRÍGUEZ DE CÓRDOBA, S. & GUINOVART, J. J. 2007. Mechanism suppressing glycogen synthesis in neurons and its demise in progressive myoclonus epilepsy. *Nat Neurosci,* 10**,** 1407-13.

WAITKUS, M. S., DIPLAS, B. H. & YAN, H. 2016. Isocitrate dehydrogenase mutations in gliomas. *Neuro Oncol,* 18**,** 16-26.

WAITKUS, M. S., DIPLAS, B. H. & YAN, H. 2018a. Biological Role and Therapeutic Potential of IDH Mutations in Cancer. *Cancer Cell,* 34**,** 186-195.

WAITKUS, M. S., PIROZZI, C. J., MOURE, C. J., DIPLAS, B. H., HANSEN, L. J., CARPENTER, A. B., YANG, R., WANG, Z., INGRAM, B. O., KAROLY, E. D., MOHNEY, R. P., SPASOJEVIC, I., MCLENDON, R. E., FRIEDMAN, H. S., HE, Y., BIGNER, D. D. & YAN, H. 2018b. Adaptive Evolution of the GDH2 Allosteric Domain Promotes Gliomagenesis by Resolving IDH1(R132H)-Induced Metabolic Liabilities. *Cancer Res,* 78**,** 36-50.

WANG, C., GUO, K., GAO, D., KANG, X., JIANG, K., LI, Y., SUN, L., ZHANG, S., SUN, C., LIU, X., WU, W., YANG, P. & LIU, Y. 2011. Identification of transaldolase as a novel serum biomarker for hepatocellular carcinoma metastasis using xenografted mouse model and clinic samples. *Cancer Lett,* 313**,** 154-66.

WANG, D., PASCUAL, J. M., YANG, H., ENGELSTAD, K., MAO, X., CHENG, J., YOO, J., NOEBELS, J. L. & DE VIVO, D. C. 2006. A mouse model for Glut-1 haploinsufficiency. *Hum Mol Genet,* 15**,** 1169-79.

WANG, X. F. & CYNADER, M. S. 2000. Astrocytes provide cysteine to neurons by releasing glutathione. *J Neurochem,* 74**,** 1434-42.

WARBURG, O., WIND, F. & NEGELEIN, E. 1927. THE METABOLISM OF TUMORS IN THE BODY. *J Gen Physiol,* 8**,** 519-30.

WARD, P. S., CROSS, J. R., LU, C., WEIGERT, O., ABEL-WAHAB, O., LEVINE, R. L., WEINSTOCK, D. M., SHARP, K. A. & THOMPSON, C. B. 2012. Identification of additional IDH mutations associated with oncometabolite R(-)-2-hydroxyglutarate production. *Oncogene,* 31**,** 2491-8.

WARD, P. S., PATEL, J., WISE, D. R., ABDEL-WAHAB, O., BENNETT, B. D., COLLER, H. A., CROSS, J. R., FANTIN, V. R., HEDVAT, C. V., PERL, A. E., RABINOWITZ, J. D., CARROLL, M., SU, S. M., SHARP, K. A., LEVINE, R. L. & THOMPSON, C. B. 2010. The common feature of leukemia-associated IDH1 and IDH2 mutations is a neomorphic enzyme activity converting alpha-ketoglutarate to 2-hydroxyglutarate. *Cancer Cell,* 17**,** 225-34.

WELLER, M., ROTH, P., PREUSSER, M., WICK, W., REARDON, D. A., PLATTEN, M. & SAMPSON, J. H. 2017. Vaccine-based immunotherapeutic approaches to gliomas and beyond. *Nat Rev Neurol,* 13**,** 363-374.

WU, J. Y. & PRENTICE, H. 2010. Role of taurine in the central nervous system. *J Biomed Sci,* 17 Suppl 1**,** S1.

XU, W., YANG, H., LIU, Y., YANG, Y., WANG, P., KIM, S. H., ITO, S., YANG, C., WANG, P., XIAO, M. T., LIU, L. X., JIANG, W. Q., LIU, J., ZHANG, J. Y., WANG, B., FRYE, S., ZHANG, Y., XU, Y. H., LEI, Q. Y., GUAN, K. L., ZHAO, S. M. & XIONG, Y. 2011a. Oncometabolite 2-hydroxyglutarate is a competitive inhibitor of alpha-ketoglutarate-dependent dioxygenases. *Cancer Cell,* 19**,** 17-30.

XU, W., YANG, H., LIU, Y., YANG, Y., WANG, P., KIM, S. H., ITO, S., YANG, C., WANG, P., XIAO, M. T., LIU, L. X., JIANG, W. Q., LIU, J., ZHANG, J. Y., WANG, B., FRYE, S., ZHANG, Y., XU, Y. H., LEI, Q. Y., GUAN, K. L., ZHAO, S. M. & XIONG, Y. 2011b. Oncometabolite 2-hydroxyglutarate is a competitive inhibitor of α-ketoglutarate-dependent dioxygenases. *Cancer Cell,* 19**,** 17-30.

XU, X., ZHAO, J., XU, Z., PENG, B., HUANG, Q., ARNOLD, E. & DING, J. 2004. Structures of human cytosolic NADP-dependent isocitrate dehydrogenase reveal a novel self-regulatory mechanism of activity. *The Journal of biological chemistry,* 279**,** 33946-33957.

YAN, H., PARSONS, D. W., JIN, G., MCLENDON, R., RASHEED, B. A., YUAN, W., KOS, I., BATINIC-HABERLE, I., JONES, S., RIGGINS, G. J., FRIEDMAN, H., FRIEDMAN, A., REARDON, D., HERNDON, J., KINZLER, K. W., VELCULESCU, V. E., VOGELSTEIN, B. & BIGNER, D. D. 2009. IDH1 and IDH2 mutations in gliomas. *N Engl J Med,* 360**,** 765-73.

ZHANG, X., RAO, A., SETTE, P., DEIBERT, C., POMERANTZ, A., KIM, W. J., KOHANBASH, G., CHANG, Y., PARK, Y., ENGH, J., CHOI, J., CHAN, T., OKADA, H., LOTZE, M., GRANDI, P. & AMANKULOR, N. 2016. IDH mutant gliomas escape natural killer cell immune surveillance by downregulation of NKG2D ligand expression. *Neuro Oncol,* 18**,** 1402-12.

ZHAO, S., LIN, Y., XU, W., JIANG, W., ZHA, Z., WANG, P., YU, W., LI, Z., GONG, L., PENG, Y., DING, J., LEI, Q., GUAN, K. L. & XIONG, Y. 2009. Glioma-derived mutations in IDH1 dominantly inhibit IDH1 catalytic activity and induce HIF-1alpha. *Science,* 324**,** 261-5.

ZHU, H., ZHANG, Y., CHEN, J., QIU, J., HUANG, K., WU, M. & XIA, C. 2017. IDH1 R132H Mutation Enhances Cell Migration by Activating AKT-mTOR Signaling Pathway, but Sensitizes Cells to 5-FU Treatment as NADPH and GSH Are Reduced. *PLoS One,* 12**,** e0169038.

ZHU, J., BERISA, M., SCHWORER, S., QIN, W., CROSS, J. R. & THOMPSON, C. B. 2019. Transsulfuration Activity Can Support Cell Growth upon Extracellular Cysteine Limitation. *Cell Metab,* 30**,** 865-876.e5.